



Characterisation and a length-based assessment model for scampi (*Metanephrops challenger*) on the Mernoo Bank (SCI 3)

New Zealand Fisheries Assessment Report 2016/55

I.D. Tuck

ISSN 1179-5352 (online)

ISBN 978-1-77665-405-5 (online)

October 2016



Requests for further copies should be directed to:

Publications Logistics Officer
Ministry for Primary Industries
PO Box 2526
WELLINGTON 6140

Email: brand@mpi.govt.nz
Telephone: 0800 00 83 33
Facsimile: 04-894 0300

This publication is also available on the Ministry for Primary Industries websites at:
<http://www.mpi.govt.nz/news-resources/publications.aspx>
<http://fs.fish.govt.nz> go to Document library/Research reports

© Crown Copyright - Ministry for Primary Industries

TABLE OF CONTENTS

EXECUTIVE SUMMARY	1
1. INTRODUCTION	2
1.1 The Mernoo Bank (SCI 3) scampi fishery	2
2. FISHERY CHARACTERISATION AND DATA	5
2.1 Commercial catch and effort data	5
2.2 Scampi stock structure	13
2.3 Seasonal patterns in scampi biology	13
2.4 Standardised CPUE indices	16
2.4.1 Core vessels and time periods	16
2.4.2 Calculation of indices	19
2.4.3 Final CPUE index	22
3. MODEL STRUCTURE	23
3.1 Seasonal and spatial structure, and the model partition	23
3.2 Biological inputs	24
3.2.1 Growth	24
3.2.2 Maturity	24
3.2.3 Natural mortality	25
3.3 Catch data	26
3.4 CPUE indices	26
3.5 Research survey indices	29
3.5.1 Photographic surveys	29
3.5.2 Trawl surveys	29
3.6 Length distributions	30
3.6.1 Commercial catch length distributions	30
3.6.2 Trawl survey length distributions	37
3.6.3 Photo survey length distributions	39
3.7 Model assumptions and priors	42
3.7.1 Scampi catchability	43
3.7.2 Priors for qs	43
3.7.3 Estimation of prior distributions	44
3.7.4 Recruitment	45
4. ASSESSMENT MODEL RESULTS	45
4.1 Initial models	45
4.2 Base models	46
4.2.1 Models excluding the trawl surveys (NT_0.15, NT_0.25, NT_0.35)	47

4.2.2	Models excluding the photographic surveys (NP_0.15, NP_0.25, NP_0.35)	52
4.3	Projections	56
5.	DISCUSSION	63
6.	ACKNOWLEDGEMENTS	64
7.	REFERENCES	64
	APPENDIX 1. CPUE standardisation diagnostics	67
	APPENDIX 2. Analysis of length composition data	77
	APPENDIX 3. MODEL NT_0.15	84
	APPENDIX 4. MODEL NT_0.25	106
	APPENDIX 5. MODEL NT_0.35	128
	APPENDIX 6. MODEL NP_0.15	150
	APPENDIX 7. MODEL NP_0.25	173
	APPENDIX 8. MODEL NP_0.35	196

EXECUTIVE SUMMARY

Tuck, I.D. (2016). Characterisation and a length-based assessment model for scampi (*Metanephrops challengeri*) on the Mernoo Bank (SCI 3).

New Zealand Fisheries Assessment Report 2016/55. 218 p.

A stock assessment of the Mernoo Bank (SCI 3) scampi stock has been undertaken through MPI project DEE201002SCID. This work has further developed an existing model for this stock, developed within a previous MPI project. The assessments presented were accepted.

A fishery characterisation was undertaken, and CPUE indices were estimated for the three areas of the stock, incorporating spatial and temporal components in the fishery. The previous model for this stock incorporated separate CPUE indices for the three time steps for each subarea, but based on more recent assessments for other scampi fisheries, and following preliminary investigations, the Shellfish Assessment Working Group (SFAWG) recommended developing a three area (stock) model, and fitting an annual CPUE index for each subarea, along with photographic and trawl survey indices. The model year was shifted slightly from the fishing year, to simplify the model to two time steps. Preliminary investigation suggested some conflict between the two survey indices, and therefore sensitivity to natural mortality (M), and inclusion of either photographic or trawl survey indices were investigated, with models taken to MCMC.

Biomass estimates were different between the two model approaches (excluding trawl or excluding photographic surveys), but current stock status was very similar (SSB_{2014}/SSB_0 54 – 60%). Projections were conducted up to 2020 on the basis of a range of catch scenarios, with the differences between the projections reflecting differences in estimated recruitment in the most recent years. Models excluding the trawl survey data suggested that with constant catches set at the TACC, stock status would improve to 70% SSB_0 by 2020. Models excluding the photographic survey data suggested that with constant catches set at the TACC, stock status would decline to 42% – 44% SSB_0 by 2020.

1. INTRODUCTION

This report undertakes a fishery characterisation for the Mernoo Bank (SCI 3) scampi stock, and applies the previously described Bayesian, length-based, two-sex population model to this stock. Previous characterisations of scampi stocks are described by Tuck (2009; 2013). The first attempt at developing a length-based population model for any scampi stock was conducted for SCI 1 (Cryer et al. 2005), implemented using the general-purpose stock assessment program CASAL v2.06 (September 2004). This model for SCI 1 was developed further and the same model structure was also applied to SCI 2 in a later project (Tuck & Dunn 2006). The model was first applied to the SCI 3 stock in 2011, although this assessment was not accepted (Tuck 2013). The current study used CASAL v 2.22 (Bull et al. 2008) with a slightly modified selectivity option. Developments in the model implementation and structure have been largely based on suggestions raised at the MFish funded Scampi Assessment Workshop (Tuck & Dunn 2009), and subsequently at Shellfish Fisheries Assessment Working Group (SFAWG) meetings. Assessments for SCI 1 and SCI 2 using this model were accepted in 2011 and 2013 (Tuck & Dunn 2012; Tuck 2014).

We describe the available data and how they were used, the parameterisation of the model, and model fits and sensitivity. This report fulfils Ministry for Primary Industries project DEE201002SCID “*Stock assessment of scampi*”, undertaking an assessment of SCI 3. The objective of this project was to conduct a stock assessment, including estimating yield for SCI 3 in 2014–15.

1.1 The Mernoo Bank (SCI 3) scampi fishery

Scampi is fished all around New Zealand, in nine fishery management areas (Figure 1). The SCI 3 fishery is one of New Zealand’s four main scampi fisheries (the others being SCI 1, SCI 2 and SCI 6A), and over the last 5 years (2009–10 to 2013–14) has contributed an average of 284 tonnes annually, having increased slightly from the previous five years (2004–05 to 2008–09 average 272 tonnes). The TACC for SCI 6A is 340 tonnes, and the total TACC for all management areas is 1231 tonnes.

The spatial distribution of the targeted scampi fishing within SCI 3 is focussed in an area on the western end of the Chatham Rise, and straddles the boundary between the old QMA 3 and QMA 4W management areas (Figure 2). Prior to introduction into the QMS, the management area boundaries for the Mernoo Bank / Chatham Rise (QMA 3 and QMA 4) fisheries were reviewed on the basis of information on average catch rates, trends in CPUE, average size, sex ratio, bathymetry, and by-catch amount and composition (Cryer 2000) resulting in changes being introduced on 1st October 2004. The fishery parameters examined were generally similar between QMA 3 and 4W but less similar for QMA 4E, and hence the former two areas were combined into SCI 3. This study also suggested that it may be appropriate to separate the Mernoo Bank / western Chatham Rise fishery from the rest of QMA 3 (Canterbury and Otago coastline), since the deep water between the two areas is a natural break between the populations, although this suggestion was not adopted by managers. Minimal scampi fishing (less than 1% of SCI 3 scampi catches) takes place outside the main Mernoo Bank / western Chatham Rise area.

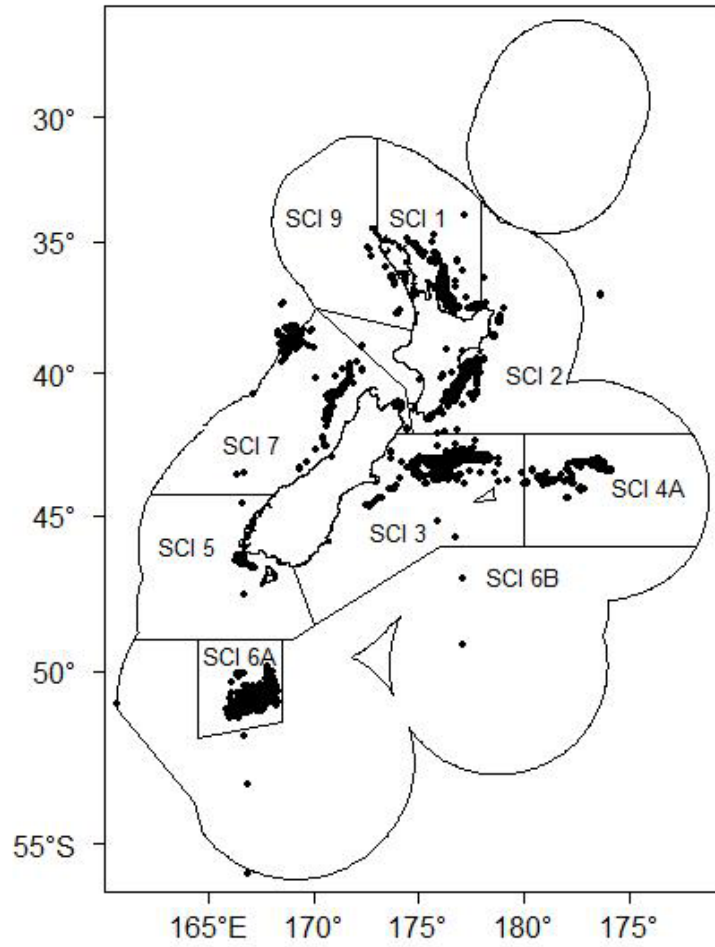


Figure 1: Spatial distribution of the scampi fishery since 1988–89. Each dot shows the mid point of one or more tows recorded on TCEPR with scampi as the target species.

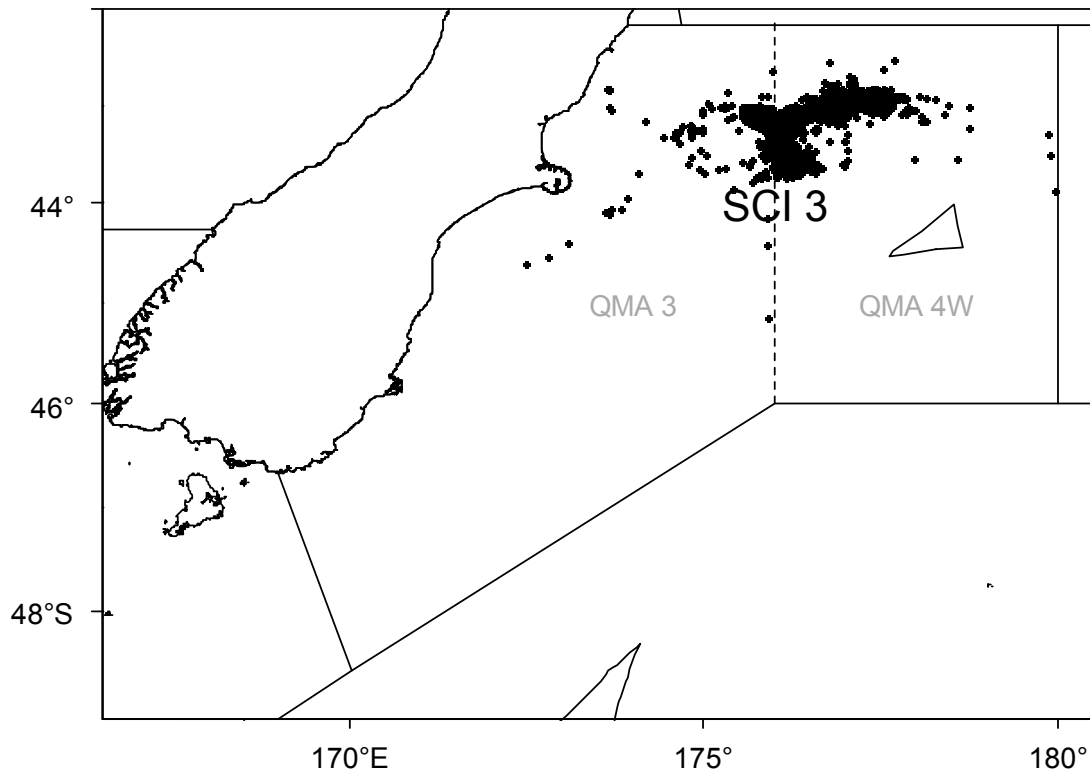


Figure 2: Spatial distribution of the scampi fishery within management area SCI 3 since 1988–89. Each dot shows the mid-point of one or more tows recorded on TCEPR with scampi as the target species. Previous (prior to the 2004–05 fishing year) scampi management areas QMA 3 and QMA 4W are also shown. The boundary between QMA 3 and QMA 4W was 176°E.

The changes to the management area boundaries mean that different parts of the SCI 3 area have different management histories. Until entry into the QMS (1 October 2004), the QMA 3 area was managed under a competitive catch limit. Individual quotas were introduced for QMA 4 in 1992–93 (allocated on the basis of the permit holders catch in 1991–92), and maintained until October 2001, when all scampi fisheries were managed with competitive catch limits. Since October 2004, all scampi fisheries have been managed with individual quotas.

Previous fishery characterisations have been undertaken for this area; by Cryer & Coburn (2000) as separate areas (QMA 3 and QMA 4W), and by Tuck (2009; 2013), as SCI 3. The more recent studies identified two separate areas within the SCI 3 fishery, one of which showed a distinct spatial shift over time (Tuck 2009).

2. FISHERY CHARACTERISATION AND DATA

2.1 Commercial catch and effort data

Scampi fishers have consistently reported catches on the Trawl Catch, Effort, and Processing Returns (TCEPR) form since its introduction in 1989–90, providing a very valuable record of catch and effort on a tow by tow basis.

Data were extracted from the MPI TCEPR database, requesting all tows where scampi (SCI) was the nominated target species, or was reported in the catch. This resulted in an extract of 303 961 fishing events, but fishing events where scampi was the target species (112 269 events) contributed 99.8% of estimated scampi catches, and so only scampi targeting events were considered further. Errors in TCEPR records are reducing in frequency, but do occur, and the raw records were groomed in the following manner. For each record, the reported data were used to estimate the duration of the trawl shot, the distance between the start and finish locations, and the mid point between the start and finish locations. Tows with zero scampi catch were excluded. All tows with zero hours tow duration recorded (but some scampi catch) were reset to the median tow duration for the trip. All tows with a tow distance greater than 50 km were reset to the median of the mid point of tows on the same day, adjacent days, or the trip, depending on available data. Where a vessel only reported start position (rather than start and finish position) for a tow, this was used instead of the mid point. Excluding fishing events with no scampi catch reduced the data set to 108 220 events, and removing additional events where the location could not be determined reduced the data set further, to 107 981 events, 2462 of which were those where the original estimated tow distance exceeded 50 km. The SCI 3 data were then extracted from this full data set on the basis of latitude and longitude. All analysis was conducted on the basis of the current management area boundaries.

Subsequent analyses were conducted on this “groomed” version of the data set (28 351 records), representing over 99% of estimated scampi catches from SCI 3, as it is considered to be the most appropriate to investigate patterns in the fishery, given that it represents the targeted scampi fishery, and latitude and longitude data are available for spatial aspects of the analysis. Previous characterisations have used a slightly different grooming approach (to that discussed above), details of which are provided in Tuck (2009). Comparisons of unstandardized CPUE data for the earlier and revised grooming approaches have previously been examined (Tuck 2014). The revised grooming slightly reduces the estimated CPUE prior to 2003 (due to rounding of the haul duration data), but the medians of the annual values appear identical after this.

The distribution of fishing activity within the SCI 3 area over time is presented in Figure 3 and Figure 4. Following some exploratory fishing, the SCI 3 fishery started in 1991–92 to the east within what was then QMA 4W, but fishing started to the west in QMA 3 the following year, with the distribution of activity remaining relatively constant for a few years. In the early 2000s the activity within QMA 4W spread further to the west, adjacent to the area fished within QMA 3, and this overall pattern continued until the 2003–04 fishing year. On the 1st October 2004 scampi was introduced into the QMS, and the management areas were revised so that QMA 4W and QMA 3 were combined to form SCI 3. Following this, the vessels active in the area had access to all the previously fished areas, and the pattern of effort shifted, with minimal effort having targeted scampi in the old QMA 3 area (to the west of 176° E) since this time, and effort developing to the south of the western part of the old QMA 4W. On the basis of the patterns observed within the fishery in this main area, three sub-areas have been identified (Figure 5), each of which show different historical fishing patterns (Table 1; Figure 6). Total annual landings for the fishery as a whole, and the subareas identified in Figure 5, and the percentage by the target scampi fishery, are presented in Table 1. Landings match the distribution of effort, with a clear shift out of subarea MO (the original QMA 3) and into MW (the western part of

the original QMA 4W) in the 2004–05 fishing year. The landings data also show patterns hidden within the effort maps, with landings from MN (the eastern part of QMA 4W) reducing between 2006–07 and 2009–10, but increasing again, and reducing in MW, from 2010–11. Over 97% of the targeted scampi catch has been reported from these main areas in any year, and over 99% over all years. Boxplots of the unstandardized CPUE (Figure 7) show reasonably similar patterns over time between areas, with catch rates initially increasing to the late 1990s or early 2000s, declining to about 2008, and then showing an increase in the most recent years (where data is available).

The breakdown of effort and catch by subarea and fishing year (Figure 8) show clear differences between the subareas. Subarea MN was previously managed within QMA 4W, and was only managed with competitive catch limits between 2001–02 and 2003–04. During this period, catches only took place in October, but prior to and since this time, fishing has been distributed throughout the year. Subarea MN was also previously managed within QMA 4W, and only had competitive catch limits between 2001–02 and 2003–04. Fishing was relatively sporadic prior to the competitive catch limit period, focussed in October during this period, and has been spread throughout the year since 2004–05 (with some indication of increased activity towards the end of the fishing year). Subarea MO was managed with competitive catch limits until 2004–05. Fishing was consistently focussed in October throughout this period, and there has been minimal activity in this subarea since 2004–05. The pattern of activity in relation to depth has remained relatively constant over time within subareas (Figure 9), but does vary between subareas, with catches from MN predominantly from the 300–400 m depth range, from MW from the 350–400 m depth range, and MO evenly spread between 350–500 m.

Table 1: Reported commercial landings (tonnes) from the 1986–87 to 2013–14 fishing years for SCI 3, catch estimated from scampi target fishery, and breakdown by spatial areas identified in Figure 5.

	Landings (MHR)	Target catch (TCEPR)	% SCI target	Catch			% of total			% of target catch in main areas
				MN	MO	MW	MN	MO	MW	
1991–92	153	160	105%	155	0	2	97%	0%	2%	98%
1992–93	296	298	101%	210	81	2	71%	27%	1%	98%
1993–94	324	312	96%	250	59	2	80%	19%	1%	100%
1994–95	292	293	100%	226	65	1	77%	22%	0%	100%
1995–96	306	304	99%	225	75	2	74%	25%	1%	100%
1996–97	304	307	101%	217	73	15	71%	24%	5%	100%
1997–98	296	299	101%	214	60	25	71%	20%	9%	100%
1998–99	292	274	94%	209	58	4	76%	21%	1%	99%
1999–00	322	293	91%	215	71	5	74%	24%	2%	100%
2000–01	333	313	94%	200	71	42	64%	23%	13%	100%
2001–02	304	278	92%	191	67	20	69%	24%	7%	100%
2002–03	264	225	85%	132	59	33	59%	26%	15%	100%
2003–04	277	236	85%	176	55	5	74%	23%	2%	100%
2004–05	335	312	93%	184	0	128	59%	0%	41%	100%
2005–06	319	291	91%	106	2	182	37%	1%	63%	100%
2006–07	307	278	90%	52	0	225	19%	0%	81%	100%
2007–08	209	176	84%	75	0	101	43%	0%	57%	100%
2008–09	190	170	89%	70	0	100	41%	0%	59%	100%
2009–10	302	278	92%	82	0	196	30%	0%	70%	100%
2010–11	256	236	92%	181	0	55	77%	0%	23%	100%
2011–12	278	257	92%	191	0	65	74%	0%	25%	100%
2012–13	267	240	90%	200	0	32	83%	0%	14%	97%
2013–14	319	301	94%	257	0	40	85%	0%	13%	99%

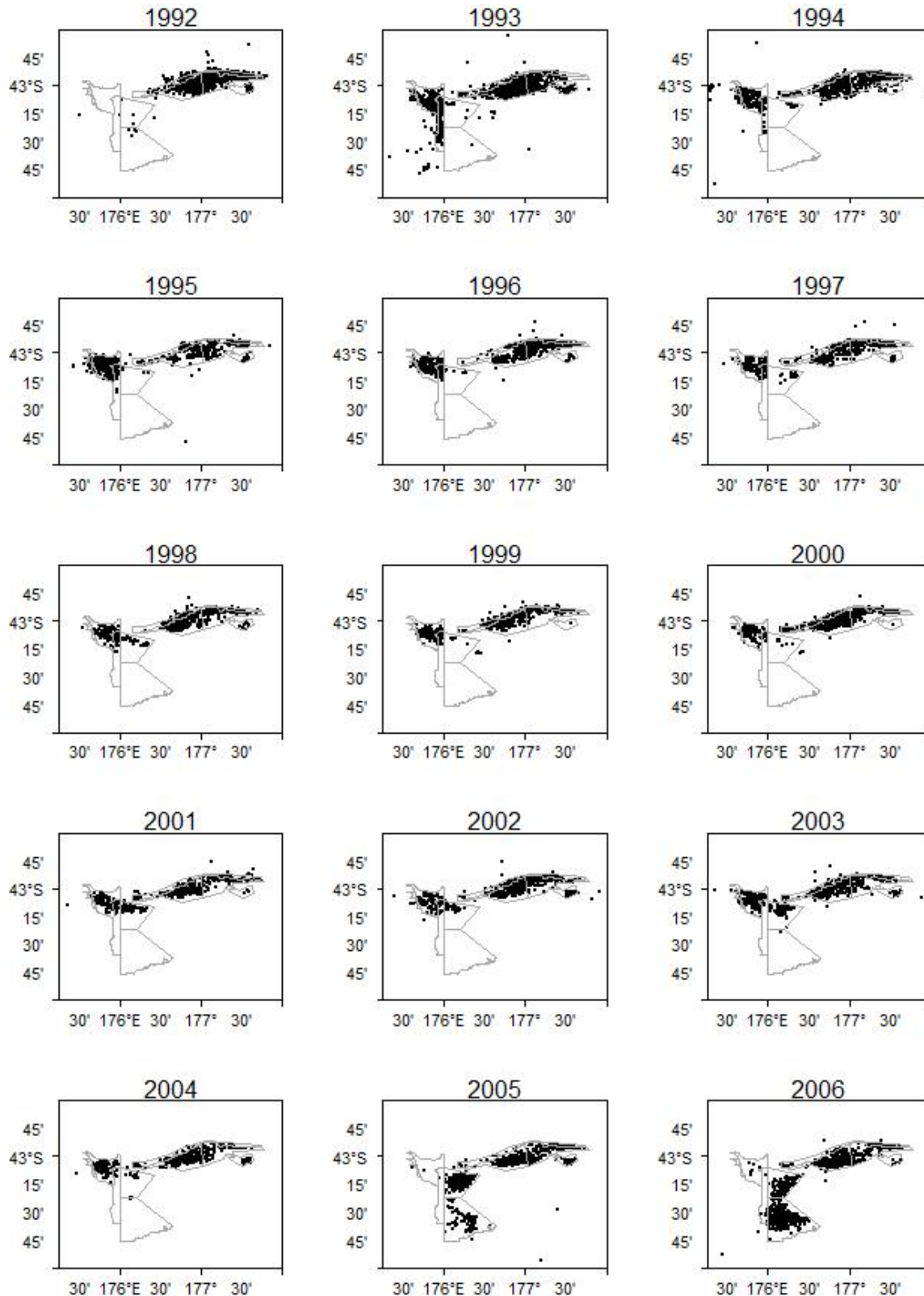


Figure 3: Spatial distribution of the main area of the SCI 3 scampi trawl fishery from 1991-92 to 2005-06. Each dot represents the mid point of one or more tows reported on TCEPR. Plots labelled by their final year, i.e., 1992 represents the 1991–92 fishing year. Grey lines represent extent of SCI 3 survey strata. General area covered by plots indicated within Figure 4.

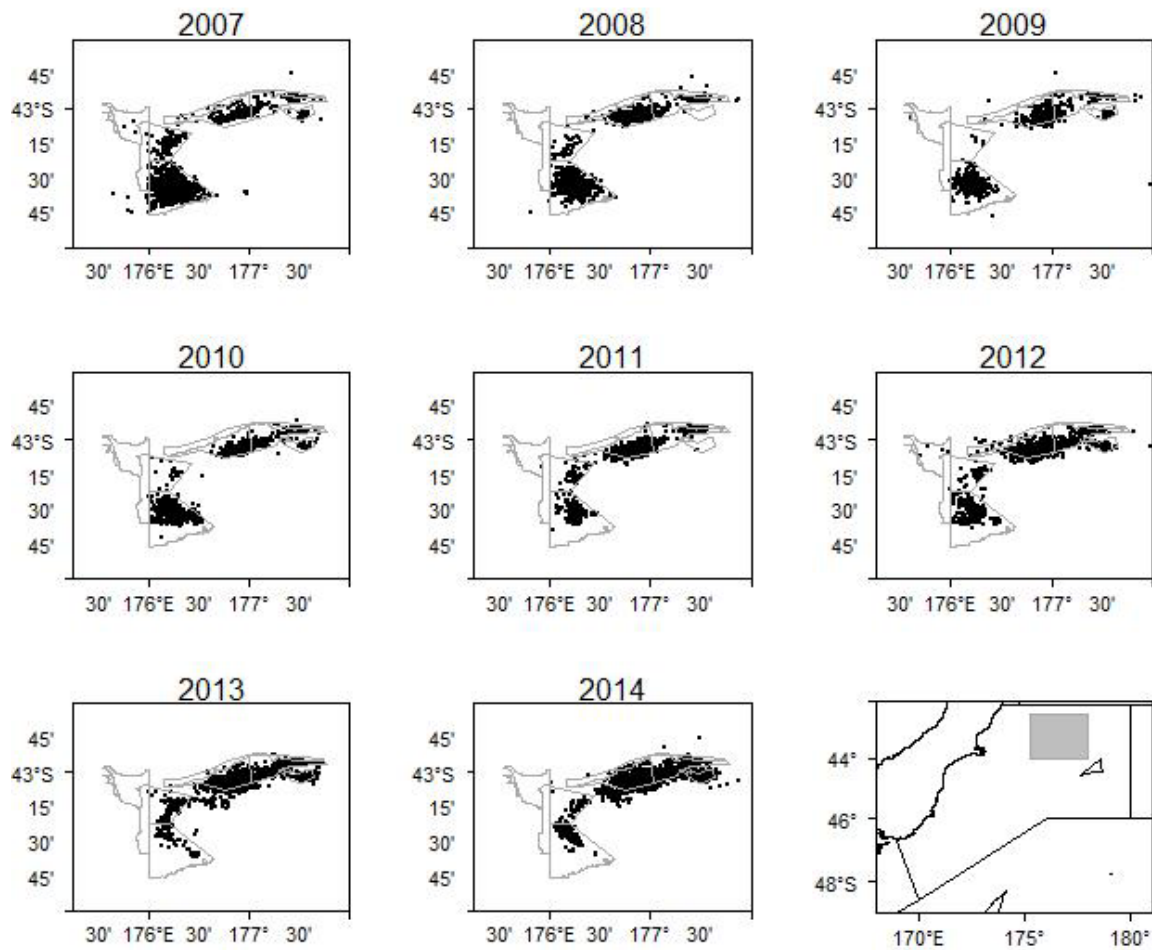


Figure 4: Spatial distribution of the main area of the SCI 3 scampi trawl fishery from 2006–07 to 2013–14. Each dot represents the mid point of one or more tows reported on TCEPR. Plots labelled by their final year, i.e., 2007 represents the 2006–07 fishing year. Grey lines represent the extent of SCI 3 survey strata. General area covered by plots indicated by shaded box in bottom right plot.

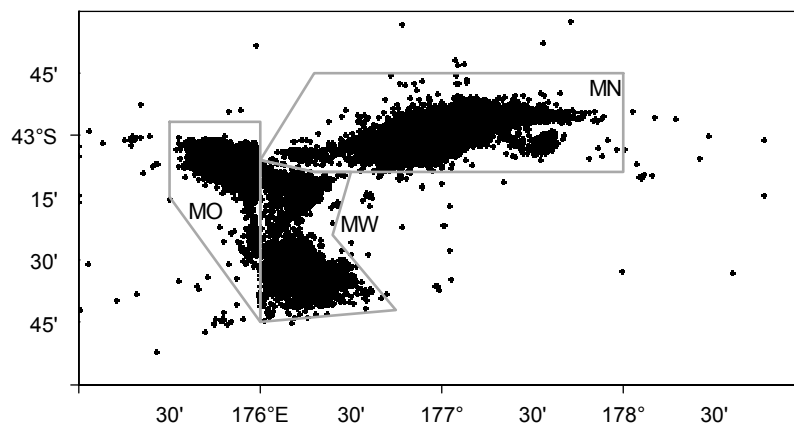


Figure 5: Sub-areas of SCI 3 used for fine scale analysis of catch and effort. Each dot represents the mid-point of one or more tows reported on a TCEPR.

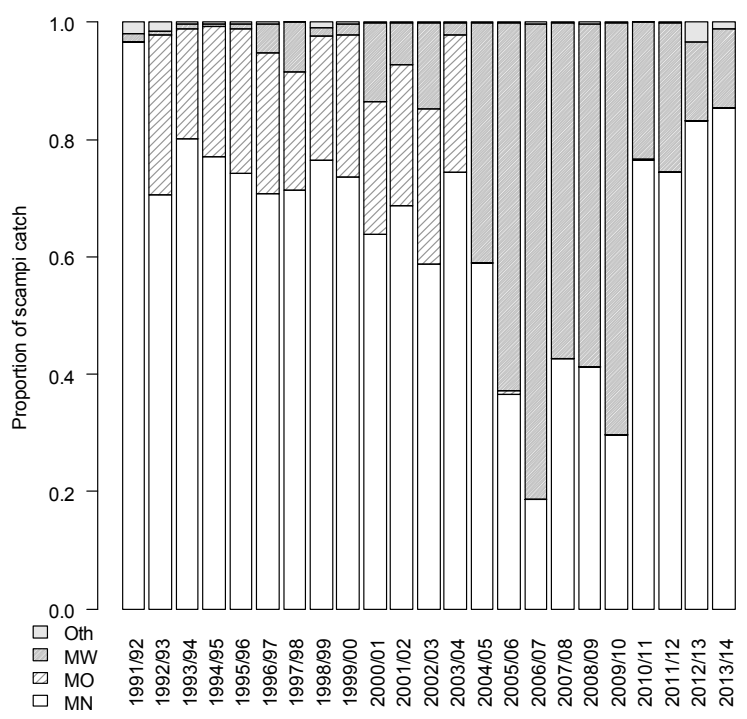
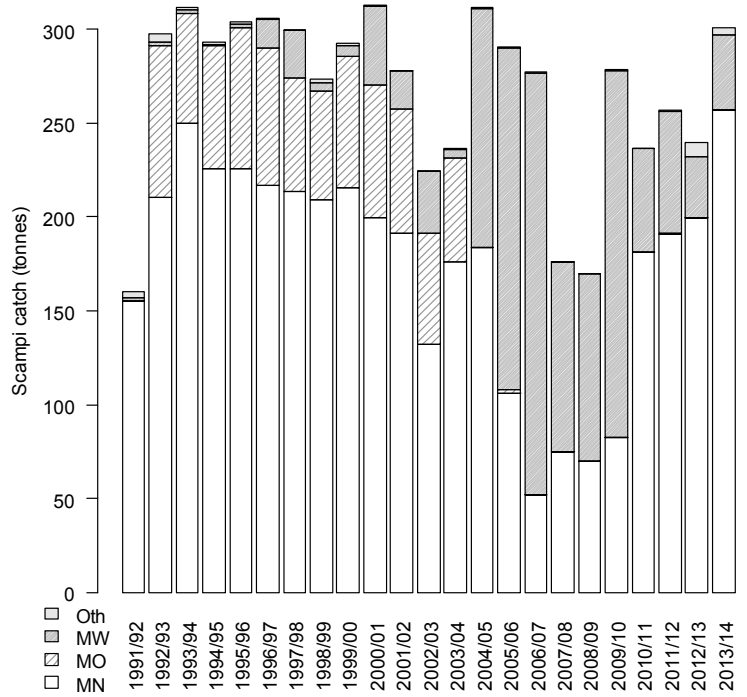


Figure 6: Barplots of scampi catch (upper plot) and catch proportion (lower plot) from SCI 3 by subarea and fishing year.

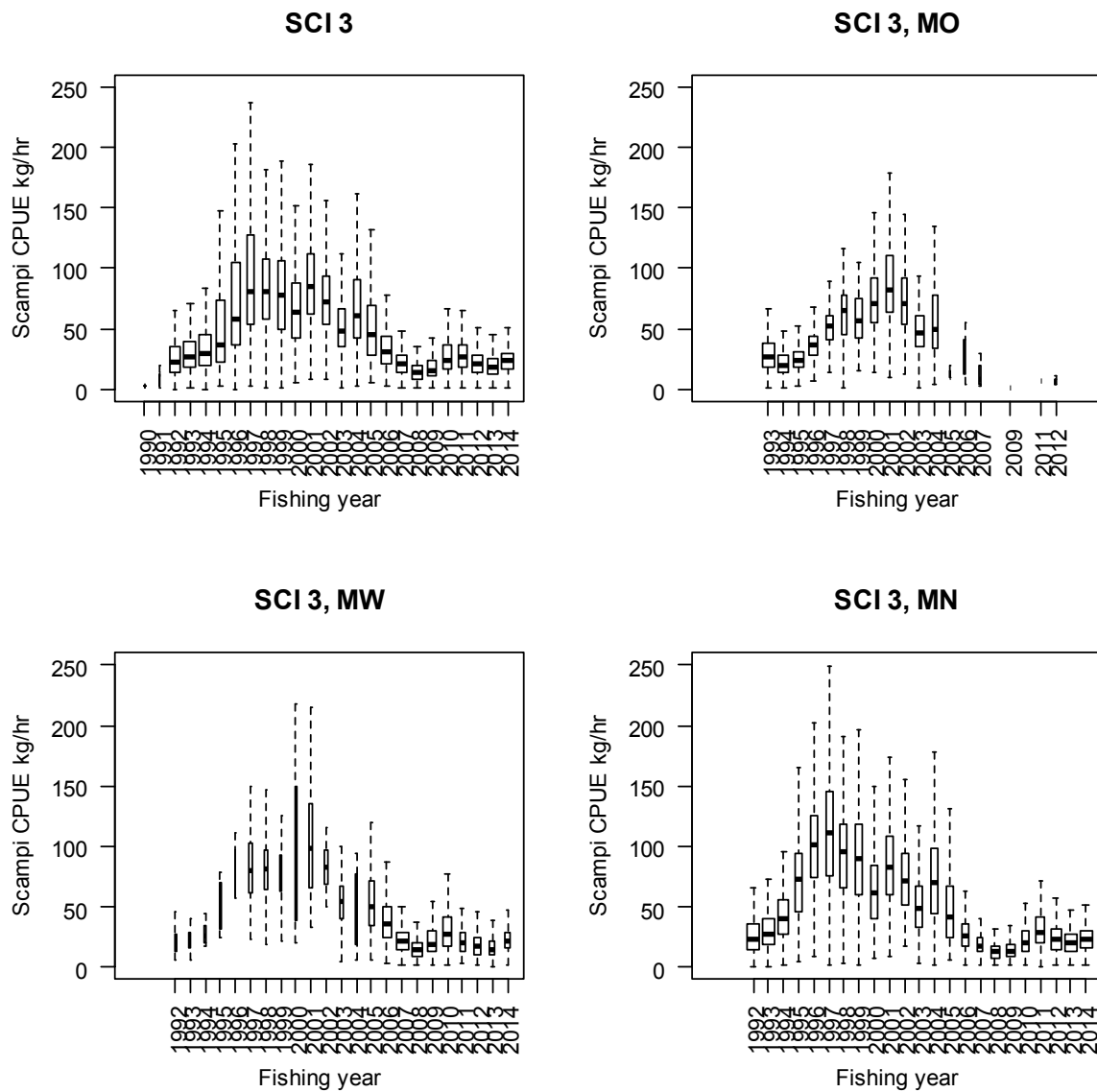


Figure 7: Boxplot (with outliers removed) of individual observations from TCEPR of unstandardized catch rate (catch (kg) divided by tow effort (hours)) with tows of zero scampi catch excluded, by fishing year for the SCI 3 fishery, and for the three subareas identified in Figure 5. Box width proportional to square root of number of observations. The solid line within each box represents the median value, the upper and lower ends of the box are the upper and lower quartiles, and the dashed lines extend out to the upper and lower adjacent values, the largest (smallest) value less (greater) than or equal to the upper (lower) quartile plus (minus) 1.5 times the interquartile range.

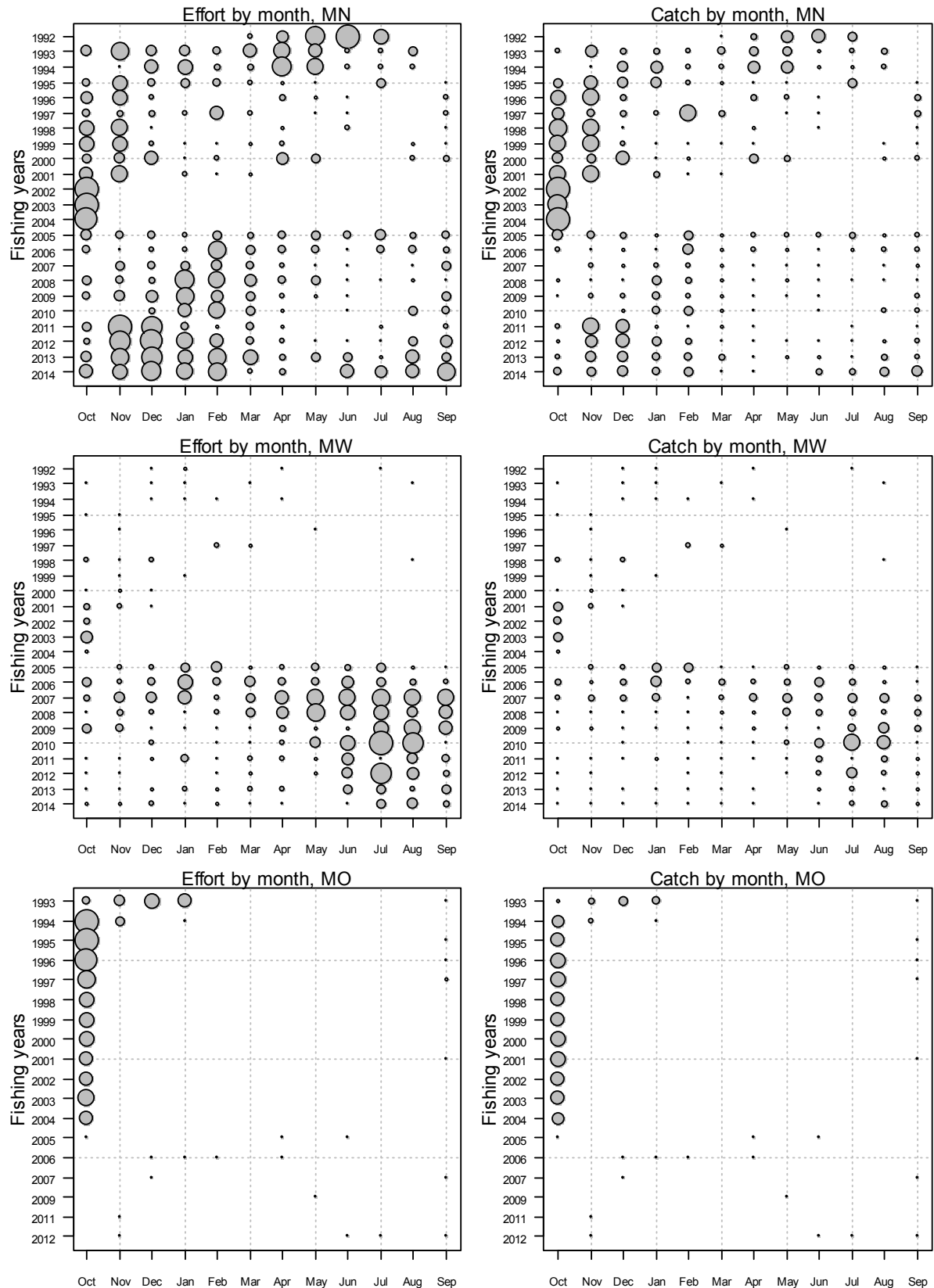


Figure 8: Monthly pattern of fishing effort (left column) and scampi catch (right column) in the scampi targeted fishery by fishing year and subarea of SCI 3. The area of the circles is proportional to the hours fishing (largest circle represents 2629 hours) and scampi catch (largest circle represents 191 tonnes), with consistent scales being used for each data type.

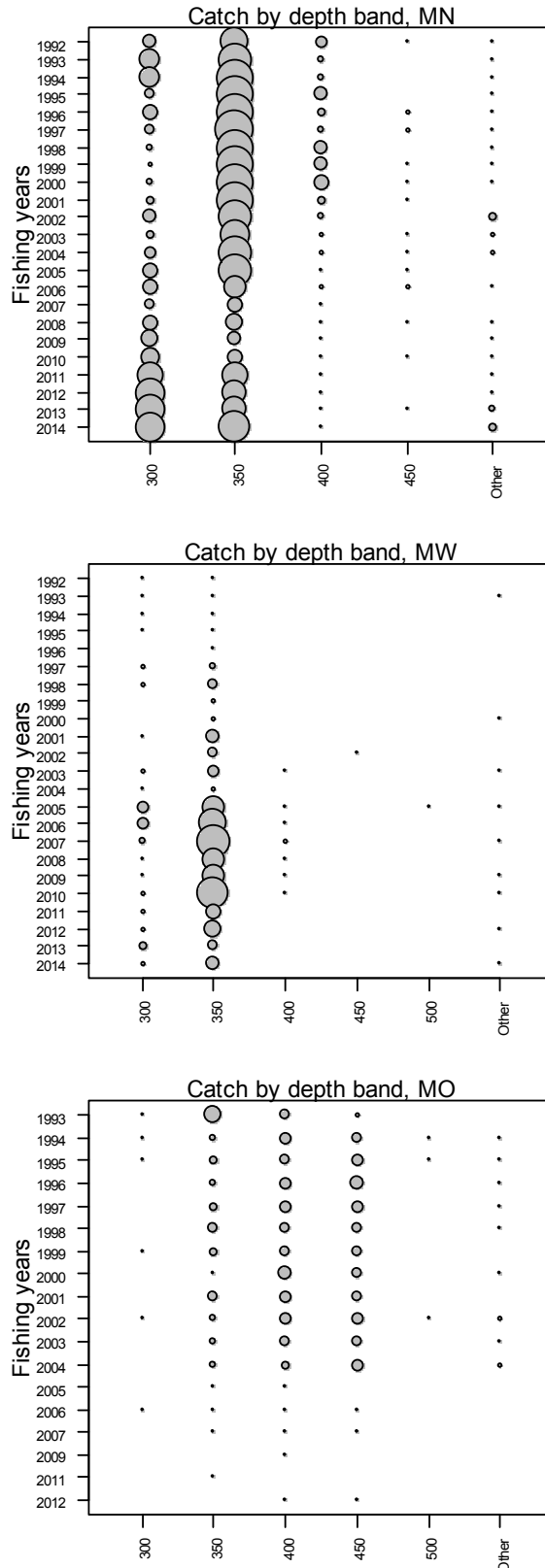


Figure 9: Annual pattern of scampi catch in the scampi targeted fishery by 50 m depth band and fishing year for each of the subareas of SCI 3. The area of the circles is proportional to the scampi catch (largest circle represents 111 tonnes), with a consistent scale being used for each plot. Depth bands represented by their lower bound, i.e., 300 represents 300–350 m band. “Other” represents catches outside the 300–500 m depth range.

2.2 Scampi stock structure

Stock structure of scampi in New Zealand waters is not well known. Preliminary electrophoretic analyses (Smith 1999) suggests that scampi in SCI 6A are genetically distinct from those in other areas, and there is substantial heterogeneity in samples from SCI 1, 2, and 4A. More recent work in South Africa on the similar species *Metanephrops mozambicus*, using mitochondrial DNA suggests that there is limited gene exchange between populations, even along the same coast (Zacarais 2013). The abbreviated larval phase of *Metanephrops* species may lead to low rates of gene mixing.

2.3 Seasonal patterns in scampi biology

Previous development of the length based model for scampi has shown that determination of appropriate time steps for the model is important in fitting to length and sex ratio data in particular (Tuck & Dunn 2006; 2009; 2012). Scampi inhabit burrows, and are not available to trawling when within a burrow. Catchability varies between the sexes on a seasonal basis in relation to moulting and reproductive behaviour, and leads to seasonal changes in the sex ratio of catches.

Current knowledge of the timing of scampi biological processes in SCI 3 are summarised in Table 2 (Tuck 2010). From patterns in the proportion of soft (post moult) animals (Figure 10), ovigerous females (Figure 11), and egg stage observed from commercial sampling (Figure 12), mature female moulting appears to be focussed around October and November, just after the hatching period (August – September). Hatching has been recorded at various times through the year, and appears to vary between stocks (Wear 1976; K. Heasman, Cawthron, pers. com.). Mating occurs after the females have moulted, while the shell is still soft, and new eggs are spawned onto the pleopods in December.

The combination of biological processes for males and females lead to different relative availabilities of the two sexes through the year, resulting in the pattern of sex ratio (displayed as proportion males) shown in Figure 13. Males are generally less abundant than females in catches between January and July (male catches being reduced during their moulting period), with males dominating from August to December.

On the basis of our understanding of the timing of biological processes for scampi in this area and the seasonal pattern in sex ratio, it was decided to shift the model year to 1st August to 31st July, slightly in advance of the New Zealand fishing year (1st October to 30th September). The previous assessment model for SCI 3 (Tuck 2013) had a model year aligned with the fishing year, and three time steps: 1; October to December (when males dominate in catches), 2; January to July (when females dominate), and 3; August to September (when males dominate in catches), with selectivity parameters shared for the steps 1 and 3. The revised approach adopted here combines the previous steps 3 and 1 into a single new step 1 (August to December), with the second time step (January to July) remaining the same. While the number of parameters remains the same (because in the previous model they were shared between steps 1 and 3), the reduction in the number of time steps reduces the run time of the model.

Table 2: Summary of scampi biological processes for SCI 3. Source; Tuck (2010) and more recent survey data.

	Jan	Feb	Mar	Apr	May	Jun	Jul	Aug	Sep	Oct	Nov	Dec
Male moult		X	?	X								
Female moult										X	X	
Mating										X	X	
Eggs spawn											X	X
Eggs hatch								X	X			

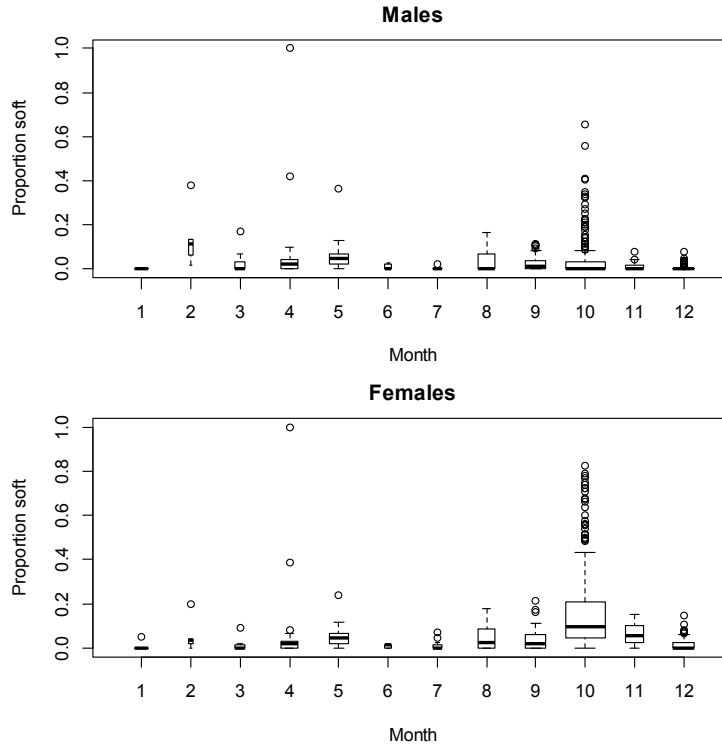


Figure 10: Boxplots of proportions of soft animals (post moult) by sex and month, as recorded by observer sampling in SCI 3. Box widths proportional to square root of number of observations for that month. The solid line within each box represents the median value, the upper and lower ends of the box are the upper and lower quartiles, and the dashed lines extend out to the upper and lower adjacent values, the largest (smallest) value less (greater) than or equal to the upper (lower) quartile plus (minus) 1.5 times the interquartile range. Outliers (values beyond the adjacent values) are shown as open circles.

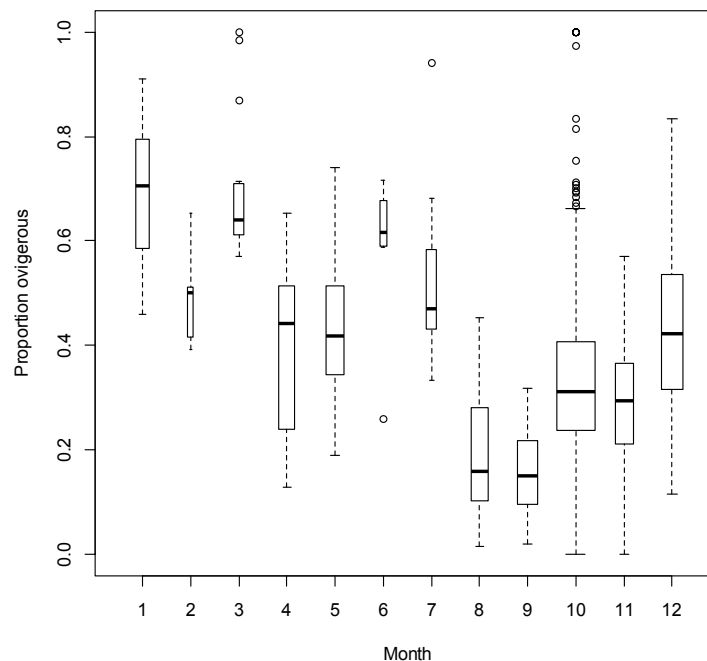


Figure 11: Boxplots of proportions of ovigerous females by month, as recorded by observer sampling in SCI 3. Box widths proportional to square root of number of observations for that month. The solid line within each box represents the median value, the upper and lower ends of the box are the upper and lower quartiles, and the dashed lines extend out to the upper and lower adjacent values, the largest (smallest) value less (greater) than or equal to the upper (lower) quartile plus (minus) 1.5 times the interquartile range. Outliers (values beyond the adjacent values) are shown as open circles.

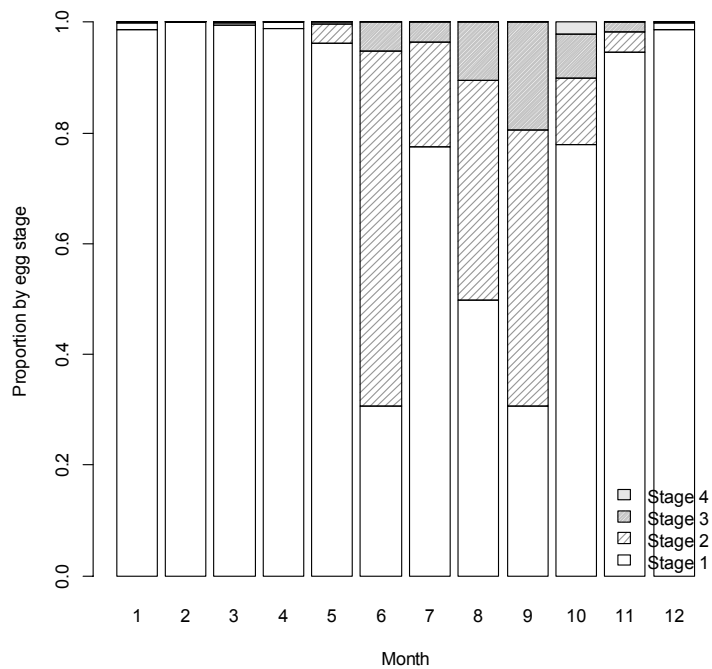


Figure 12: Barplots of the proportion of ovigerous females by egg stage and month, from observer sampling in SCI 3.

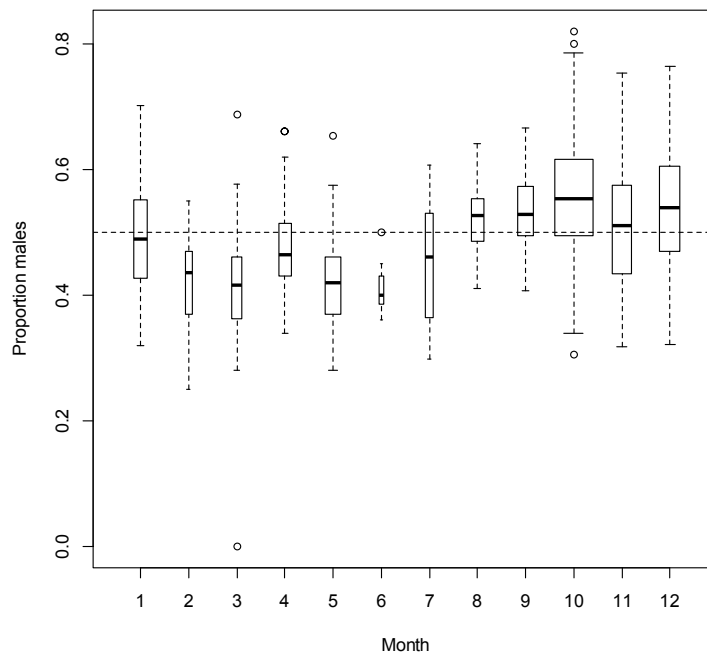


Figure 13: Boxplots of proportion of males in catches by month from observer sampling in SCI 3. Box widths are proportional to square root of number of observations. The solid line within each box represents the median value, the upper and lower ends of the box are the upper and lower quartiles, and the dashed lines extend out to the upper and lower adjacent values, the largest (smallest) value less (greater) than or equal to the upper (lower) quartile plus (minus) 1.5 times the interquartile range. Outliers (values beyond the adjacent values) are shown as open circles.

2.4 Standardised CPUE indices

2.4.1 Core vessels and time periods

A plot of vessel activity (number of scampi targeted tows recorded) over time is presented for the core area of SCI 3 (300–500 m depth, subareas MN, MW and MO) (Figure 14) and shows that 26 vessels have been active in the area over the history of the fishery. Ten vessels were active through most of the first decade of the fishery, some stopped while others started during the 2002–03 and 2003–04 years, and six vessels have been consistently active since 2004–05, with other vessels also active in some years.

Figure 15 (upper plot) shows the proportion of the total catch (over the history of the fishery) in relation to the number of years the vessels contributing that catch have been active in the fishery, and on the basis of this, a cut-off of a minimum of 10 years of activity has been selected to identify eleven core vessels. Over the full history of the fishery, these vessels contribute over 88% of the scampi catches by scampi targeted fishing. The lower plot of Figure 15 shows the proportion of catch accounted for in each year by vessels active for 10 or more years. Similar analyses in previous characterisations (e.g., Tuck 2014) have also examined a 5 year vessel activity cut-off, but for SCI 3, this results in the same vessels being selected. Other than the 1992–93 and 2002–03 to 2003–04 periods, the core vessels (active for over 10 years) have accounted for over 80% of targeted scampi catches in each year, and often well over 90%.

Vessels E, H, J and P have been consistently active through the history of the fishery (Figure 16), while vessels D, I and L were consistently active up until 2003–04, but have then been far more intermittent in the area. Vessels F and G were consistently active from the start of the fishery until 2008–09. Vessel O has been active in the area since 1996–97, and vessel X has been active since 2002–03.

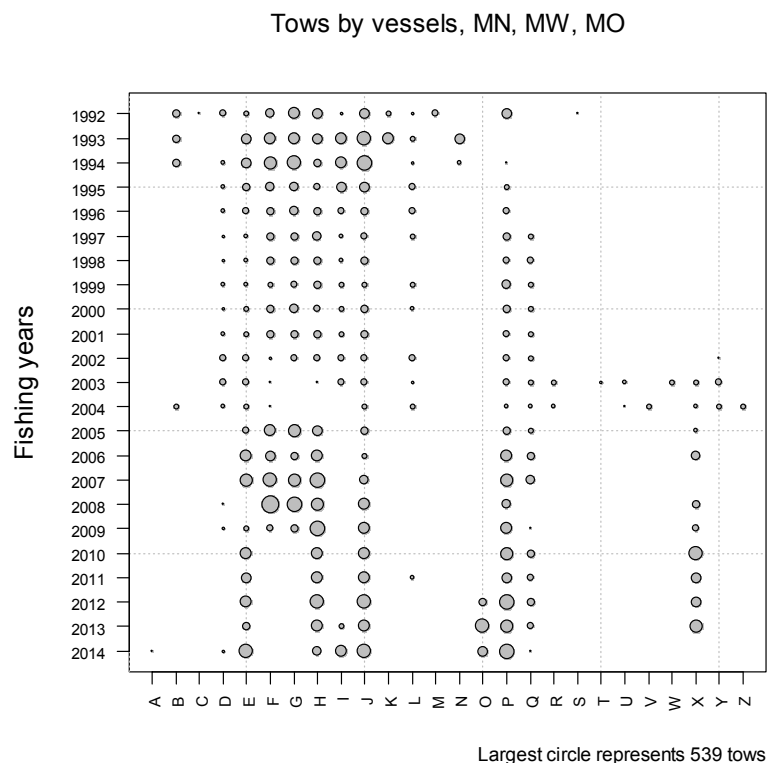


Figure 14: Pattern of fishing activity by vessel and fishing year for SCI 3. The area of the circles is proportional to the number of tows recorded.

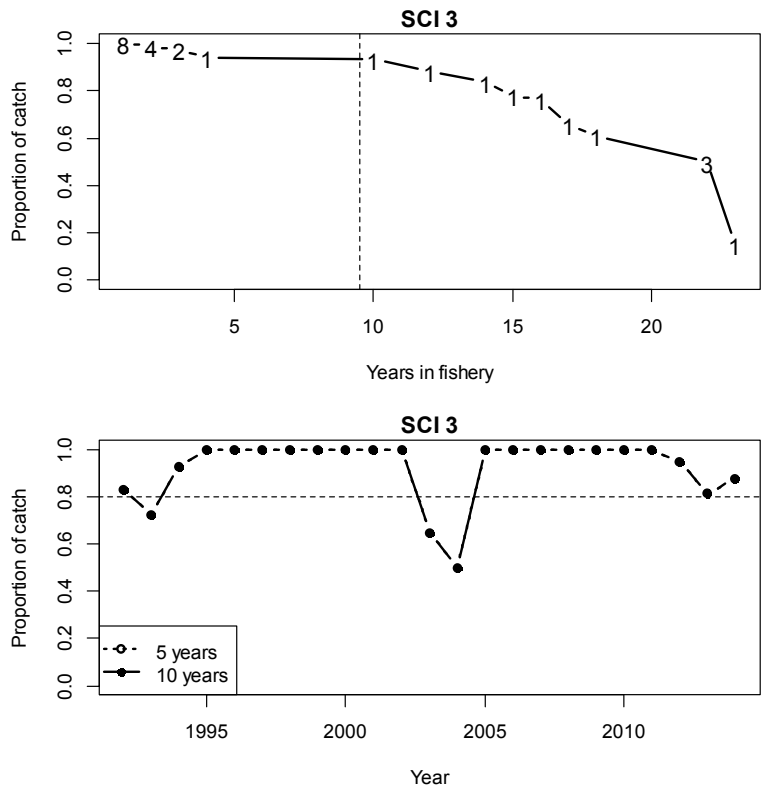


Figure 15: Catch breakdown by vessel. Upper plot - Proportion of total scampi catch (all years) plotted against the number of years the vessels reporting that catch have been active in the fishery. Numbers indicate number of vessels active for that duration. Vertical dotted line represents cut off for core vessels. Lower plot – Proportion of annual catch reported by vessels active in the fishery for 5 and 10 years.

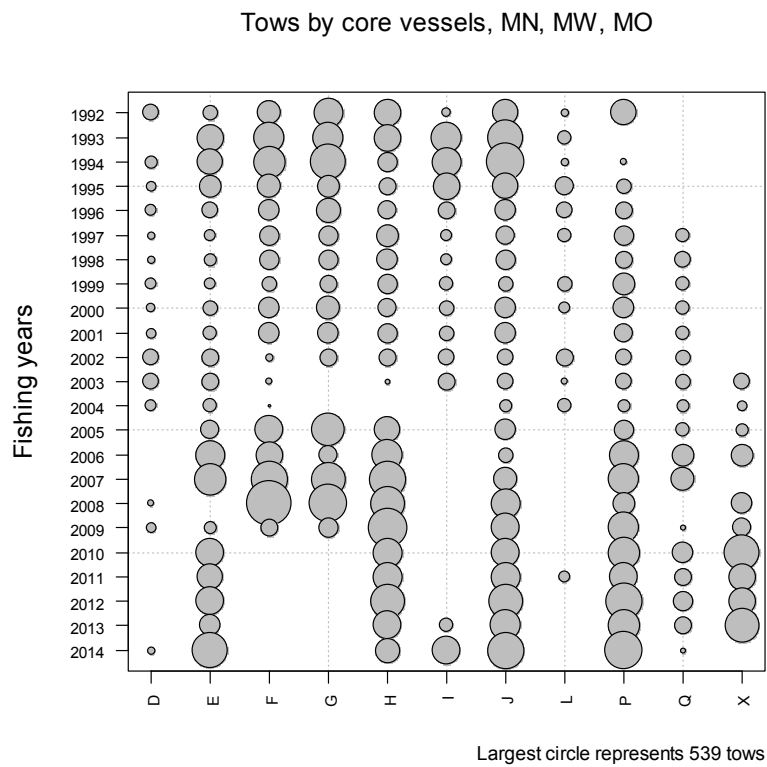


Figure 16: Core vessel pattern of fishing activity by vessel and fishing year for SCI 3. The area of the circles is proportional to the number of tows recorded.

As described above, the patterns of fishing activity have changed considerably over the history of the fishery. Therefore, the amount of data (number of commercial tows) contributing to the indices varies considerably between areas and time steps over time. While each index value (for an area, year and time step) has a CV estimated, index values from low numbers of tows are unlikely to be representative of the overall subarea and time step, and it may be appropriate to exclude some points from the indices. Having selected the core vessels, the numbers of tows available were examined by subarea, fishing year and time step (Figure 17), and an arbitrary cut-off level of fewer than 5 tows was selected. Subarea MN has been relatively well sampled by the core vessels, while subarea MO was only well sampled in time step 1, between 1993 and 2004. Subarea MW was not well sampled in the early years of the fishery, but has data for most years for time step 1 since the late 1990s, and since 2005 for time step 2. The approach of excluding poorly sampled periods and areas from the calculation of standardised indices has been used previously for this fishery (Tuck 2013), and while it is acknowledged that it potentially introduces some bias, in that low numbers of tows are more likely in areas or times of low catch rate, it seems unlikely that such low numbers of tows would provide a reliable index.

Having excluded poorly sampled subarea / year / time step combinations (45 fishing events, spread across 22 subarea / year / time step combinations), the core vessels were rechecked to confirm that they still met the requirements of contributing data for at least 10 years, which they did.

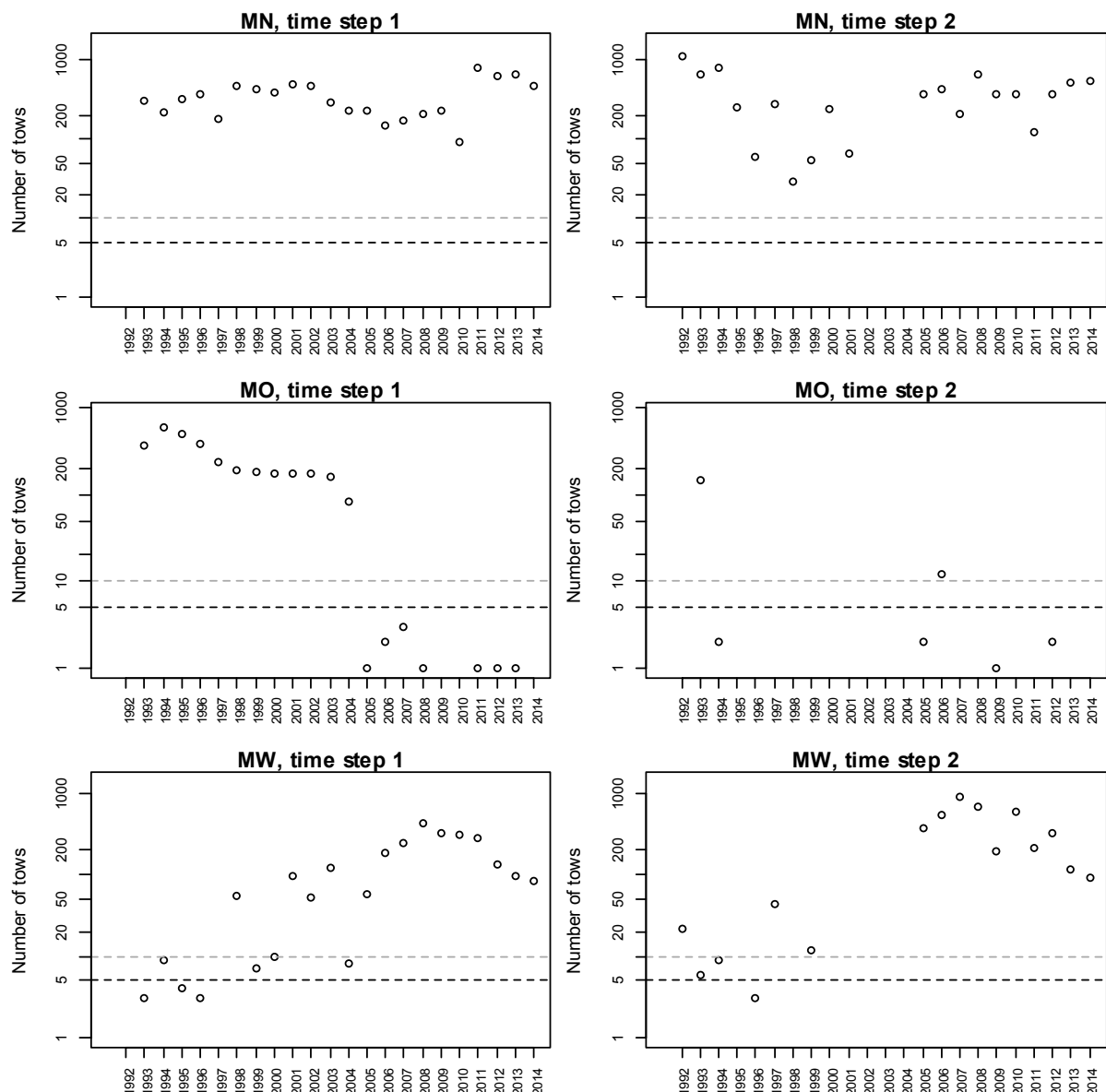


Figure 17: Numbers of commercial tows available within the core vessel dataset by time step and fishing year for each subarea. Dashed lines represent arbitrary cut offs at 5 and 10 tows.

2.4.2 Calculation of indices

Standard indices were calculated from the data recorded by the eleven core vessels (25 731 fishing event records). Within the previous preliminary assessment of SCI 3, a three stock model was developed, with separate abundance indices fitted for each time step in each subarea (Tuck 2013), but more recently the SFAWG has suggested a general simplification of the scampi assessment model structure. Therefore, an initial model was examined allowing for the potential of model year \times subarea \times time step interactions. Scampi catch of core vessels was modelled using a year index (forced), model time step, subarea, vessel, time of day, state of moon, depth, fishing duration and trawl gear parameters.

The time of day of each tow was calculated in relation to nautical dawn and dusk (time when the sun is 12 degrees below the horizon in the morning and evening), as calculated by the *crepuscule* function of the *maptools* package in R. Individual tows were characterised on the basis of whether they included dawn (shot before dawn, hauled after dawn and before dusk), day (shot after dawn, hauled before dusk), dusk (shot before dusk, hauled after dusk and before dawn) or night (shot after dusk and

hailed before dawn). Longer tows including more than one period (i.e. shot before dusk and hauled after dawn) were excluded from this part of the analysis (excluding 55 records).

Individual hauls were also categorised in terms of moon state, on the assumption that tidal current strength at the sea floor will be related to the lunar cycle. Tows were categorised by their date in relation to the lunar cycle, as Full moon (more than 26 days since full moon, or less than 3 days since full moon), Waning (4 – 11 days since full moon), New moon (12 – 18 days since full moon), and Waxing (19 – 26 days since full moon).

Within the core vessels identified, three have changed gear configuration (twin rig to triple rig), and two have changed engine power over the history of the fishery. Engine power was fitted within the model as a third order polynomial, and gear configuration as a two level factor (twin or triple rig). Gear configuration for a particular vessel and date was determined on the basis of information provided by the fishing industry as to when vessels changed from twin to triple, and all tows after this date are defined as triple rig. It is acknowledged that vessels may change configuration within a trip depending on gear damage or fishing conditions, but it is unclear how reliably this has been recorded on TCEPR forms in the past (as effort width). Preliminary examination of the data for the core vessels suggested the values recorded were generally realistic, and following some minor grooming, “effort width” was also included as a term (third order polynomial) as a term in the model.

In addition, examination of the data for SCI 3 (Tuck 2013) identified a distinct shift in trawl duration between 2002–03 and 2006–07 (from about 5 hours to 7 hours). This shift (in SCI 3) was fleet-wide, and associated with a modification to the top of the trawl to reduce the bycatch (John Finlayson, Sanford Ltd. *pers comm.*), enabling vessels to fish for longer on each tow. Boxplots of tow duration over time have been examined for each of the core vessels identified for SCI 3 (Figure 18), and show a relatively rapid shift in trawl duration around the mid 2000s, from roughly 5 to 7 hours. For each vessel, the timing of the gear modification was estimated from examination of tow durations in SCI 3, and fitted as a two level factor in the model.

Catch indices were derived using generalised linear modelling (GLM) procedures (Vignaux 1994; Francis 1999), using the statistical software package R. The response variable in the GLM was the natural logarithm of scampi catch. The fishing-year (combined with any time step or depth strata for the index) was entered as a categorical covariate (explanatory) term on the right-hand side of the model. Standardised CPUE abundance indices (canonical) were derived from the exponential of the fishing-year covariate terms as described in Francis (1999).

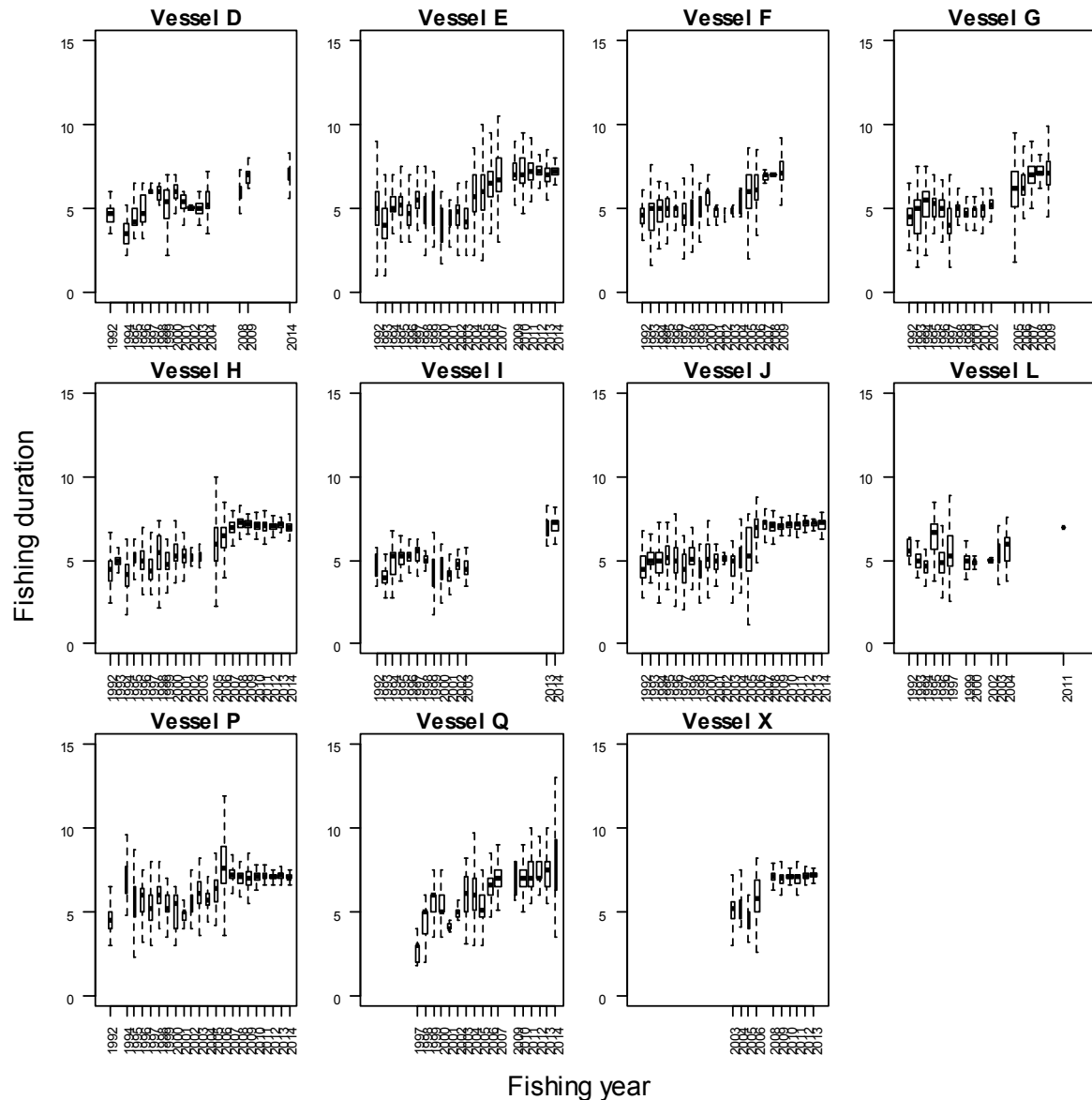


Figure 18: Boxplots of tow duration (hours) for scampi targeted fishing in SCI 3 for the eleven core vessels identified. Box widths proportional to square root of number of observations. The solid line within each box represents the median value, the upper and lower ends of the box are the upper and lower quartiles, and the dashed lines extend out to the upper and lower adjacent values, the largest (smallest) value less (greater) than or equal to the upper (lower) quartile plus (minus) 1.5 times the interquartile range.

In order to accommodate a non-linear relationship with the response variable (log catch), the continuous variables (effort, engine power, gear width) were “offered” to the GLMs as third order polynomials. Vessel, depth (binned into the 50 m bands), time of day, state of tide, twin or triple rig, and bycatch modification were “offered” to the GLM’s as factors. Some effects (e.g., gear width) were represented by more than one term, and the model was allowed to select which (if any) were retained. A forward fitting, stepwise, multiple-regression algorithm was used to fit GLMs to groomed catch, effort and characterisation data. The stepwise algorithm generates a final regression model iteratively and uses a simple model with a single predictor variable, fishing year, as the initial or base model. The reduction in residual deviance relative to the null deviance is calculated for each additional term added to the base model. The term that results in the greatest reduction in residual

deviance is added to the base model if this results in an improvement in residual deviance of more than 1%. The algorithm repeats this process, updating the model, until no new terms can be added.

Preliminary investigations into different error distributions using a simple standardisation model

$$\text{Log}(\text{catch}) \sim \text{fishing_year}$$

(comparing log normal, gamma and weibull) identified that the gamma distribution provided a slight improvement in the distribution of residuals, and this error distribution was used for calculation of the indices reported below. Diagnostic plots for the three compared error distributions, and for the final standardisation model, are presented in Appendix 1.

2.4.3 Final CPUE index

Stepwise regression analysis of the dataset with the full model to estimate the CPUE indices for SCI 3 resulted in an initial model with model year, fishing duration, time of day (TOD), vessel, subarea, and a second order interaction between model year and subarea retained (Table 3). The model explained 55% of the variation in the data. Depth and time step were not retained within the model, either as separate terms, or as part of an interaction, suggesting that they do not contribute much to explaining the deviance in the model.

Table 3: Analysis of deviance table for initial standardisation model selected by stepwise regression for SCI 3.

	Df	Deviance explained	Additional deviance explained (%)
NULL			
model_year	22	7853.2	38.18
TOD	3	7263	4.65
subarea	2	6691.9	4.50
vessel	10	6368.9	2.54
poly(fishing_duration, 3)	3	6105.7	2.07
model_year:subarea	32	5619.8	3.83

A second model was examined combining model_year and subarea into a single term, which explained 55% of the variation in the data, and also retained time of day, vessel and fishing duration (Table 4). Predicted CPUE (for vessel H with a 7 hour fishing duration) from the model matched the pattern observed in the unstandardized data for each of the subareas (Figure 19), and the WG agreed to use this standardised CPUE analysis for the abundance index.

Table 4: Analysis of deviance table for final standardisation model selected by stepwise regression for SCI 3.

	Df	Deviance explained	Additional deviance explained (%)	Overall influence (%)*
NULL				
model_year_subarea	56	5944.1	46.79	
TOD	3	593.4	4.67	3.36
vessel	10	308.5	2.43	3.21
poly(fishing_duration, 3)	3	237.1	1.87	8.56

*- Overall influence as in table 1 of Bentley et al. (2012)

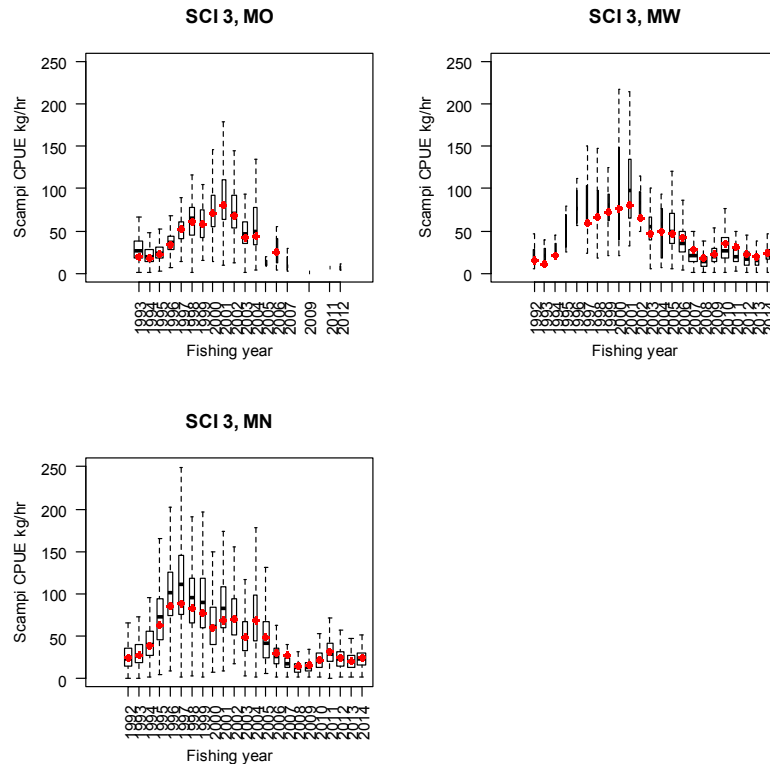


Figure 19: Annual standardised CPUE by area predicted (for vessel H for a 7 hour tow) from the final model (red dots), and boxplots of unstandardized CPUE. Box widths proportional to square root of number of observations. The solid line within each box represents the median value, the upper and lower ends of the box are the upper and lower quartiles, and the dashed lines extend out to the upper and lower adjacent values, the largest (smallest) value less (greater) than or equal to the upper (lower) quartile plus (minus) 1.5 times the interquartile range.

3. MODEL STRUCTURE

3.1 Seasonal and spatial structure, and the model partition

The model partitions scampi by area (MN, MO, and MW), stock (one stock per area), sex, and length class. The model assumes that the three subareas are completely separate and that there is no movement, either by adults or recruitment, between them. No recaptures have been made from the tagged scampi released in SCI 3, but recaptures from other New Zealand stocks suggest very limited movement (Cryer & Stotter 1999; Tuck et al. 2009), and this is supported by acoustic tracking of both the European scampi *Nephrops norvegicus* (albeit in shallower waters) and *Metanephrops challengeri* (Chapman et al. 1974; Tuck et al. 2015b). Larval development of scampi appears to be partially abbreviated (compared to similar shallow water species), in that there only appears to be one larval stage, with a duration of three to four days (Wear 1976). The postlarvae appear to be benthic orientated (Wear 1976), and it has therefore been assumed that there is little potential for larval exchange between the subareas. Genetic studies on *Metanephrops mozambicus* support this (Zacarias 2013). By assessing the three areas within the same model, catches, survey indices and length distributions can be specific to each area, but other parameters (growth, natural mortality, selectivity, catchability) can be shared.

Growth between length classes is determined by sex-specific, length-based growth parameters. Individuals enter the partition by recruitment and are removed by natural mortality and fishing mortality. The model's annual cycle is based on the fishing year and is divided into the two time-steps described above (on basis of Table 2). The choice of two time steps was based on the current

understanding of scampi biology and sex ratio in catches. Note that model references to “year” within this report refer to the modelled year, and are labelled as the most recent calendar year, e.g. the fishing year 1998–99 is referred to as “1999” throughout. As described above, the modelled year (August to July) runs slightly in advance of the fishing year. Previous models for SCI 3 included spatial structure (Tuck 2013), and given the distinct changes in exploitation patterns in the area, the Working Group considered that this should be maintained, but the temporal structure of the model has been simplified.

The model uses capped logistic length based selectivity curves for commercial fishing and research trawl surveys, but allowed to vary with sex and time step. While the sex ratio data suggest that the relative catchability of the sexes varies through the year (hence the model time structure adopted), there is no reason to suggest that assuming equal availability, selectivity at size would be different between the sexes. Therefore the two sex selectivity implementation developed within CASAL for previous scampi assessments (Tuck & Dunn 2012) was applied. This allows the L_{50} (size at which 50% of individuals are retained) and a_{95} (size at which 95% of individuals are retained) selectivity parameters to be estimated as single values shared by both sexes in a particular time step, but allows for different availability between the sexes through estimation of different a_{\max} (maximum level of selectivity) values for each sex. The burrow based photographic survey abundance indices are not sex specific, and a standard logistic length based selectivity curve is applied.

3.2 Biological inputs

3.2.1 Growth

Recent scampi assessments have estimated growth within the model from tag recapture data (Tuck & Dunn 2012; Tuck 2015). Although surveys in 2009 and 2010 released over 5000 tagged scampi, returns have been very low, and there are insufficient data to estimate growth.

As an alternative, the previous SCI 3 model used a simple (one area) model to estimate growth, and then fixed this in more complex models, also examining sensitivity to faster and slower growth (Tuck 2013). The Working Group suggested that growth could potentially be estimated within the model without tagging data, and preliminary investigations suggested that this was feasible, so this approach was adopted.

3.2.2 Maturity

Female maturity can be estimated from gonad staging or the presence of eggs on the pleopods. Gonad stages are recorded from research survey catches (although only on scampi not tagged and released), while the presence and development stage of eggs on pleopods are recorded from research survey and observer sampling. No data are available for the maturity of male scampi, so their maturity ogive was assumed to be identical to that of females, although studies on *N. norvegicus* have suggested that male maturity may occur at a larger size (although possibly the same age) than females (Tuck et al. 2000). Maturity is not considered to be a part of the model partition, but proportion ovigerous at length was fitted within the model based on a logistic ogive with a binomial likelihood (Bull et al. 2008). Analysis of the proportion mature data was modelled as a function of length within a GLM framework, with a quasi distribution of errors and a logit link (McCullagh & Nelder 1989),

$$P_{\text{mature}} = a + b * \text{Length}$$

which equates to the logistic model. The model was weighted by the number measured at each length. After obtaining estimates for the parameters a and b , the length at which 50% are mature (L_{50}) was calculated from:

$$L_{50} = -\frac{a}{b}$$

with selection range (SR) calculated from:

$$SR = \frac{(2 \cdot \ln(3))}{b}$$

The L_{50} estimate for the SCI 3 data was 43.2 mm, with a selection range a_{10} to a_{90} of 6.5 mm (Figure 20).

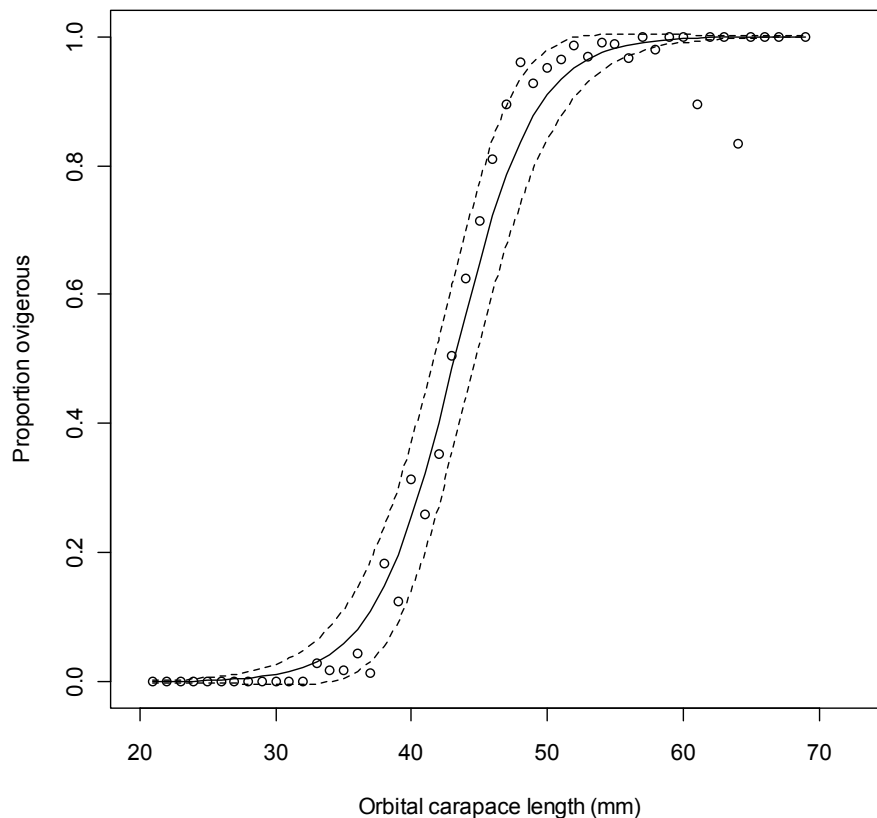


Figure 20: Proportions of female scampi carrying eggs (ovigerous) at length, from sampling in January to March period, just after spawning period. Solid line represents logistic curve fitted to the data (L_{50} 43.2 mm and selection range 6.5 mm). Dashed line represents plus or minus one Standard Error.

3.2.3 Natural mortality

The instantaneous rate of natural mortality, M , has not been estimated directly for any scampi species, but estimates have been made (0.2 – 0.25) based on the estimate of the K parameter from a von Bertalanffy growth curve (Cryer & Stotter 1999) using a correlative method (Pauly 1980; Charnov et al. 1983). Morizur (1982) used length distributions from ‘quasi-unexploited’ *Nephrops* stocks to obtain estimates for annual M of 0.2–0.3. The values most commonly assumed for assessment of *Nephrops* stocks in the Atlantic is 0.3 for males and immature females, and 0.2 for mature females (assumed less vulnerable to predation during the ovigerous period) (Bell et al. 2006). For New Zealand scampi, M has previously been fixed at 0.2 (Tuck & Dunn 2012), or both 0.2 and 0.3 (Tuck 2014). Within the current assessment, preliminary investigation suggested that attempting to estimate M within the model would not be useful, and so M was fixed at 0.25, with sensitivities runs examined with M at 0.15 and 0.35.

3.3 Catch data

Data for the model were collated over the spatial and temporal strata as defined in the model structure. Catches in these three sub-areas represent over 98% of scampi catches from SCI 3, and are presented in Table 5.

Table 5: Estimated landed catch (t) from SCI 3, by sub-area and time-step.

Fishing year	MN_1	MN_2	MW_1	MW_2	MO_1	MO_2
1991	0.00	0.00	0.00	0.00	0.00	0.00
1992	0.00	154.83	0.00	0.00	0.35	2.11
1993	77.85	114.81	54.91	25.65	1.15	0.35
1994	65.73	191.78	58.38	0.49	1.13	1.32
1995	141.21	92.77	65.14	0.00	1.00	0.00
1996	190.99	23.41	75.16	0.00	1.00	1.37
1997	102.75	114.09	71.52	0.00	0.00	15.11
1998	220.65	5.70	62.09	0.00	23.41	0.00
1999	196.59	9.34	57.90	0.00	2.48	3.67
2000	145.83	60.35	70.50	0.00	5.44	0.00
2001	194.18	18.88	70.50	0.00	41.89	0.00
2002	191.17	0.00	66.91	0.00	20.03	0.00
2003	132.01	0.00	59.43	0.00	32.96	0.00
2004	176.00	0.00	55.40	0.00	4.86	0.00
2005	83.60	84.67	0.09	0.09	20.95	99.00
2006	31.24	72.50	0.17	1.96	45.73	135.10
2007	35.63	27.02	0.23	0.00	51.57	137.10
2008	19.68	61.24	0.01	0.00	50.37	68.13
2009	23.65	39.56	0.00	0.01	38.98	31.84
2010	13.44	58.87	0.00	0.00	58.35	132.54
2011	178.47	18.94	0.05	0.00	63.97	30.19
2012	121.72	51.99	0.04	0.07	22.26	48.79
2013	114.20	75.66	0.02	0.00	17.29	22.18
2014	124.67	90.90	0.00	0.00	14.45	14.83

3.4 CPUE indices

The annual CPUE indices estimated within the standardisation (Figure 19) were fitted within the model as abundance indices. There has been considerable discussion on whether CPUE is proportional to abundance for scampi (Tuck 2009), with rapid increases in both CPUE and trawl survey catch rates for a number of stocks in the early to mid 1990s (and changes in sex ratio in trawl survey catches) initially being considered related to changes in catchability. Later analysis (Tuck & Dunn 2009) suggested that the observed changes in sex ratio were related to slight changes in the survey timing in relation to the moult cycle. Similar patterns in CPUE are observed over the same period for rock lobster (Starr 2009; Starr et al. 2009), and scampi in SCI 3 (Tuck 2013), which may suggest broad scale environmental drivers influencing crustacean recruitment. The CPUE patterns for SCI 1 are mirrored by trawl survey catch rates, suggesting that they do not reflect fisher learning. While not considered appropriate for use as an index in the model (Tuck 2013), a scampi abundance index generated from the middle depths (*RV Tangaroa*) trawl survey shows a very similar temporal pattern to the standardised CPUE indices for SCI 3, also supporting the suggestion that the increases in scampi catch rate observed during the 1990s do not reflect fisher learning.

The standardised CPUE index for each subarea was fitted using the approach of Clark & Hare (2006), as recommended by Francis (2011). This approach fits lowess smoothers with different degrees of

smoothing (Figure 21 to Figure 23), and uses the residuals from each fit to estimate the CV. While examination of the individual series suggested that different CVs might be appropriate for different areas, there was no reason to believe that the reliability of the index varied between subarea, and from visual examination of the fits, the Working Group determined that a CV of 0.25 was appropriate for the CPUE series for each subarea.

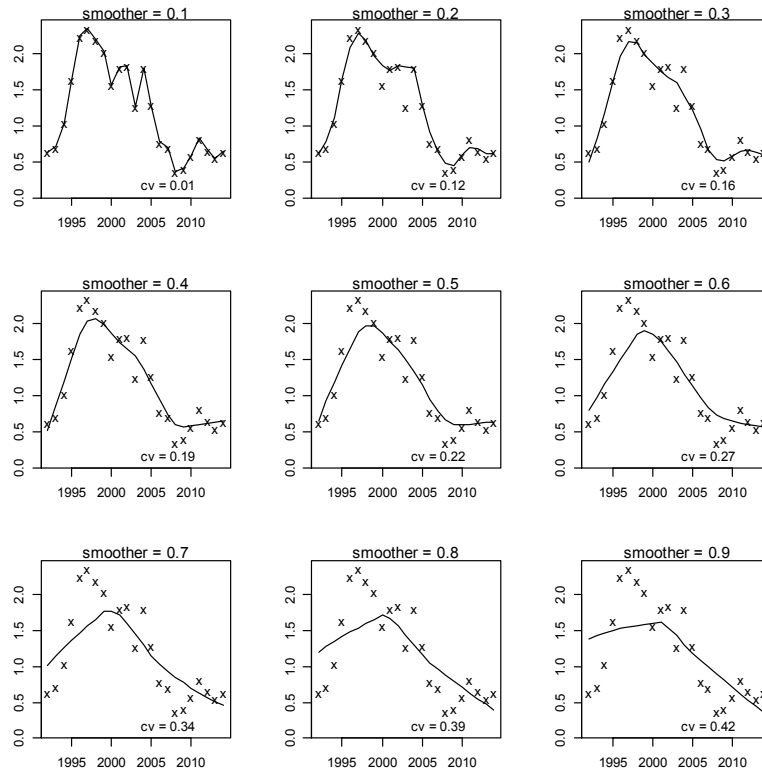


Figure 21: Fits of lowess smoothers to the standardised CPUE index for the MN subarea.

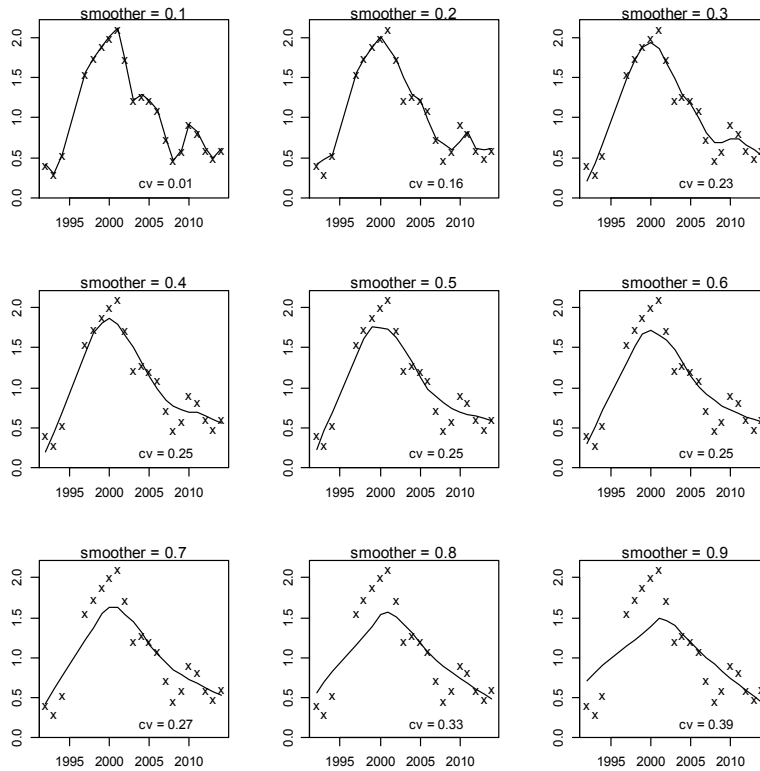


Figure 22: Fits of lowess smoothers to the standardised CPUE index for the MW subarea.

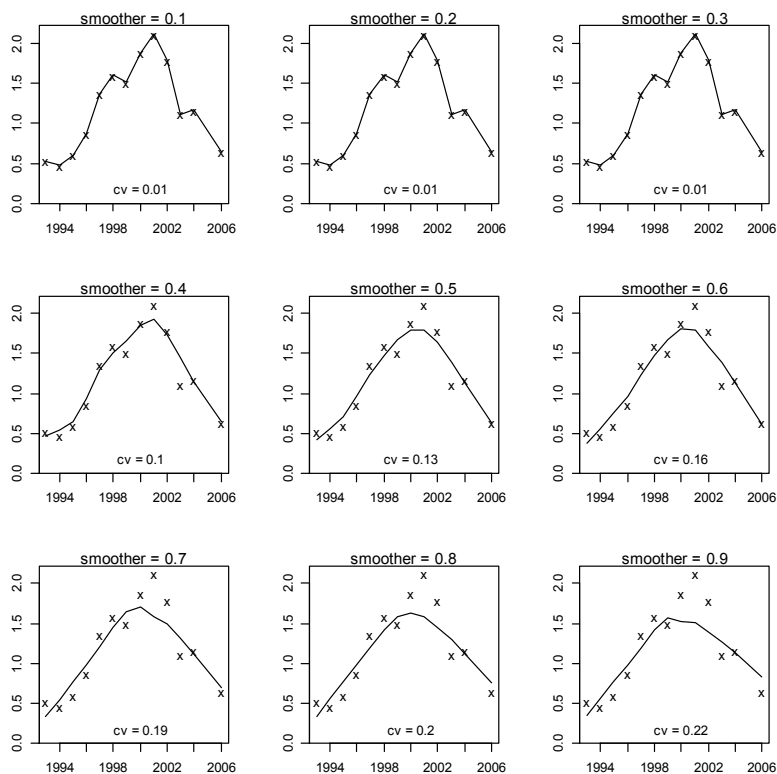


Figure 23: Fits of lowess smoothers to the standardised CPUE index for the MO subarea.

3.5 Research survey indices

Trawl and photographic surveys have been undertaken from the RV *Kaharoa* in August and November 2001, and October 2009, 2010 and 2013. In 2001, pre and post fishery surveys were conducted in the MO subarea (the fishery occurring over a few weeks in October). This survey was for the QMA 3 management area, and did not cover the MN and MW subareas. The more recent surveys were for the SCI 3 management area, and covered all three subareas.

3.5.1 Photographic surveys

Photographic surveys of SCI 3 have been conducted in 2001, 2009, 2010 and 2013 (Cryer et al. 2003; Tuck et al. 2011a; Tuck et al. 2011b; Tuck et al. 2015a). The surveys provide two indices of scampi abundance, one based on major burrow openings, and one based on visible scampi. Both indices are subject to uncertainty, either from burrow detection and occupancy rates (for burrow based indices) or emergence patterns (for visible scampi based indices) (Tuck et al. 2015b). The burrow index has been used to date within assessments for SCI 1, SCI 2 and SCI 3 (Tuck & Dunn 2012; Tuck 2013), but in SCI 6A scampi appear to spend less time in burrows (Tuck et al. 2007), and the visible scampi index has been used (Tuck & Dunn 2012; Tuck 2015). Scaled survey estimates (by survey strata and subarea) are provided for scampi burrows in Table 6. Details of the estimation of the catchability priors are provided in Section 3.7.

Table 6: Scaled photo survey estimates of scampi burrow abundance (millions) in SCI 3 by subarea.

	MN		MW		MO	
	Abundance	CV	Abundance	CV	Abundance	CV
2002					224.2	0.09
2010	98.8	0.09	112.3	0.13	48.2	0.15
2011	173.3	0.06	123.1	0.12	69.5	0.11
2014	331.3	0.08	151.0	0.10	154.0	0.11

3.5.2 Trawl surveys

Trawl catch rates from scampi surveys have been scaled up to strata to provide relative biomass estimates in Table 7. The biomass indices were used in the assessment model. Research trawl data are also available from a Chatham Rise middle depths trawl survey time series, but this survey targets hoki, hake and ling across the whole region, with station coverage being low within the main scampi fishery areas, and the trawl gear used is not considered appropriate for sampling scampi. Details of the estimation of the catchability priors are provided in Section 3.7.

Table 7: Time series of trawl survey scampi biomass (tonnes) and CV for SCI 3 by subarea.

	MN		MW		MO	
	Biomass	CV	Biomass	CV	Biomass	CV
2002					272.5	0.24
2010	82.3	0.25	295.0	0.36	40.2	0.37
2011	119.4	0.07	347.0	0.06	49.0	0.11
2014	246.9	0.06	175.0	0.30	126.5	0.27

3.6 Length distributions

3.6.1 Commercial catch length distributions

Ministry for Primary Industries observers have collected scampi length frequency data from scampi targeted fishing on commercial vessels in SCI 3 since 1991–92. The numbers of tows by subarea and time step for which length data are available are presented by fishing year in Table 8.

Examination of data from other scampi fisheries has suggested that the size composition of catches may vary with depth (Tuck 2015) and so patterns in the sex ratio and mean size from the scampi observer length frequency data were examined using multivariate tree regression (using the R package *mvpert*). Data were analysed for each year separately at the observed tow level, with response variables regressed on the explanatory variables month and depth bin. Pruning was conducted to give the tree with the smallest cross-validated relative error. No consistent depth splits were identified, and the temporal splits were consistent with those already proposed for the model structure (Table 2). It was therefore considered unnecessary to stratify the length sampling by depth.

The Working Group also previously expressed interest in any potential “observer” or “trip” effect in the data. Boxplots of scampi mean size per tow for each trip (Figure 24) show that the median size per tow has generally varied between about 40 mm and 50 mm. No trips stand out as being well outside the range.

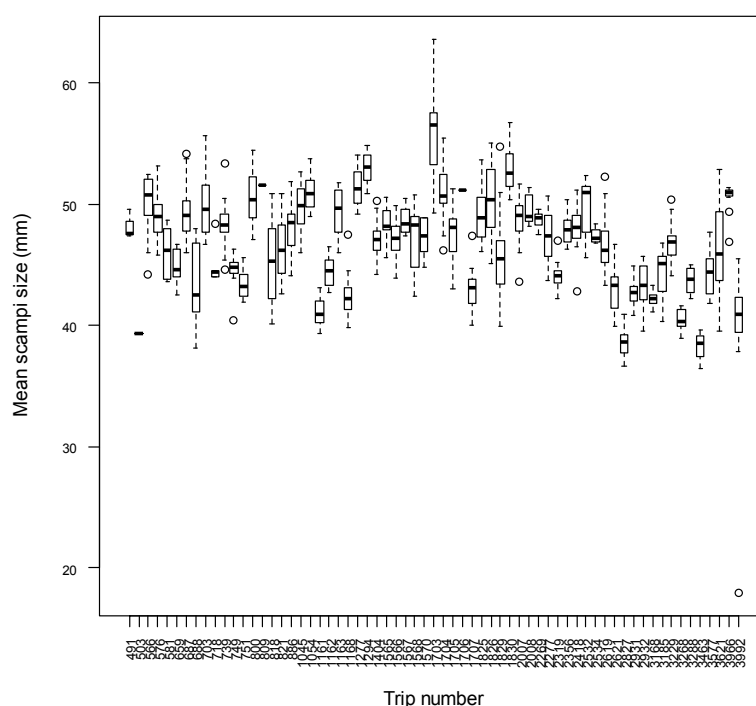


Figure 24: Boxplots of scampi mean size per tow by observer trip. Trips are plotted in chronological order. The solid line within each box represents the median value, the upper and lower ends of the box are the upper and lower quartiles, and the dashed lines extend out to the upper and lower adjacent values, the largest (smallest) value less (greater) than or equal to the upper (lower) quartile plus (minus) 1.5 times the interquartile range. Outliers (values beyond the adjacent values) are shown as open circles.

The numbers of tows sampled per subarea and time step varied (Table 8), and it was decided to exclude data where only one tow was available. For the year-time step combinations retained,

proportional length distributions (and associated CVs) were calculated using CALA (Francis & Bian 2011), using the approaches previously implemented in NIWA's *Catch-at-Age* software (Bull & Dunn 2002). Plots of the proportional length distribution are shown by year by time step in Figure 25 to Figure 31.

Table 8: Numbers of scampi observer length frequency samples from SCI 3, by model year, subarea and time step.

Year	MN		MO		MW		Trips
	TS 1	TS 2	TS 1	TS 2	TS 1	TS 2	
1991/92					4		2
1992/93	15	34					4
1993/94	31	46	49		7		8
1994/95	23	18	50		2		4
1995/96	6		12		1*		1
1996/97							
1997/98	22		13		4		2
1998/99	23		19				4
1999/00	22		7		6		2
2000/01	17		17		1*		1
2001/02	6		29		9		5
2002/03	49		18		7		5
2003/04	53		21		1*		4
2004/05	20				8		2
2005/06		15				7	2
2006/07	10				17	20	4
2007/08	11	7		1*	13	41	4
2008/09		2				11	1
2009/10	11				47		2
2010/11	54	14			17		5
2011/12		4					1
2012/13	49	4		1*	6	8	2
2013/14	8	11	5			4	2

* - where only a single tow was sampled from a subarea time step combination, the data were excluded from the model.

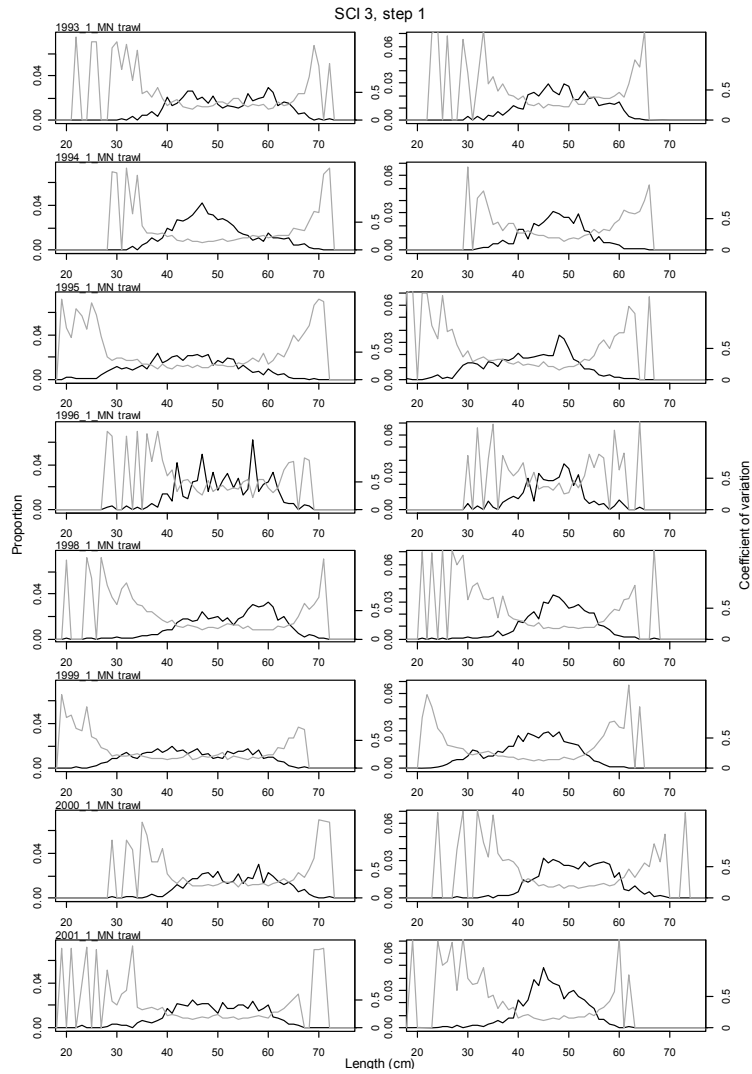


Figure 25: Proportional length frequency distributions (black line) and CVs (grey line) for commercial catches by model year and time step 1 for SCI 3, subarea MN. Males plotted on left, females on right.

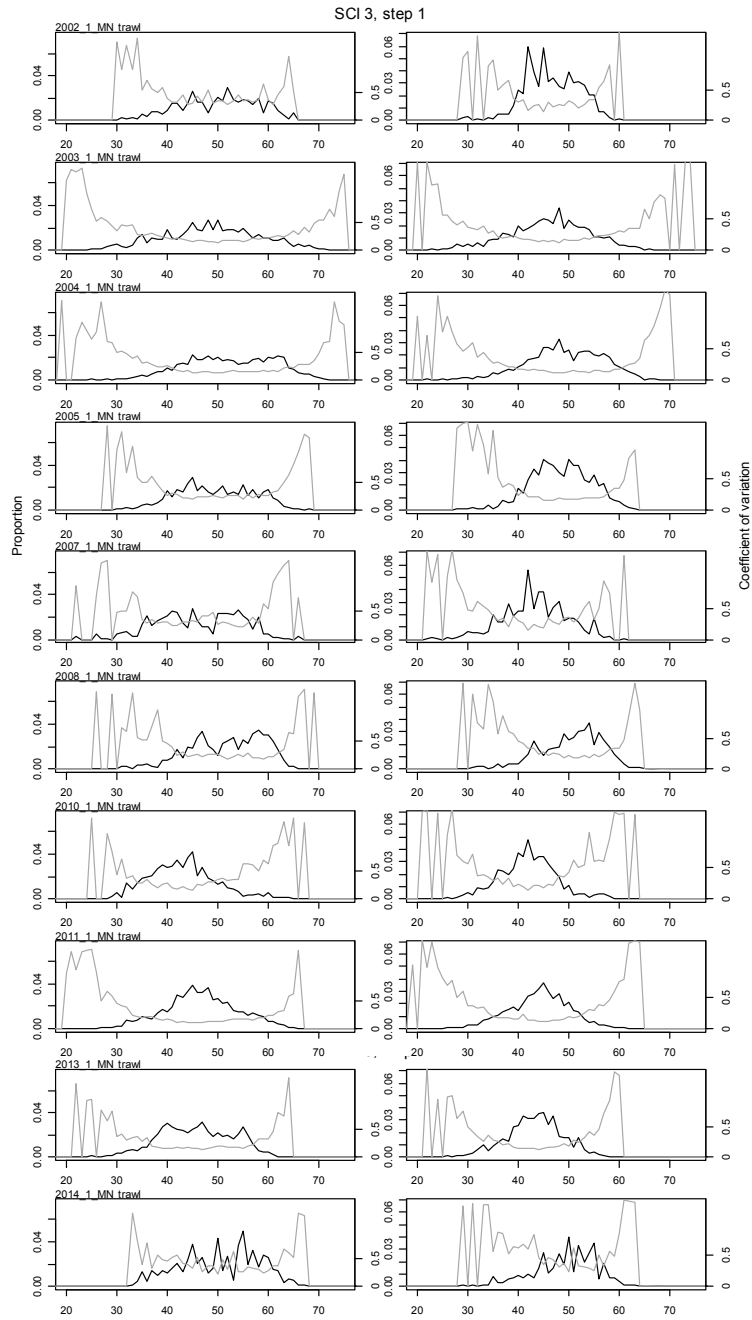


Figure 26: Proportional length frequency distributions (black line) and CVs (grey line) for commercial catches by model year and time step 1 (continued) for SCI 3, subarea MN. Males plotted on left, females on right.

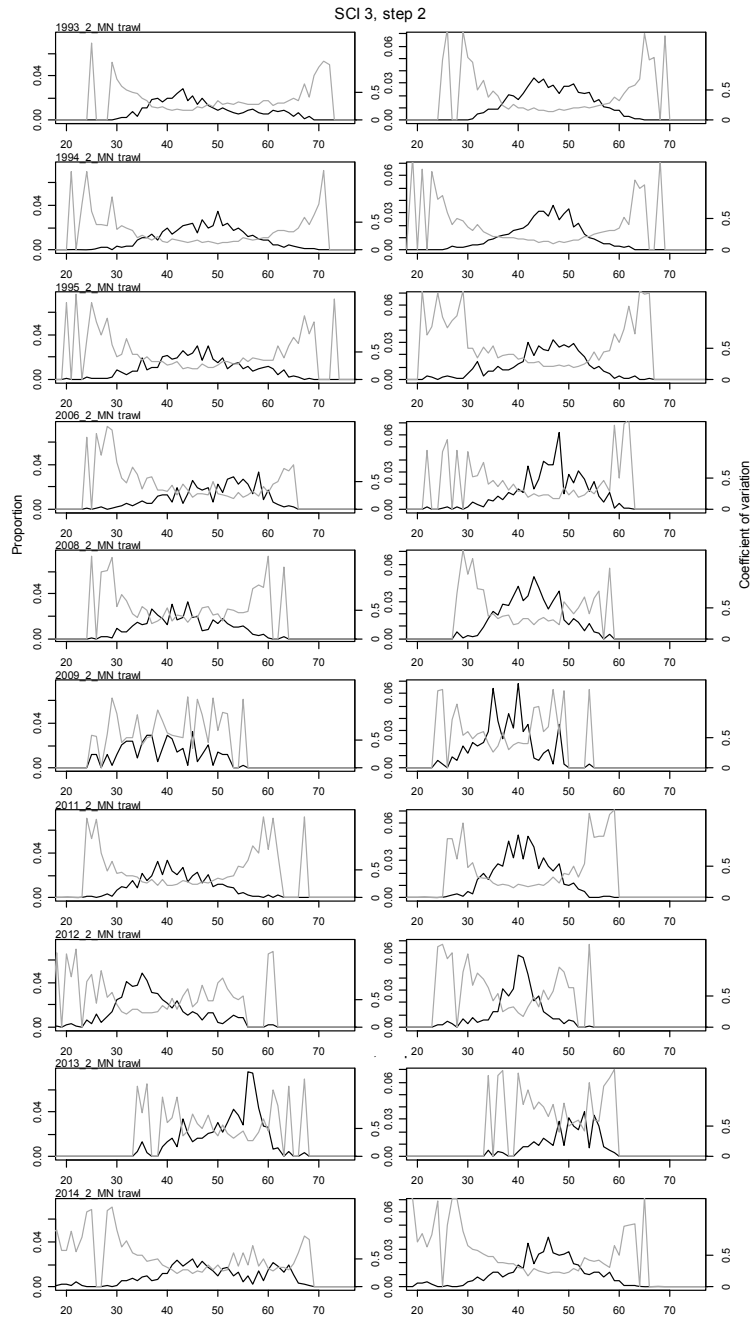


Figure 27: Proportional length frequency distributions (black line) and CVs (grey line) for commercial catches by model year and time step 2 for SCI 3, subarea MN. Males plotted on left, females on right.

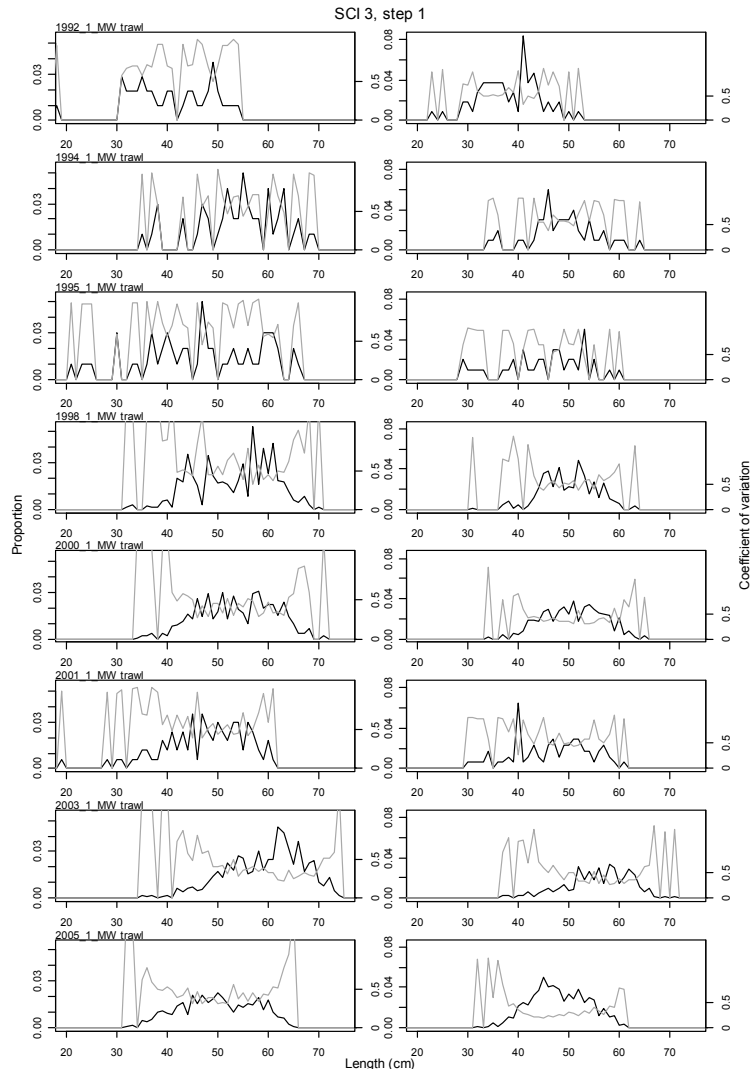


Figure 28: Proportional length frequency distributions (black line) and CVs (grey line) for commercial catches by model year and time step 1 for SCI 3, subarea MW. Males plotted on left, females on right.

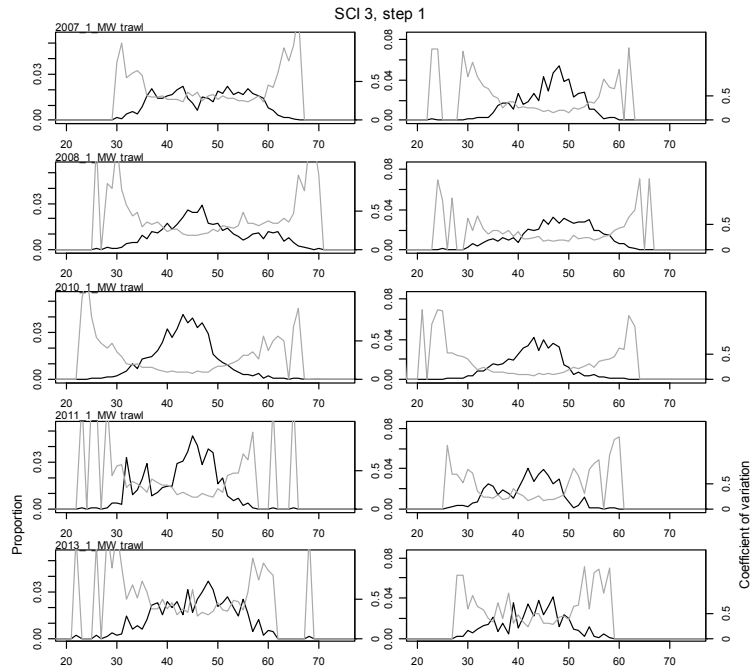


Figure 29: Proportional length frequency distributions (black line) and CVs (grey line) for commercial catches by model year and time step 1 (continued) for SCI 3, subarea MW. Males plotted on left, females on right.

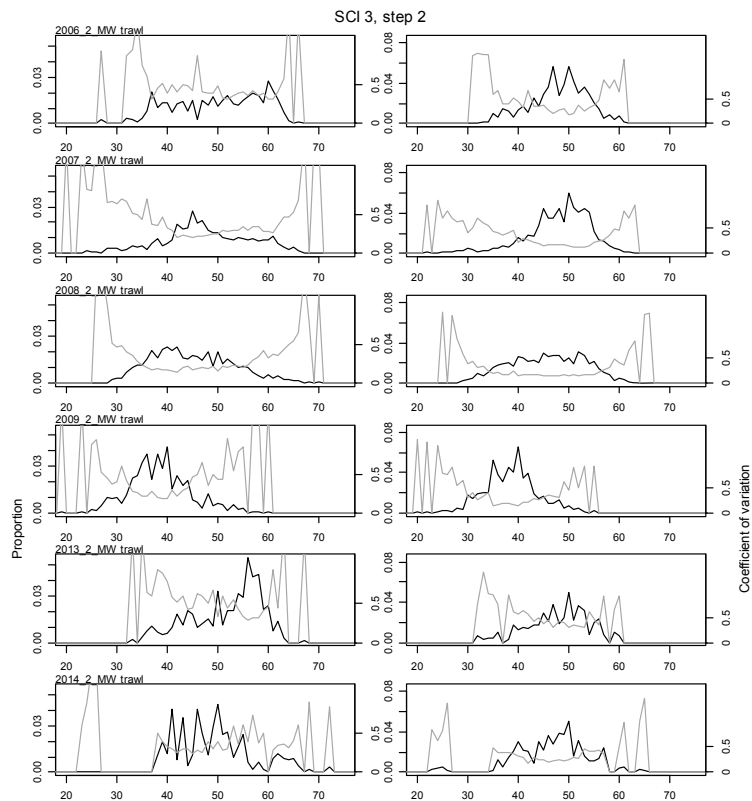


Figure 30: Proportional length frequency distributions (black line) and CVs (grey line) for commercial catches by model year and time step 2 for SCI 3, subarea MW. Males plotted on left, females on right.

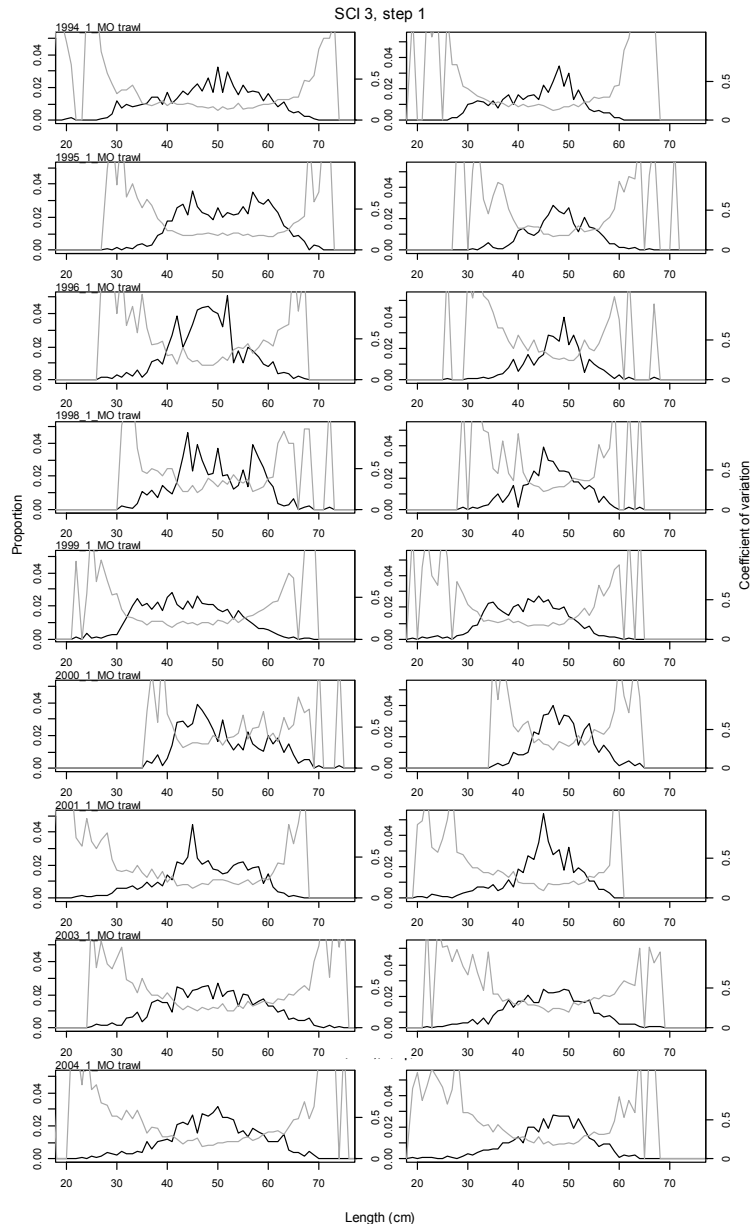


Figure 31: Proportional length frequency distributions (black line) and CVs (grey line) for commercial catches by model year and time step 1 for SCI 3, subarea MO. Males plotted on left, females on right.

3.6.2 Trawl survey length distributions

Length frequency samples from research trawling have been taken by scientific staff on all surveys (Table 7). Estimates of the length frequency distributions (with associated CVs) were derived using the NIWA CALA software (Francis & Bian 2011), using 1 mm OCL (Orbital Carapace Length) length classes by sex, and are presented in Figure 32 to Figure 34.

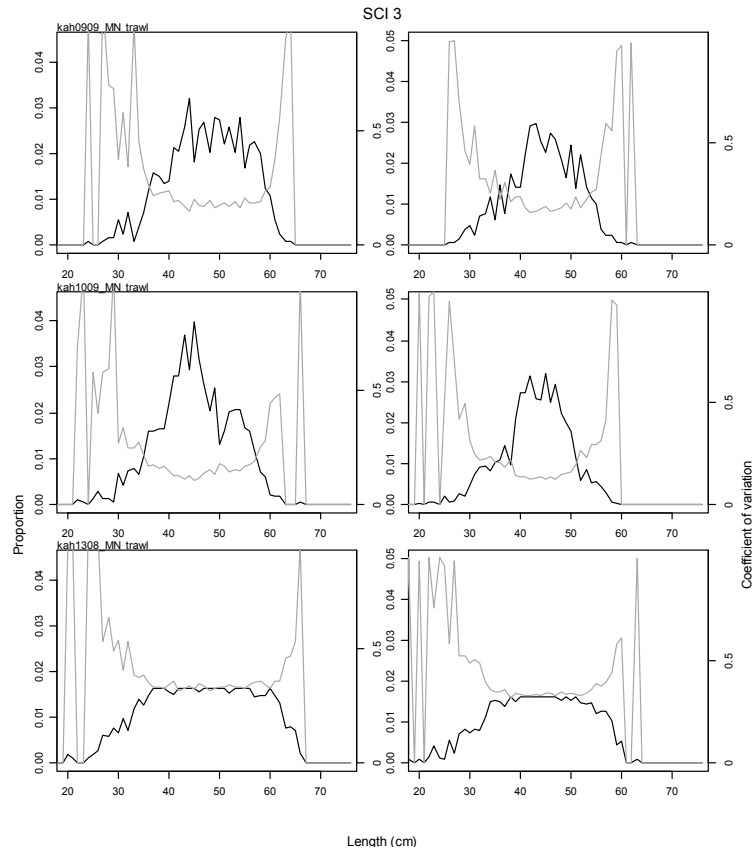


Figure 32: Proportional length frequency distributions (black line) and CVs (grey line) for research survey catches by model year for SCI 3, subarea MN. Males plotted on left, females on right.

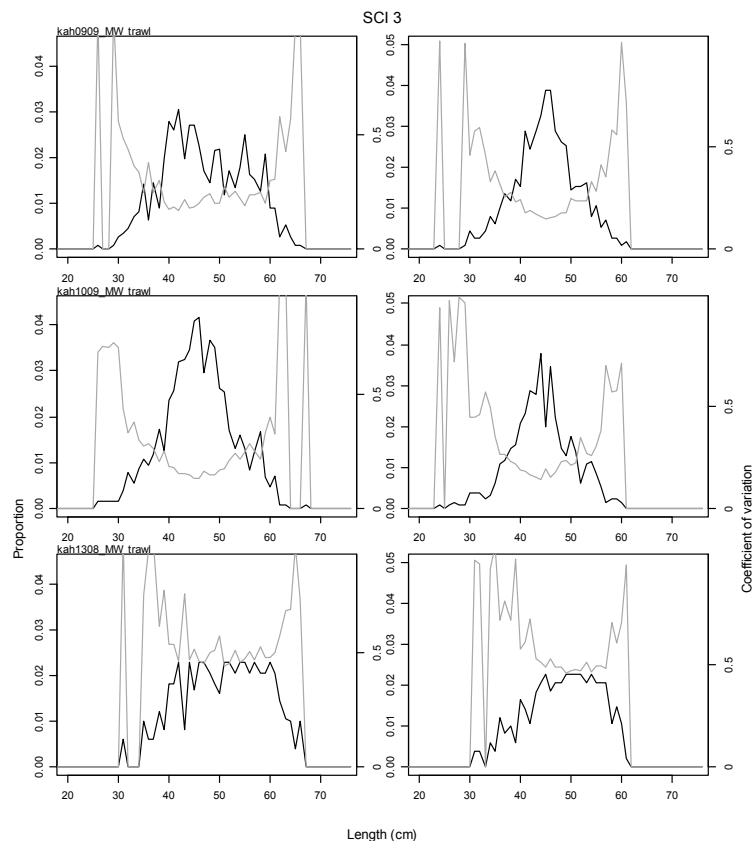


Figure 33: Proportional length frequency distributions (black line) and CVs (grey line) for research survey catches by model year for SCI 3, subarea MW. Males plotted on left, females on right.

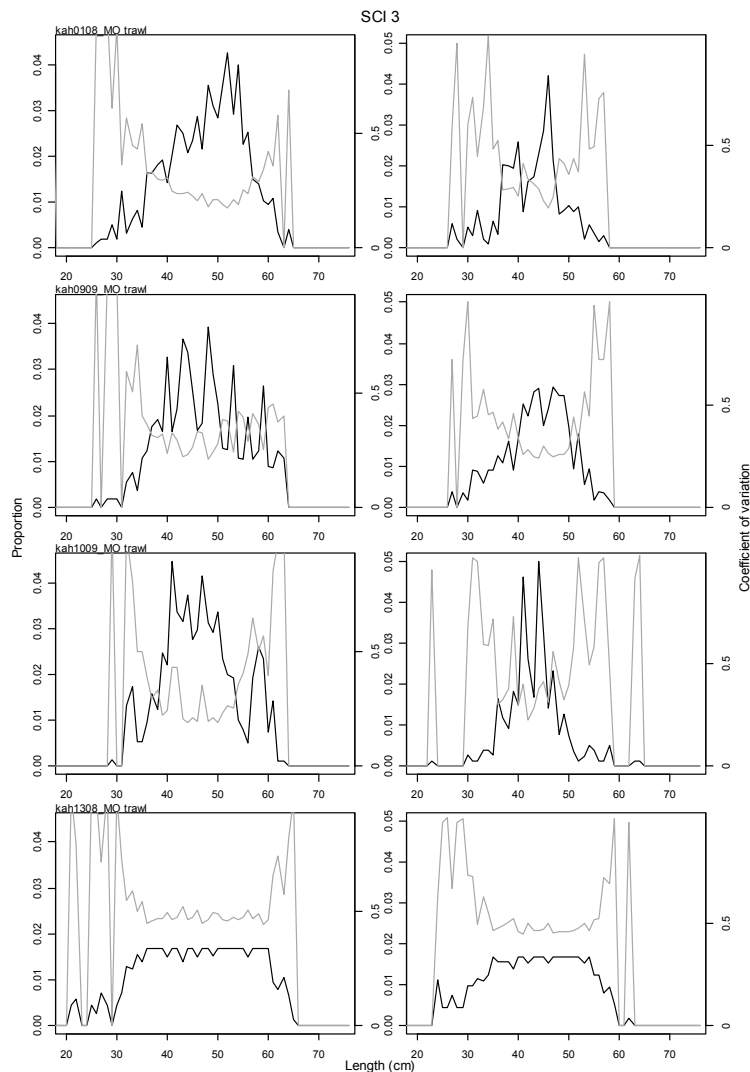


Figure 34: Proportional length frequency distributions (black line) and CVs (grey line) for research survey catches by model year for SCI 3, subarea MO. Males plotted on left, females on right.

3.6.3 Photo survey length distributions

Length frequency distributions were estimated for the relative photographic abundance series, by measuring the widths of a large sample of major burrow openings in the images, and converting these to orbital carapace lengths using a regression of OCL on major opening width (Cryer et al. 2005), augmented with additional data collected from more recent surveys. To estimate the CVs at length for each year, we used a bootstrap procedure, resampling with replacement from the original observations of burrow width, converting each observation to an estimated scampi size (in OCL), and using an error term sampled from a normal distribution fitted to the regression residuals. Compared with the length frequency distributions from trawl catches, this procedure gave very large CVs, but we think this is realistic given the uncertainties involved in generating a length frequency distribution from burrow sizes. Estimates of the length frequency distributions (with associated CVs) for scampi generating burrows are presented in Figure 35 to Figure 37.

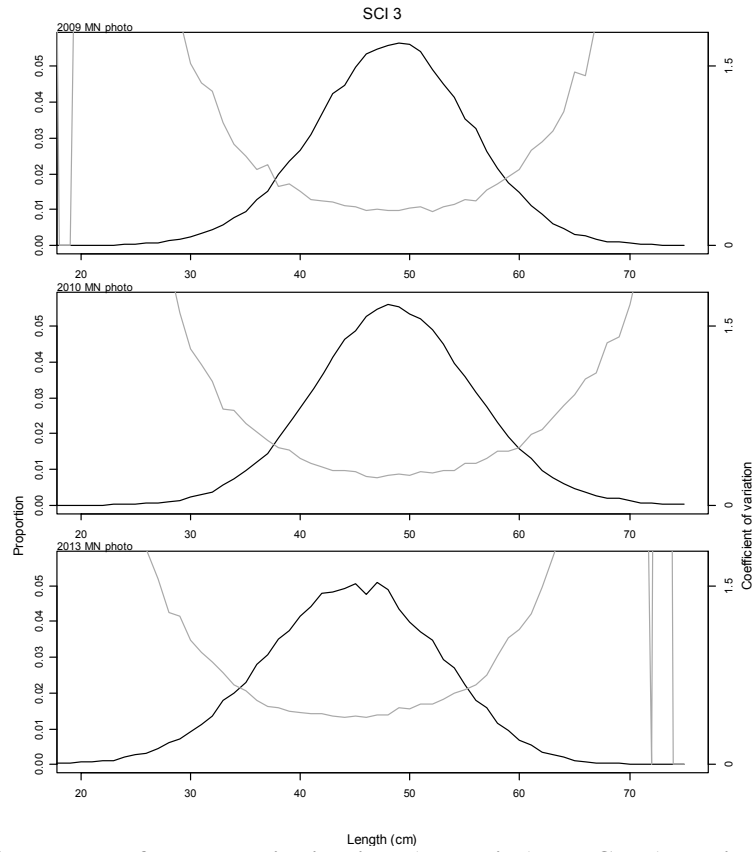


Figure 35: Proportional length frequency distributions (black line) and CVs (grey line) for estimated scampi size distribution from photo survey observations of burrows by model year for SCI 3, subarea MN.

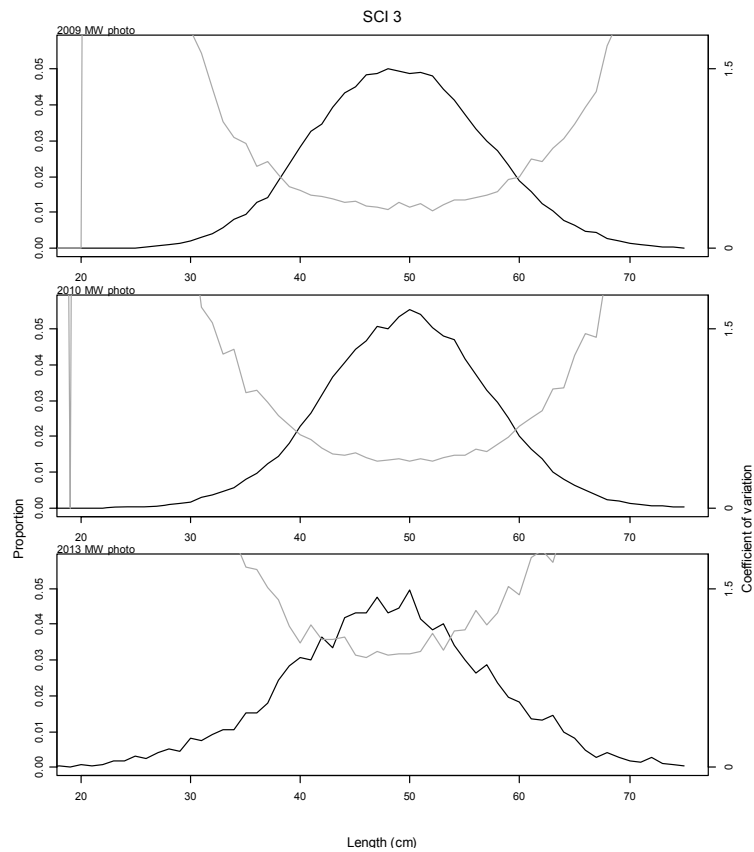


Figure 36: Proportional length frequency distributions (black line) and CVs (grey line) for estimated scampi size distribution from photo survey observations of burrows by model year for SCI 3, subarea MW.

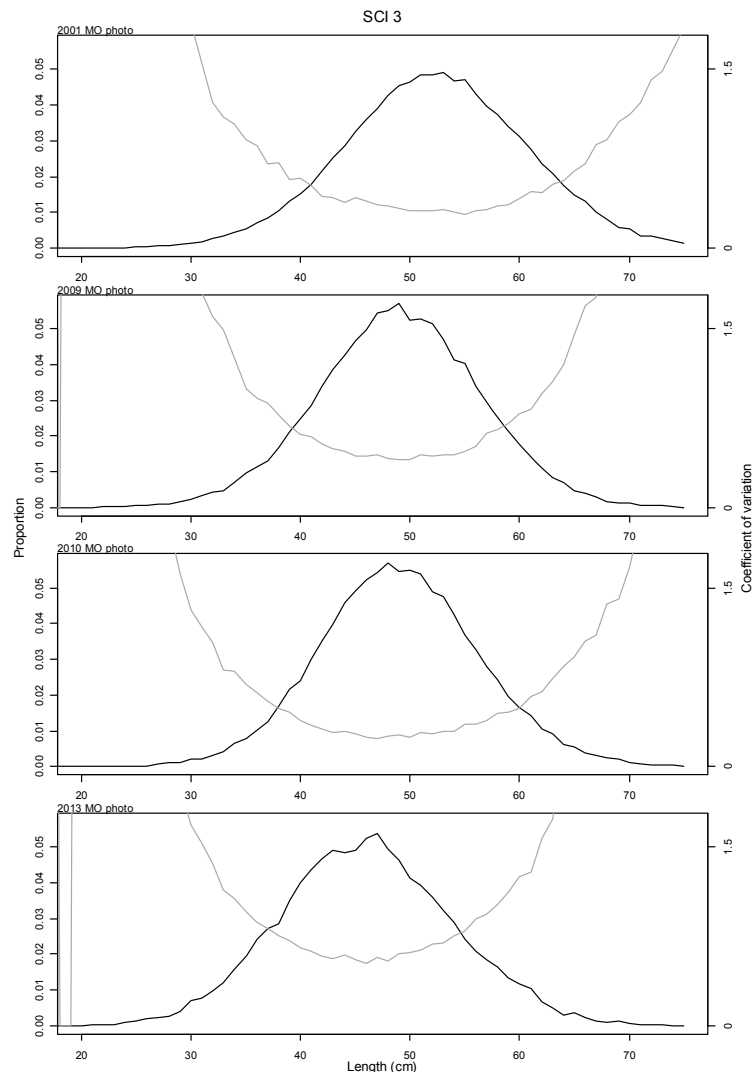


Figure 37: Proportional length frequency distributions (black line) and CVs (grey line) for estimated scampi size distribution from photo survey observations of burrows by model year for SCI 3, subarea MO.

3.7 Model assumptions and priors

Maximum Posterior Density (MPD) fits were found within CASAL using a quasi-Newton optimiser and the BETADIFF automatic differentiation package (Bull et al. 2008). Fitting was done inside the model except for the weighting of the abundance and length frequency data. For the length frequency data, observation-error CVs were estimated using CALA, converted to equivalent observation-error multinomial N s, and used within the model. The appropriate multinomial N s to account for both observation and process error were then calculated from the model residuals (method TA1.8 of Francis 2011), and these final N s were used in all models reported. This generally resulted in small N s for the commercial length frequency data in particular, and therefore relatively low weighting within the model. For the CPUE indices, the approach proposed by Clark & Hare (2006), and recommended by Francis (2011) was applied, estimating appropriate CV by fitting a smoother to the index. Process error for trawl and photo survey indices were fixed at 10%. CASAL was also used to run Monte-Carlo Markov Chains (MCMC) on the base models. MPD output was analysed using the extract and plot utilities in the CASAL library running under the general analytical package R.

The initial model was based on that described previously (Tuck & Dunn 2009; 2012; Tuck 2014; 2015). The model inputs include catch data, abundance indices (CPUE, trawl and photo surveys) and associated length frequency distributions. The parameters estimated by the base model include SSB_0 and R_0 , and time series of SSB and year class strength, selectivity parameters for commercial and research trawling, and the photo survey, and associated catchability coefficients. To reduce the number of fitted parameters, the catchability coefficients (qs) for commercial fishing, research trawling, and photographic surveys have previously been assumed to be “nuisance” rather than free parameters. At the request of the Working Group, models were also run with the qs as free parameters. The only informative priors used in the initial model were for q -Photo, q -Trawl, and the YCS vector (which constrains the variability of recruitment).

3.7.1 Scampi catchability

Catchability is considered to be the proportion of the scampi population that a particular survey index represents. Previous priors for scampi catchability have been largely based on information on *Nephrops* emergence and occupancy rates from European studies conducted in far shallower waters than *Metanephrops* populations inhabit (Tuck & Dunn 2012), but the acoustic tagging study conducted at the Mernoo Bank in October 2010 offered an opportunity to estimate priors for occupancy and emergence from New Zealand data (Tuck 2013). Acoustic tagging was repeated successfully within the SCI 1 and SCI 2 surveys in 2012, and was also conducted within the SCI 6A and SCI 3 surveys in 2013 (although less successfully). The data collected within these studies have been used to estimate catchability priors, based on the approach described by Tuck et al. (2015b).

Acoustic tags were fitted to scampi, and released with a moored hydrophone which recorded tag detections, when animals were emerged from burrows. Tag detection were analysed to investigate temporal patterns, and overall detection rate (Tuck et al. 2015b). Some tag detections showed distinct cyclical patterns (12.6 hour cycle), but other animals showed no clear patterns, and over the duration of the study the median proportion of scampi detectable was 53%. On the basis of shallow water trials with the acoustic tags, and scampi observations, it is assumed that these detections include scampi in burrow entrances and scampi walking free on the seabed (all of which would be visible to the photographic survey). Using the overall proportion detectable (over the duration of the mooring deployment) as an estimate of the proportion of scampi that would be visible in photographs at a particular time of day, the density of visible scampi in each survey can be scaled to a population density estimate. Overall proportion detectable also provides a catchability for estimates of visible scampi. The population density estimate was used in conjunction with photographic survey estimates of scampi burrows, and emerged scampi, to provide estimates of burrow count and trawl survey catchability, respectively. Uncertainty in each component was accounted for through resampling from the original distributions (1000 iterations), and the mean and upper and lower bound (2.5th and 97.5th quantiles) of the estimated catchability distributions (Table 9) were fitted within a binomial GLM (probit link) to estimate the slope and intercept of the cumulative frequency distribution, which in turn were used to estimate the mean and standard deviation of the lognormal distribution of the priors for the various catchability terms used in the assessment model (Figure 38).

3.7.2 Priors for qs

***q*-Photo**

This is the proportion of the scampi population represented by the count of major burrow openings. The best estimate is 2.387 (major burrow openings divided by estimated scampi density). Upper and lower estimates are taken as the 2.5th and 97.5th percentiles of the distribution.

q-Trawl

This is the proportion of the scampi population represented by the trawl survey catches. The best estimate is 0.108 (scampi out of burrows divided by estimated scampi density). Upper and lower estimates are taken as the 2.5th and 97.5th percentiles of the distribution.

q-Scampi

This is the proportion of the scampi population represented by the count of visible scampi. The best estimate is 0.526 (scampi out of burrows divided by estimated scampi density). Upper and lower estimates are taken as the 2.5th and 97.5th percentiles of the distribution.

3.7.3 Estimation of prior distributions

The bounds and best estimate were assumed to represent the 2.5th, 50th and 97.5th percentiles of the prior distribution. These values were fitted within a binomial GLM (probit link) to estimate the slope and intercept of the cumulative frequency distribution, which in turn were used to estimate the mean and standard deviation of the lognormal distribution of the prior. The distributions of the priors for *q-Photo* and *q-Trawl* are presented in Figure 38.

Table 9: Component factors for estimation of priors for *q-Scampi*, *q-Photo*, and *q-Trawl*.

	Lower	Best	Upper	Source
Major opening	0.0794	0.0794	0.0794	survey
Visible scampi	0.0175	0.0175	0.0175	survey
Scampi "out"	0.0036	0.0036	0.0036	survey
Scampi as % of openings		22%		Visible/openings
% of scampi "out"		21%		Out/visible
Emergence	28%	53%	72%	Acoustic tags
Est scampi density	0.063	0.033	0.024	Visible/emergence
Est occupancy	80%	42%	31%	Est density/major
<i>q-Trawl</i>	0.057	0.108	0.149	Out/Est density
<i>q_scampi</i>	0.277	0.526	0.722	Visible/Est density
<i>q_photo</i>	1.257	2.387	3.276	Major/Est density

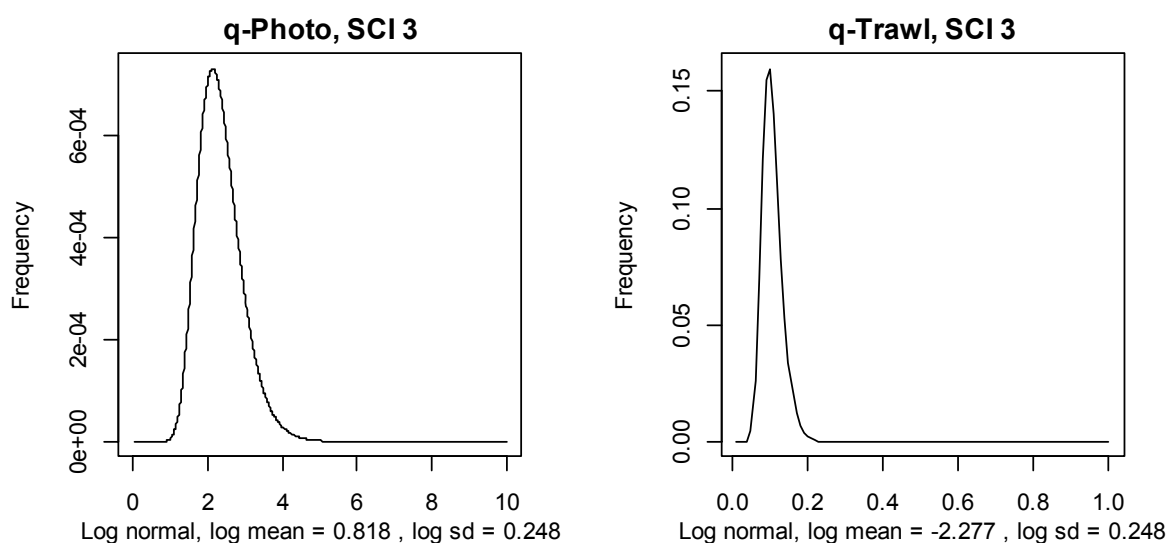


Figure 38: Estimated distribution of *q-Photo* and *q-Trawl* for SCI 3.

3.7.4 Recruitment

Few data are available on scampi recruitment. Relative year class strengths were fixed at 1 for the two most recent years, and were assumed to average 1.0 over all other years. In the initial model development (Cryer et al. 2005) lognormal priors on relative year class strengths were assumed, with mean 1.0 and CV of 0.2, and the sensitivity of year class strength (YCS) variation was examined in further developments (Tuck & Dunn 2006). More recent model investigations, particularly those fitting the CPUE indices, suggest that the constraint on variability in YCS may be too severe, and the SFAWG suggested increasing the CV (Tuck & Dunn 2012). In the current implementation, lognormal priors on relative year class strengths were assumed, with mean 1.0 and CV of 1.0. The relationship between stock size and recruitment for scampi is unknown, and a Beverton Holt relationship with a steepness of 0.8 has been assumed. New Zealand scampi have very low fecundity (Wear 1976; Fenaughty 1989) (in the order of tens to hundreds of eggs carried by each female), so very successful recruitment is probably not plausible at low abundance. Recruitment enters the model partition as a year class, with a normally distributed OCL of mean 10 mm and CV of 0.4.

4. ASSESSMENT MODEL RESULTS

4.1 Initial models

Details of differences between models examined within sensitivity analyses are presented in Table 10. An initial single area model (Model 1) was examined, but given the contrasting fishing histories of the three areas, was not considered appropriate. As described in Section 3.1, a three area (three stock) model was applied, with series of CPUE, photo survey, and trawl survey indices for each area (Model 2). Preliminary models did not suggest that the three stocks had significantly different YCS patterns, and so the SFAWG proposed estimating a single shared YCS (Model 3). This is also supported by biological understanding (in that YCS variability is considered to be related to broad environmental drivers, which would apply to all three stocks) although it is acknowledged that a shared YCS tends to drive the three areas to have the same stock trajectory. Fits to the individual survey and abundance indices were improved when commercial fishery and survey catchability were allowed to vary between stocks (Model 4). The previous assessment had shared these parameters between stocks (Tuck 2013), but given the different fishing histories and seasonal patterns, the SFAWG considered the estimation of stock specific catchabilities (other than for the photo survey) to be appropriate. In addition, preliminary examination of the sensitivity of the model to estimating catchability terms as free parameters was examined (Model 5). Although stock status was estimated to be very similar between models estimating catchability terms as free or nuisance parameters, MCMC traces for free parameter models did not stabilise, despite running far longer chains than for nuisance parameter models.

Key parameter and quantity estimates from the MPD fits for the models are presented in Table 11. Fits to the CPUE indices did not differ greatly between any of the models. All the models showed an increase in biomass at the start of the series, with a fluctuating decline over time. Across the five models examined, estimates of SSB_0 for the combined stocks varied from 9345 to 12 718 tonnes, and stock trajectories were quite consistent, with the estimates of SSB_{2014}/SSB_0 ranging from 51% to 64%.

Table 10: General details of models examined within sensitivity analyses for SCI 3.

Model	Stocks	YCS	qs	q estimation
1	1			Nuisance
2	3	Separate	Shared	Nuisance
3	3	Shared	Shared	Nuisance
4	3	Shared	Separate	Nuisance
5	3	Shared	Separate	Free

Table 11: Estimated key parameters and quantities from MPD fits for SCI 3 initial model runs.

Parameter/Quantity	Model 1	Model 2	Model 3	Model 4	Model 5
CPUE-Commercialq	0.00006	0.00018	0.00016		
CPUE-Commercialq[MN]				0.00020	0.00020
CPUE-Commercialq[MO]				0.00031	0.00030
CPUE-Commercialq[MW]				0.00019	0.00019
TrawlSurveyq	0.064	0.045	0.044		
TrawlSurveyq[MN]				0.061	0.061
TrawlSurveyq[MO]				0.044	0.044
TrawlSurveyq[MW]				0.107	0.107
PhotoSurvey_q	3.468	4.409	3.96	5.60	5.60
initialization.B0	12718	11822	12646	9345	9347
initialization.B0[MN]		4834	5070	3955	3958
initialization.B0[MO]		3100	4671	3438	3437
initialization.B0[MW]		3888	2905	1952	1952
B2014/B0	0.56	0.64	0.53	0.51	0.51
B2014[MN]/ B0[MN]		0.63	0.48	0.45	0.45
B2014[MO]/ B0[MO]		0.64	0.62	0.63	0.63
B2014[MW]/B0[MW]		0.63	0.54	0.52	0.52
maturity_props.all	a50	43.33	43.33	43.33	43.33
	a to 95	7.03	7.03	7.03	7.03
selectivity[Fishing_1]	a50	34.88	34.23	36.63	36.84
	a to 95	9.89	10.31	10.87	10.90
	amax M	1.05	1.12	1.29	1.32
selectivity[Fishing_2]	a50	33.44	33.43	34.62	34.63
	a to 95	7.91	7.91	7.79	7.74
	amax M	0.81	0.83	0.96	0.96
selectivity[TrawlSurvey]	a50	36.35	33.29	34.08	34.80
	a to 95	12.48	9.06	10.25	11.29
	amax M	1.08	1.27	1.37	1.30
selectivity[photosurvey]	a50	39.35	43.66	42.74	43.66
	a to 95	10.41	12.33	14.02	12.33
growth[1].g_male	g20	14.26	14.39	10.33	10.32
	g40	3.49	3.97	2.06	2.10
growth[1].g_female	g20	13.26	14.26	12.72	12.34
	g40	1.05	1.38	0.55	0.52

4.2 Base models

Model 4 (shared YCS, separate catchabilities for each stock) identified contrasting trends between the photographic and trawl surveys, particularly for the MN and MW stocks, and also inconsistencies between the catchabilities and their priors. It was therefore decided that models excluding either the trawl survey or the photographic survey should be investigated as base models. Attempts to estimate natural mortality within preliminary models (not presented) did not generate realistic results, and so sensitivity to M was also examined (base value 0.25, sensitivity runs at 0.15 and 0.35). Various model output plots and diagnostics are presented as an Appendix for each model. Key parameter and quantity estimates from the MPD fits for the models are presented in Table 12.

Table 12: Estimated key parameters and quantities from MPD fits for SCI 3 natural mortality sensitivity runs for models excluding the trawl survey (NT), or excluding the photographic survey (NP).

Parameter/Quantity		NT_0.15	NT_0.25	NT_0.35	NP_0.15	NP_0.25	NP_0.35
CPUE-Commercialq[MN]		0.0001	0.0001	0.0001	0.0003	0.0003	0.0003
CPUE-Commercialq[MO]		0.0002	0.0001	0.0001	0.0011	0.0009	0.0009
CPUE-Commercialq[MW]		0.0002	0.0001	0.0001	0.0003	0.0002	0.0002
TrawlSurveyq[MN]					0.0695	0.0639	0.0669
TrawlSurveyq[MO]					0.0810	0.0773	0.0811
TrawlSurveyq[MW]					0.0960	0.0783	0.0765
PhotoSurvey_q		3.3002	2.4128	1.9690			
B0 total		12243	19127	28042	6611	7845	7804
initialization.B0[MN]		5358	8121	12021	3104	3315	3084
initialization.B0[MO]		2884	4471	6574	810	849	809
initialization.B0[MW]		4001	6535	9447	2696	3681	3912
B2014 total		7522	11045	15976	3362	3989	4194
B2014 MN		2904	4445	6668	1254	1425	1421
B2014 MO		2125	2834	3938	517	523	517
B2014 MW		2492	3766	5369	1590	2041	2256
% total		0.61	0.58	0.57	0.51	0.51	0.54
%MN		0.54	0.55	0.55	0.40	0.43	0.46
%MO		0.74	0.63	0.60	0.64	0.62	0.64
%MW		0.62	0.58	0.57	0.59	0.55	0.58
selectivity[Fishing_1]	a50	32.52	36.52	40.46	34.59	36.58	36.08
	a to 95	8.43	10.52	11.90	10.09	11.03	13.40
	amax M	1.38	1.45	1.36	1.05	1.02	1.08
selectivity[Fishing_2]	a50	31.94	34.29	36.95	33.05	34.27	33.58
	a to 95	7.02	7.61	8.62	7.17	7.44	9.02
	amax M	1.02	1.05	1.00	0.87	0.83	0.84
selectivity[TrawlSurvey]	a50				31.14	34.07	34.76
	a to 95				9.27	10.84	12.31
	amax M				1.56	1.46	1.44
selectivity[photosurvey]	a50	37.37	42.15	45.63			
	a to 95	12.89	13.60	13.14			
growth[1].g_male	g20	9.43	9.12	9.20	10.51	12.90	16.88
	g40	1.23	1.63	2.02	1.27	2.91	5.12
growth[1].g_female	g20	13.09	13.38	11.67	10.10	12.22	15.96
	g40	-0.26	0.91	1.17	-1.09	0.41	2.26

4.2.1 Models excluding the trawl surveys (NT_0.15, NT_0.25, NT_0.35)

The outputs and diagnostics for the three models excluding the trawl survey data and examining the sensitivity to M are presented in Appendix 3 (NT_0.15), Appendix 4 (NT_0.25) and Appendix 5 (NT_0.35). The fits to the CPUE indices were similar for the M=0.25 and M=0.35 models, but with the lower M (0.15), the model was less able to fit the data (Figure 39). Fits to the photographic survey abundance index generally improved with increasing M, but were not able to match the decline in abundance between 2002 and 2010 (only data for MO subarea), or the increase in abundance observed since 2010 (Figure 40). All three models estimated similar YCS patterns (Figure 41), with very high recruitment in 1993, and above average recruitment in either 2010 (M=0.15) or 2011. Selectivity curves were sensitive to M (moving to the right with increasing natural mortality) (Figure 42), but were consistent with changes in sex ratio observed in the fishery (males more available in the first time step). Fits to the observer length frequencies were variable (shown in the relevant Appendix), with the data weighting giving observer length frequency samples low effective sample size, while fits to the photographic survey length frequencies were generally better, and effective sample size larger, but there was little difference in the fits between models. The estimated combined SSB₀ increased

markedly with M , and ranged from 12 243 t ($M=0.15$) to 28 042 t ($M=0.35$), although SSB_{2014} as a percentage of SSB_0 was far more consistent, ranging from 57% – 61%. The three models consistently estimated the MO subarea to have the most optimistic stock status (relative to SSB_0), and the MN subarea to have the least, but all estimates were above 50% SSB_0 .

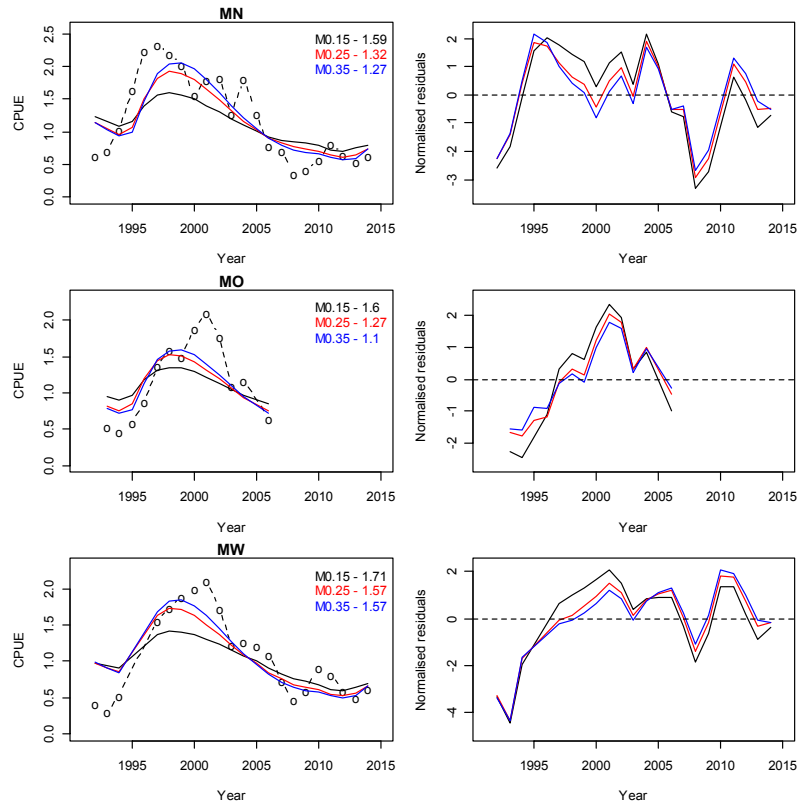


Figure 39: Fits to CPUE indices (left column) and normalised residuals (right column) for each subarea for models excluding trawl survey data with M fixed at 0.15 (black), 0.25 (red) or 0.35 (blue).

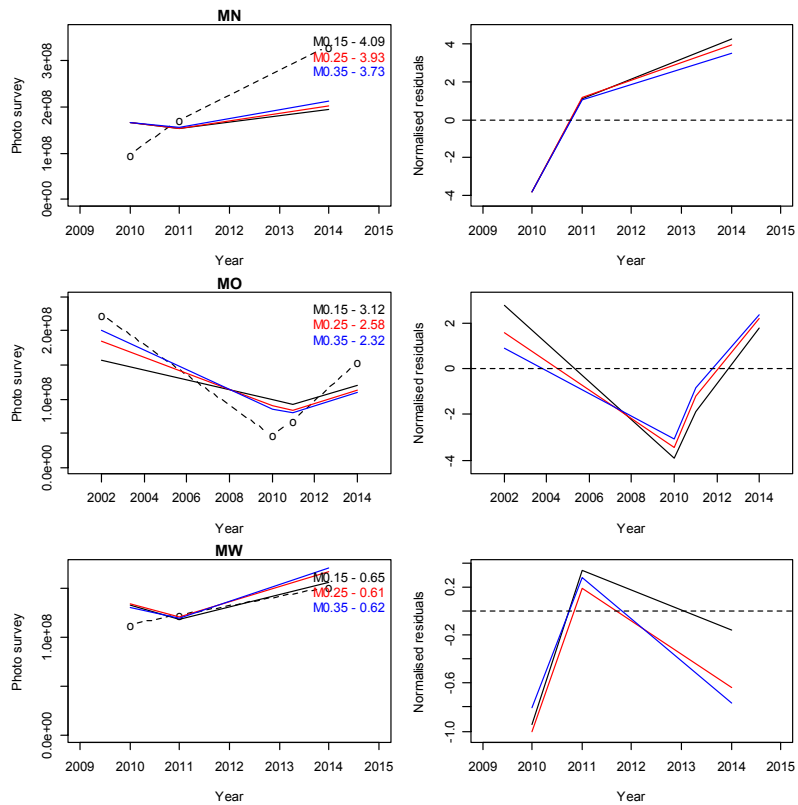


Figure 40: Fits to photographic survey indices (left column) and normalised residuals (right column) for each subarea for models excluding trawl survey data with M fixed at 0.15 (black), 0.25 (red) or 0.35 (blue).

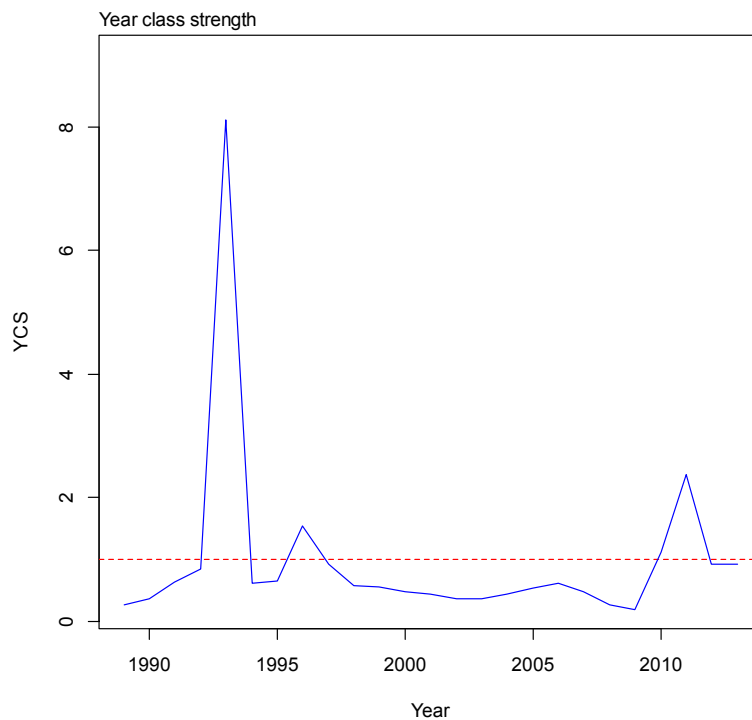


Figure 41: Year class strength for models excluding trawl surveys with M fixed at 0.15 (black), 0.25 (red) or 0.35 (blue).

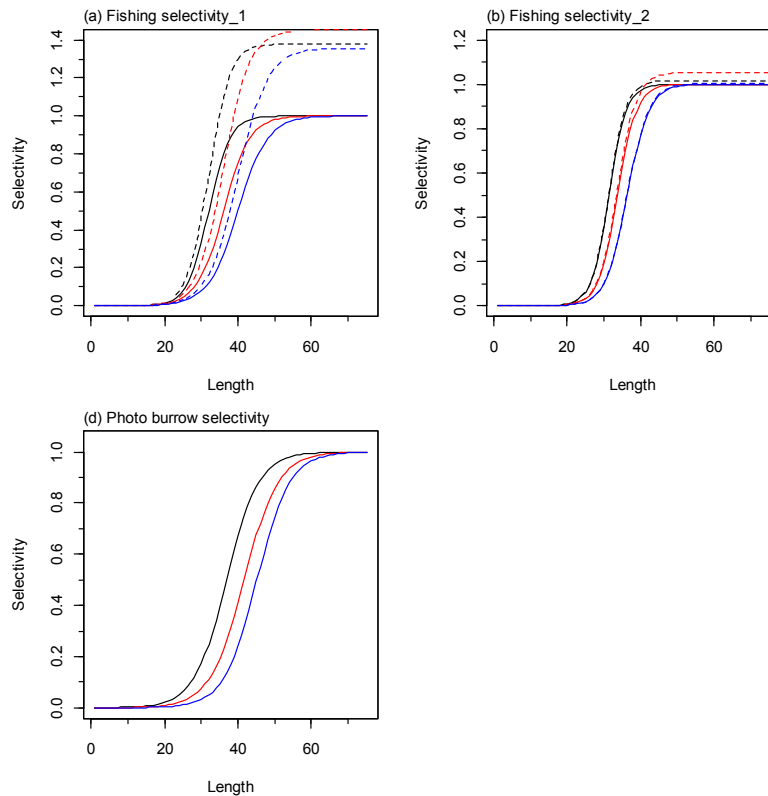


Figure 42: Fishery and survey selectivity curves for models excluding trawl surveys, with M fixed at 0.15 (black), 0.25 (red) or 0.35 (blue). Solid line – females, dotted line – males. The scampi photo index is not sexed, and a single selectivity applies.

The likelihood profile when B_0 is fixed (for one subarea) shows a minimum at just under 20 000 t (total SSB, three subareas combined) (shown for the NT_0.25 model; A4. 25), although it is relatively flat in this region of the curve. The various data sets do not provide any consistent signal, and none are particularly informative, other than suggesting that the combined SSB_0 is greater than about 8000 t. The prior for q -photo appears quite influential.

MCMC runs

MCMC runs were explored for all three models, and are presented for each in the Appendices, but are only discussed in detail for the NT_0.25 model. Three independent MCMC chains were started a random step away from the MPD for the model, and run for 5 million simulations, with every one thousandth sample saved, giving a set of 5000 samples. The three chains were examined for evidence of lack of convergence (A4. 26 – A4. 28), and having dropped the first 1500 samples from each, concatenated to produce a sample chain for projections. While there was some divergence between the chains, estimates of SSB_{2014}/SSB_0 were reasonably stable, and considered acceptable by the SFAWG. The posterior distributions of the photo survey catchability were within the prior distribution (A4. 31), with the MPD estimates also located within the posterior distribution. The posterior trajectory of overall SSB (Figure 43, individual subarea plots provided in Appendices) suggests an increase in SSB until 1999, followed by a decline to 2009, a slower decline to a stable period around 2012 and 2013, and an increase in 2014. YCS shows a peak around 1993, then a series of below average years, but above average values in 2010 and 2011 (leading to the increase in SSB in 2014). The median estimate of current status (SSB_{2014}/SSB_0) for the combined subareas is 60% (ranging from 57% to 65% for individual subareas), with 100% probability (individually or combined) that SSB_{2014} is above 40% SSB_0 (Table 13).

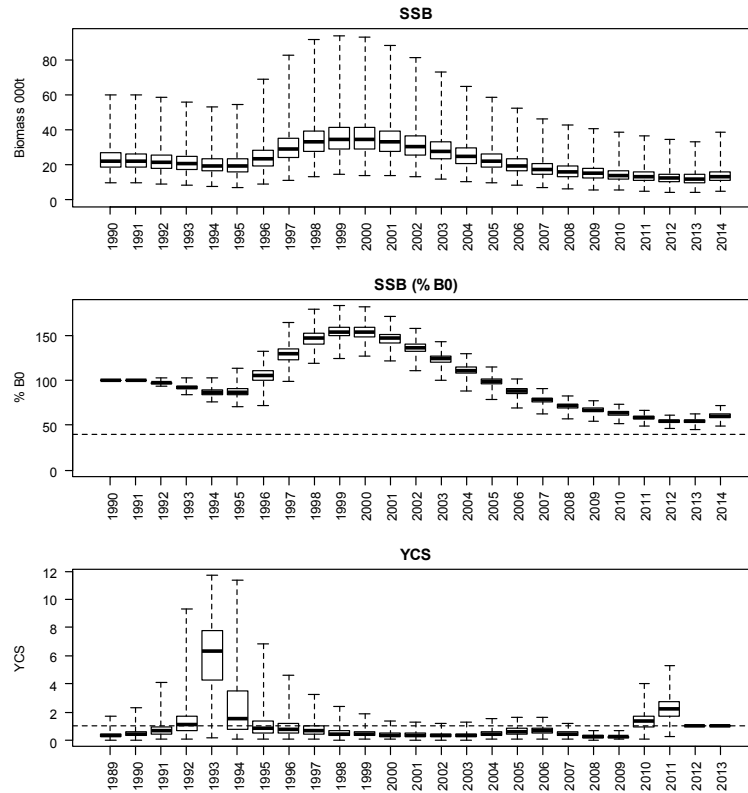


Figure 43: Posterior trajectory of combined SSB, SSB_{2014}/SSB_0 and YCS for model NT_0.25. The solid line within each box represents the median value, the upper and lower ends of the box are the upper and lower quartiles, and the dashed lines extend out to the upper and lower adjacent values, the largest (smallest) value less (greater) than or equal to the upper (lower) quartile plus (minus) 1.5 times the interquartile range.

Table 13: Estimates of SSB_0 , SSB_{2014} , SSB_{2014}/SSB_0 and the probability of SSB_{2014} being below 10% SSB_0 , below 20% SSB_0 , or above 40% SSB_0 , from MCMC runs for models excluding the trawl survey data. Estimates provided at the subarea and combined stock level.

	SSB_0	SSB_{2014}	SSB_{2014}/SSB_0	P $SSB_{2014} < 10\%SSB_0$	P $SSB_{2014} < 20\%SSB_0$	P $SSB_{2014} > 40\%SSB_0$
NT_0.15						
MN	6162	3564	0.58	0.000	0.000	1.000
MW	4630	3007	0.65	0.000	0.000	1.000
MO	3433	2577	0.75	0.000	0.000	1.000
SCI 3	14258	9177	0.64	0.000	0.000	1.000
NT_0.25						
MN	9550	5489	0.57	0.000	0.000	1.000
MW	7539	4516	0.60	0.000	0.000	1.000
MO	5294	3442	0.65	0.000	0.000	1.000
SCI 3	22424	13497	0.60	0.000	0.000	1.000
NT_0.35						
MN	13606	7706	0.57	0.000	0.000	1.000
MW	10644	6116	0.57	0.000	0.000	1.000
MO	7489	4512	0.60	0.000	0.000	1.000
SCI 3	31895	18371	0.58	0.000	0.000	1.000

4.2.2 Models excluding the photographic surveys (NP_0.15, NP_0.25, NP_0.35)

The outputs and diagnostics for the three models excluding the photographic survey data and examining the sensitivity to M are presented in Appendix 6 (NP_0.15), Appendix 7 (NP_0.25) and Appendix 8 (NP_0.35). As with the models excluding the trawl survey data, the fits to the CPUE indices were similar for the $M=0.25$ and $M=0.35$ models, but with the lower M (0.15), the model was less able to fit the data (Figure 44). Fits to the trawl survey abundance index improved slightly with increasing M , but were not able to match well the patterns observed (Figure 45), and only showed an improvement in the fit (compared to a model including both trawl and photographic surveys, not shown) for the MW subarea. The three models estimated similar YCS patterns, with slight differences in the timing of peaks that were related to M (Figure 46), and no evidence of above average recruitment in the most recent years. Selectivity curves were far less sensitive to M than the models excluding the trawl survey data (Figure 47), and maintained consistency with changes in sex ratio observed in the fishery. As with the models discussed above, fits to the observer length frequency distributions were variable (shown in the relevant Appendix), with the data weighting giving observer length frequency samples low effective sample size, while fits to the trawl survey length frequency distributions were generally better, and effective sample size larger, but there was little difference in the fits between models. The estimated combined SSB_0 was lower than the models excluding the trawl survey data, and increased with M , ranging from 6611 t ($M=0.15$) to 7804 t ($M=0.35$), although SSB_{2014} as a percentage of SSB_0 was more comparable with the other models, ranging from 51% – 54%. As with the other models, these models consistently estimated the MO subarea to have the most optimistic stock status (relative to SSB_0), and the MN subarea to have the least, but all estimates were above 40% SSB_0 .

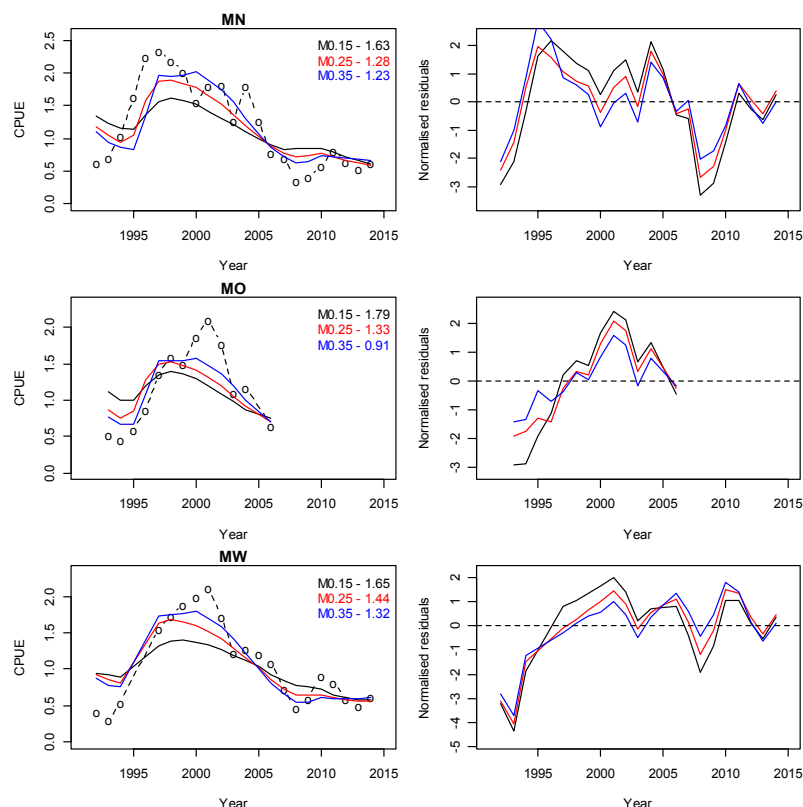


Figure 44: Fits to CPUE indices (left column) and normalised residuals (right column) for each subarea for models excluding photographic survey data with M fixed at 0.15 (black), 0.25 (red) or 0.35 (blue).

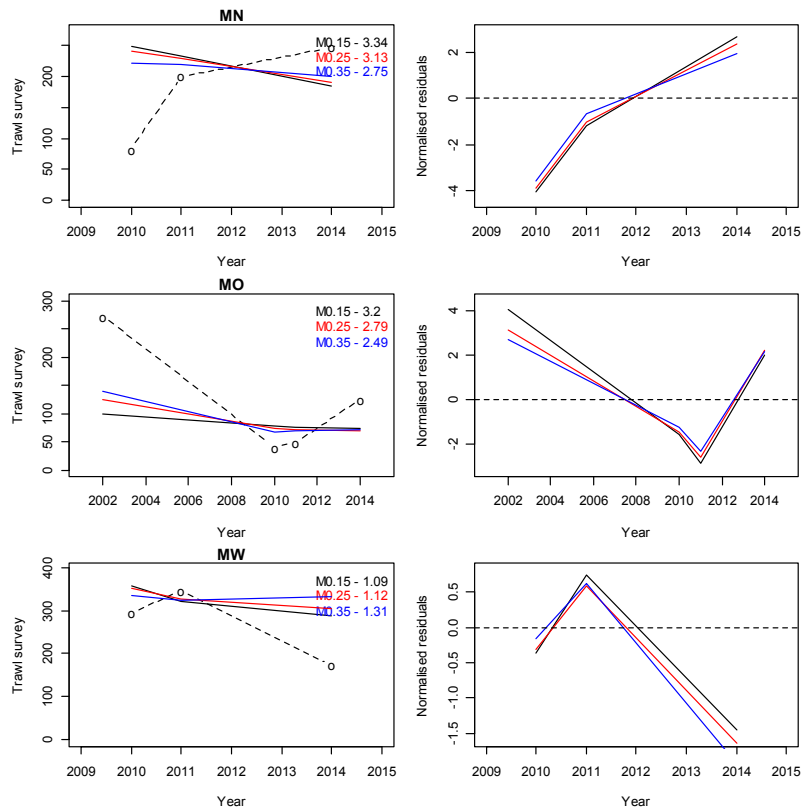


Figure 45: Fits to trawl survey indices (left column) and normalised residuals (right column) for each subarea for models excluding photographic survey data with M fixed at 0.15 (black), 0.25 (red) or 0.35 (blue).

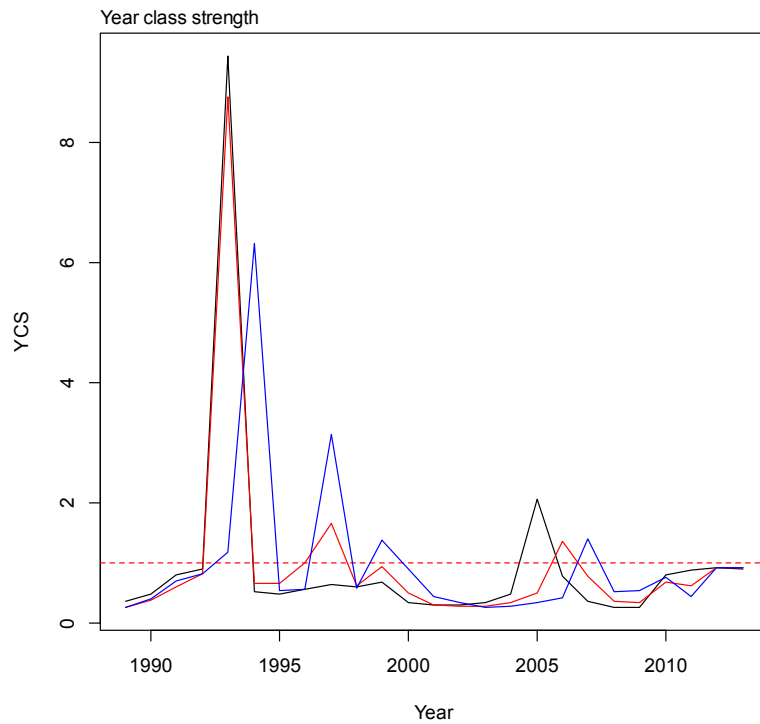


Figure 46: Year class strength for models excluding photographic surveys with M fixed at 0.15 (black), 0.25 (red) or 0.35 (blue).

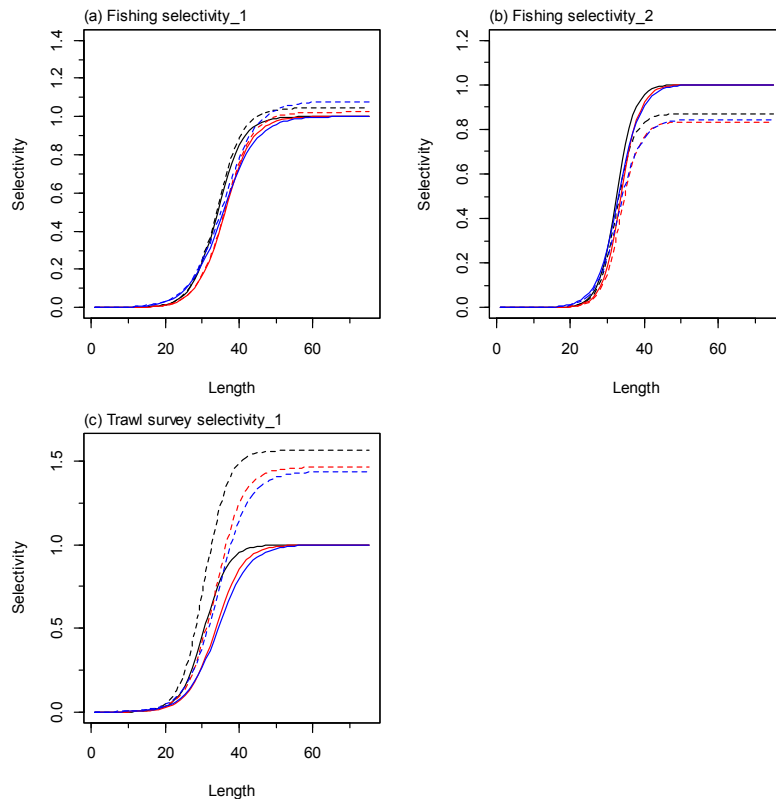


Figure 47: Fishery and survey selectivity curves for models excluding photographic surveys, with M fixed at 0.15 (black), 0.25 (red) or 0.35 (blue). Solid line – females, dotted line – males.

The likelihood profile when B_0 is fixed (for one subarea) shows a minimum at just under 8000 t (total SSB, three subareas combined) (shown for the NP_0.25 model; A7. 25). The likelihood profile is slightly more U shaped than the equivalent for the model excluding trawl data (A4. 25). The various data sets do not provide any consistent signal, and none are particularly informative, other than suggesting that the combined SSB_0 is greater than about 6000 t. The prior for *q-trawl* appears quite influential.

MCMC runs

MCMC runs were explored for all three models, and are presented for each in the Appendices, but are only discussed in detail for the NP_0.25 model. Three independent MCMC chains were started a random step away from the MPD for the model, and run for a minimum of 2.7 million simulations (determined by the minimum length of the three chains at the time analysis needed to be conducted), with every 1000th sample saved, giving a set of 2700 samples. The three chains were examined for evidence of lack of convergence (A7. 26 – A7. 28), and concatenated to produce a sample chain for projections. The three chains were quite consistent, and did not provide evidence of lack of convergence, and were considered acceptable by the SFAWG. The posterior distributions of the trawl survey catchabilities were within the prior distribution (A7. 31), with the MPD estimates also located within the posterior distribution. The posterior trajectory of overall SSB (Figure 48, individual subarea plots provided in Appendices) suggests an increase in SSB until 1999, followed by a decline to 2008, and a slower decline to 2014. YCS shows strong recruitment in 1993 and 1994, with only 1997, 1999 and 2007 estimated at or above average. The median estimate of current status (SSB_{2014}/SSB_0) for the combined subareas is 54% (ranging from 45% to 65% for individual subareas), with 70% to 88% probability (depending on M) that SSB_{2014} for MN is above 40% SSB_0 , and 100% probability that the other subareas or the combined biomass is above 40% SSB_0 (Table 14).

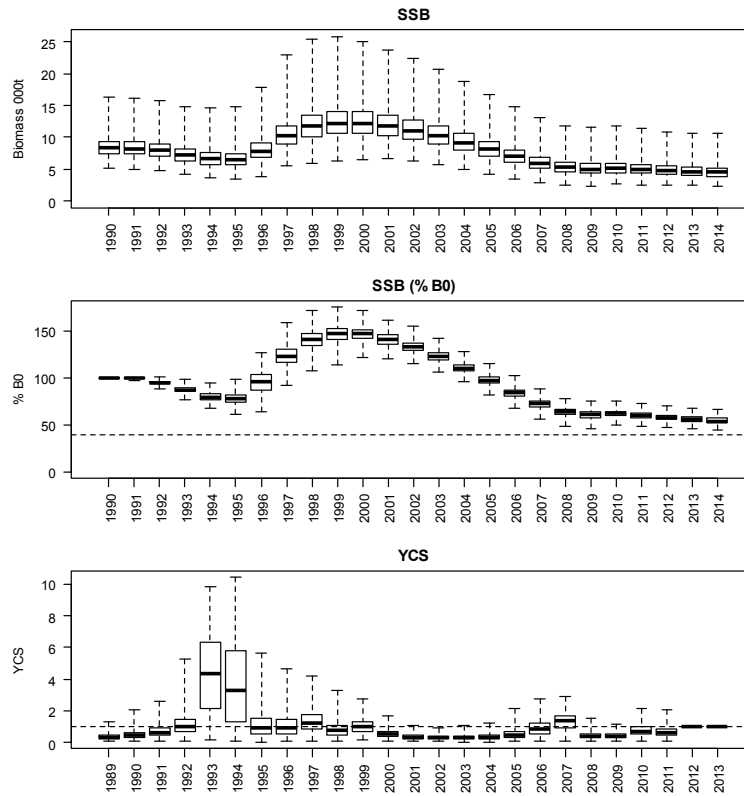


Figure 48: Posterior trajectory of combined SSB, SSB_{2014}/SSB_0 and YCS for model NP_0.25. The solid line within each box represents the median value, the upper and lower ends of the box are the upper and lower quartiles, and the dashed lines extend out to the upper and lower adjacent values, the largest (smallest) value less (greater) than or equal to the upper (lower) quartile plus (minus) 1.5 times the interquartile range.

Table 14: Estimates of SSB_0 , SSB_{2014} , SSB_{2014}/SSB_0 and the probability of SSB_{2014} being below 10% SSB_0 , below 20% SSB_0 , or above 40% SSB_0 , from MCMC runs for models excluding the photographic survey data. Estimates provided at the subarea and combined stock level.

	SSB_0	SSB_{2014}	SSB_{2014}/SSB_0	P $SSB_{2014} < 10\%SSB_0$	P $SSB_{2014} < 20\%SSB_0$	P $SSB_{2014} > 40\%SSB_0$
NP_0.15						
MN	3243	1405	0.43	0.000	0.000	0.706
MW	2829	1734	0.61	0.000	0.000	1.000
MO	949	646	0.68	0.000	0.000	1.000
SCI 3	7162	3898	0.54	0.000	0.000	1.000
NP_0.25						
MN	3391	1542	0.45	0.000	0.000	0.835
MW	3799	2200	0.58	0.000	0.000	1.000
MO	924	597	0.65	0.000	0.000	1.000
SCI 3	8330	4485	0.54	0.000	0.000	1.000
NP_0.35						
MN	3341	1569	0.47	0.000	0.000	0.887
MW	4179	2416	0.58	0.000	0.000	1.000
MO	930	595	0.64	0.000	0.000	1.000
SCI 3	8653	4729	0.55	0.000	0.000	1.000

While the two model approaches (excluding either the trawl survey or the photographic survey data) provide very different estimates of SSB_0 and current SSB (Figure 49), the estimated stock status ($\%SSB_0$) follows a very similar trajectory, only showing a slight divergence in the most recent years. The model excluding the trawl survey data shows a slight increase in $\%SSB_0$ while the model excluding the photographic survey data remains stable. YCS trajectories remain similar between models until 2010, where the increase in the photographic survey index observed in the most recent years is interpreted as an increase in recruitment.

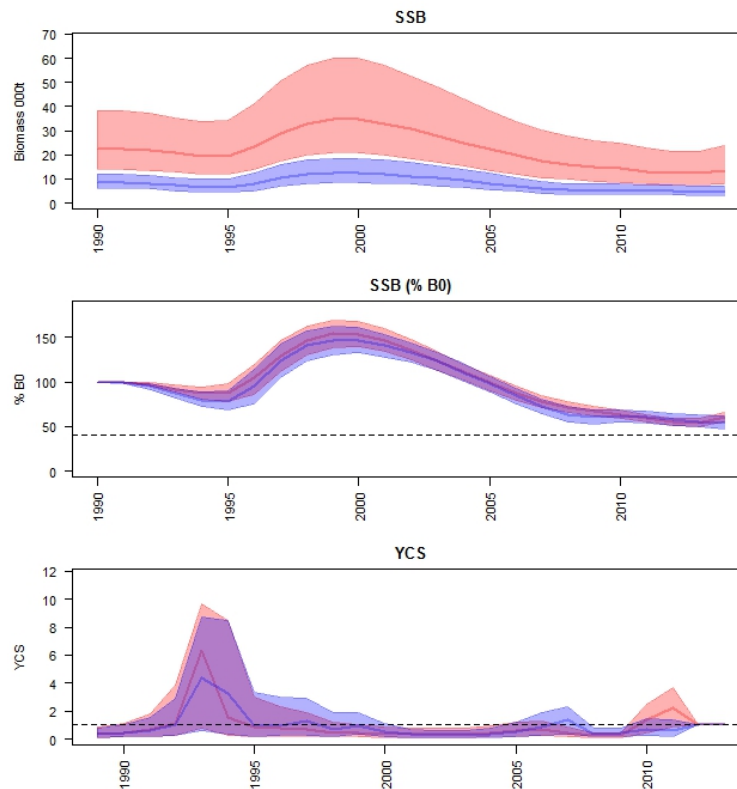


Figure 49: Comparison of combined SCI 3 stock SSB , $\%SSB_0$, and YCS for the model excluding trawl survey (red) and photographic survey (blue) data. The thick line represents the median, and shaded area the 95% credible interval, of the posterior distribution.

4.3 Projections

The assessments reported SSB_0 and $SSB_{current}$ and used the ratio of current and projected SSB to SSB_0 as preferred indicators. Projections were conducted up to 2020 on the basis of scenarios maintaining catches by subarea at current levels (Status quo), or increasing catches to the TACC (either in the current proportions between subareas (TACC(SQ)), or with all available additional catch taken from the MO subarea (TACC(MO))) (Table 15). These two TACC scenarios are believed to encompass the range of extremes possible, but in reality if catches are increased to the TACC, some balance between the two scenarios is likely, with more effort in the currently very lightly exploited MO subarea. Projections have been conducted by randomly resampling year class strengths from the last decade estimated within the model (2002 – 2011). The SSB and stock status relative to SSB_0 , and probability of exceeding the default Harvest Strategy Standard target and limit reference points are reported for the catch scenarios for model NT_0.25 (Table 16) and model NP_0.25 (Table 17).

Table 15: Allocation of catches (tonnes) to subarea and time step for the catch scenarios used in the projections for SCI 3.

Scenario	Total catch	Subarea time step					
		MN 1	MN 2	MO 1	MO 2	MW 1	MW 2
Status quo	279 Average of last 5 yrs	121.30	65.12	0.02	0.02	38.78	54.20
TACC (SQ)	340 Status quo scaled to TACC	147.59	79.23	0.03	0.02	47.19	65.95
TACC (MO)	340 Status quo with extra taken from MO	121.30	65.12	30.28	30.28	38.78	54.20

For the model excluding the trawl survey data, each of the catch scenarios examined predict the increase in SSB to continue until 2016 or 2017, followed by a more stable period, with SSB_{2020} projected to be 70% SSB_0 for the SCI 3 stock, and 65% to 76% SSB_0 for individual subareas (Table 16). Projections varied slightly between the TACC catch scenario options, with TACC(SQ) (current catches scaled to TACC) leading to a slightly reduced stock status for subareas MN and MW, while TACC(MO) (current catches from MN and MW fixed and additional catch all taken from MO) leading to reduced stock status for subarea MO. Across all the scenarios, there is a greater than 99.9% probability of SSB_{2020} being above 40% SSB_0 at the stock level, and greater than 98% probability at the subarea level. Projected stock trajectories for the different catch scenarios are shown for model NT_0.25 in Figure 50 to Figure 52.

Table 16: Results from projection runs showing SSB_0 , SSB_{curr} , SSB_{2018} and SSB_{2020} estimates and probability of exceeding Harvest Strategy Standard target and limit reference points for the model excluding trawl survey ($M=0.25$), with different catch scenarios for SCI 3.

	Status quo				TACC (SQ)				TACC (MO)			
	MN	MW	MO	SCI 3	MN	MW	MO	SCI 3	MN	MW	MO	SCI 3
SSB_0	9550	7539	5294	22424	9550	7539	5294	22424	9550	7539	5294	22424
SSB_{2014}	5489	4516	3442	13497	5489	4516	3442	13497	5489	4516	3442	13497
SSB_{2014}/SSB_0	0.57	0.60	0.65	0.60	0.57	0.60	0.65	0.60	0.57	0.60	0.65	0.60
SSB_{2018}/SSB_0	0.69	0.72	0.78	0.73	0.68	0.72	0.78	0.72	0.69	0.72	0.75	0.72
SSB_{2018}/SSB_{2014}	1.20	1.21	1.20	1.21	1.18	1.20	1.20	1.20	1.20	1.21	1.16	1.20
SSB_{2020}/SSB_0	0.66	0.70	0.76	0.71	0.65	0.69	0.76	0.70	0.66	0.70	0.72	0.70
SSB_{2020}/SSB_{2014}	1.15	1.16	1.16	1.17	1.13	1.15	1.16	1.16	1.15	1.16	1.11	1.16
P $SSB_{2014} < 10\%SSB_0$	0.000	0.000	0.000	0.000	0.000	0.000	0.000	0.000	0.000	0.000	0.000	0.000
P $SSB_{2014} < 20\%SSB_0$	0.000	0.000	0.000	0.000	0.000	0.000	0.000	0.000	0.000	0.000	0.000	0.000
P $SSB_{2014} > 40\%SSB_0$	1.000	1.000	1.000	1.000	1.000	1.000	1.000	1.000	1.000	1.000	1.000	1.000
P $SSB_{2018} < 10\%SSB_0$	0.000	0.000	0.000	0.000	0.000	0.000	0.000	0.000	0.000	0.000	0.000	0.000
P $SSB_{2018} < 20\%SSB_0$	0.000	0.000	0.000	0.000	0.000	0.000	0.000	0.000	0.000	0.000	0.000	0.000
P $SSB_{2018} > 40\%SSB_0$	0.999	1.000	1.000	1.000	0.999	1.000	1.000	1.000	0.999	1.000	1.000	1.000
P $SSB_{2018} > SSB_{2014}$	0.880	0.911	0.925	0.965	0.852	0.893	0.925	0.954	0.880	0.911	0.849	0.954
P $SSB_{2020} < 10\%SSB_0$	0.000	0.000	0.000	0.000	0.000	0.000	0.000	0.000	0.000	0.000	0.000	0.000
P $SSB_{2020} < 20\%SSB_0$	0.000	0.000	0.000	0.000	0.000	0.000	0.000	0.000	0.000	0.000	0.000	0.000
P $SSB_{2020} > 40\%SSB_0$	0.990	0.998	1.000	1.000	0.984	0.997	1.000	1.000	0.990	0.998	1.000	1.000
P $SSB_{2020} > SSB_{2014}$	0.729	0.760	0.804	0.880	0.687	0.736	0.804	0.855	0.729	0.760	0.686	0.855

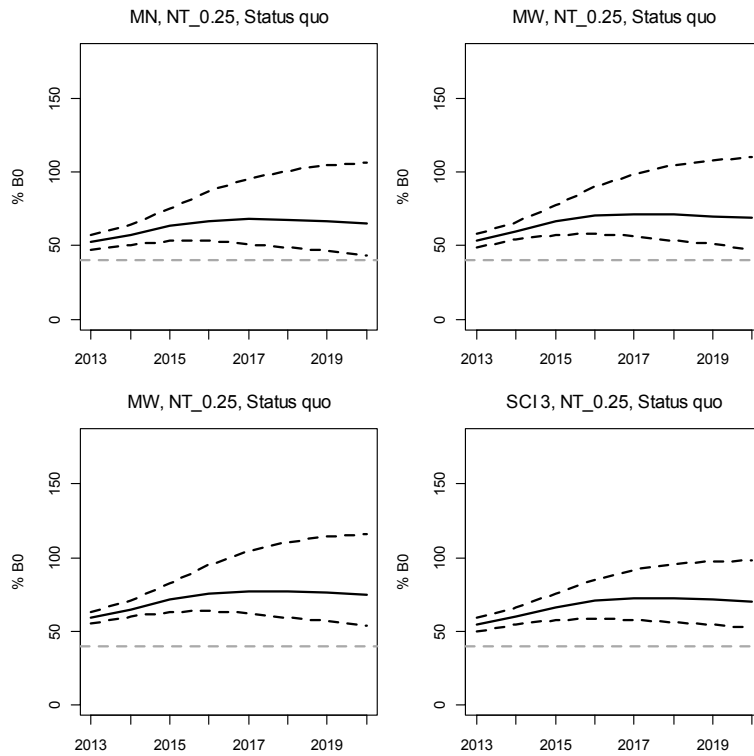


Figure 50: Projected stock trajectory (as a % of SSB₀) for subareas and the overall SCI 3 stock from model NT_0.25 for the status quo constant future catches. Solid black line represents median of projections, while dashed black lines represent 2.5th and 97.5th quantiles. Horizontal dashed grey line represents 40% SSB₀.

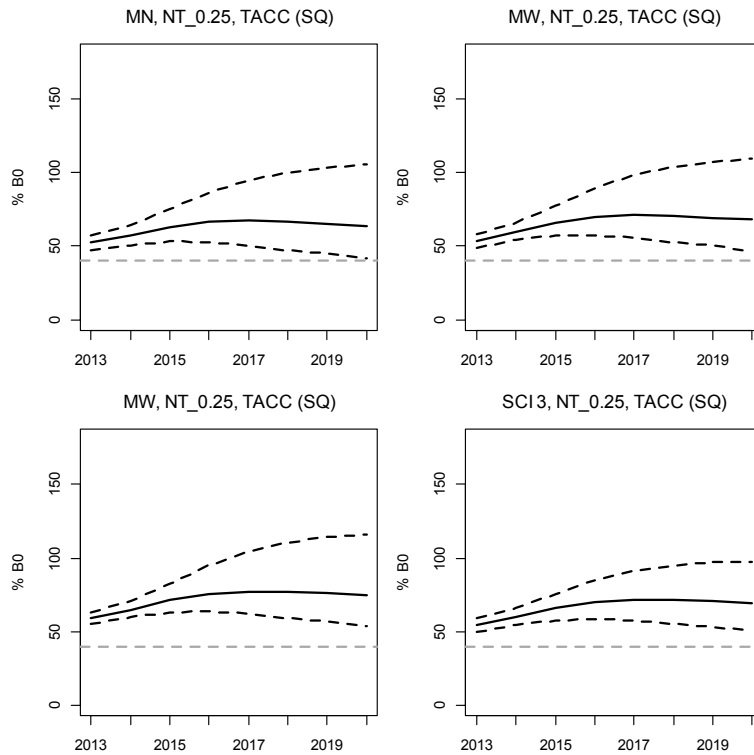


Figure 51: Projected stock trajectory (as a % of SSB₀) for subareas and the overall SCI 3 stock from model NT_0.25 for the TACC (SQ) constant future catches. Solid black line represents median of projections, while dashed black lines represent 2.5th and 97.5th quantiles. Horizontal dashed grey line represents 40% SSB₀.

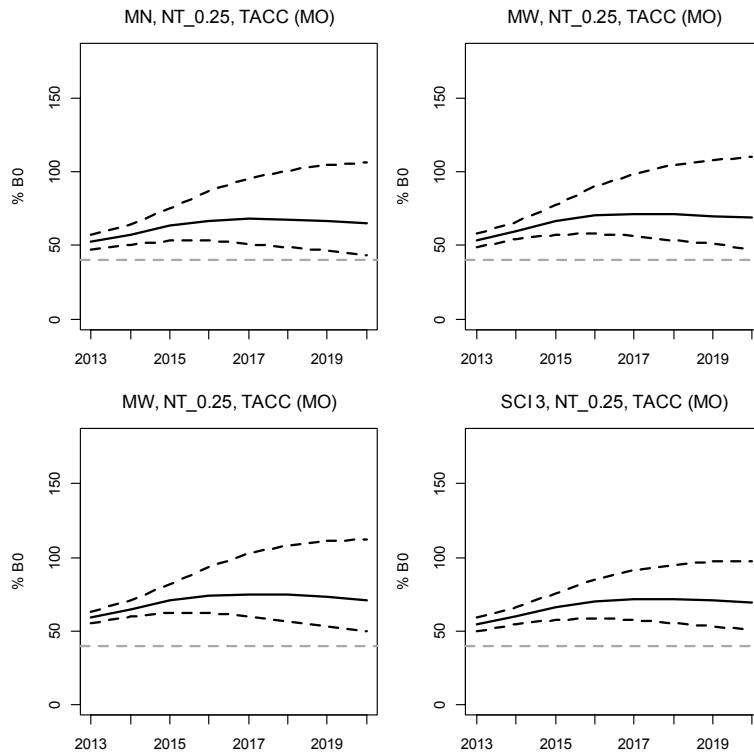


Figure 52: Projected stock trajectory (as a % of SSB_0) for subareas and the overall SCI 3 stock from model NT_0.25 for the TAC (MO) constant future catches. Solid black line represents median of projections, while dashed black lines represent 2.5th and 97.5th quantiles. Horizontal dashed grey line represents 40% SSB_0 .

Projections for the model excluding the photographic survey data were less optimistic (Table 17). Each of the catch scenarios examined predict a gradual decline in SSB, with SSB_{2020} projected to be 42% to 44% SSB_0 for the SCI 3 stock, and 29% to 59% SSB_0 for individual subareas (Table 17). As with the model excluding the trawl survey data, projections varied slightly between the TACC catch scenario options, with TACC(SQ) (current catches scaled to TACC) leading to a slightly reduced stock status for subareas MN and MW, while TACC(MO) (current catches from MN and MW fixed and additional catch all taken from MO) leading to reduced stock status for subarea MO. The projections indicate a 57% probability of SSB_{2020} being above 40% SSB_0 at the stock level with catches increased to the TACC, while maintaining catches at current levels gives a 69% probability of SSB_{2020} being above 40% SSB_0 . Projected stock trajectories for the different catch scenarios are shown for model NP_0.25 in Figure 53 to Figure 55.

Table 17: Results from projection runs showing SSB_0 , SSB_{curr} , SSB_{2018} and SSB_{2020} estimates and probability of exceeding Harvest Strategy Standard target and limit reference points for the model excluding photographic survey ($M=0.25$), with different catch scenarios for SCI 3.

	Status quo				TACC (SQ)				TACC (MO)			
	MN	MW	MO	SCI 3	MN	MW	MO	SCI 3	MN	MW	MO	SCI 3
SSB_0	3391	3799	924	8330	3391	3799	924	8330	3391	3799	924	8330
SSB_{2014}	1542	2200	597	4485	1542	2200	597	4485	1542	2200	597	4485
SSB_{2014}/SSB_0	0.45	0.58	0.65	0.54	0.45	0.58	0.65	0.54	0.45	0.58	0.65	0.54
SSB_{2018}/SSB_0	0.36	0.51	0.61	0.47	0.33	0.50	0.61	0.45	0.36	0.51	0.45	0.45
SSB_{2018}/SSB_{2014}	0.80	0.89	0.94	0.87	0.74	0.87	0.94	0.83	0.80	0.89	0.70	0.83
SSB_{2020}/SSB_0	0.33	0.48	0.59	0.44	0.29	0.47	0.59	0.42	0.33	0.48	0.38	0.42
SSB_{2020}/SSB_{2014}	0.73	0.84	0.92	0.82	0.64	0.81	0.92	0.77	0.73	0.84	0.59	0.77
P $SSB_{2014} < 10\%SSB_0$	0.000	0.000	0.000	0.000	0.000	0.000	0.000	0.000	0.000	0.000	0.000	0.000
P $SSB_{2014} < 20\%SSB_0$	0.000	0.000	0.000	0.000	0.000	0.000	0.000	0.000	0.000	0.000	0.000	0.000
P $SSB_{2014} > 40\%SSB_0$	0.835	1.000	1.000	1.000	0.835	1.000	1.000	1.000	0.835	1.000	1.000	1.000
P $SSB_{2018} < 10\%SSB_0$	0.002	0.000	0.000	0.000	0.006	0.000	0.000	0.000	0.002	0.000	0.000	0.000
P $SSB_{2018} < 20\%SSB_0$	0.040	0.000	0.000	0.000	0.092	0.000	0.000	0.000	0.040	0.000	0.002	0.000
P $SSB_{2018} > 40\%SSB_0$	0.345	0.902	1.000	0.832	0.262	0.867	1.000	0.758	0.345	0.902	0.676	0.757
P $SSB_{2018} > SSB_{2014}$	0.137	0.219	0.334	0.112	0.081	0.180	0.334	0.072	0.137	0.219	0.030	0.072
P $SSB_{2020} < 10\%SSB_0$	0.012	0.000	0.000	0.000	0.043	0.000	0.000	0.000	0.012	0.000	0.003	0.000
P $SSB_{2020} < 20\%SSB_0$	0.125	0.000	0.000	0.000	0.223	0.001	0.000	0.000	0.125	0.000	0.053	0.001
P $SSB_{2020} > 40\%SSB_0$	0.272	0.787	0.988	0.689	0.182	0.731	0.988	0.573	0.272	0.787	0.430	0.574
P $SSB_{2020} > SSB_{2014}$	0.104	0.188	0.309	0.086	0.062	0.147	0.309	0.050	0.104	0.188	0.019	0.050

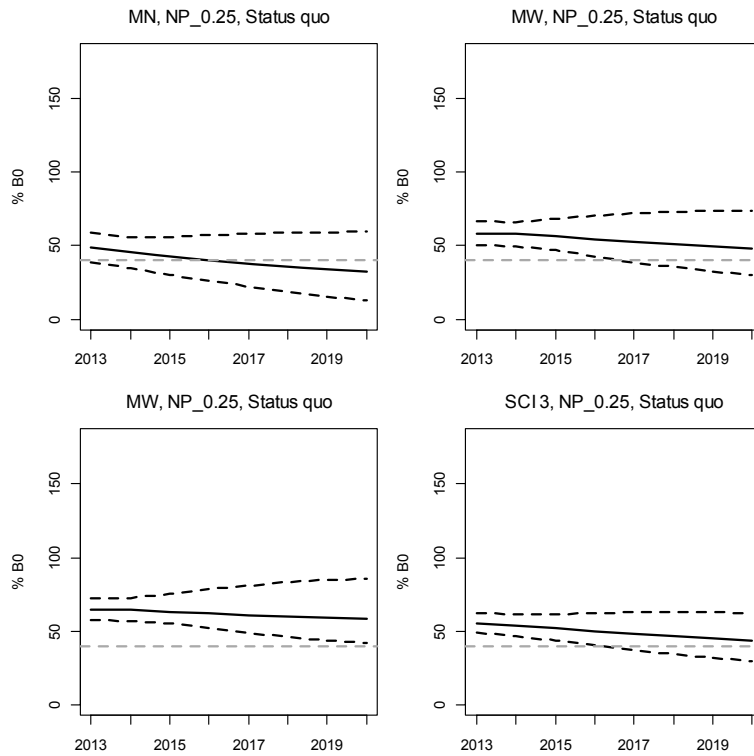


Figure 53: Projected stock trajectory (as a % of SSB₀) for subareas and the overall SCI 3 stock from model NP_0.25 for the status quo constant future catches. Solid black line represents median of projections, while dashed black lines represent 2.5th and 97.5th quantiles. Horizontal dashed grey line represents 40% SSB₀.

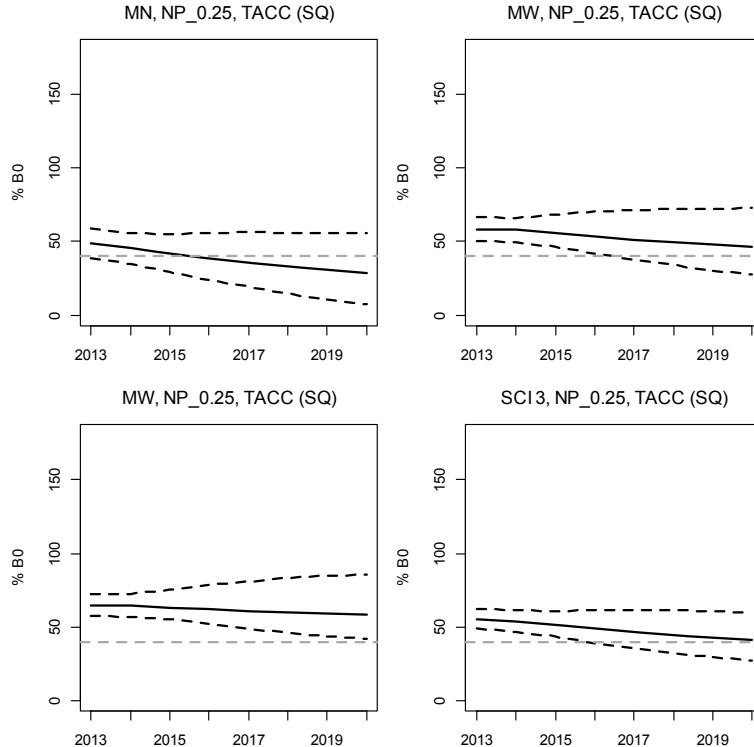


Figure 54: Projected stock trajectory (as a % of SSB₀) for subareas and the overall SCI 3 stock from model NP_0.25 for the TACC (SQ) constant future catches. Solid black line represents median of projections, while dashed black lines represent 2.5th and 97.5th quantiles. Horizontal dashed grey line represents 40% SSB₀.

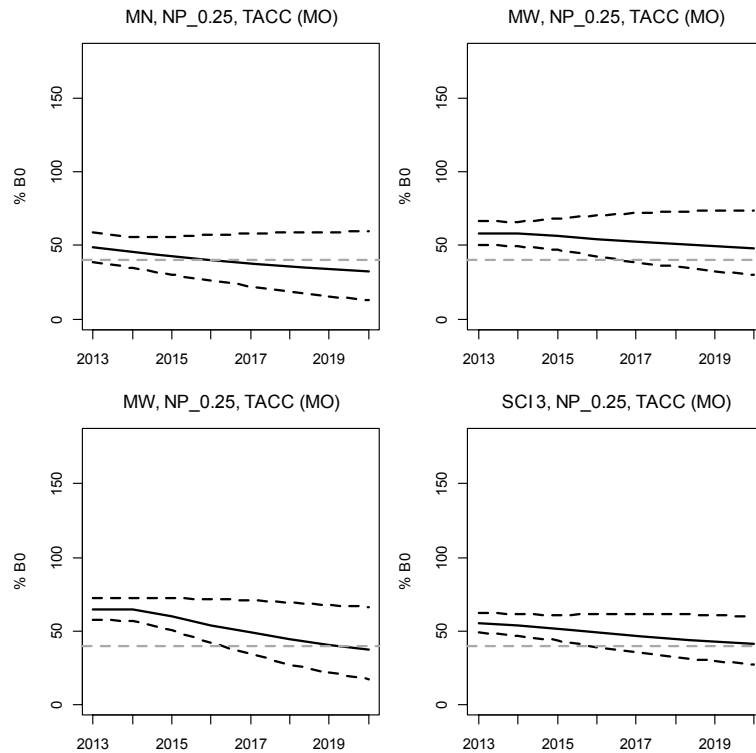


Figure 55: Projected stock trajectory (as a % of SSB₀) for subareas and the overall SCI 3 stock from model NP_0.25 for the TACC (MO) constant future catches. Solid black line represents median of projections, while dashed black lines represent 2.5th and 97.5th quantiles. Horizontal dashed grey line represents 40% SSB₀.

5. DISCUSSION

An assessment of the SCI 3 stock was last attempted in 2012 (Tuck 2013), and the current study has developed the model further. The assessment was accepted, although contrasting trends between trawl and photographic surveys meant that two models were explored, one excluding the trawl survey data, and one excluding the photographic survey data.

Preliminary analysis suggested that slight modifications were needed to the previously adopted model structure for this area, and a three (subarea) stock, two time step model was developed, with shared YCS and some shared catchability parameters. The model year was shifted slightly from the fishing year, to combine the months from August to December into a single time step. Base models were developed, with M fixed at 0.15, 0.25 and 0.35. A single annual standardised CPUE index was calculated for each subarea, and along with trawl survey or photographic survey data, were fitted as abundance indices, with associated length frequency distributions. MCMC diagnostics did not show evidence of lack of convergence, and the models were accepted by the Shellfish Assessment Working Group.

Biomass estimates were different between the two model approaches, but stock status was very similar, the main difference being the model excluding the trawl survey (and including the photographic survey) estimating a slight increase in biomass in the most recent years, associated with above average YCS around 2011. Projections were conducted up to 2020 on the basis of a range of catch scenarios, with the differences between the MCMC runs also reflected in the projections. Models excluding the trawl survey data suggested that the current SSB is 60% SSB₀, and with constant catches set at the TACC, this would increase to 70% SSB₀ by 2020. Models excluding the photographic

survey data suggested that the current SSB is 54% SSB₀, and with constant catches set at the TACC, this would decrease to 42% to 44% SSB₀ by 2020.

6. ACKNOWLEDGEMENTS

This work was funded by the Ministry for Primary Industries under project DEE201002SCID, and builds on a series of scampi assessment projects funded by the Ministry. I thank the many NIWA and Ministry of Fisheries staff who measured scampi over the years, and the members of the NIWA scampi image reading team. Development of the model structure benefitted greatly from comments by Paul Breen in particular, along with other members of the Shellfish Fisheries Assessment Working Group. This report was reviewed by Peter Horn (NIWA, Wellington).

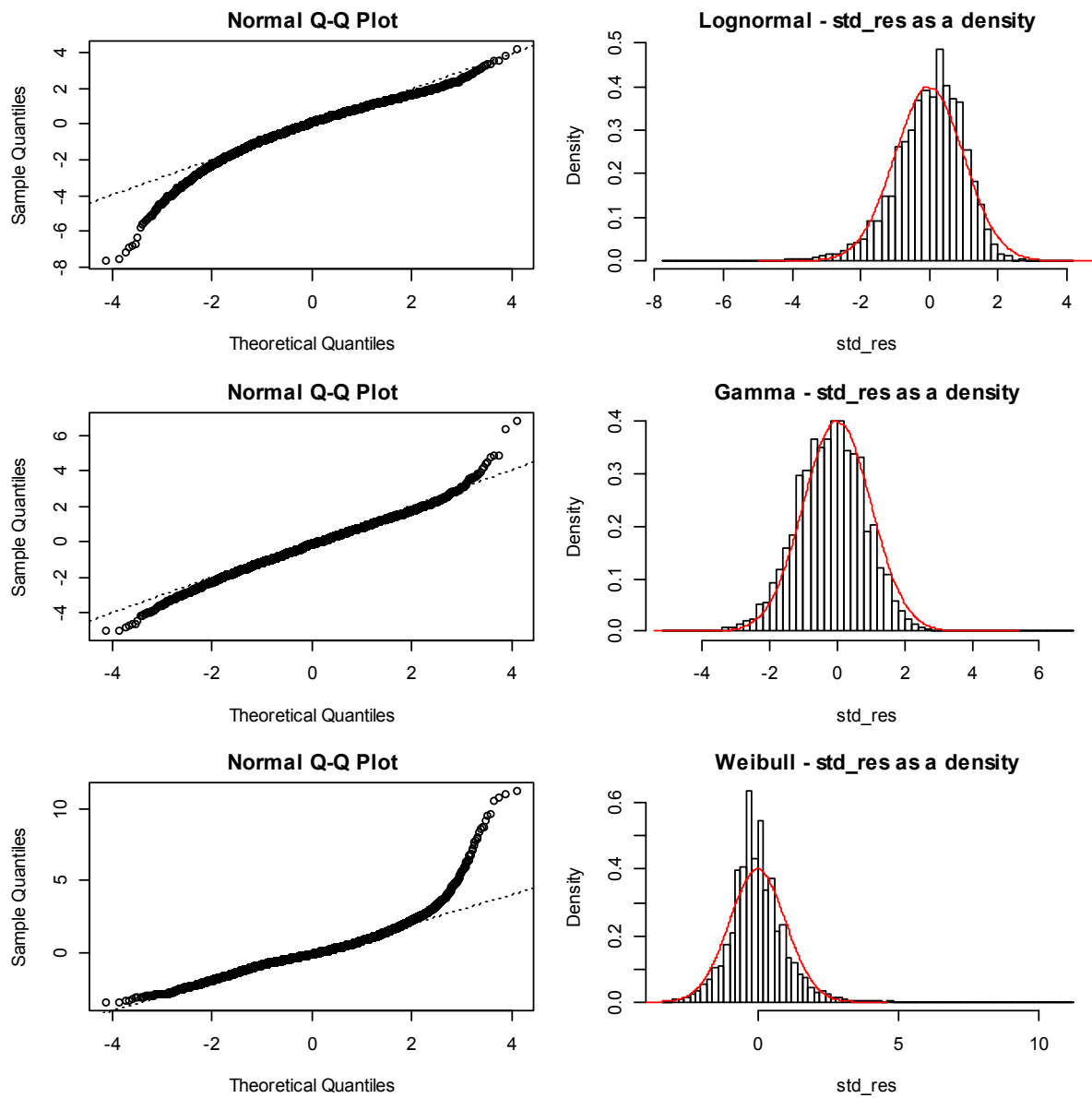
7. REFERENCES

- Bell, M.C., Redant, F., Tuck, I.D. (2006) *Nephrops* species. In: B. Phillips (Ed). *Lobsters: biology, management, aquaculture and fisheries*. Blackwell Publishing, Oxford: 412–461.
- Bentley, N., Kendrick, T.H., Starr, P.J., Breen, P.A. (2012) Influence plots and metrics: tools for better understanding fisheries catch-per-unit-effort standardisations. *ICES Journal of Marine Science*, 69: 84–88.
- Bull, B., Dunn, A. (2002) Catch-at-age: User manual v 1.06.2002/09/12. *NIWA Internal Report*, 114.
- Bull, B., Francis, R.I.C.C., Dunn, A., McKenzie, A., Gilbert, D.J., Smith, M.H., Bian, R. (2008) CASAL (C++ algorithmic stock assessment laboratory). *NIWA Technical Report No.*, 130.
- Chapman, C.J., Johnstone, A.D.F., Urquhart, G.G. (1974) Preliminary acoustic tracking studies on *Nephrops norvegicus*. *Department of Agriculture and Fisheries for Scotland, Marine Laboratory Internal Report*: 15.
- Charnov, E.L., Berrigan, D., Shine, R. (1983) The M/k ratio is the same for fish and reptiles. *American Naturalist*, 142: 707–711.
- Clark, W.G., Hare, S.R. (2006) Assessment and management of Pacific halibut: data, methods, and policy. *International Pacific Halibut Commission Scientific Report*: 111.
- Cryer, M. (2000) A consideration of current management areas for scampi in QMAs 3, 4, 6A and 6B. *Final Research Report for Ministry of Fisheries Project MOF1999-04K*, Objective 1: 52.
- Cryer, M., Coburn, R. (2000) Scampi stock assessment for 1999. *New Zealand Fisheries Assessment Report*, 2000/7.
- Cryer, M., Dunn, A., Hartill, B. (2005) Length-based population model for scampi (*Metanephrops challenger*) in the Bay of Plenty (QMA 1). *New Zealand Fisheries Assessment Report*, 2005/27: 55 p.
- Cryer, M., Hartill, B., Drury, J., Tuck, I.D., Armiger, H., Smith, M., Middleton, C. (2003) Indices of relative abundance for scampi, *Metanephrops challenger*, based on photographic surveys before and after fishing in QMA 3, 2001. *Final Research Report for Ministry of Fisheries research project SCI2000-02*, Obj 3: 33.
- Cryer, M., Stotter, D.R. (1999) Movement and growth rates of scampi inferred from tagging, Alderman Islands, western Bay of Plenty. *NIWA Technical Report No.*, 49.

- Fenaughty, C. (1989) Reproduction in *Metanephrops challengeri*. *Unpublished Report MAF Fisheries, Wellington*: 46.
- Francis, R.I.C.C. (1999) The impact of correlations in standardised CPUE indices. *New Zealand Fisheries Assessment Research Document*: 30.
- Francis, R.I.C.C. (2011) Data weighting in statistical fisheries stock assessment models. *Canadian Journal Fisheries and Aquatic Science*, 68: 1124–1138.
- Francis, R.I.C.C., Bian, R. (2011) Catch-at-length and -age (CALA) User Manual: 83.
- McCullagh, P., Nelder, J.A. (1989) *Generalised Linear Models*. Chapman and Hall, London: 511 p.
- Morizur, Y. (1982) Estimation de la mortalité pour quelques stocks de langoustine, *Nephrops norvegicus*. *ICES CM*, 1982/K:10.
- Pauly, D. (1980) On the interrelationships between natural mortality, growth parameters, and mean environmental temperature in 175 fish stocks. *Journal du Conseil International pour l'Exploration du Mer*, 39: 175–192.
- Smith, P.J. (1999) Allozyme variation in scampi (*Metanephrops challengeri*) fisheries in New Zealand. *New Zealand journal of Marine and Freshwater Research*, 33: 491-497.
- Starr, P.J. (2009) Rock lobster catch and effort data: summaries and CPUE standardisations, 1979–80 to 2007–08. *New Zealand Fisheries Assessment Report*, 2009/38: 73 p.
- Starr, P.J., Breen, P.A., Kendrick, T.H., Haist, V. (2009) Model and data used for the 2008 stock assessment of rock lobsters (*Jasus edwardsii*) in CRA 3. *New Zealand Fisheries Assessment Report*, 2009/22: 62 p.
- Tuck, I., Hartill, B., Parkinson, D., Smith, M., Armiger, H., Rush, N., Drury, J. (2011a) Estimating the abundance of scampi - Relative abundance of scampi, *Metanephrops challengeri*, from photographic surveys in SCI 3 (2009 & 2010). *Final Research Report for Ministry of Fisheries research projects SCI200901 & SCI 201001*.
- Tuck, I.D. (2009) Characterisation of scampi fisheries and the examination of catch at length and spatial distribution of scampi in SCI 1, 2, 3, 4A and 6A. *New Zealand Fisheries Assessment Report*, 2009/27: 102 p.
- Tuck, I.D. (2010) Scampi burrow occupancy, burrow emergence, and catchability. *New Zealand Fisheries Assessment Report*, 2010/13: 58 p. <http://webcat.niwa.co.nz/documents/FAR2010-13.pdf>
- Tuck, I.D. (2013) Characterisation and length-based population model for scampi (*Metanephrops challengeri*) on the Mernoo Bank (SCI 3). *New Zealand Fisheries Assessment Report*, 2013/24: 165 p.
- Tuck, I.D. (2014) Characterisation and length-based population model for scampi (*Metanephrops challengeri*) in the Bay of Plenty (SCI 1) and Hawke Bay/Wairaraoa (SCI 2). *New Zealand Fisheries Assessment Report*, 2014/33: 172 p.
- Tuck, I.D. (2015) Characterisation and length-based population model for scampi (*Metanephrops challengeri*) at the Auckland Islands (SCI 6A). *New Zealand Fisheries Assessment Report*, 2015/21: 164 p.

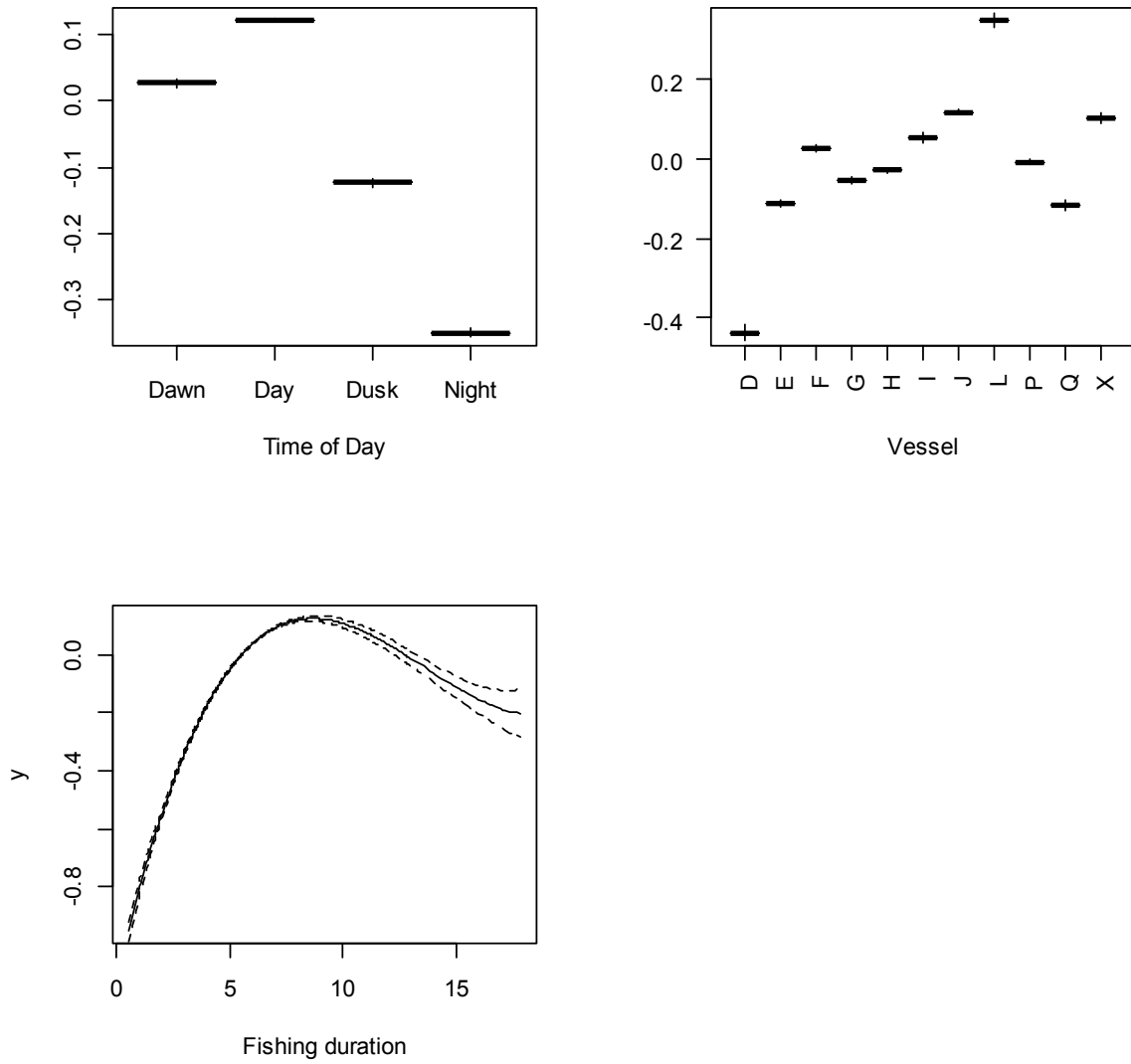
- Tuck, I.D., Atkinson, R.J.A., Chapman, C.J. (2000) Population biology of the Norway lobster, *Nephrops norvegicus* (L.) in the Firth of Clyde, Scotland. II. Fecundity and size at onset of maturity. *ICES Journal of Marine Science*, 57: 1222–1237.
- Tuck, I.D., Dunn, A. (2006) Length based population model for scampi (*Metanephrops challengeri*) in the Bay of Plenty (SCI 1) and Wairarapa / Hawke Bay (SCI 2). *Final Research Report for Ministry of Fisheries research project SCI2005-01*, Objectives 2 & 3: 93.
- Tuck, I.D., Dunn, A. (2009) Length-based population model for scampi (*Metanephrops challengeri*) in the Bay of Plenty (SCI 1) and Wairarapa / Hawke Bay (SCI 2). *Final Research Report for Ministry of Fisheries research project SCI2008-03*, Obj 1: 30.
- Tuck, I.D., Dunn, A. (2012) Length-based population model for scampi (*Metanephrops challengeri*) in the Bay of Plenty (SCI 1), Wairarapa / Hawke Bay (SCI 2) and Auckland Islands (SCI 6A). *New Zealand Fisheries Assessment Report*, 2012/1: 125 p.
- Tuck, I.D., Hartill, B., Parkinson, D., Drury, J., Smith, M., Armiger, H. (2009) Estimating the abundance of scampi - Relative abundance of scampi, *Metanephrops challengeri*, from a photographic survey in SCI 6A (2009). *Final Research Report for Ministry of Fisheries research project SCI2008-01*, Objectives 1 & 2: 26.
- Tuck, I.D., Hartill, B., Parkinson, D., Smith, M., Armiger, H., Rush, N., Drury, J. (2011b) Estimating the abundance of scampi – Relative abundance of scampi, *Metanephrops challengeri*, from photographic surveys in SCI 3 (2009 & 2010). *Final Research Report for Ministry of Fisheries research projects SCI2009-01 & SCI2010-01*: 29.
- Tuck, I.D., Parkinson, D., Armiger, H., Smith, M., Miller, A., Rush, N., Spong, K. (2015a) Estimating the abundance of scampi in SCI 3 (Mernoo Bank) in 2013. *New Zealand Fisheries Assessment Report*, 2015/23: 49 p.
- Tuck, I.D., Parkinson, D., Hartill, B., Drury, J., Smith, M., Armiger, H. (2007) Estimating the abundance of scampi - relative abundance of scampi, *Metanephrops challengeri*, from a photographic survey in SCI 6A (2007). *Final Research Report for Ministry of Fisheries research project SCI2006-02*, Objectives 1 & 2: 29.
- Tuck, I.D., Parsons, D.M., Hartill, B.W., Chiswell, S.M. (2015b) Scampi (*Metanephrops challengeri*) emergence patterns and catchability. *ICES Journal of Marine Science*, 72 (Supplement 1): i199-i210. <http://icesjms.oxfordjournals.org/content/early/2015/01/08/icesjms.fsu244.abstract>
- Vignaux, M. (1994) Catch per unit effort (CPUE) analysis of west coast South Island and Cook Strait spawning hoki fisheries, 1987–93. *New Zealand Fisheries Assessment Research Document*: 29.
- Wear, R.G. (1976) Studies on the larval development of *Metanephrops challengeri* (Balss, 1914) (Decapoda, Nephropidae). *Crustaceana*, 30: 113–122.
- Zacarais, L.D. (2013) Genetic population structure of deep-water prawns *Haliporoides triarthrus* and langoustines *Metanephrops mozambicus* in the South West Indian Ocean: use of mitochondrial DNA to investigate metapopulation structure. *School of Life Sciences*. University of KwaZulu-Natal, Durban: 87.

APPENDIX 1. CPUE standardisation diagnostics

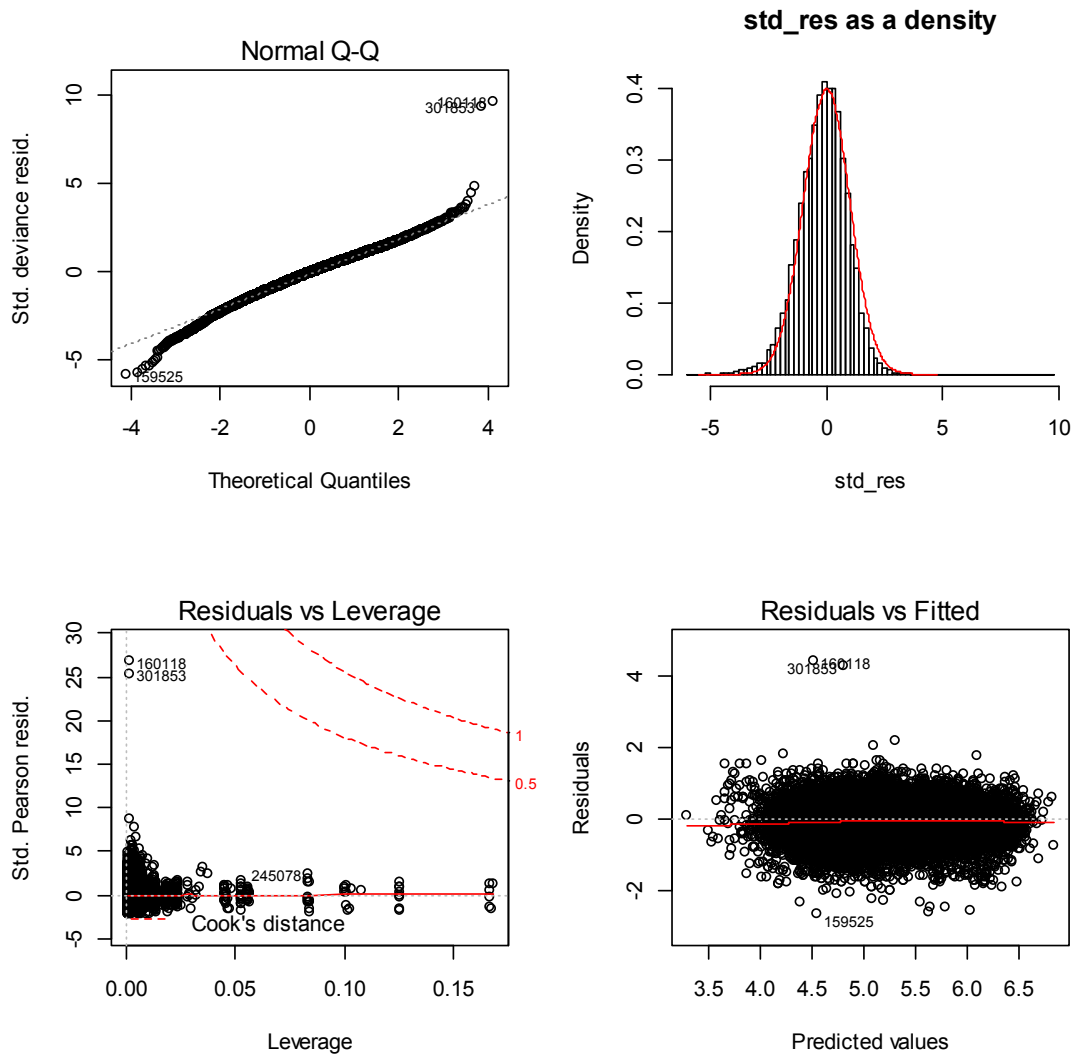


A1. 1: Plots of the distributions of standardised residuals for simple standardised CPUE models with log normal (top panel), gamma (middle panel), and Weibull (bottom panel) error distributions.

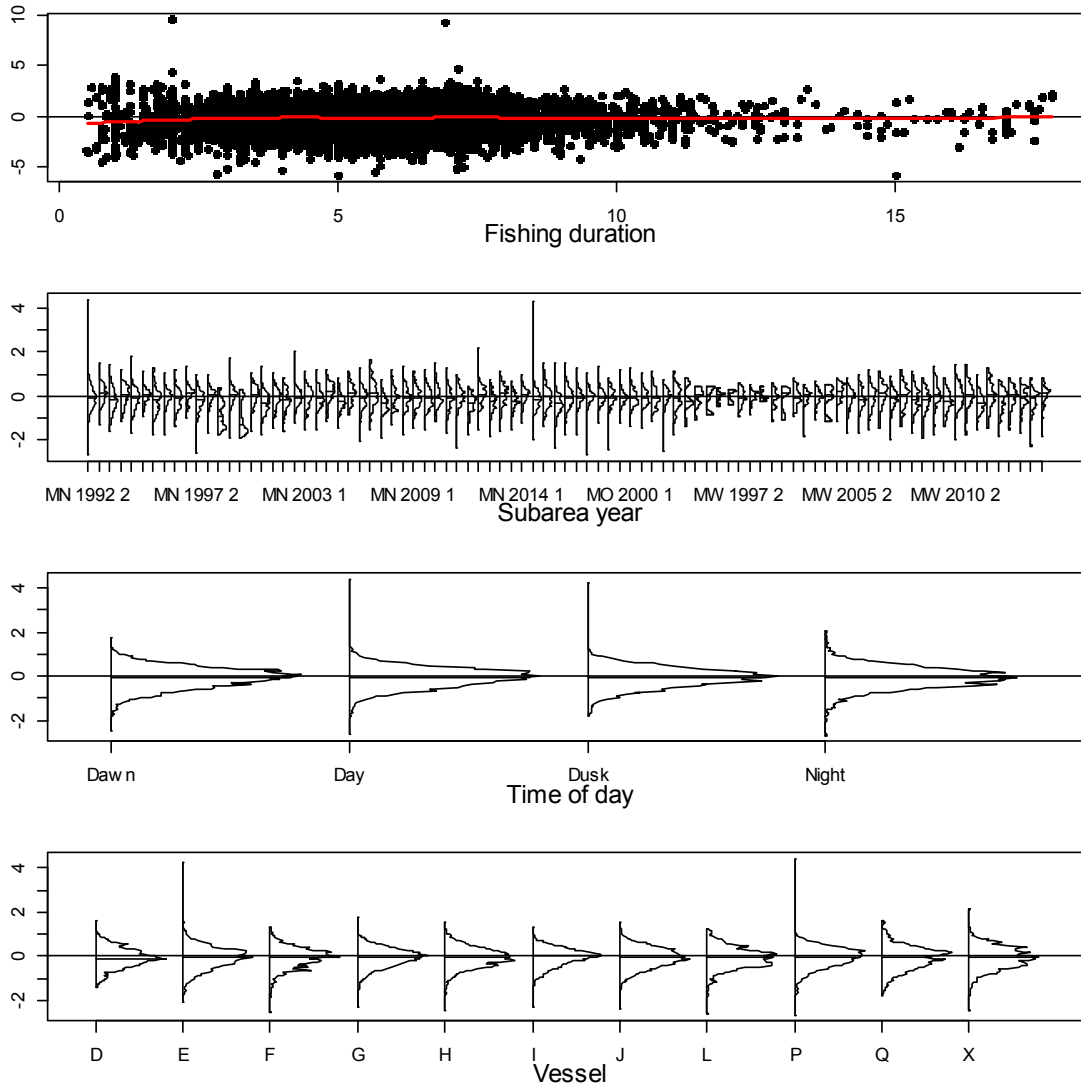
Annual CPUE index



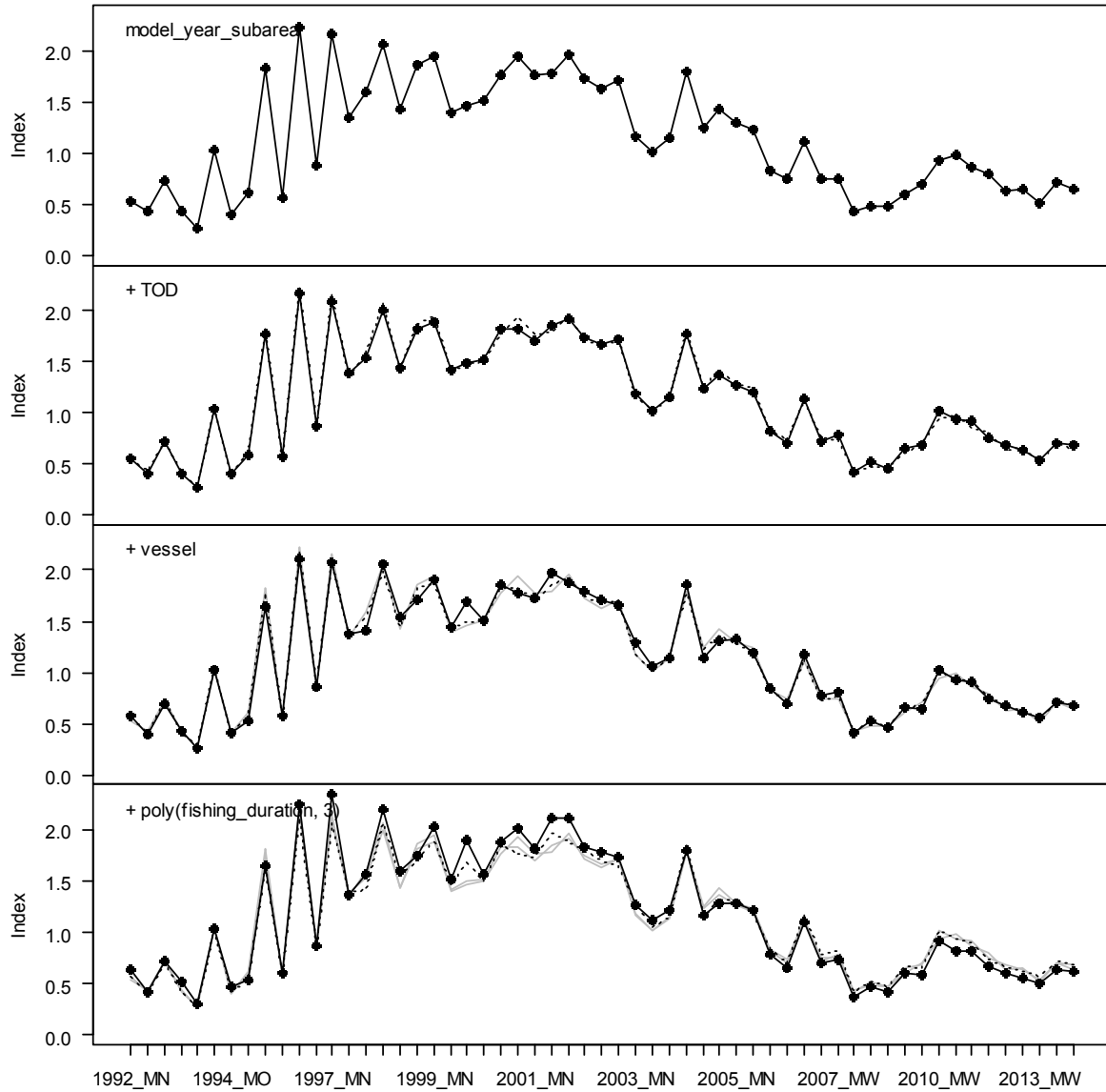
A1. 2: Termplot for final SCI 3 CPUE standardisation model (Table 4).



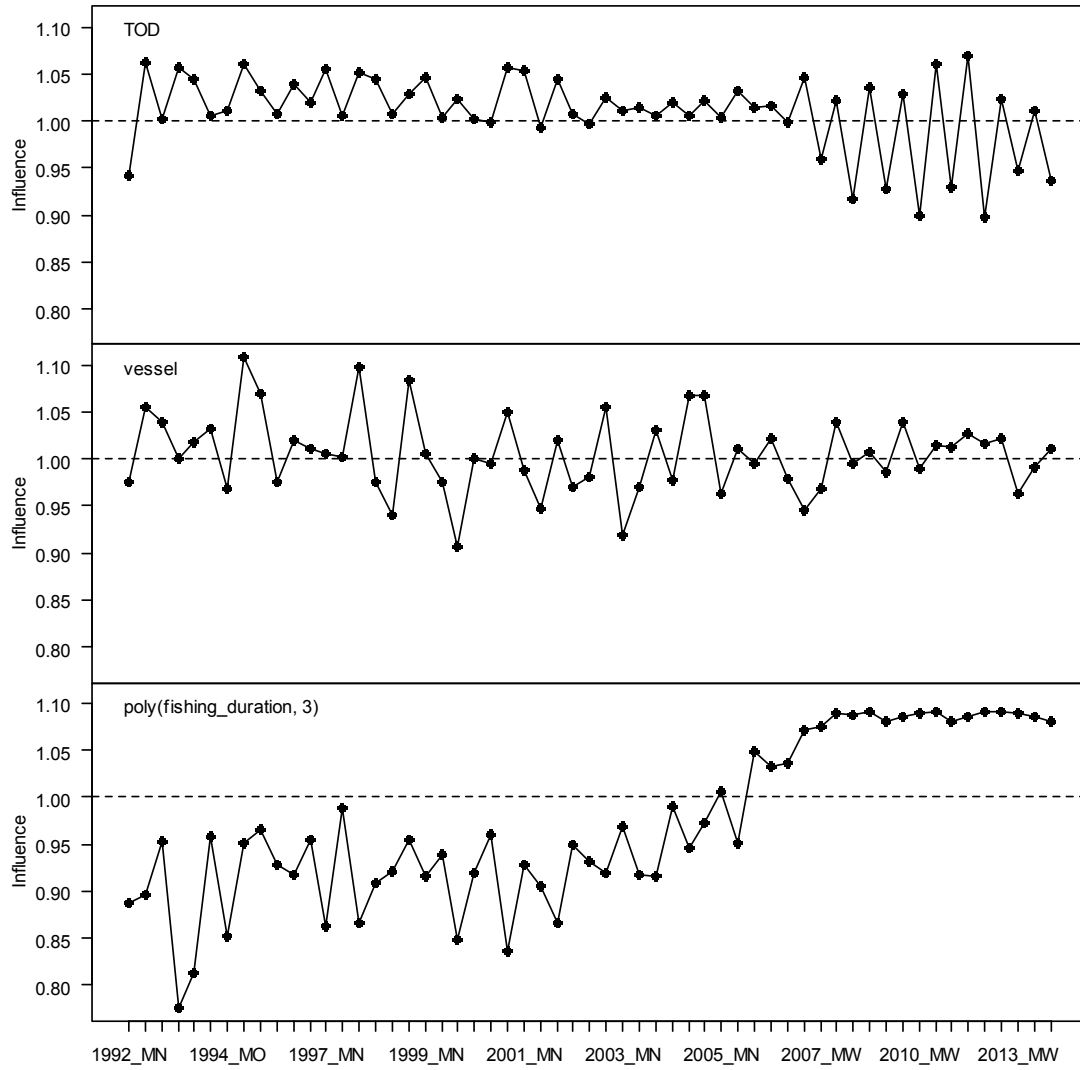
A1. 3: Diagnostic plots for final SCI 3 CPUE standardisation model (Table 4).



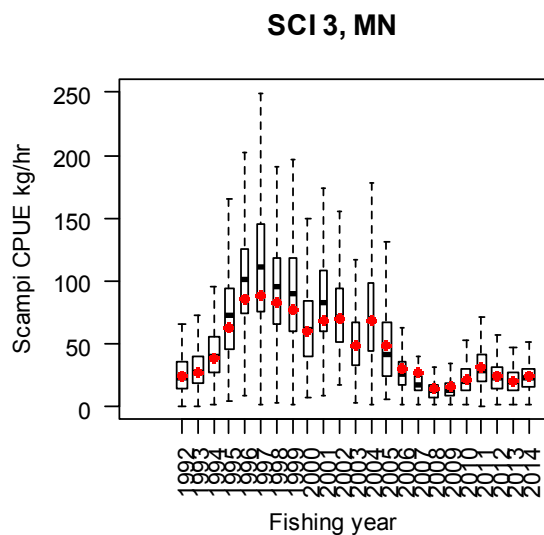
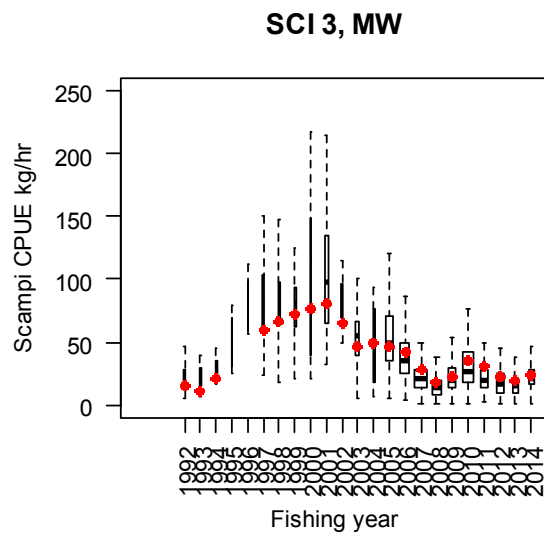
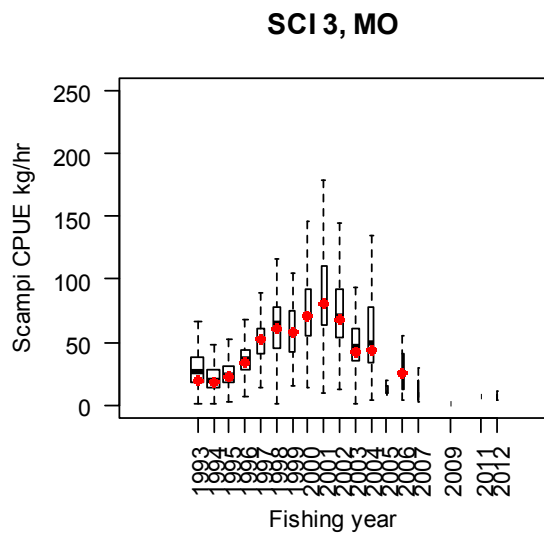
A1. 4: Distributions of residuals for final SCI 3 CPUE standardisation model (Table 4).



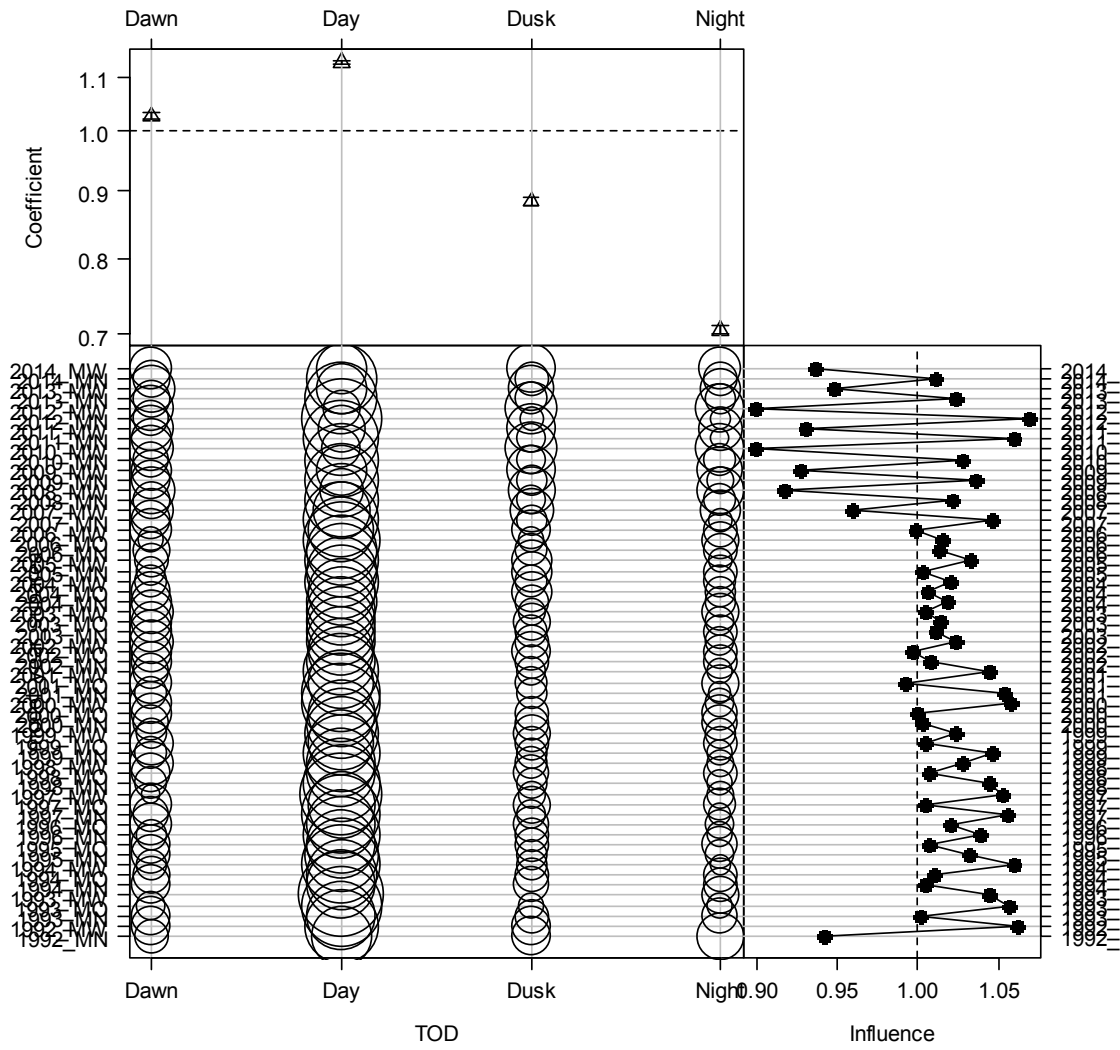
A1. 5: Step influence plot for final SCI 3 CPUE standardisation model (Table 4).



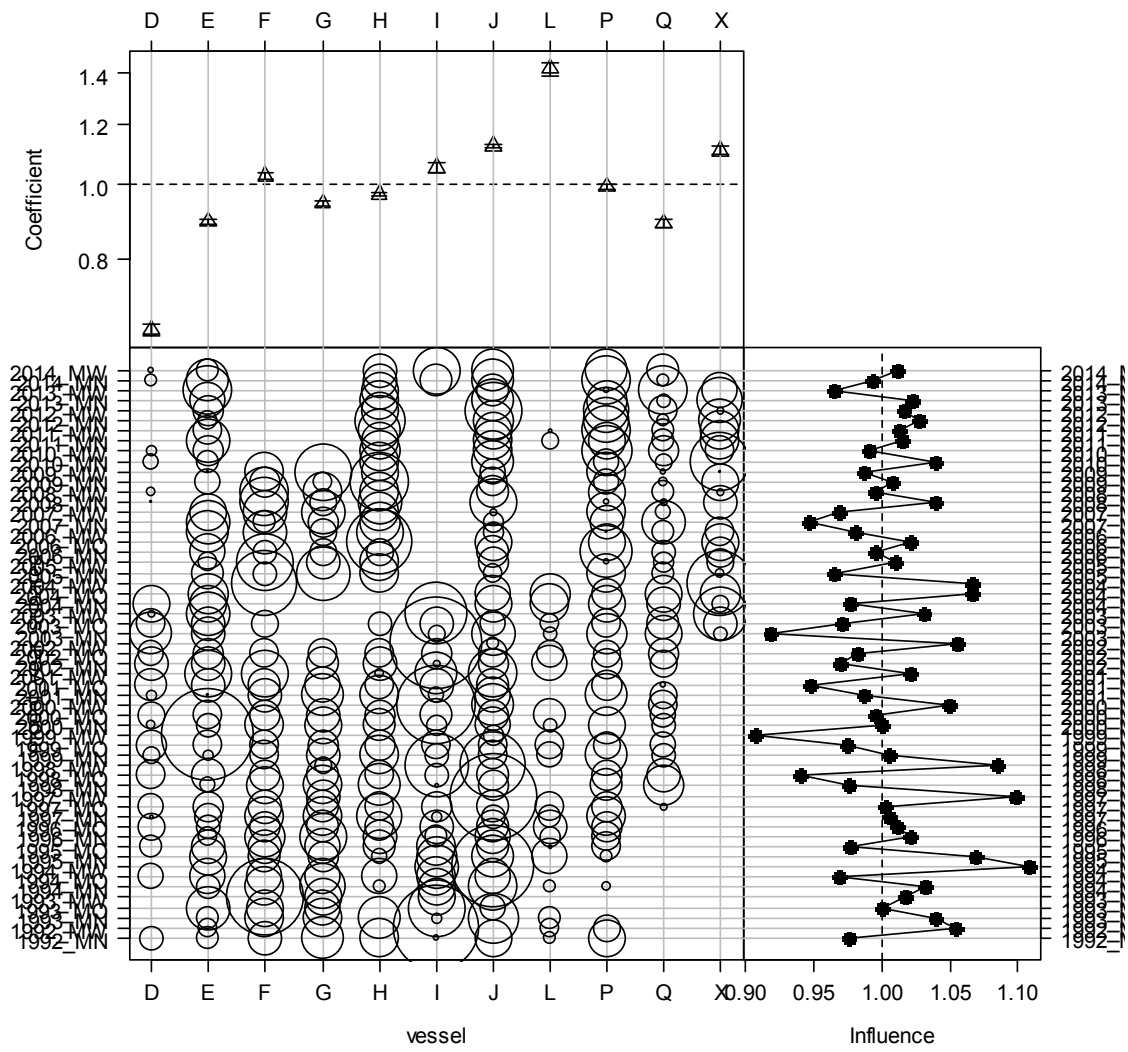
A1. 6: Year influence plots for each explanatory variable for final SCI 3 CPUE standardisation model (Table 4).



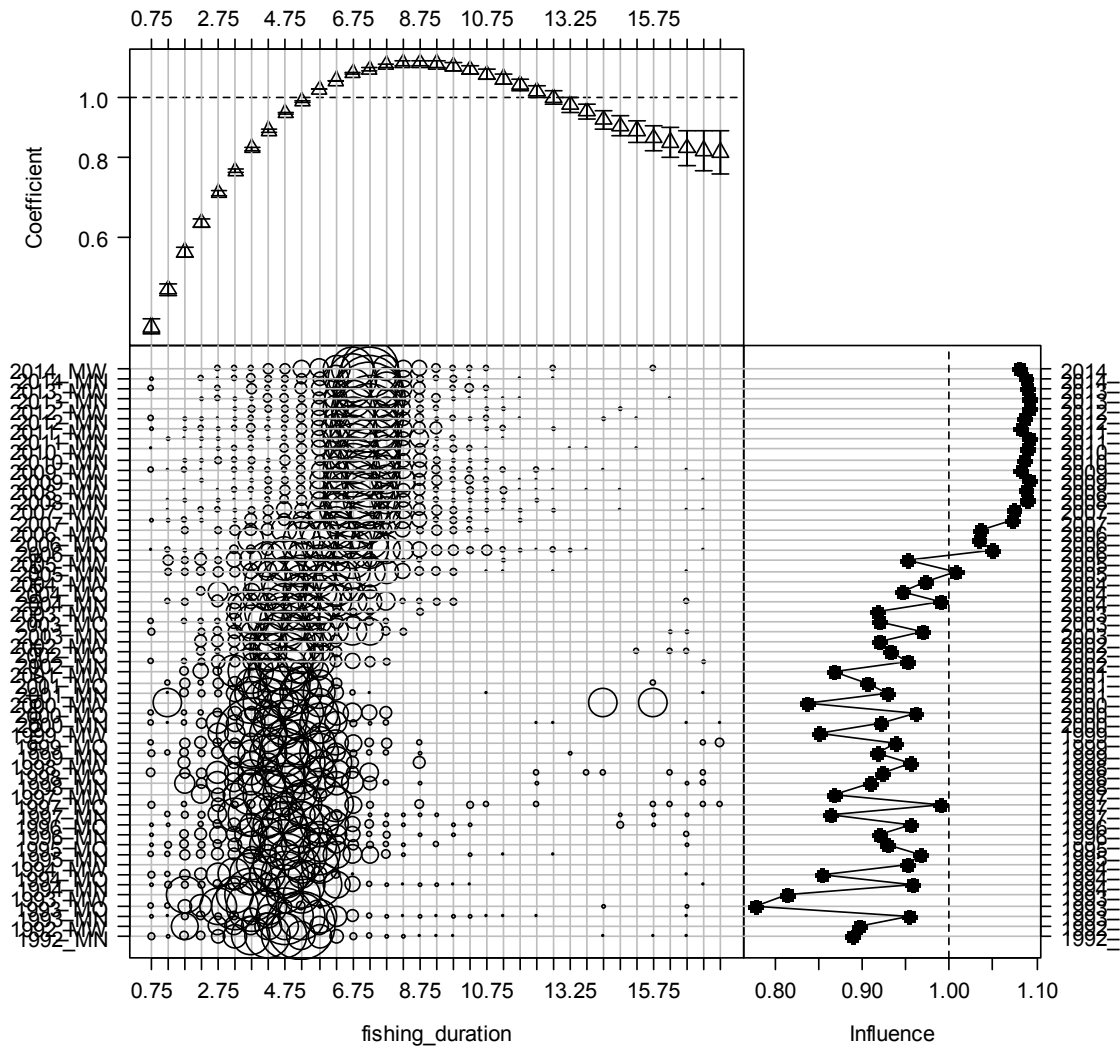
A1. 7: Plot of standardised and unstandardized CPUE indices for SCI 3.



A1. 8: Coefficient-distribution influence plot for time of day (TOD) for final SCI 3 CPUE standardisation model (Table 4).



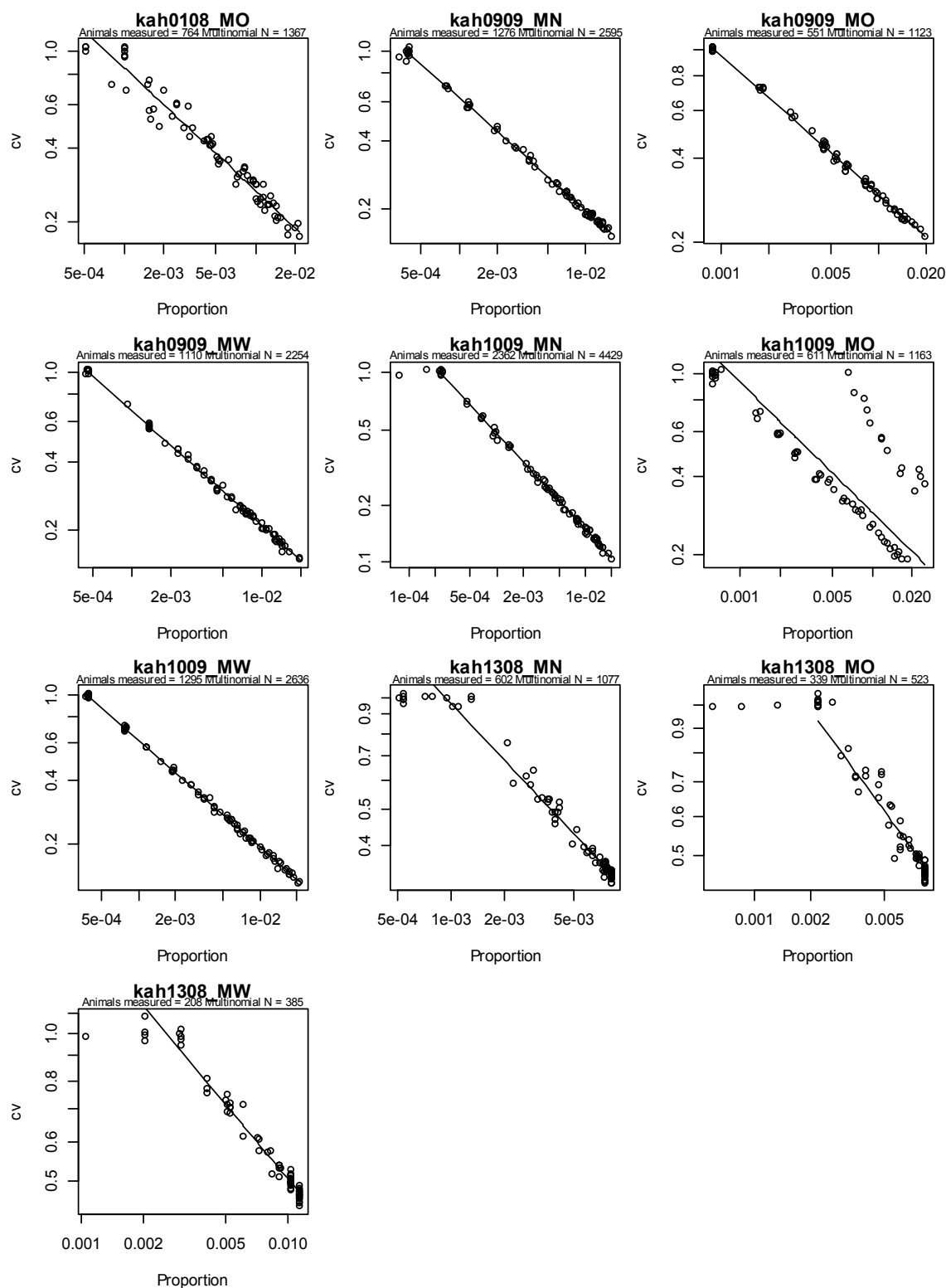
A1. 9: Coefficient-distribution influence plot for vessel for final SCI 3 CPUE standardisation model (Table 4).



A1. 10: Coefficient-distribution influence plot for fishing duration for final SCI 3 CPUE standardisation model (Table 4).

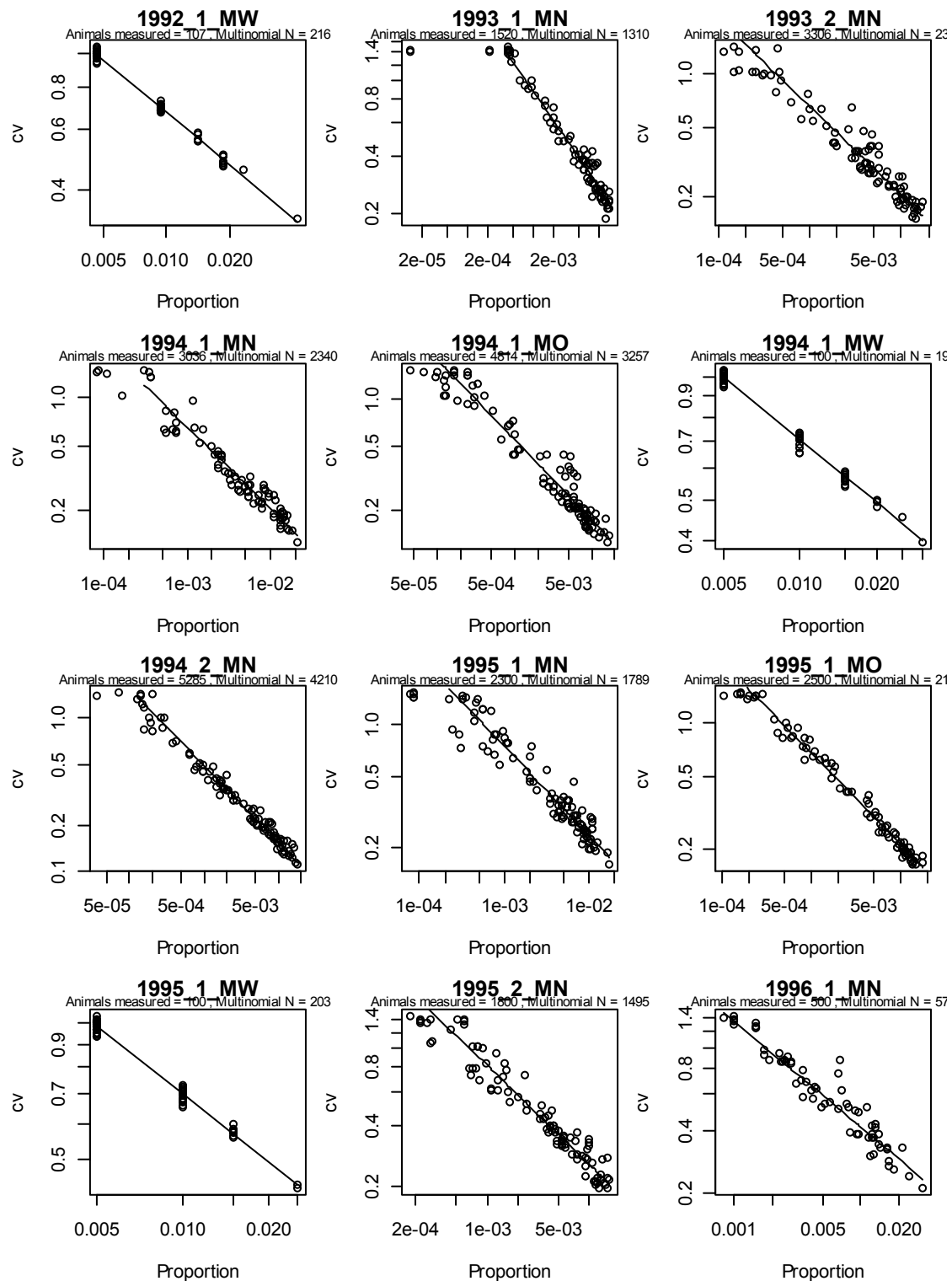
APPENDIX 2. Analysis of length composition data

Trawl survey length frequency

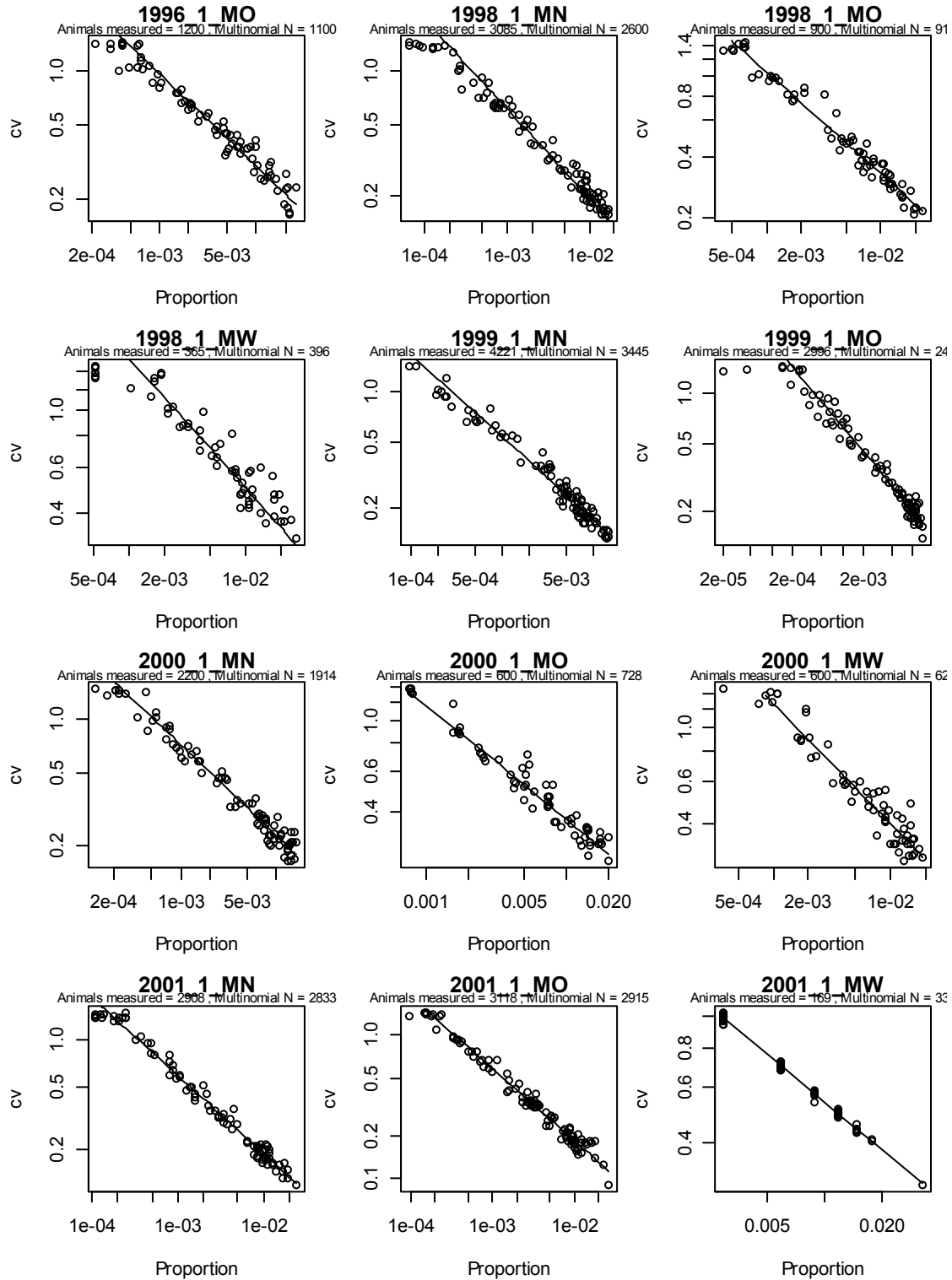


A2. 1: Observation-error CVs for the trawl survey proportions-at-length data sets. Each point represents a proportion at a specific length and sex for a given year. The diagonal line, which is the same in each panel, is added to aid comparison between panels; it shows the relationship between proportion and CV that would hold with simple multinomial sampling with sample size 500.

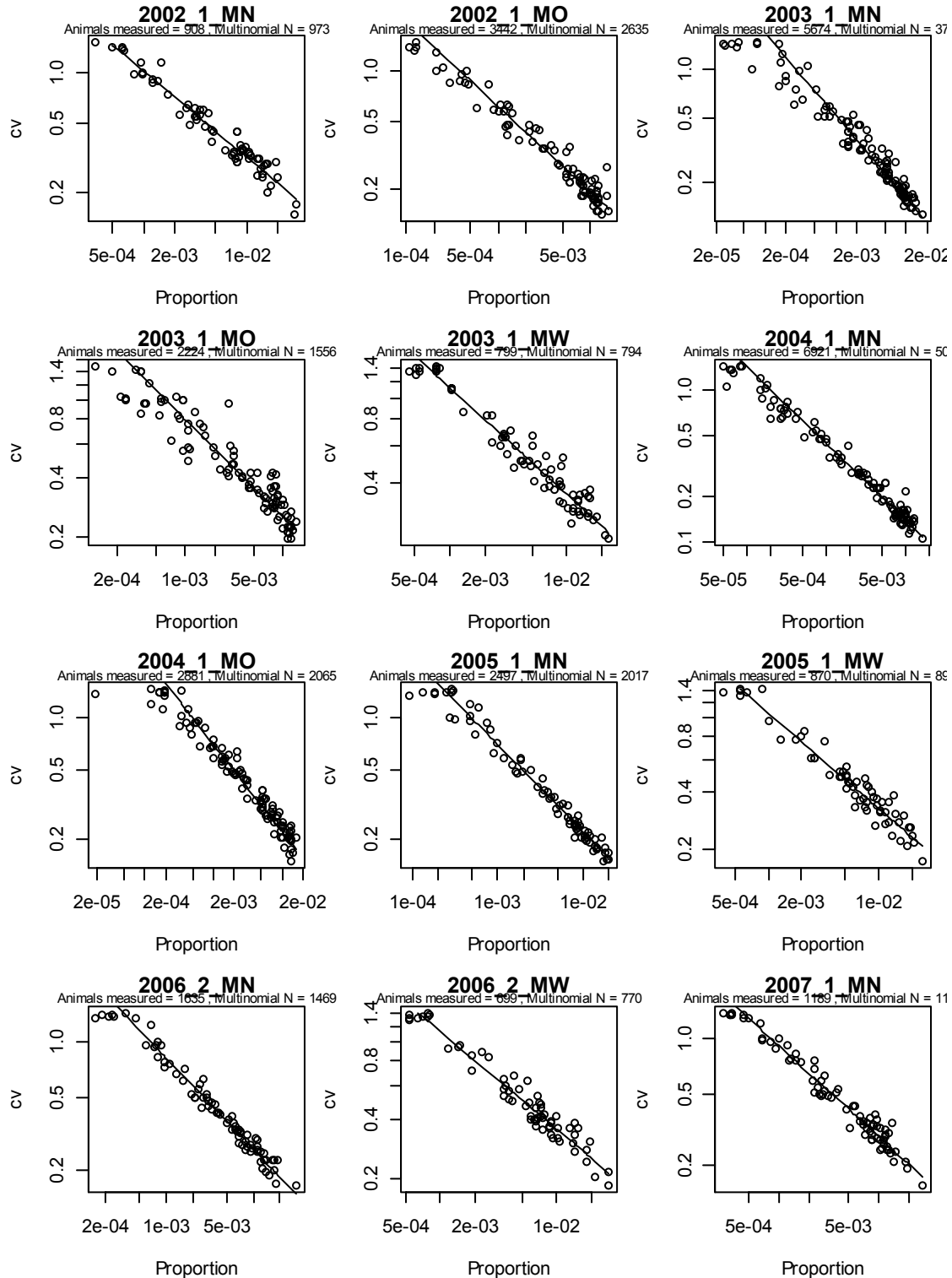
Observer length frequency



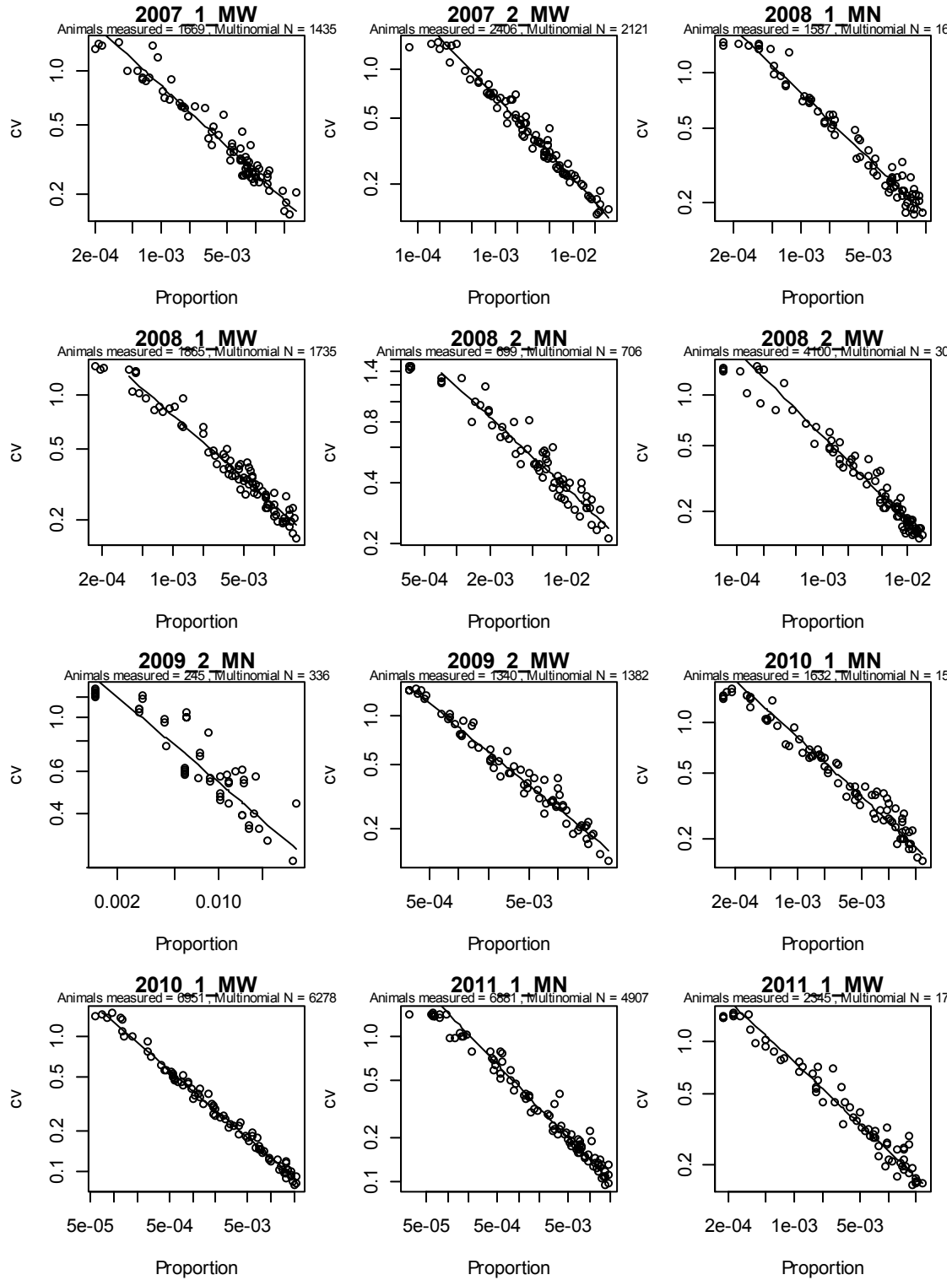
A2. 2: Observation-error CVs for the observer proportions-at-length data sets. Each point represents a proportion at a specific length and sex for a given year. The diagonal line, which is the same in each panel, is added to aid comparison between panels; it shows the relationship between proportion and CV that would hold with simple multinomial sampling with sample size 500.



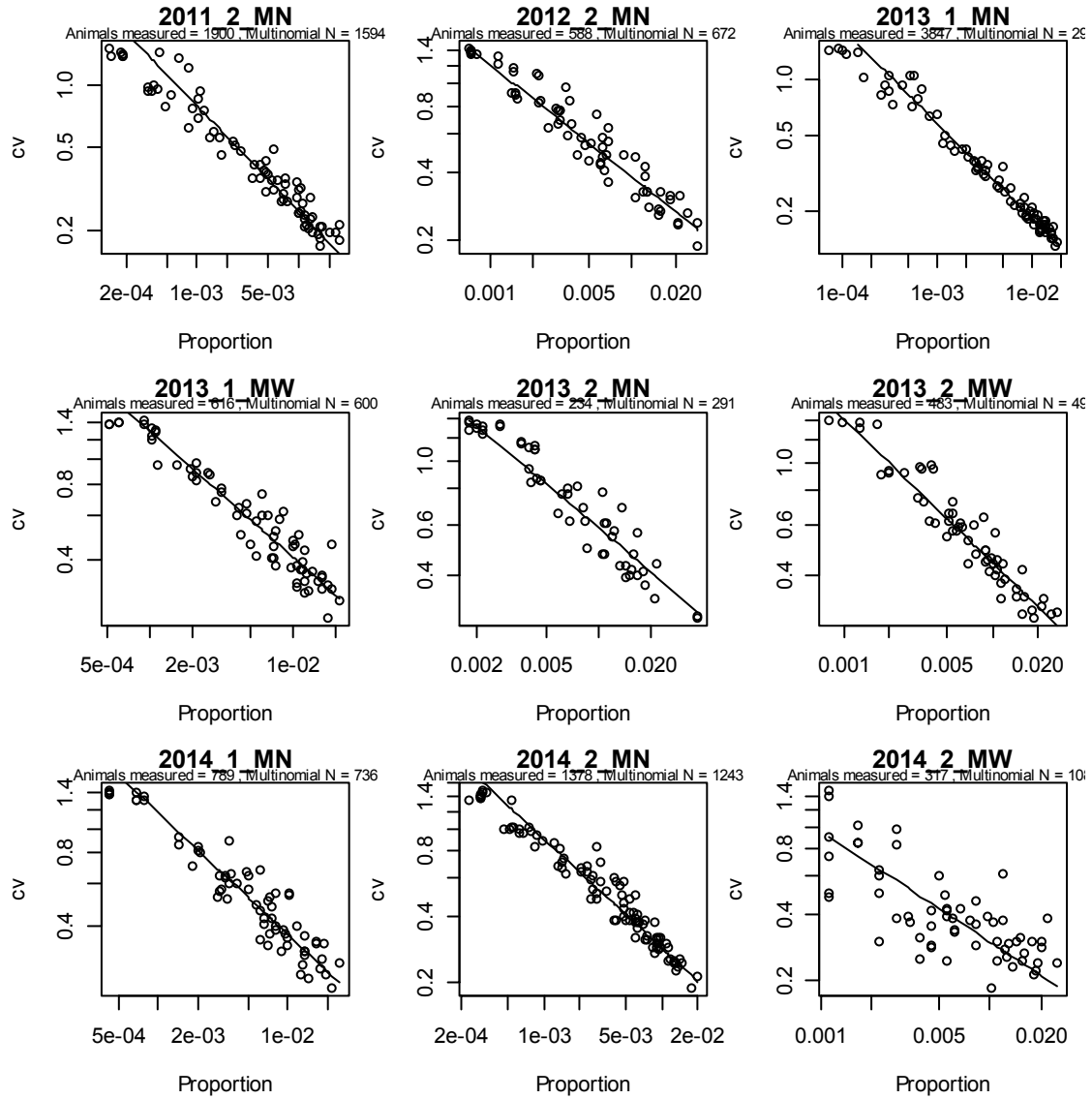
A2. 3: Observation-error CVs for the observer proportions-at-length data sets. Each point represents a proportion at a specific length and sex for a given year. The diagonal line, which is the same in each panel, is added to aid comparison between panels; it shows the relationship between proportion and CV that would hold with simple multinomial sampling with sample size 500.



A2. 4: Observation-error CVs for the observer proportions-at-length data sets. Each point represents a proportion at a specific length and sex for a given year. The diagonal line, which is the same in each panel, is added to aid comparison between panels; it shows the relationship between proportion and CV that would hold with simple multinomial sampling with sample size 500.

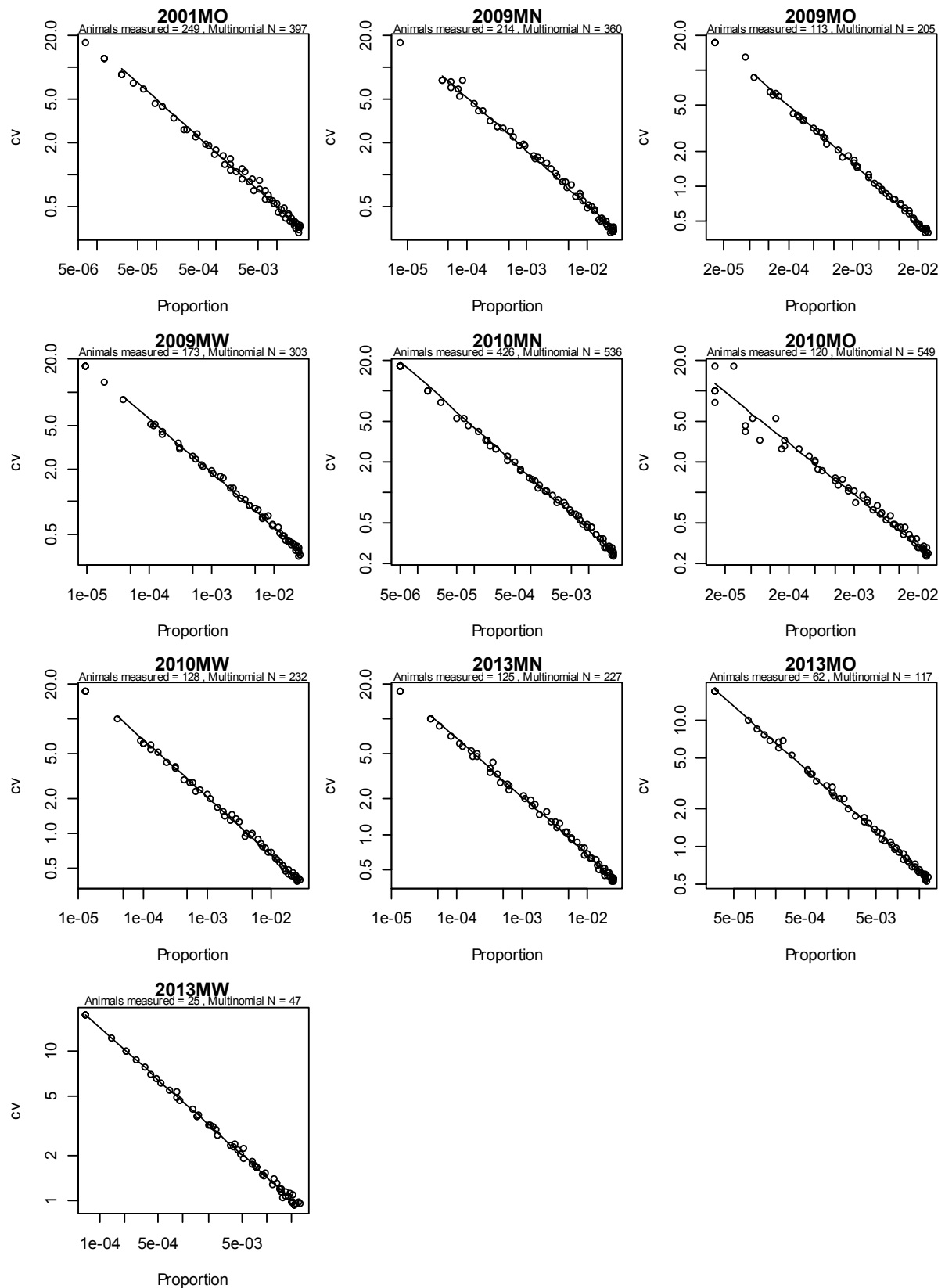


A2. 5: Observation-error CVs for the observer proportions-at-length data sets. Each point represents a proportion at a specific length and sex for a given year. The diagonal line, which is the same in each panel, is added to aid comparison between panels; it shows the relationship between proportion and CV that would hold with simple multinomial sampling with sample size 500.



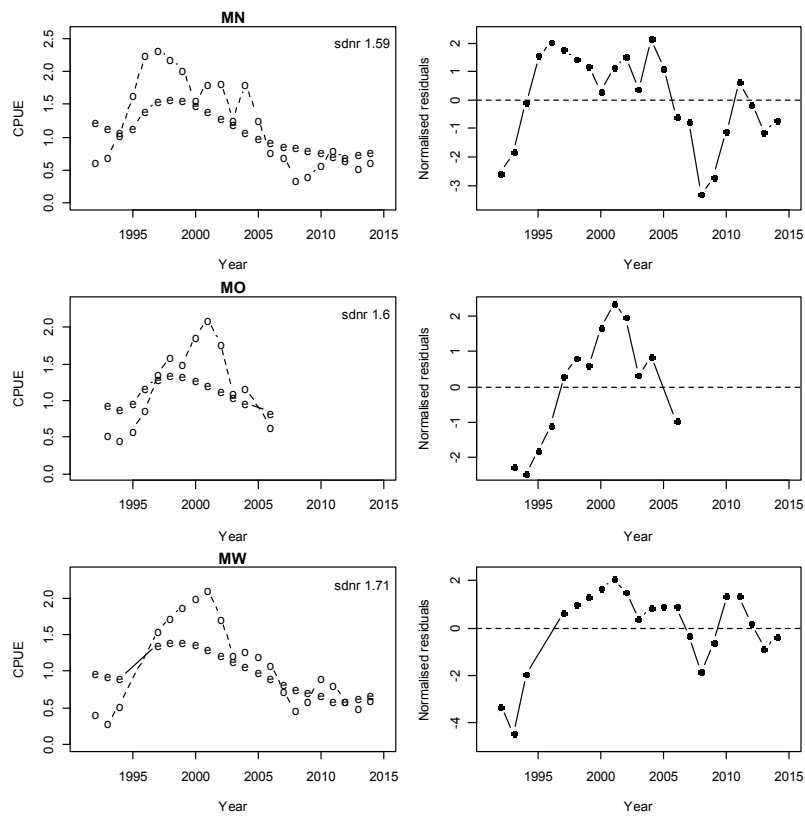
A2. 6: Observation-error CVs for the observer proportions-at-length data sets. Each point represents a proportion at a specific length and sex for a given year. The diagonal line, which is the same in each panel, is added to aid comparison between panels; it shows the relationship between proportion and CV that would hold with simple multinomial sampling with sample size 500.

Photo survey

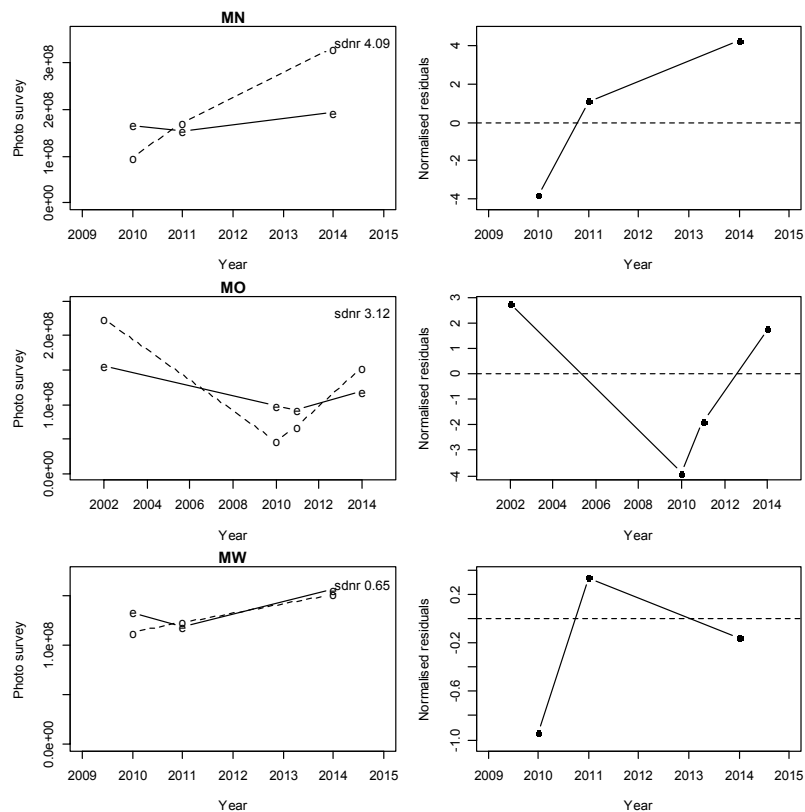


A2. 7: Observation-error CVs for the photo survey proportions-at-length data sets. Each point represents a proportion at a specific length and sex for a given year. The diagonal line, which is the same in each panel, is added to aid comparison between panels; it shows the relationship between proportion and CV that would hold with simple multinomial sampling with sample size 500.

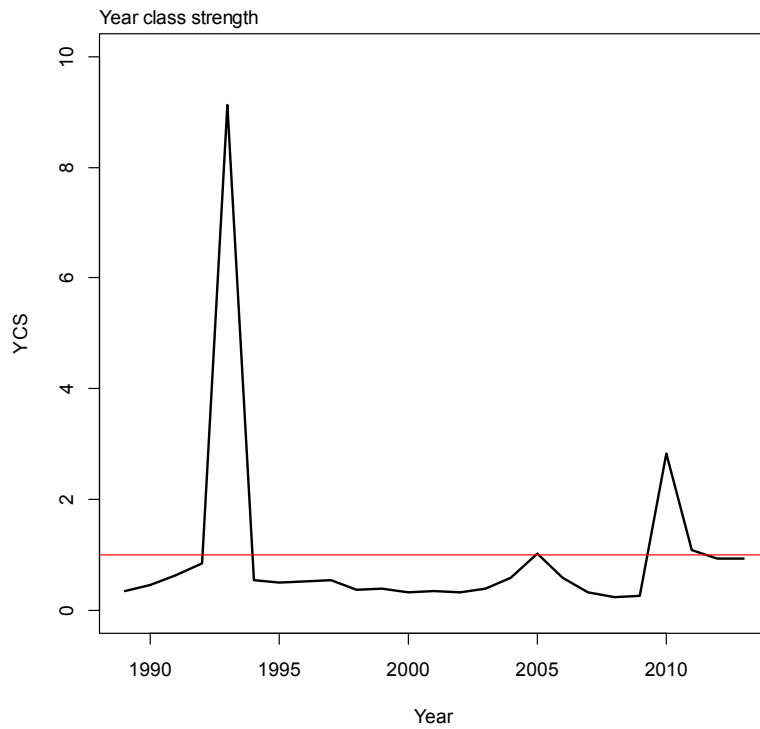
APPENDIX 3. MODEL NT_0.15



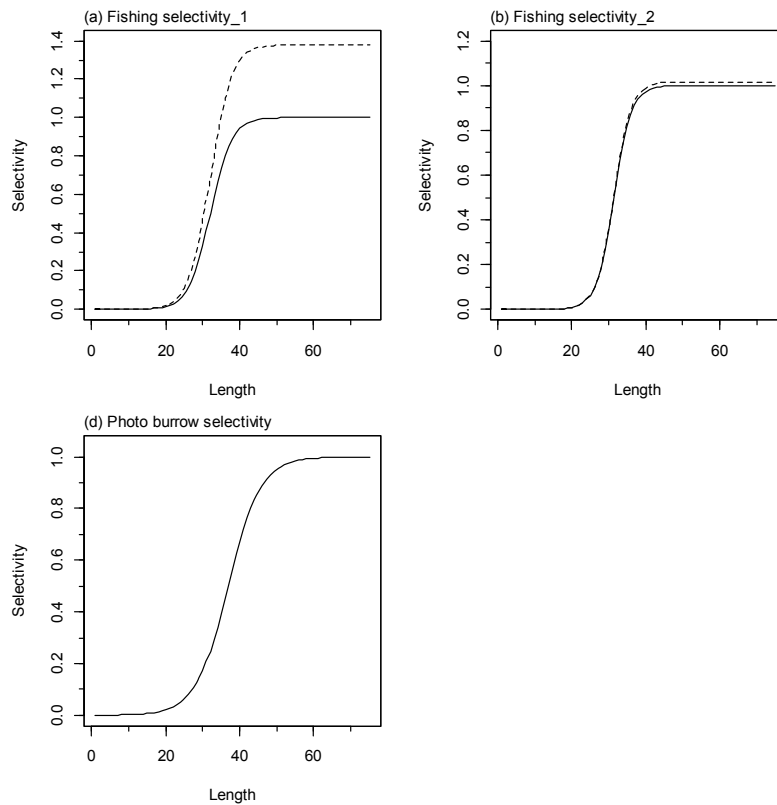
A3. 1: Fits to CPUE indices (left column) and normalised residuals (right column) for each subarea for SCI 3 NT_0.15.



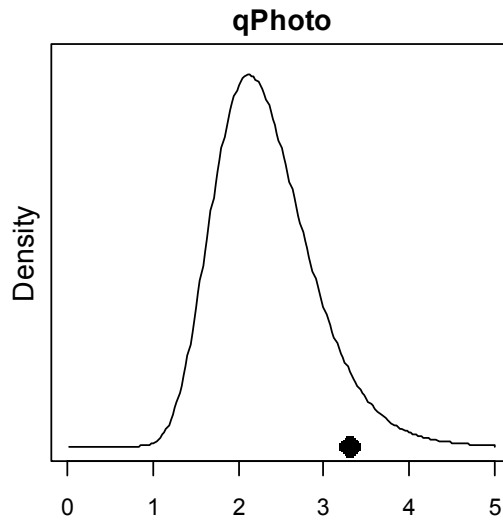
A3. 2: Fits to photographic survey indices (left column) and normalised residuals (right column) for each subarea for SCI 3 NT_0.15.



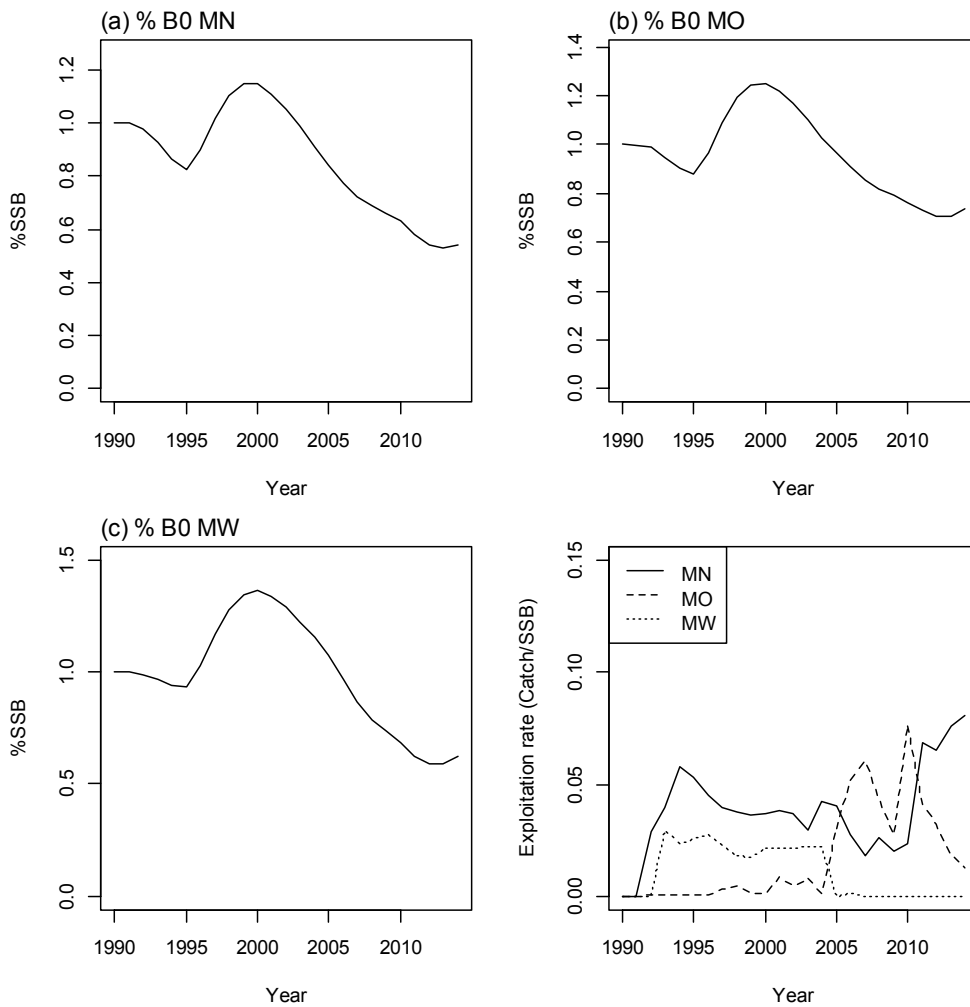
A3. 3: Year class strength for SCI 3 NT_0.15.



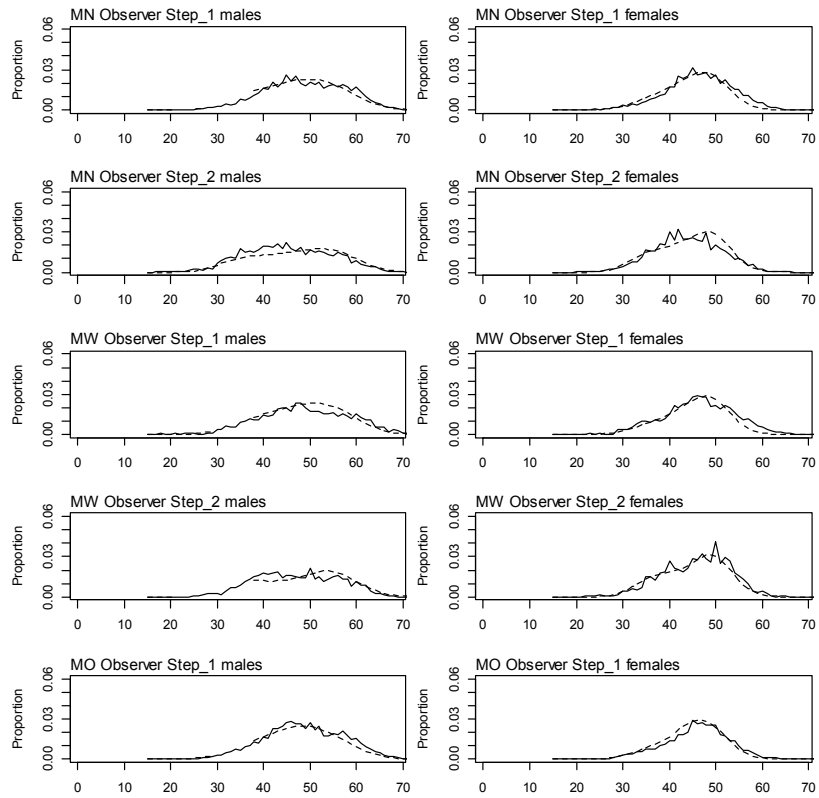
A3. 4: Fishery and survey selectivity curves for SCI 3 NT_0.15. Solid line – females, dotted line – males. The scampi photo index is not sexed, and a single selectivity applies.



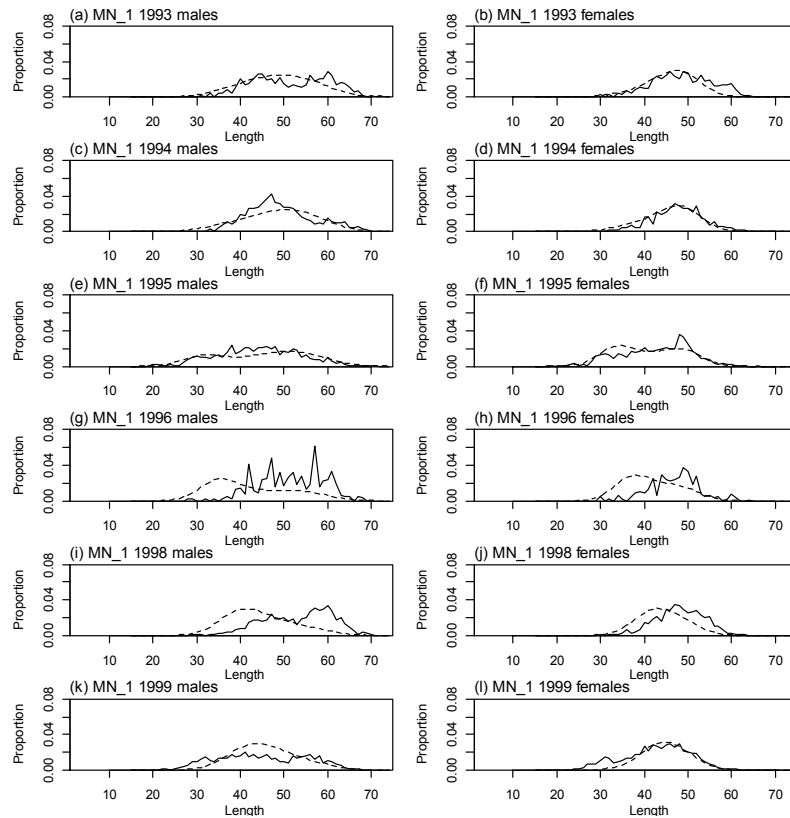
A3. 5: Catchability estimates from MPD model run, plotted in relation to prior distribution for SCI 3 NT_0.15.



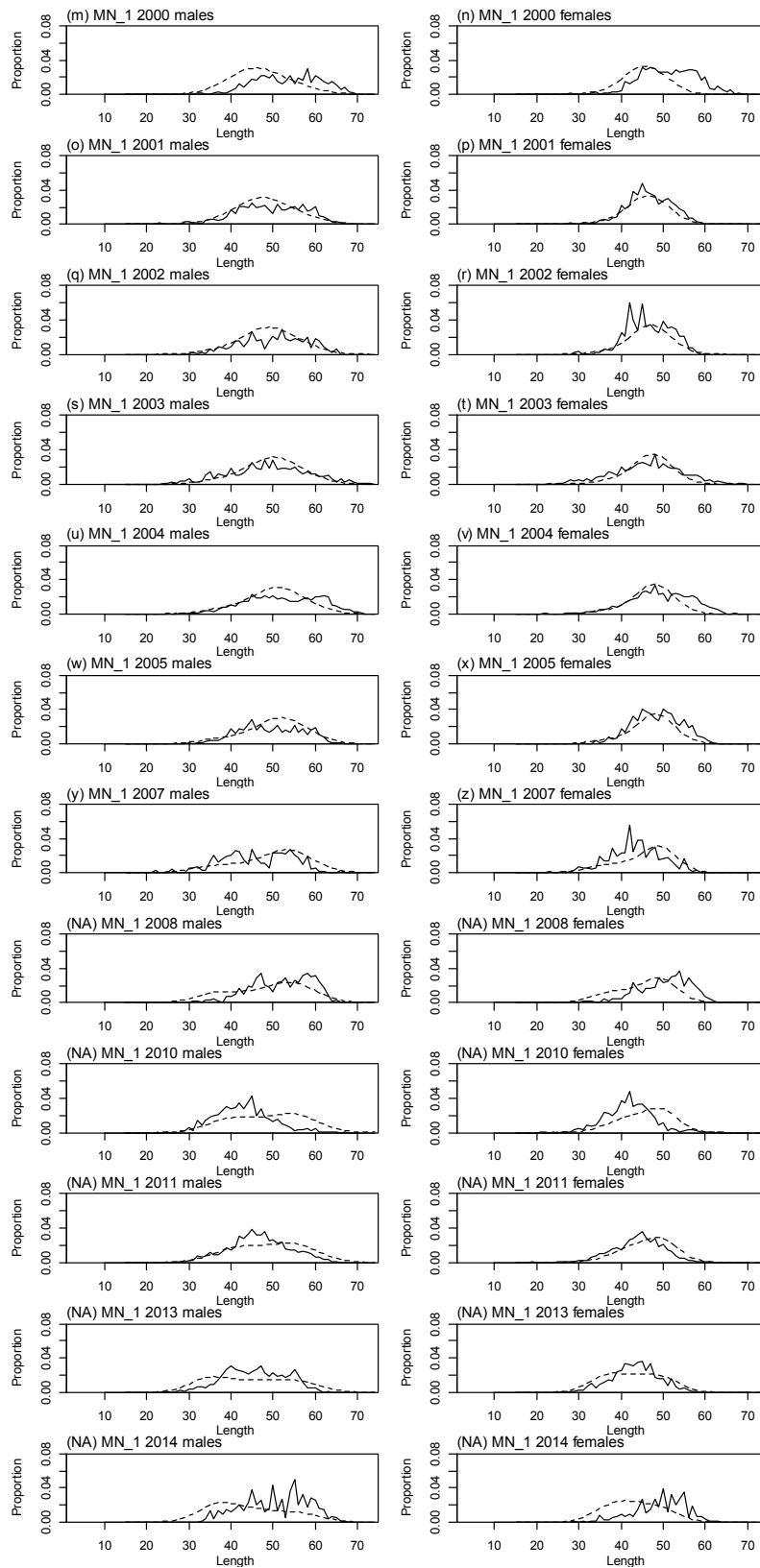
A3. 6: Stock trajectories (%SSB₀) for each subarea estimated from the MPD model run, and estimated exploitation rates for SCI 3 NT_0.15.



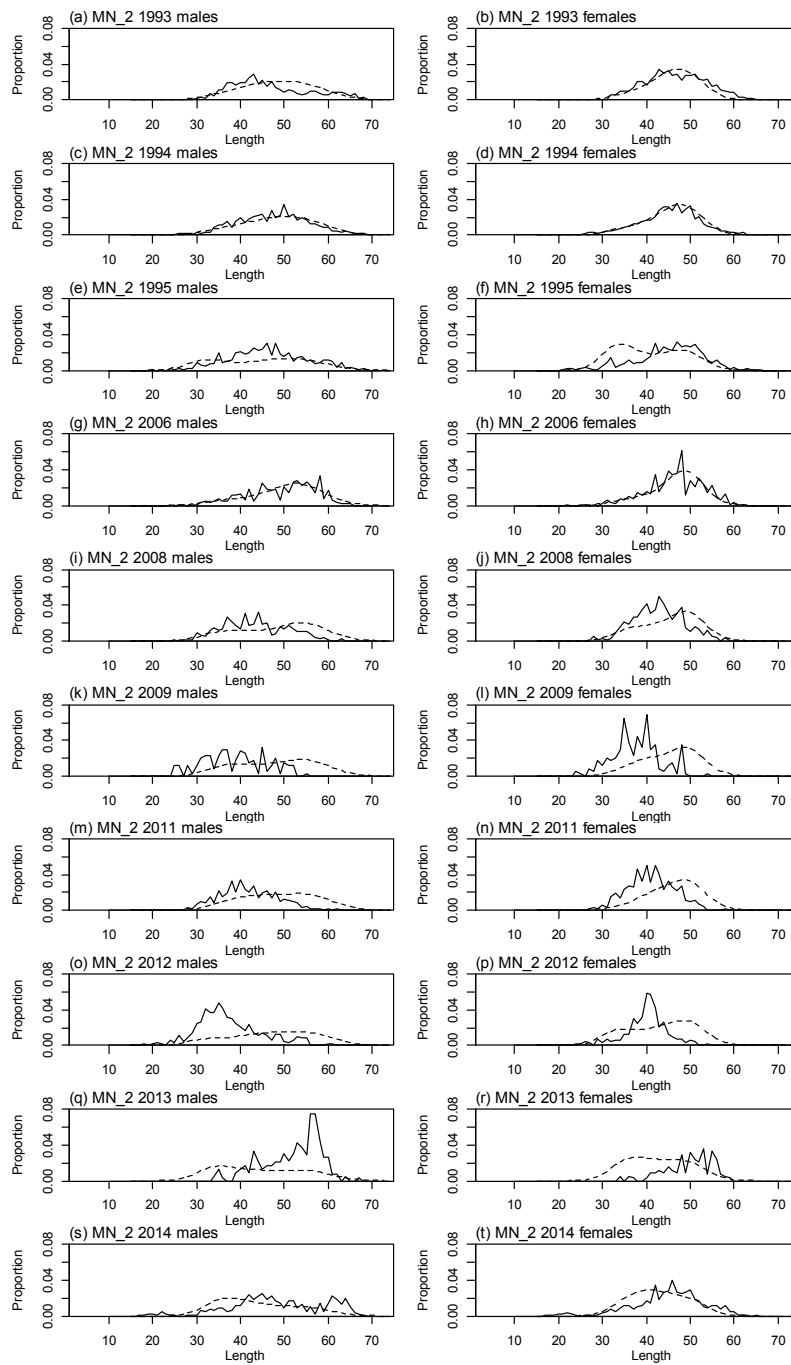
A3. 7: Average observed (solid line) and fitted (dashed line) length frequency distributions for observer samples for SCI 3 NT_0.15.



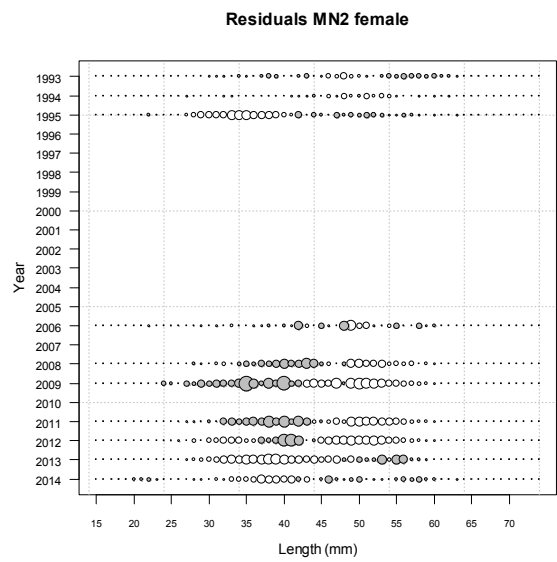
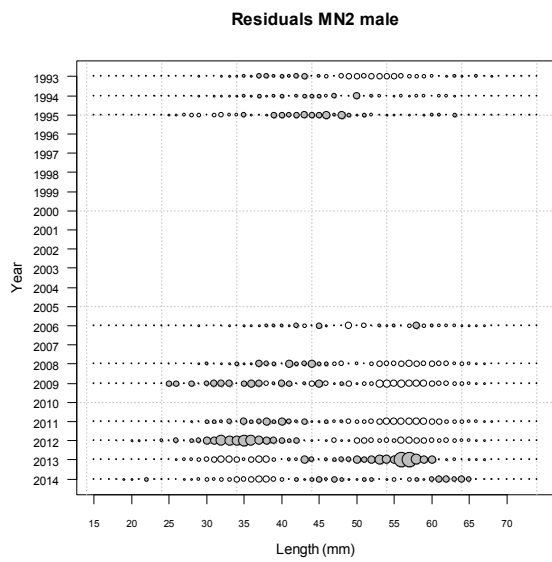
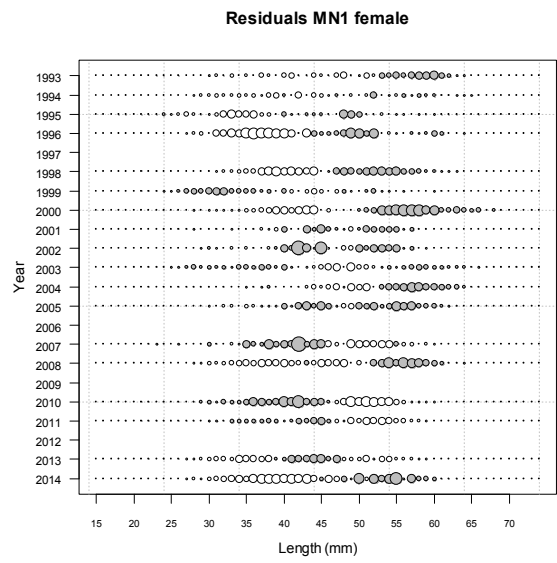
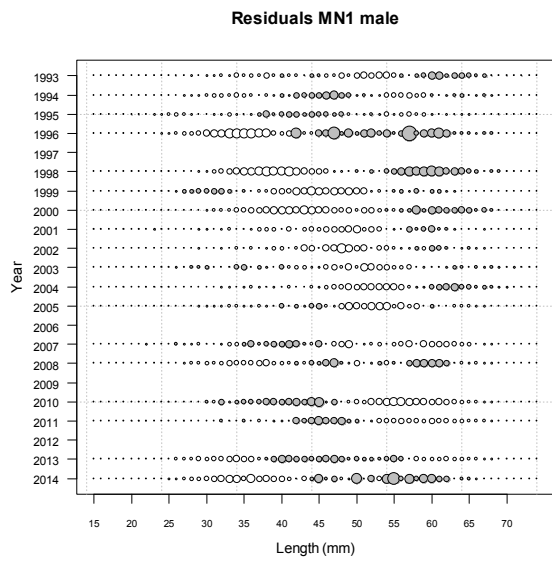
A3. 8: Observed (solid line) and fitted (dashed line) length frequency distributions for observer samples, MN time step 1 for SCI 3 NT_0.15.



A3.8 ctd.: Observed (solid line) and fitted (dashed line) length frequency distributions for observer samples, MN time step 1 for SCI 3 NT_0.15.



A3. 9: Observed (solid line) and fitted (dashed line) length frequency distributions for observer samples, MN time step 2 for SCI 3 NT_0.15.



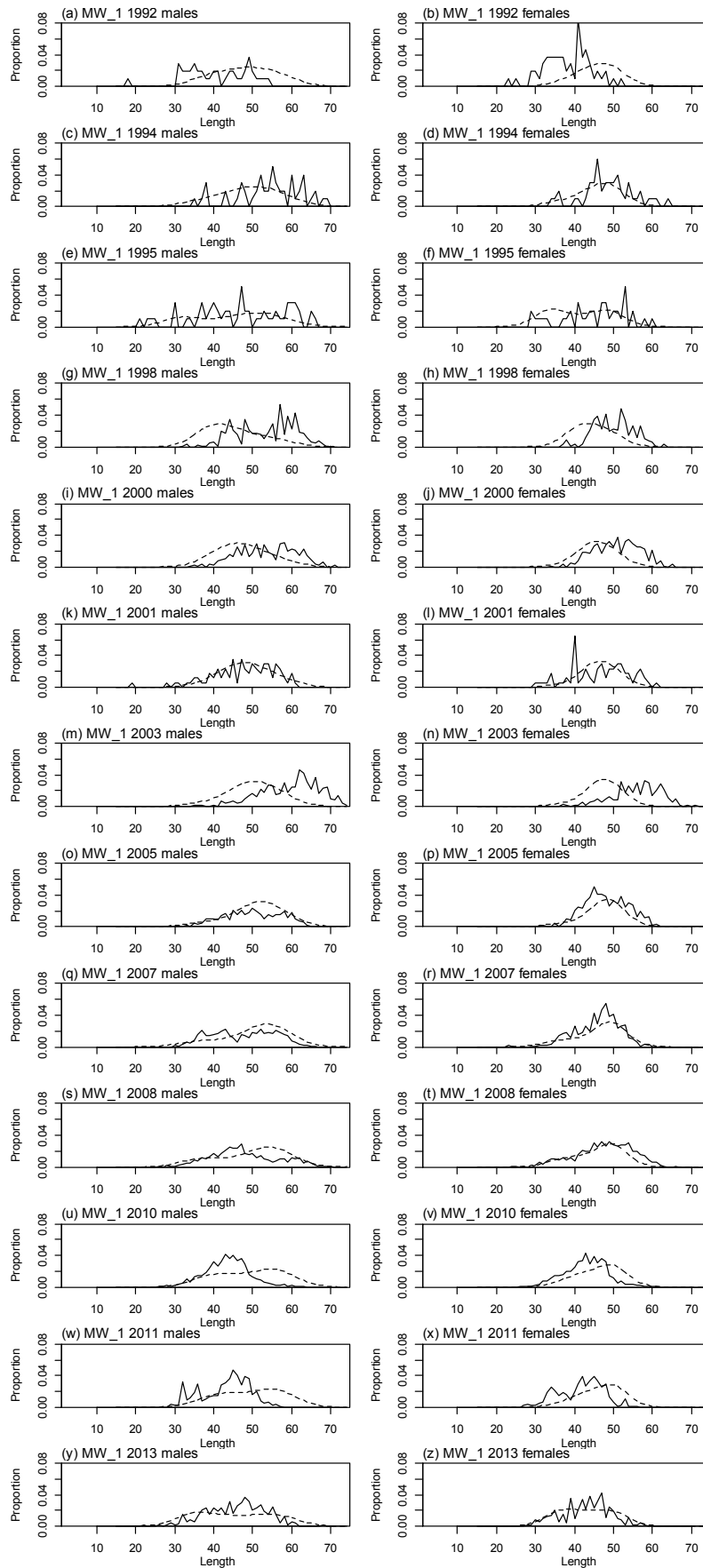
A3. 10: Bubble plots of residuals of fits to length frequency distributions for observer sampling from MN, time step 1 and 2, for SCI 3 NT_0.15.

A3. 11: Numbers of scampi measured, estimated multinomial N sample size, and effective sample size used within the SCI 3 NT_0.15 model for length frequency distributions for observer samples, MN time step 1.

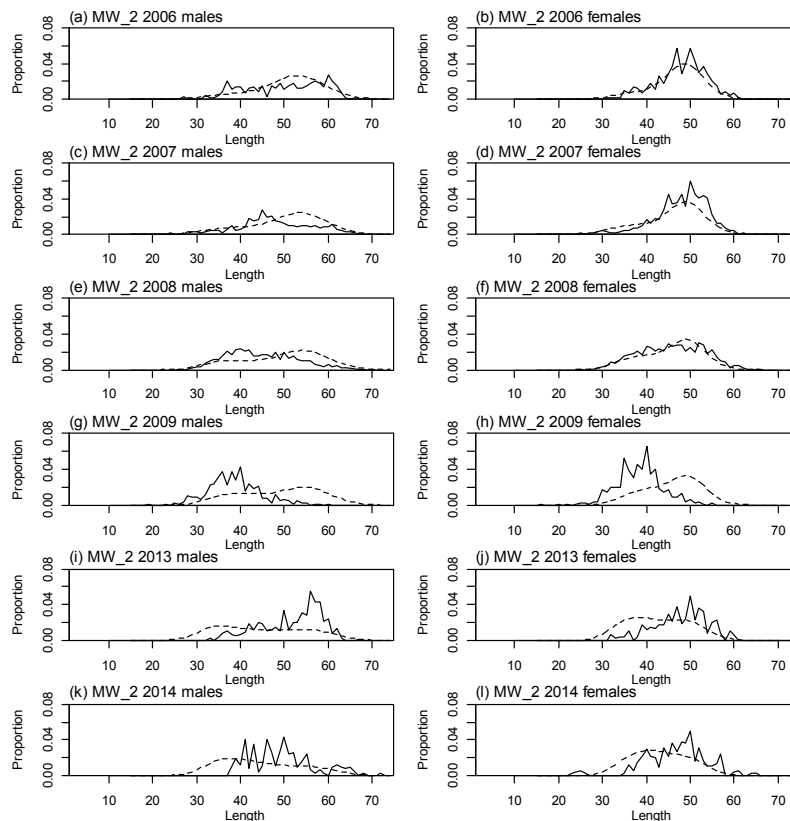
	Measured	Multinomial N	Effective sample size
N_1993	1 089	1 520	3.74
N_1994	2 090	3 036	7.47
N_1995	1 498	2 300	5.66
N_1996	465	500	1.23
N_1998	1 843	3 085	7.59
N_1999	1 921	4 221	10.39
N_2000	1 727	2 200	5.41
N_2001	1 528	2 908	7.16
N_2002	510	908	2.23
N_2003	2 824	5 674	13.96
N_2004	3 856	6 921	17.03
N_2005	1 448	2 497	6.14
N_2007	829	1 189	2.93
N_2008	1 087	1 587	3.91
N_2010	948	1 632	4.02
N_2011	3 273	6 881	16.93
N_2013	2 613	3 847	9.47
N_2014	403	789	1.94

A3. 12: Numbers of scampi measured, estimated multinomial N sample size, and effective sample size used within the SCI 3 NT_0.15 model for length frequency distributions for observer samples, MN time step 2.

	Measured	Multinomial N	Effective sample size
N_1993	1 639	3 306	13.09
N_1994	2 923	5 285	20.93
N_1995	1 260	1 800	7.13
N_2006	1 086	1 635	6.47
N_2008	535	699	2.77
N_2009	186	245	0.97
N_2011	1 019	1 900	7.52
N_2012	333	588	2.33
N_2013	352	234	0.93
N_2014	1 443	1 378	5.46



A3. 13: Observed (solid line) and fitted (dashed line) length frequency distributions for observer samples, MW time step 1 for SCI 3 NT_0.15.



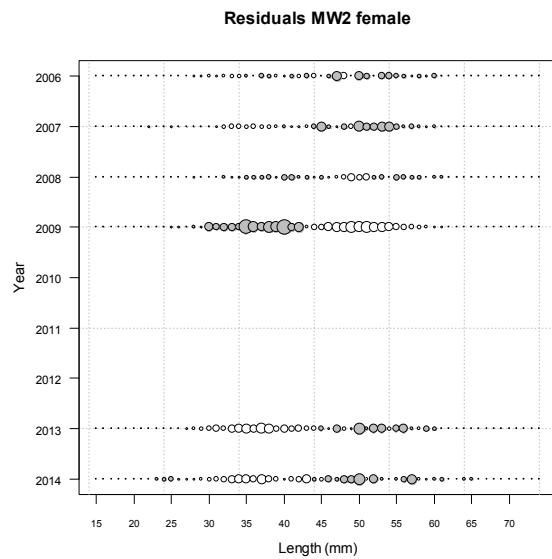
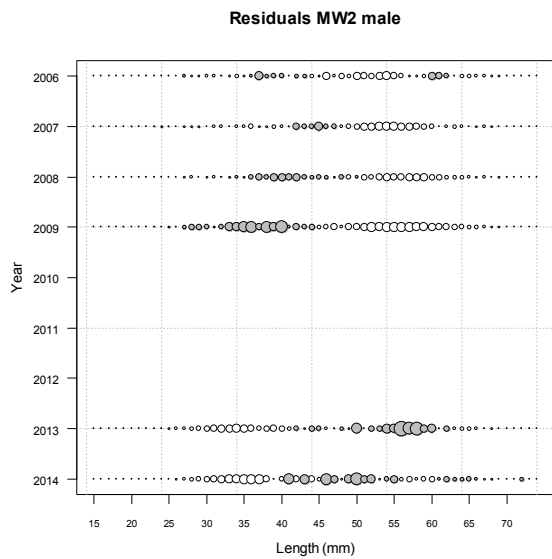
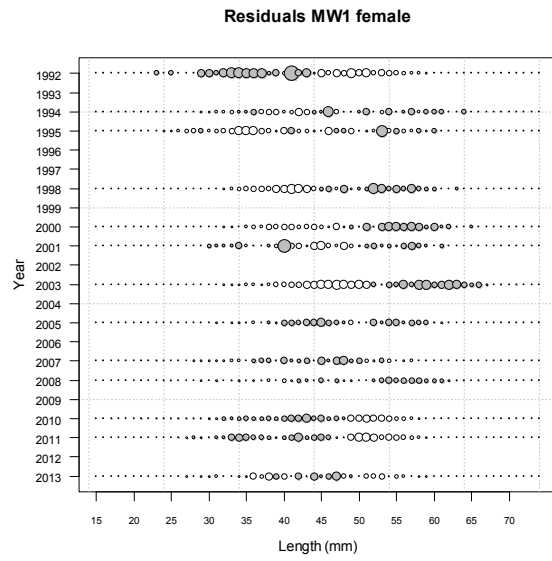
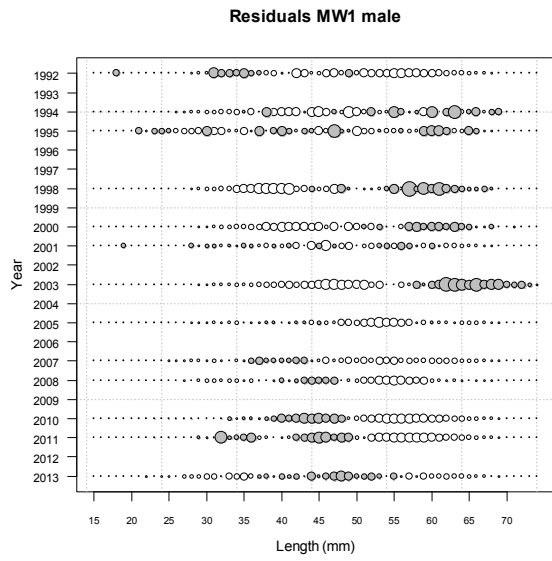
A3. 14: Observed (solid line) and fitted (dashed line) length frequency distributions for observer samples, MW time step 2 for SCI 3 NT_0.15.

A3. 15: Numbers of scampi measured, estimated multinomial N sample size, and effective sample size used within the SCI 3 NT_0.15 model for length frequency distributions for observer samples, MW time step 1.

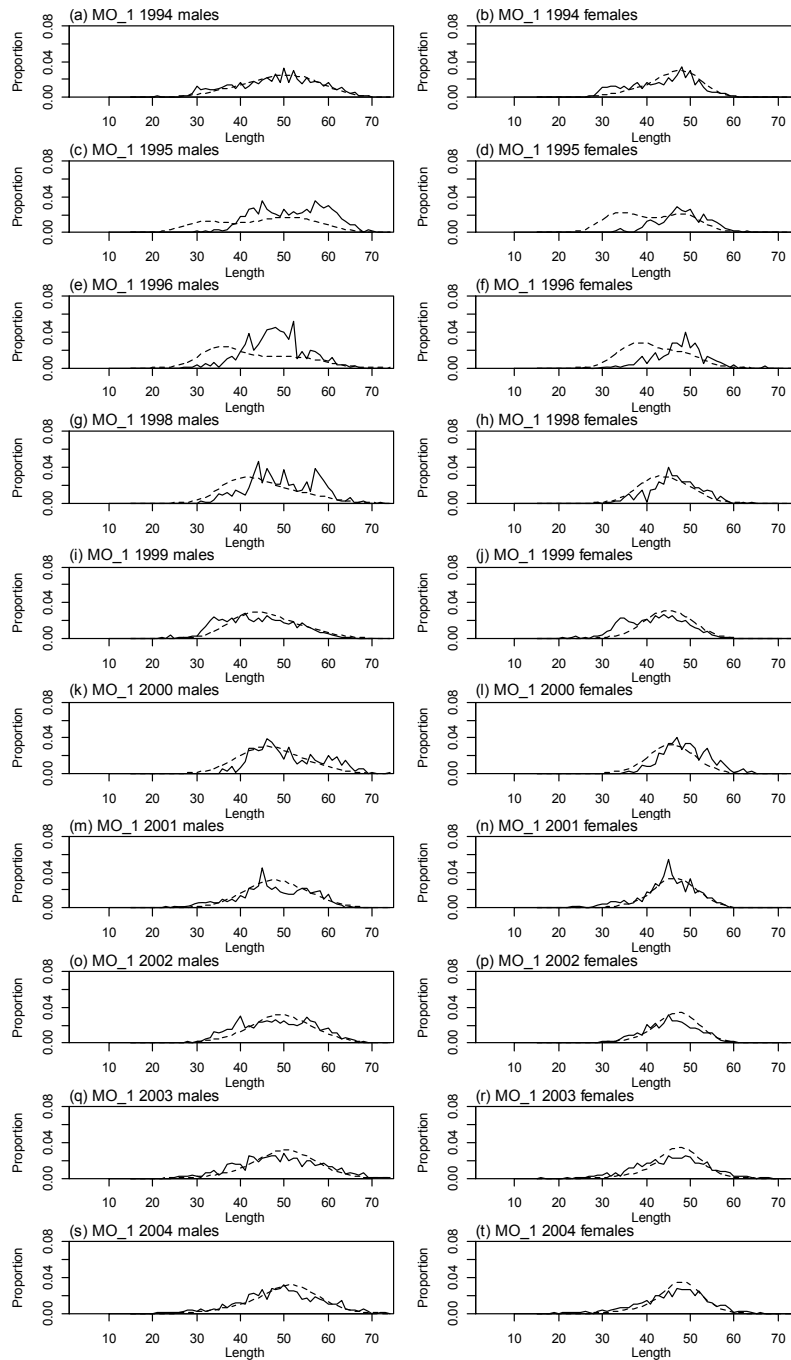
	Measured	Multinomial N	Effective sample size
N_1992	229	107	0.22
N_1994	242	100	0.21
N_1995	241	100	0.21
N_1998	365	365	0.75
N_2000	521	600	1.23
N_2001	251	169	0.35
N_2003	578	799	1.64
N_2005	593	870	1.79
N_2007	1 082	1 669	3.43
N_2008	1 201	1 865	3.83
N_2010	3 163	6 951	14.27
N_2011	712	2 345	4.82
N_2013	495	616	1.26

A3. 16: Numbers of scampi measured, estimated multinomial N sample size, and effective sample size used within the SCI 3 NT_0.15 model for length frequency distributions for observer samples, MW time step 2.

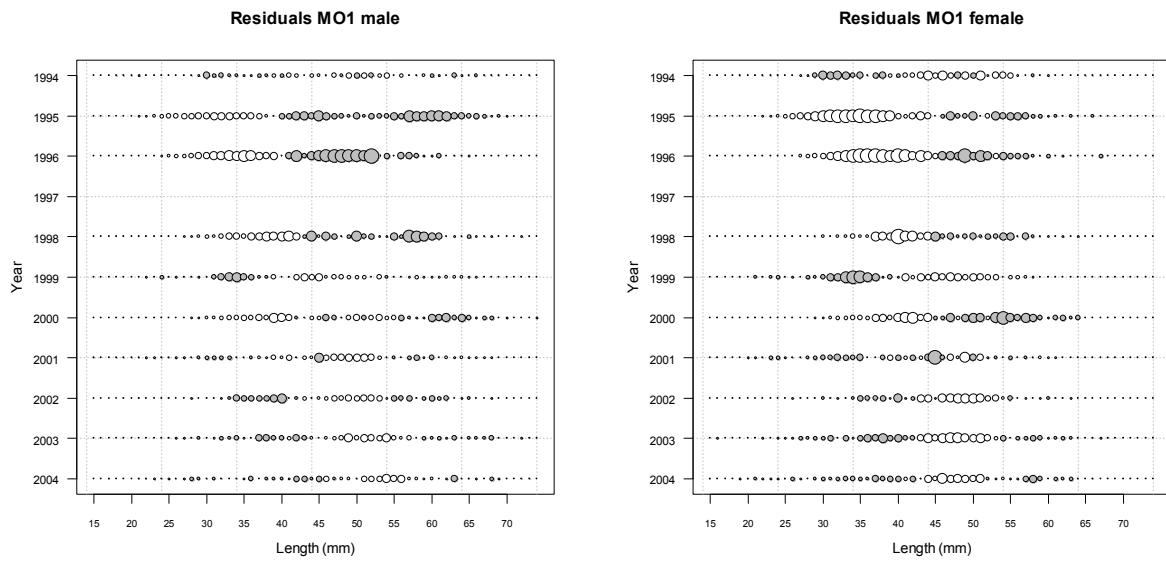
	Measured	Multinomial N	Effective sample size
N_2006	659	699	1.93
N_2007	1333	2406	6.65
N_2008	2278	4100	11.33
N_2009	693	1340	3.70
N_2013	550	483	1.33
N_2014	460	317	0.88



A3. 17: Bubble plots of residuals of fits to length frequency distributions for observer sampling from MW, time step 1 and 2, for SCI 3 NT_0.15.



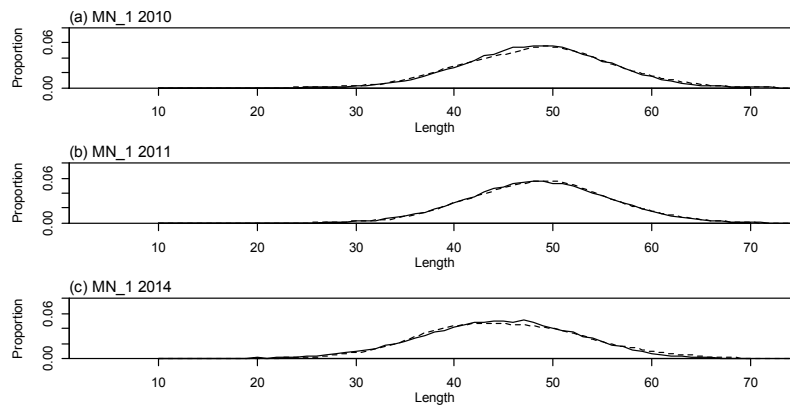
A3. 18: Observed (solid line) and fitted (dashed line) length frequency distributions for observer samples, MO time step 1 for SCI 3 NT_0.15.



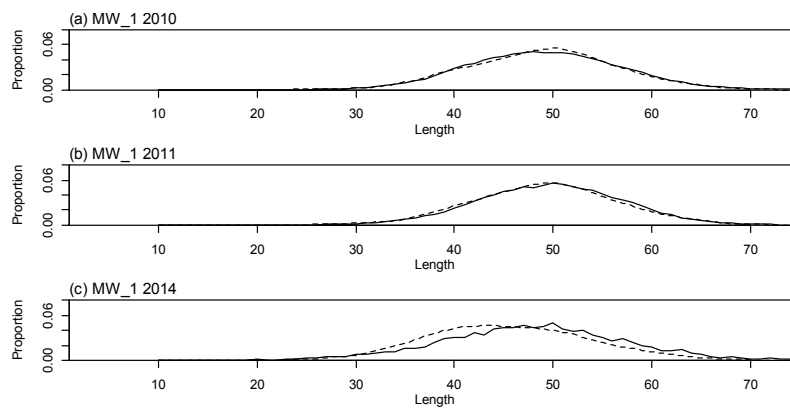
A3. 19: Bubble plots of residuals of fits to length frequency distributions for observer sampling from MO, time step 1, for SCI 3 NT_0.15.

A3. 20: Numbers of scampi measured, estimated multinomial N sample size, and effective sample size used within the SCI 3 NT_0.15 model for length frequency distributions for observer samples, MO time step 1.

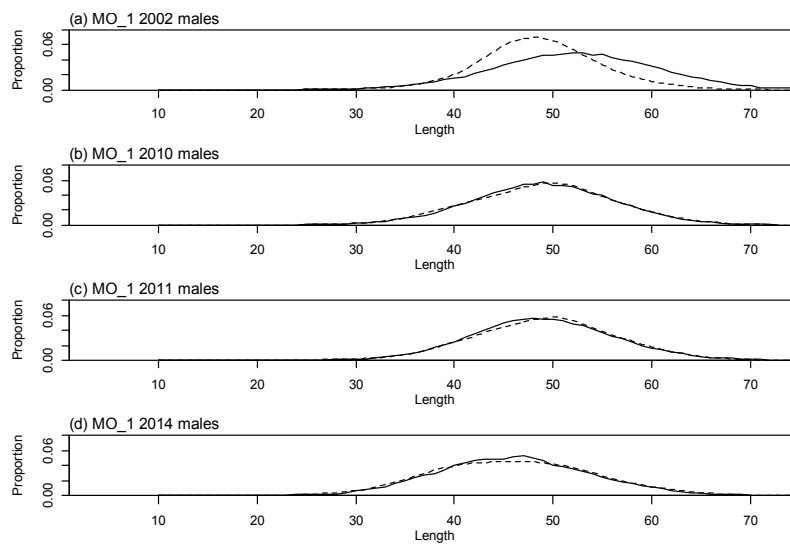
	Measured	Multinomial N	Effective sample size
N_1994	2 665	4 814	14.09
N_1995	2 474	2 500	7.32
N_1996	752	1 200	3.51
N_1998	870	900	2.63
N_1999	1 492	2 996	8.77
N_2000	608	600	1.76
N_2001	1 749	3 118	9.13
N_2002	1 768	3 442	7.71
N_2003	1 367	2 224	6.51
N_2004	1 557	2 881	8.43



A3. 21: Observed (solid line) and fitted (dashed line) length frequency distributions for MN photographic survey scampi size estimation within the SCI 3 NT_0.15 model.



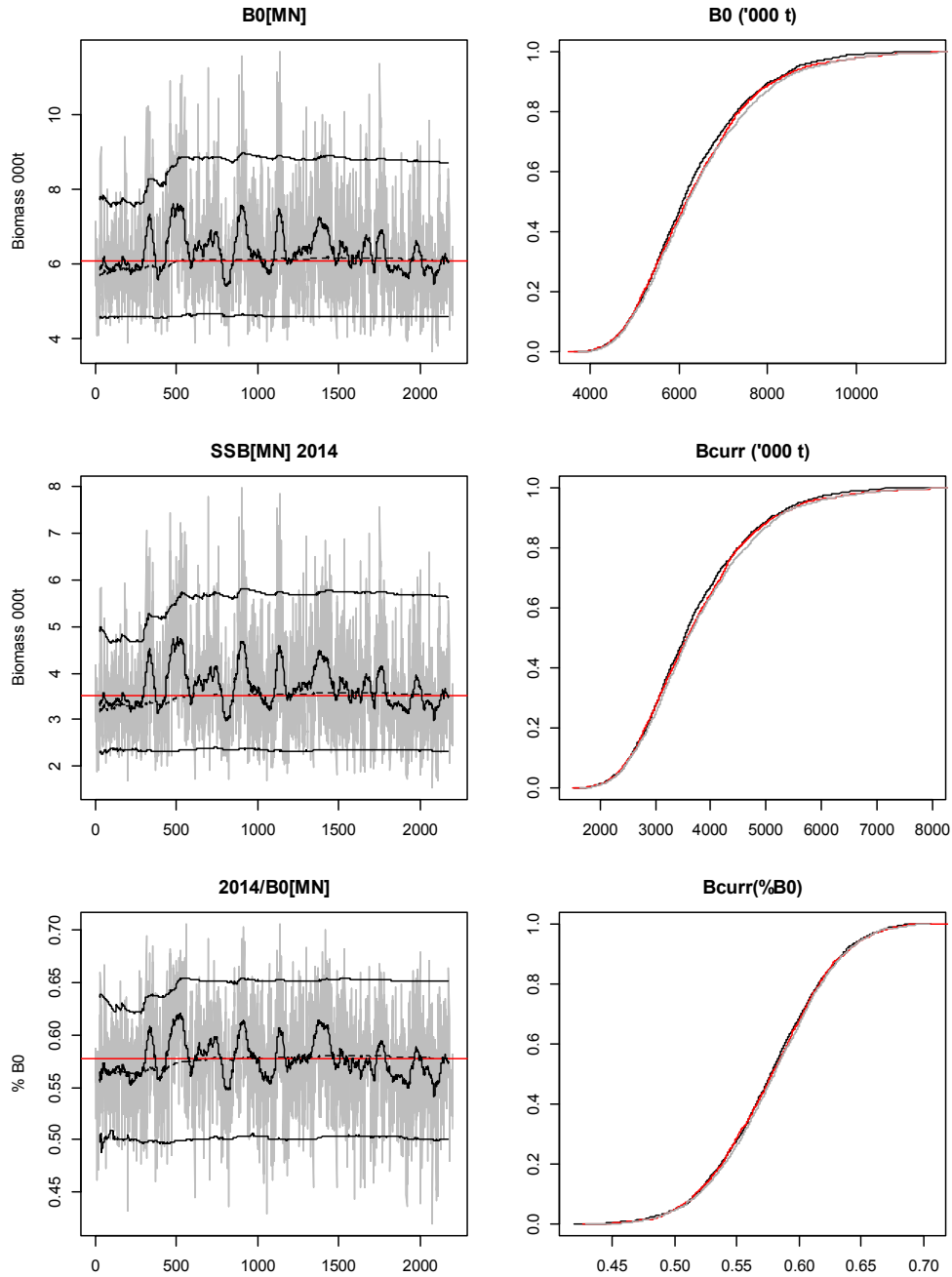
A3. 22: Observed (solid line) and fitted (dashed line) length frequency distributions for MW photographic survey scampi size estimation within the SCI 3 NT_0.15 model.



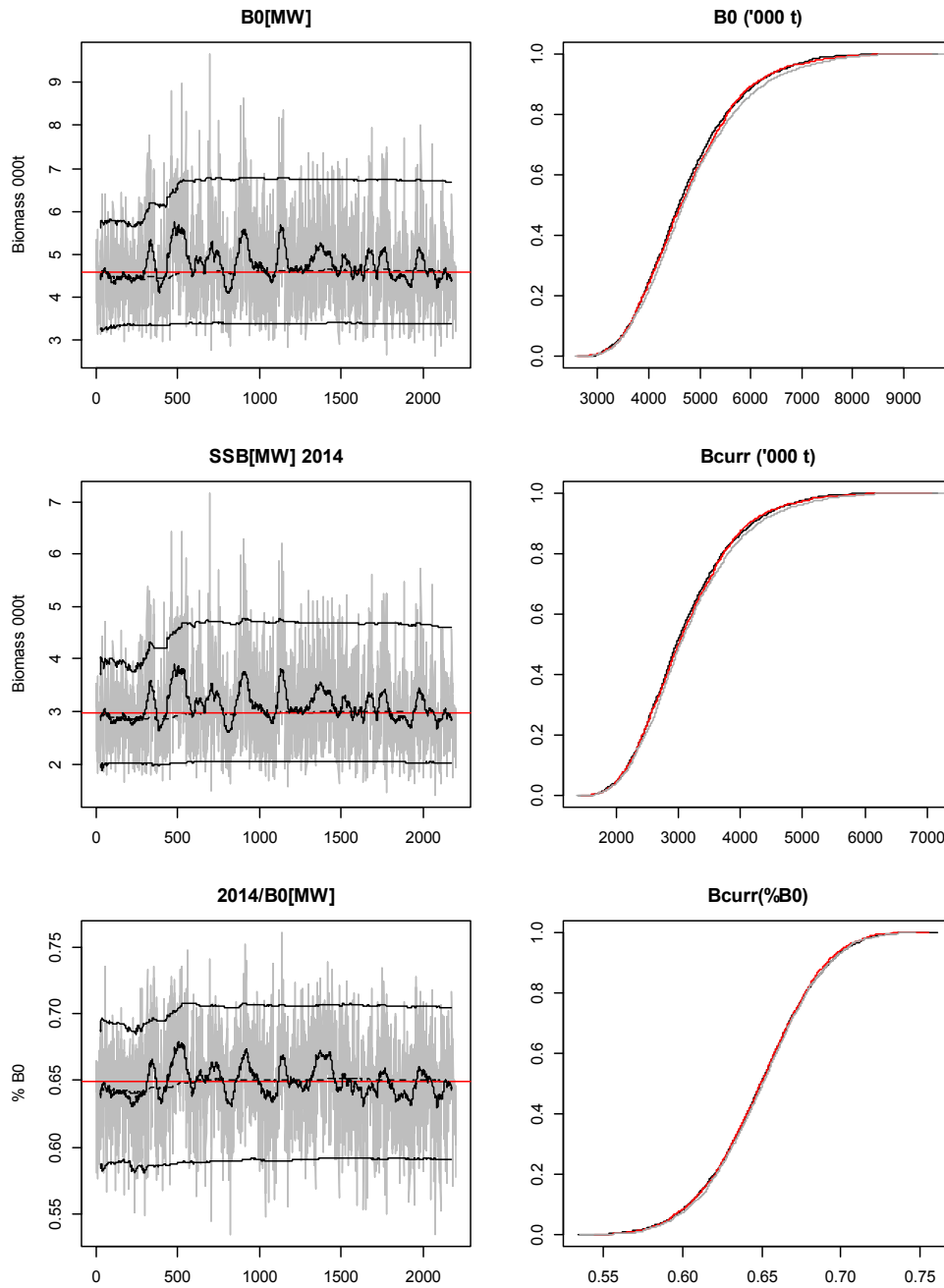
A3. 23: Observed (solid line) and fitted (dashed line) length frequency distributions for MO photographic survey scampi size estimation within the SCI 3 NT_0.15 model.

A3. 24: Numbers of scampi burrows measured, estimated multinomial N sample size, and effective sample size used within the model for length frequency distributions for photographic survey samples within the SCI 3 NT_0.15 model.

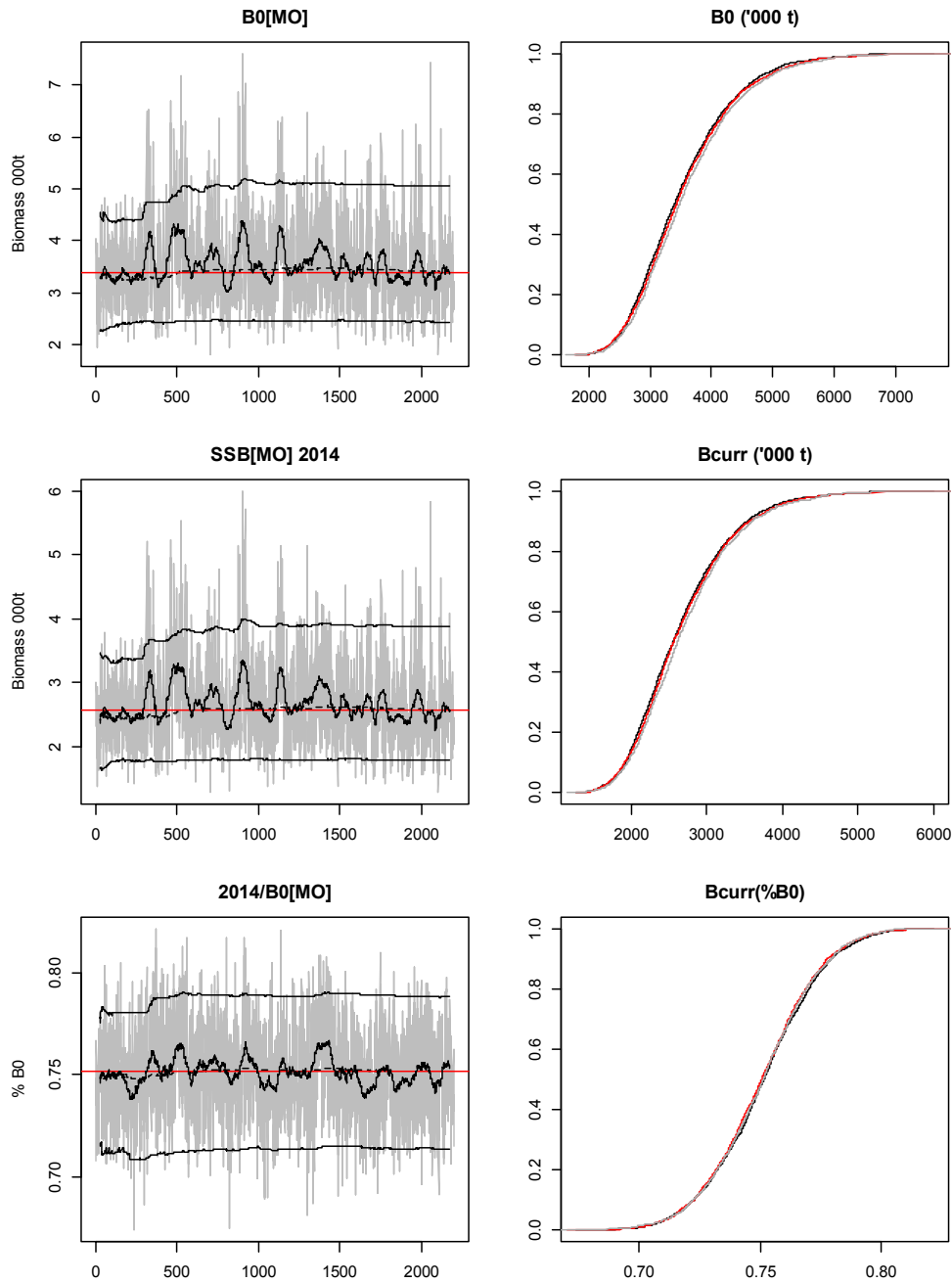
MN	Measured	Multinomial N	Effective sample size
N_2010	360	214	3 069.21
N_2011	536	426	4 569.71
N_2014	227	125	1 935.31
MW	Measured	Multinomial N	Effective sample size
N_2010	303	173	876.84
N_2011	232	128	671.38
N_2014	47	24	136.01
MO	Measured	Multinomial N	Effective sample size
N_2002	397	249	16.36
N_2010	205	113	8.45
N_2011	549	120	22.63
N_2014	117	62	4.82



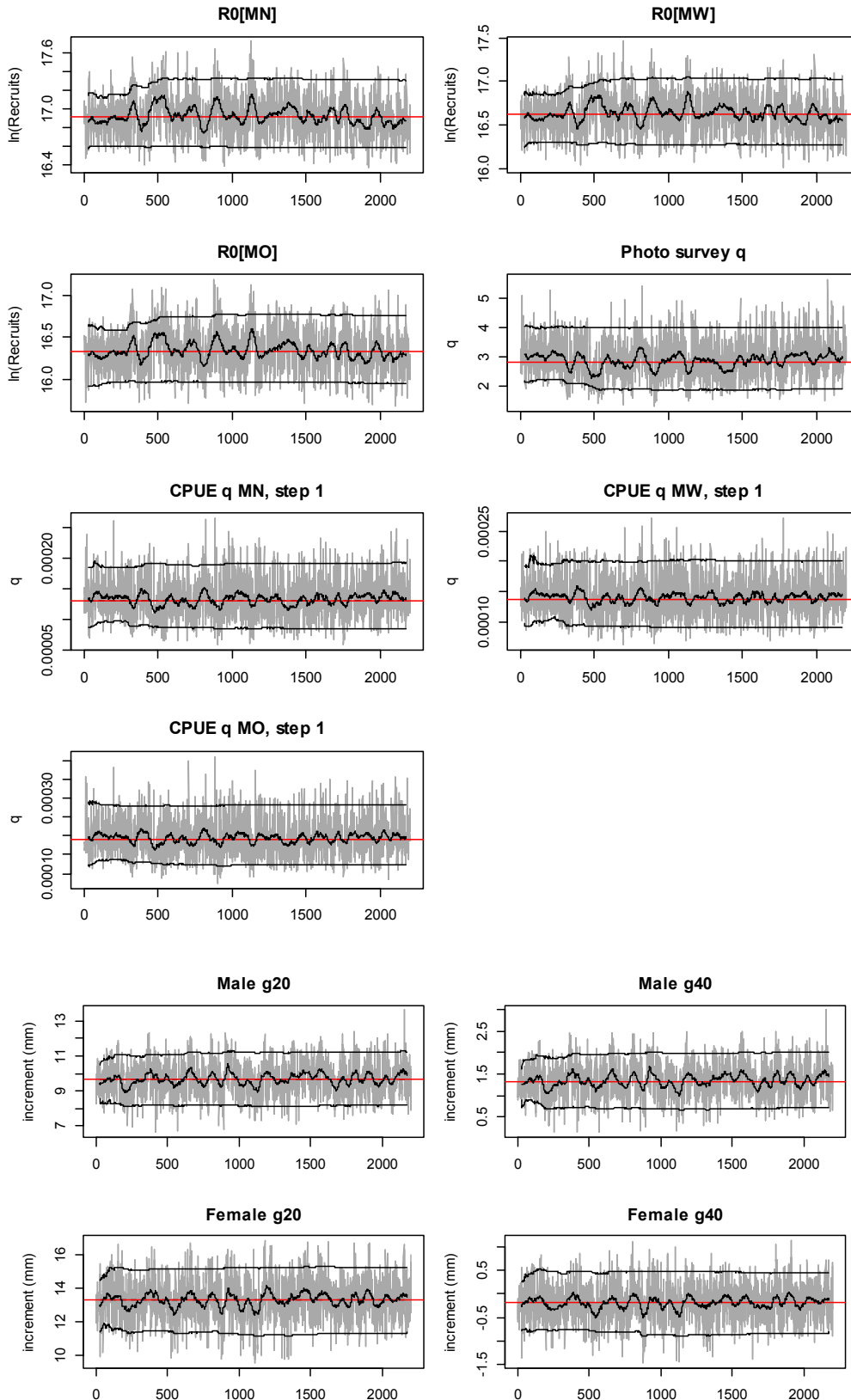
A3. 25: MCMC traces for SSB_0 , SSB_{2014} , and SSB_{2014}/SSB_0 terms for the MN subarea within the SCI 3 NT_0.15 model for SCI 3 (trace – grey line, cumulative moving median – dashed black line, moving average and cumulative moving 2.5%, 97.5% quantiles – solid black lines, overall median – solid red line, left plots), along with cumulative frequency distributions for three independent MCMC chains (shown as red, grey and black lines, right plots).



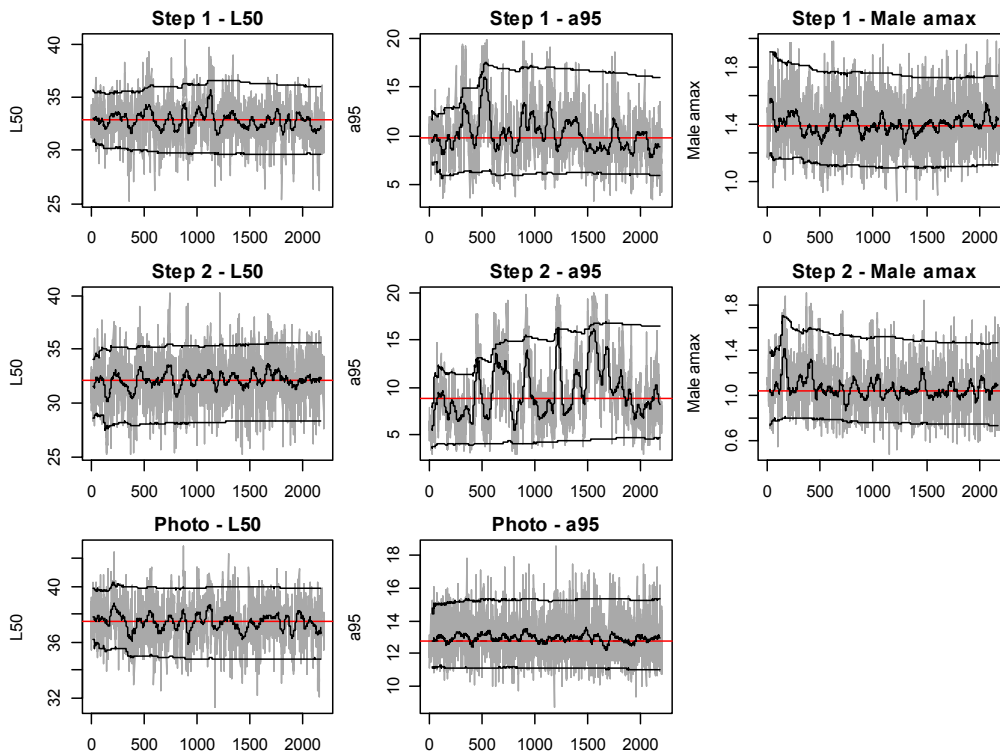
A3. 26: MCMC traces for SSB_0 , SSB_{2014} , and SSB_{2014}/SSB_0 terms for the MW subarea within the SCI 3 NT_0.15 model for SCI 3 (trace – grey line, cumulative moving median – dashed black line, moving average and cumulative moving 2.5%, 97.5% quantiles – solid black lines, overall median – solid red line, left plots), along with cumulative frequency distributions for three independent MCMC chains (shown as red, grey and black lines, right plots).



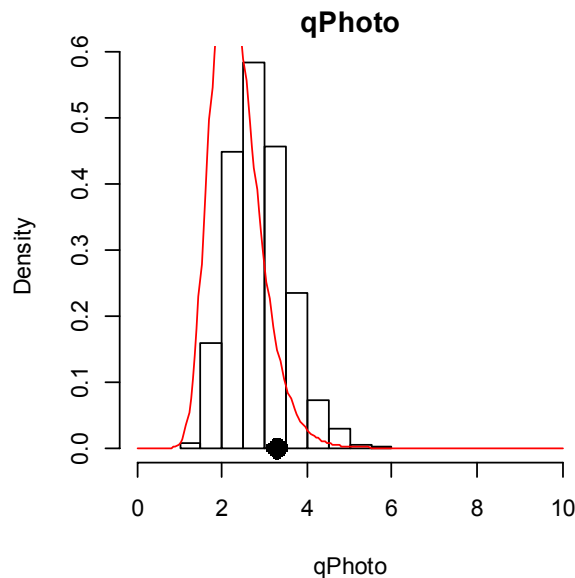
A3. 27: MCMC traces for SSB_0 , SSB_{2014} , and SSB_{2014}/SSB_0 terms for the MN subarea within the SCI 3 NT_0.15 model for SCI 3 (trace – grey line, cumulative moving median – dashed black line, moving average and cumulative moving 2.5%, 97.5% quantiles – solid black lines, overall median – solid red line, left plots), along with cumulative frequency distributions for three independent MCMC chains (shown as red, grey and black lines, right plots).



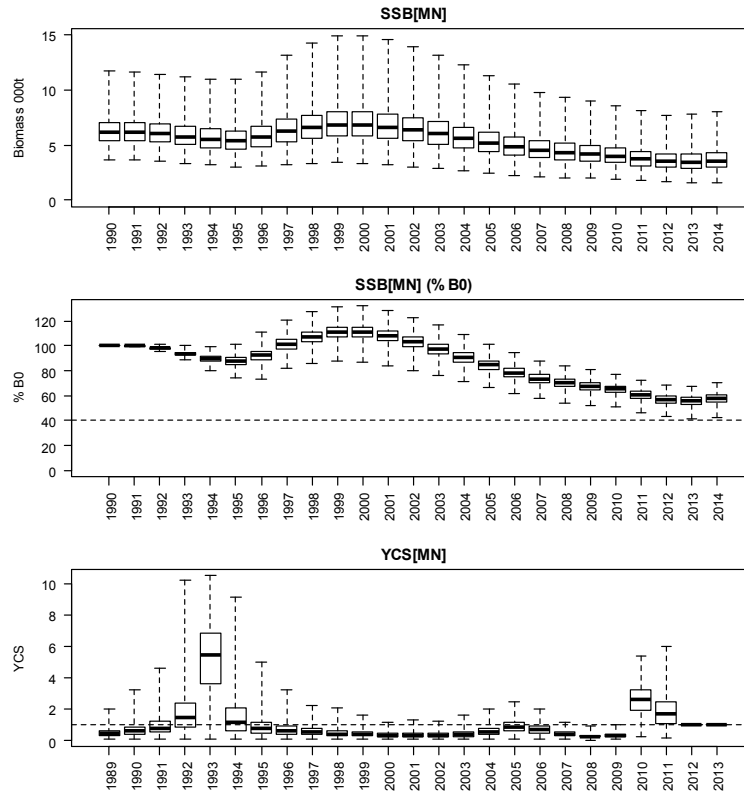
A3. 28: MCMC traces for R_0 , photo survey q , commercial fishery q , and growth increment terms within the SCI 3 NT_0.15 model for SCI 3 (trace – grey line, cumulative moving median – dashed black line, moving average and cumulative moving 2.5%, 97.5% quantiles – solid black lines, overall median – solid red line, left plots), along with cumulative frequency distributions for three independent MCMC chains (shown as red, grey and black lines, right plots).



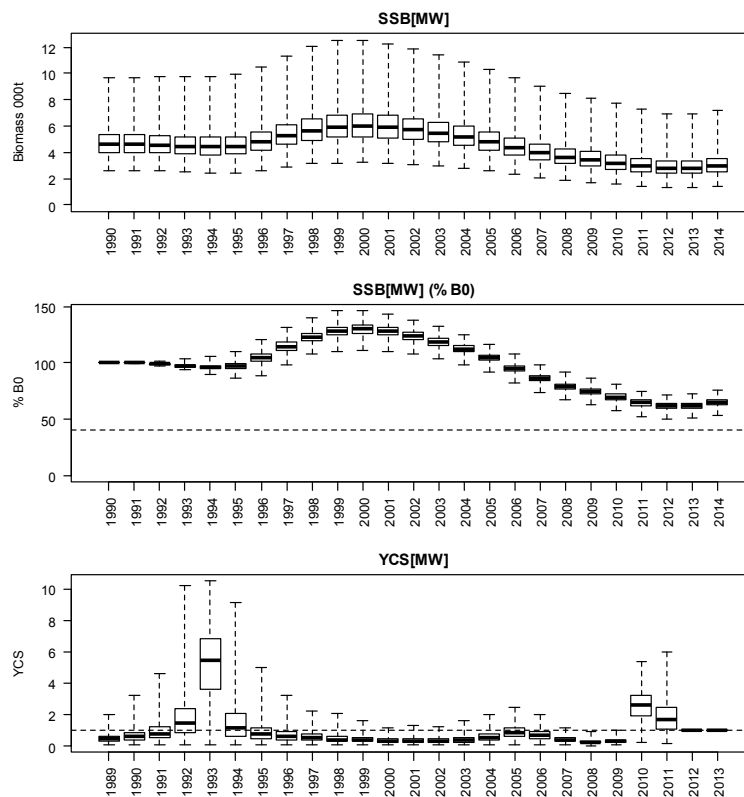
A3. 29: MCMC traces for selectivity parameters within the SCI 3 NT_0.15 model for SCI 3 (trace – grey line, cumulative moving median – dashed black line, moving average and cumulative moving 2.5%, 97.5% quantiles – solid black lines, overall median – solid red line, left plots), along with cumulative frequency distributions for three independent MCMC chains (shown as red, grey and black lines, right plots).



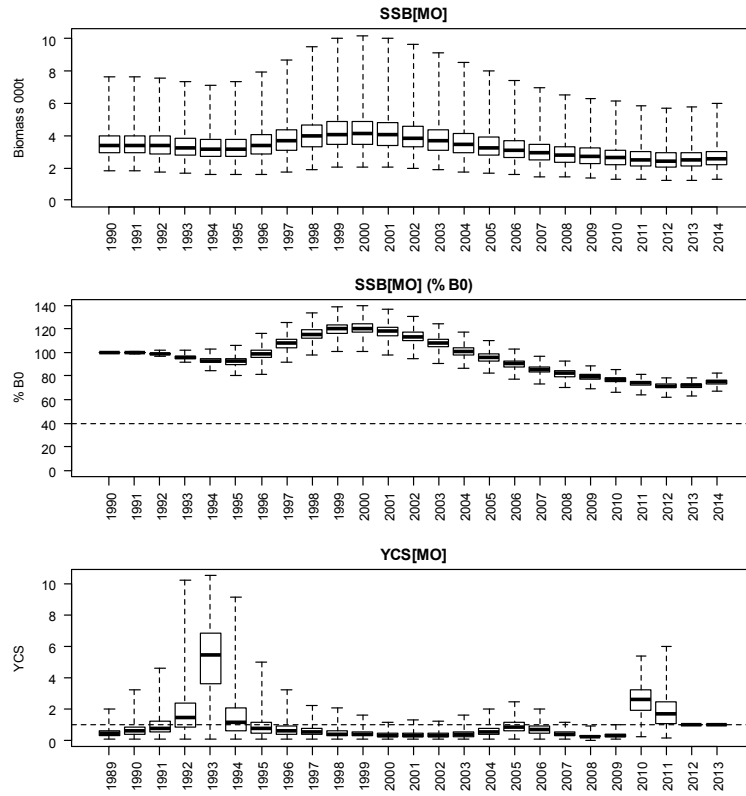
A3. 30: Marginal posterior distribution (histogram), MPD estimate (solid symbol) and distribution of prior (line) for photo survey catchability term within the SCI 3 NT_0.15 model.



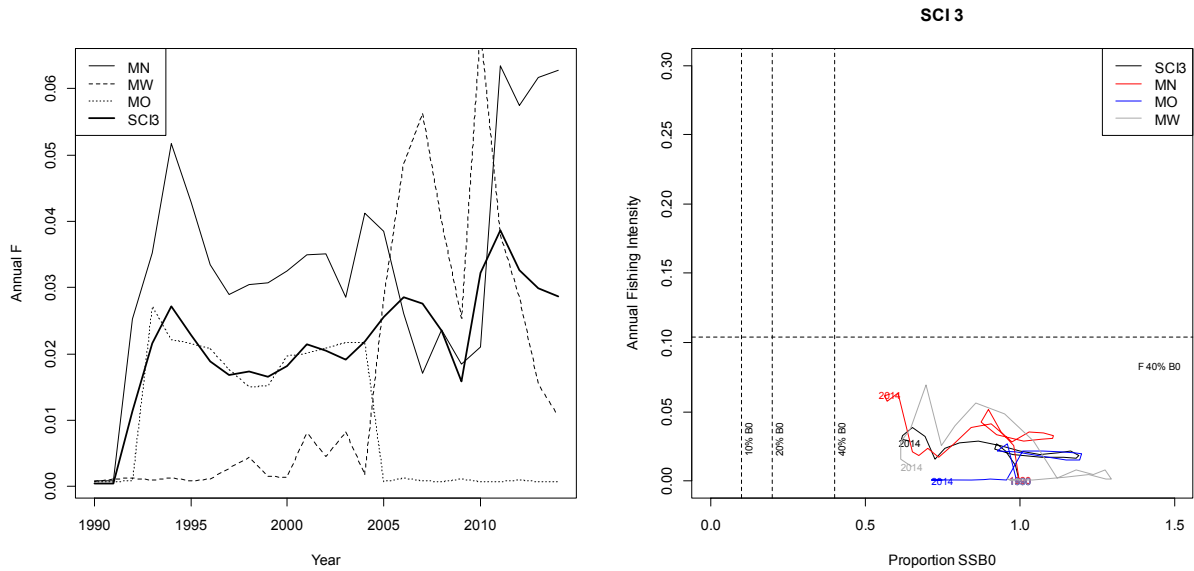
A3. 31: Posterior trajectory of SSB, SSB_{2014}/SSB_0 and YCS for the MN subarea within the SCI 3 NT_0.15 model.



A3. 32: Posterior trajectory of SSB, SSB_{2014}/SSB_0 and YCS for the MW subarea within the SCI 3 NT_0.15 model.

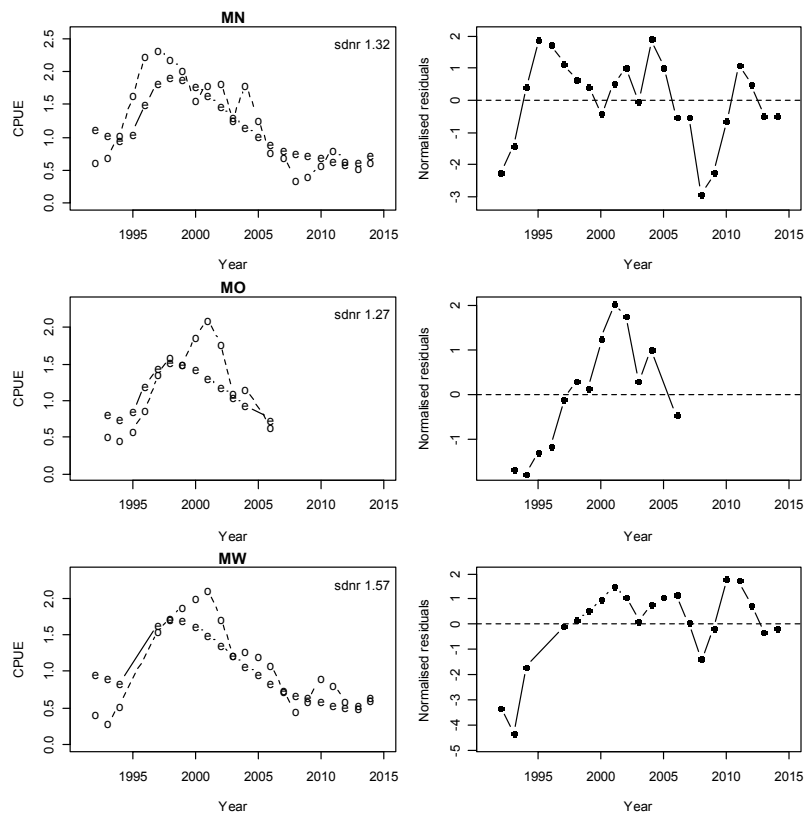


A3. 33: Posterior trajectory of SSB, SSB₂₀₁₄/SSB₀ and YCS for the MO subarea within the SCI 3 NT_{0.15} model.

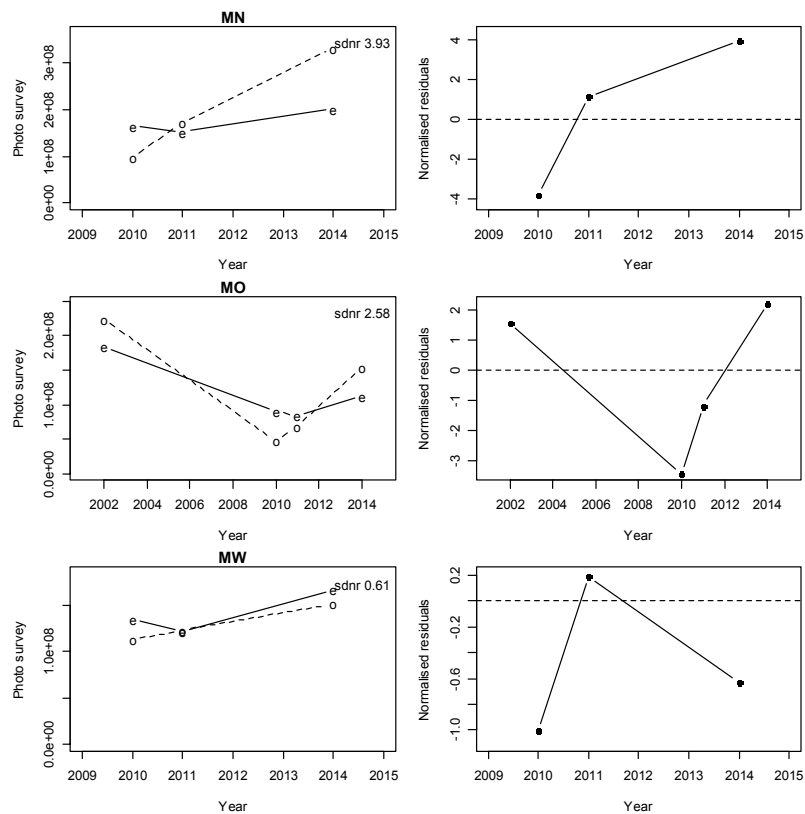


A3. 34: Estimated annual equivalent F (left) and phase plot (right) from the SCI 3 NT_{0.15} model.

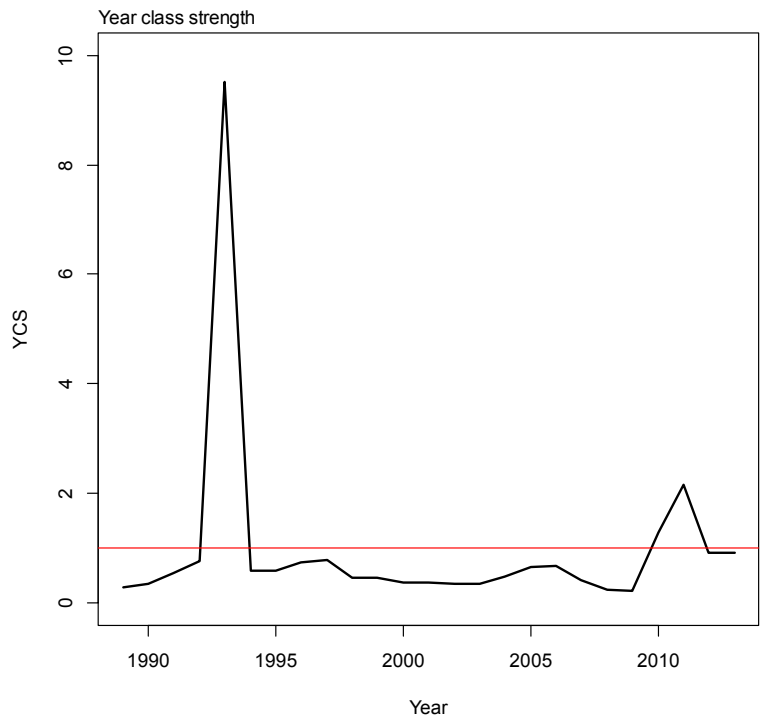
APPENDIX 4. Model NT_0.25



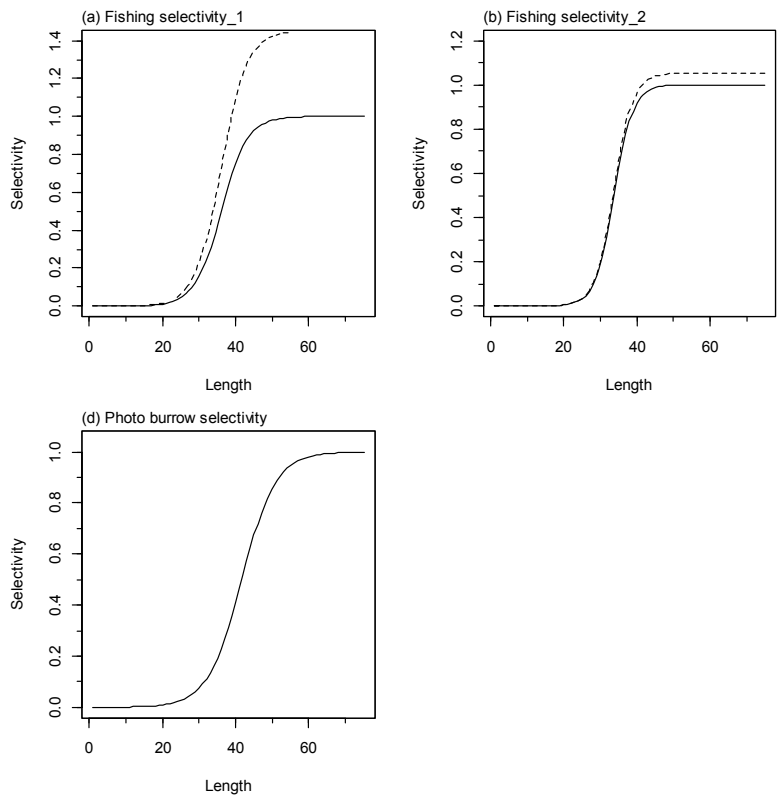
A4. 1: Fits to CPUE indices (left column) and normalised residuals (right column) for each subarea for SCI 3 NT_0.25.



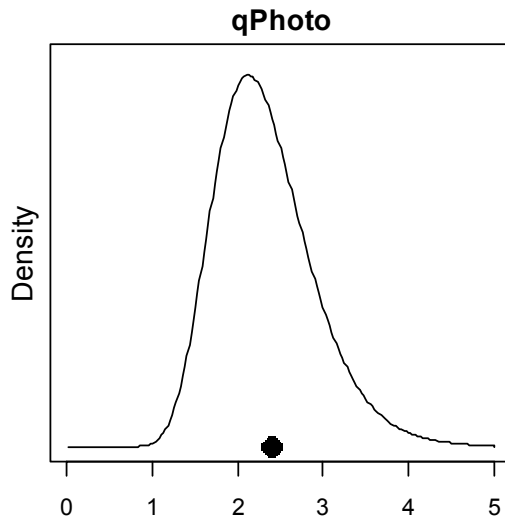
A4. 2: Fits to photographic survey indices (left column) and normalised residuals (right column) for each subarea for SCI 3 NT_0.25.



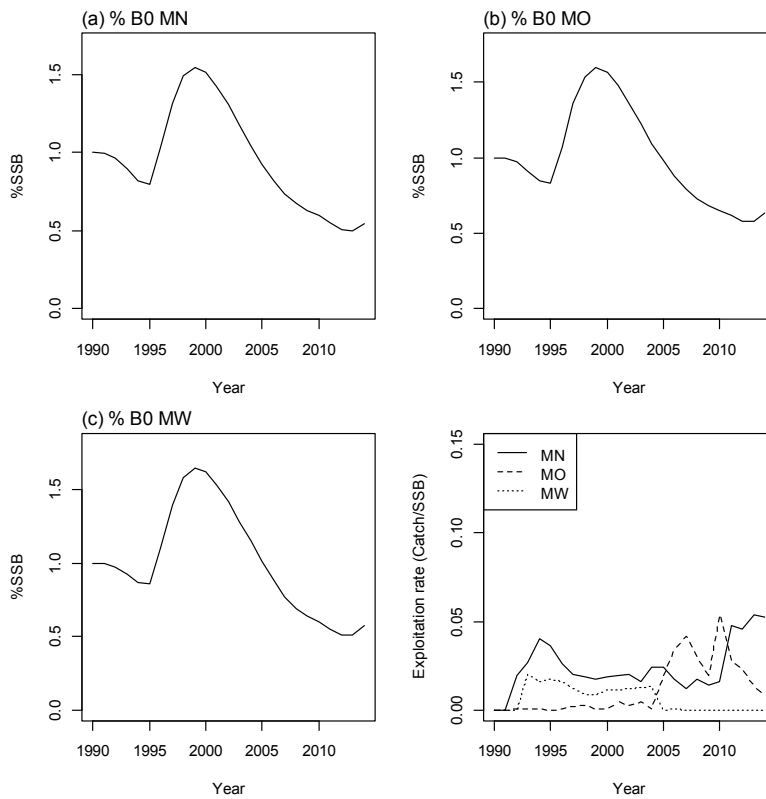
A4. 3: Year class strength for SCI 3 NT_0.25.



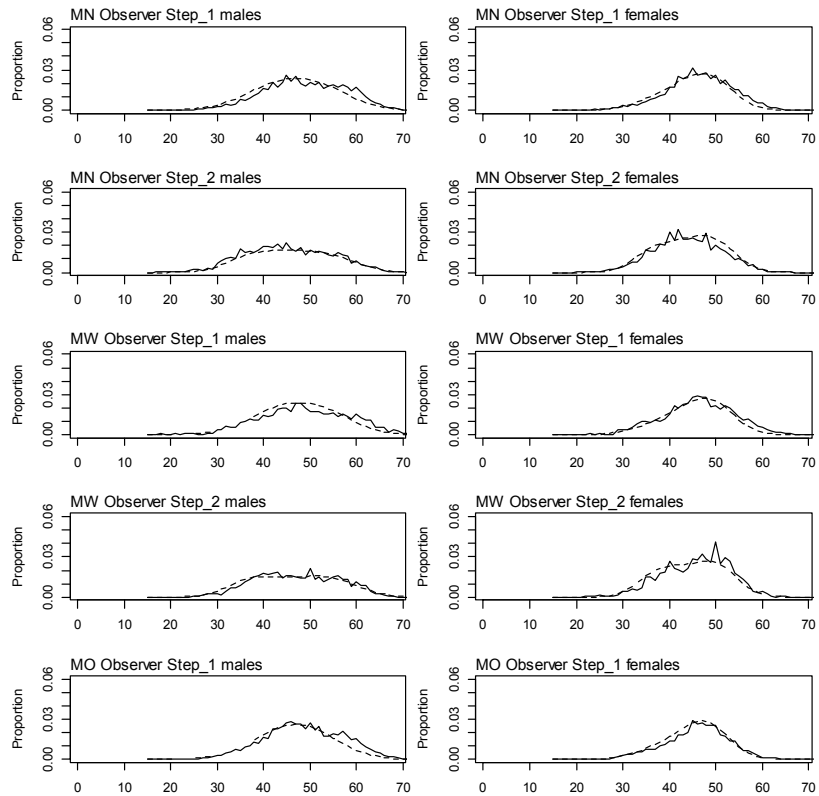
A4. 4: Fishery and survey selectivity curves for SCI 3 NT_0.25. Solid line – females, dotted line – males. The scampi photo index is not sexed, and a single selectivity applies.



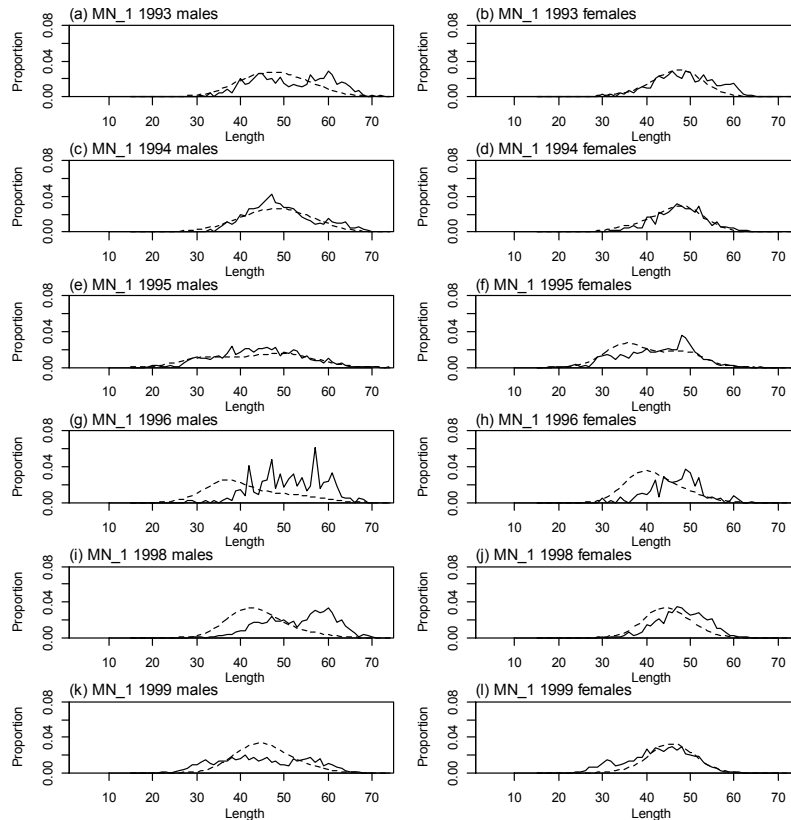
A4. 5: Catchability estimate from MPD model run, plotted in relation to prior distribution for SCI 3 NT_0.25.



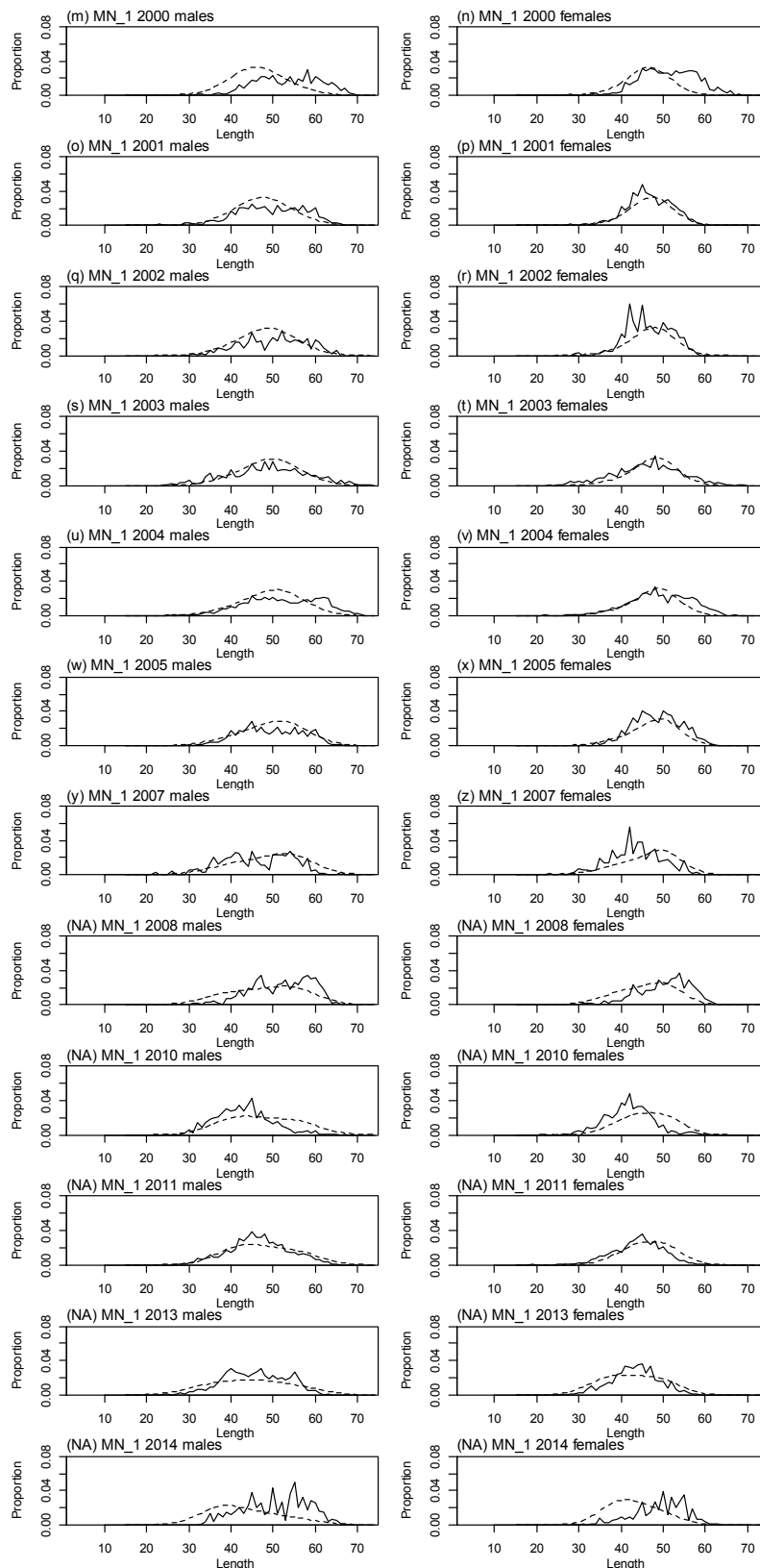
A4. 6: Stock trajectories (%SSB₀) for each subarea estimated from the MPD model run, and estimated exploitation rates for SCI 3 NT_0.25.



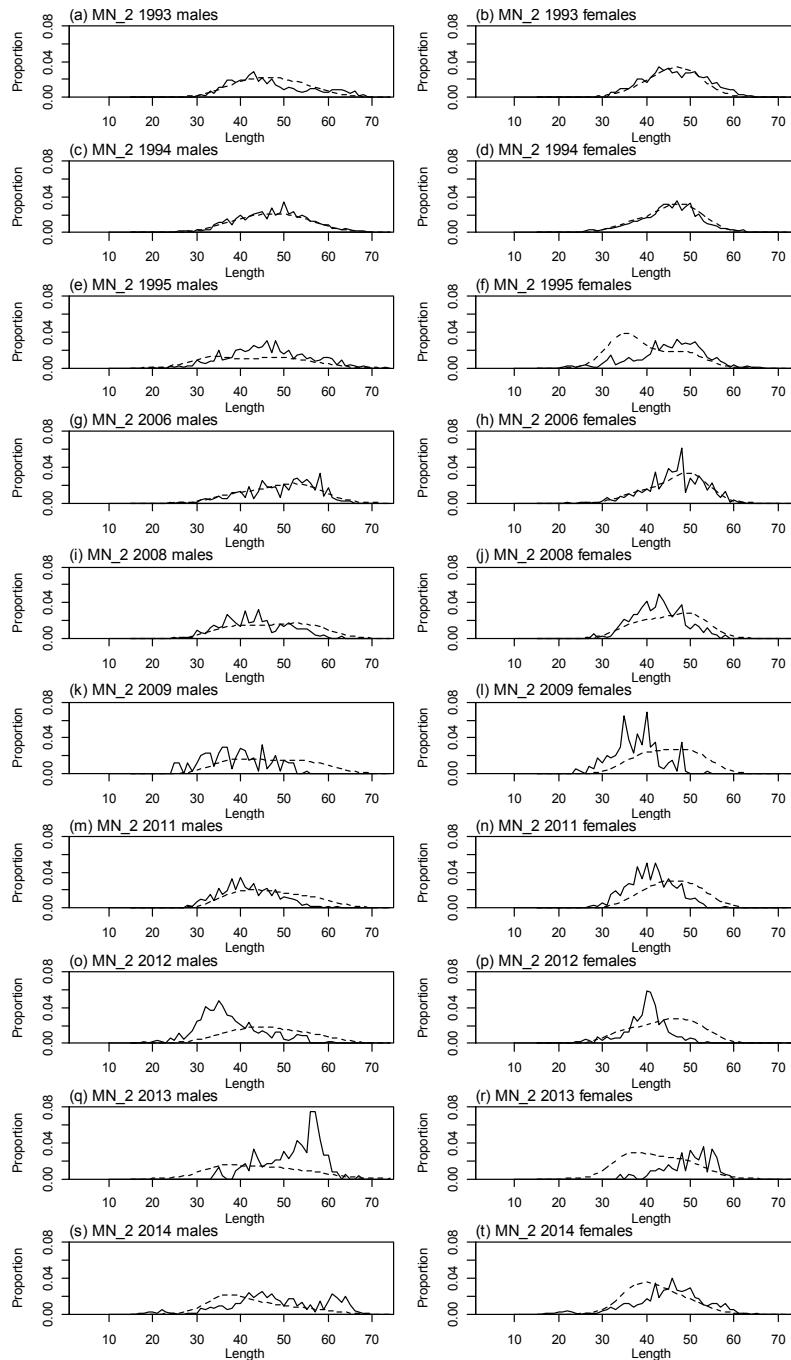
A4. 7: Average observed (solid line) and fitted (dashed line) length frequency distributions for observer samples for SCI 3 NT_0.25.



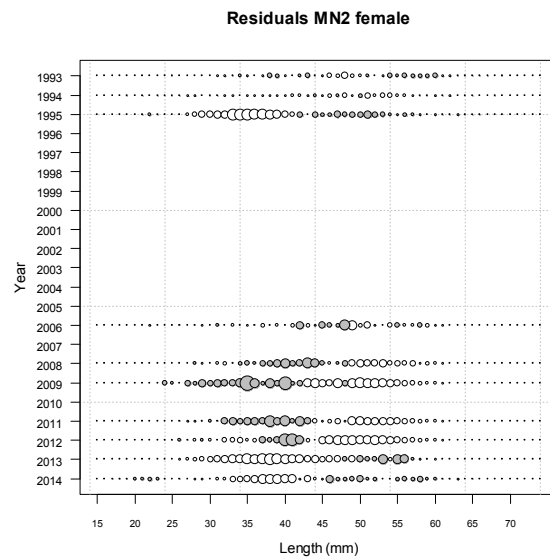
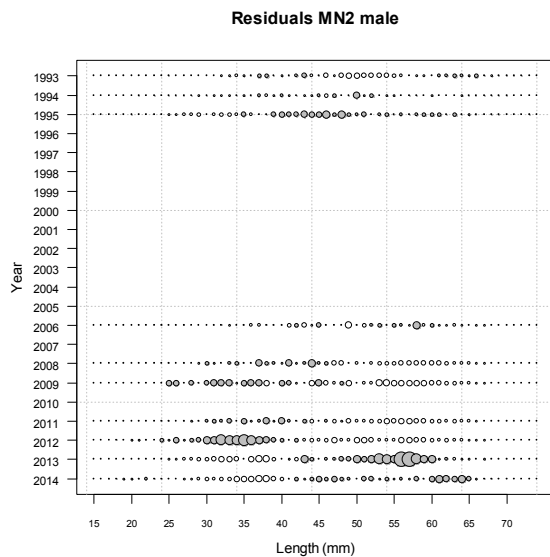
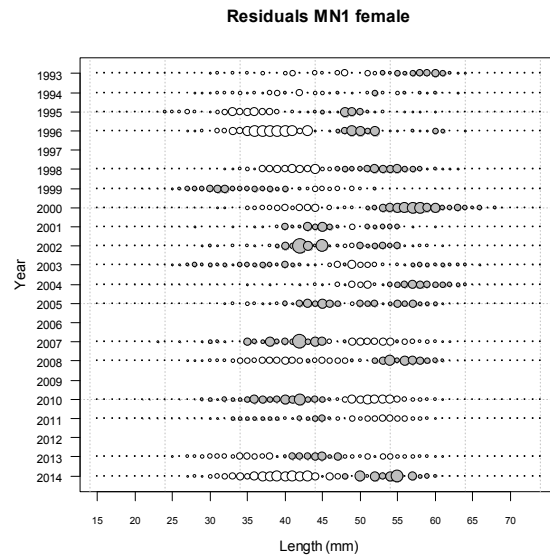
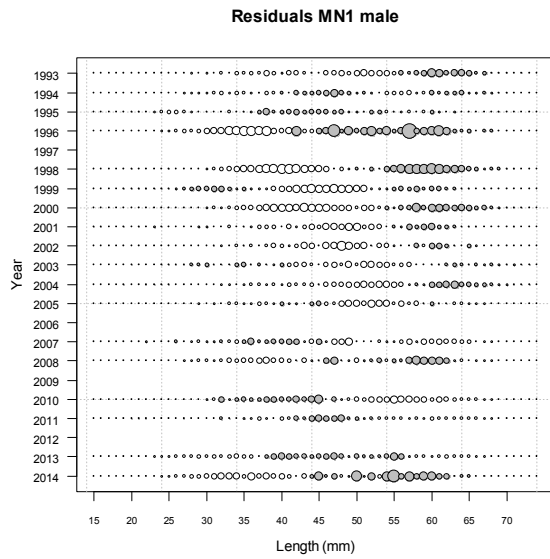
A4. 8: Observed (solid line) and fitted (dashed line) length frequency distributions for observer samples, MN time step 1 for SCI 3 NT_0.25.



A4. 8 ctd: Observed (solid line) and fitted (dashed line) length frequency distributions for observer samples, MN time step 1 for SCI 3 NT_{0.25}.



A4. 9: Observed (solid line) and fitted (dashed line) length frequency distributions for observer samples, MN time step 2 for SCI 3 NT_{0.25}.



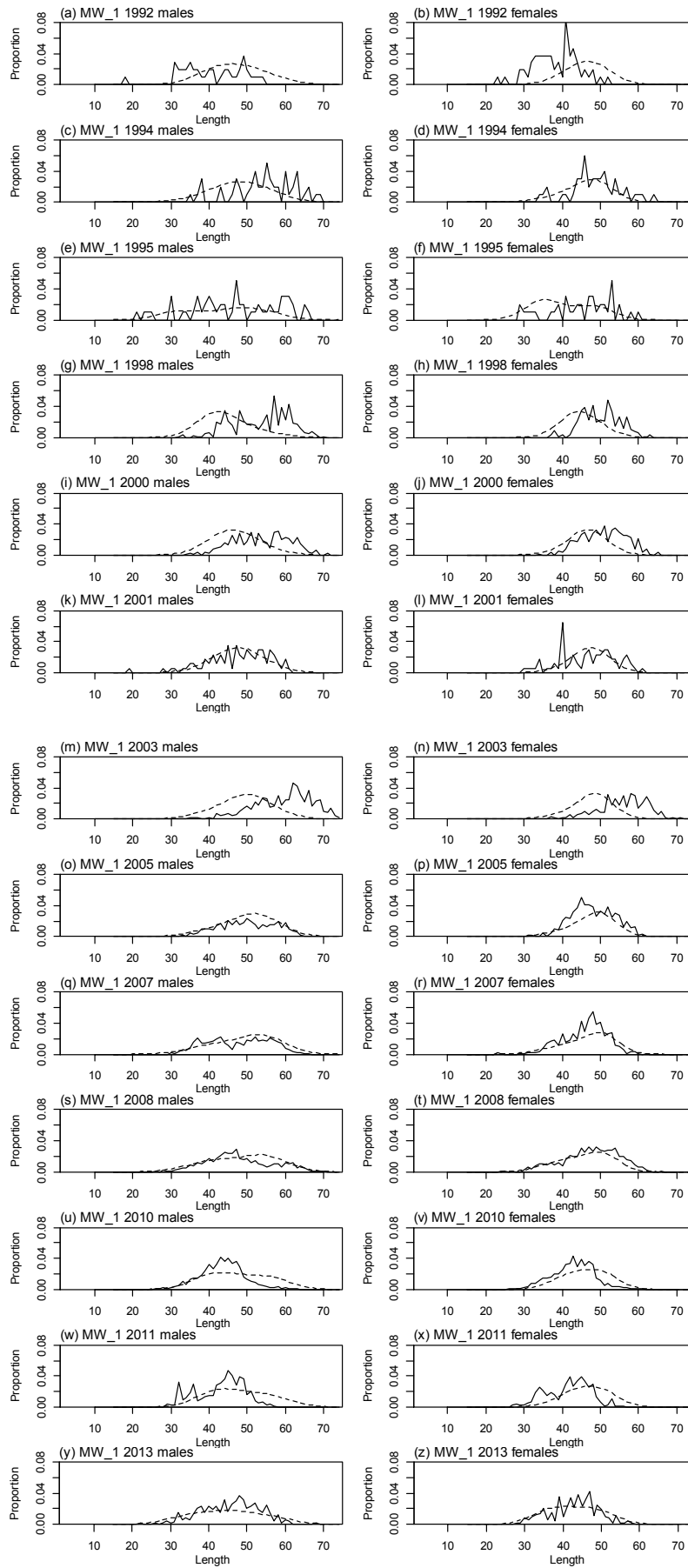
A4. 10: Bubble plots of residuals of fits to length frequency distributions for observer sampling from MN, time step 1 and 2, for SCI 3 NT_0.25.

A4. 11: Numbers of scampi measured, estimated multinomial N sample size, and effective sample size used within the SCI 3 NT_0.25 model for length frequency distributions for observer samples, MN time step 1.

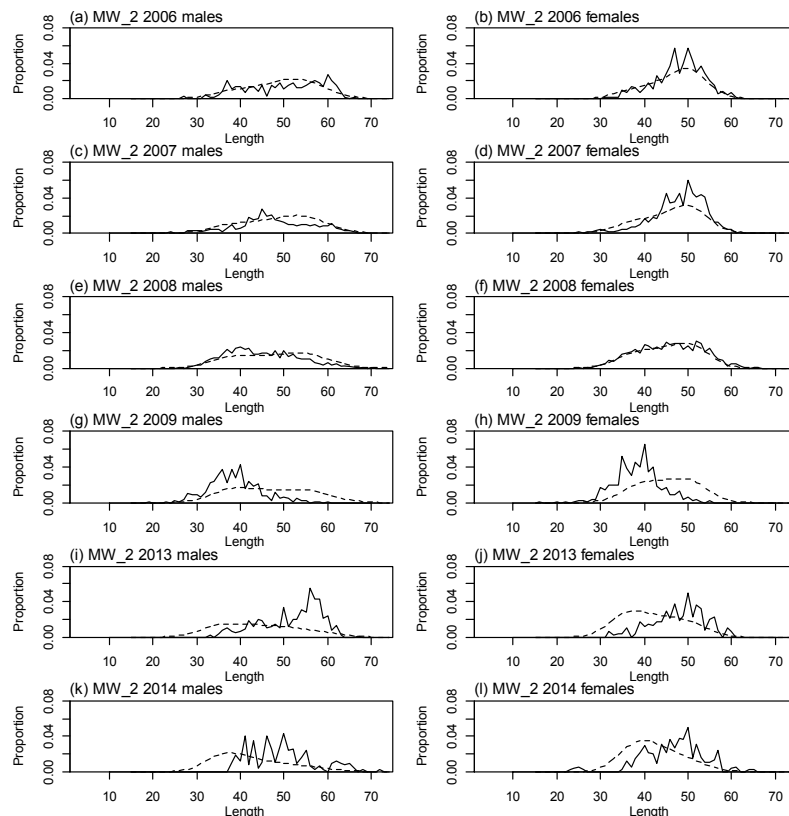
	Measured	Multinomial N	Effective sample size
N_1993	1 089	1 520	3.56
N_1994	2 090	3 036	7.10
N_1995	1 498	2 300	5.38
N_1996	465	500	1.17
N_1998	1 843	3 085	7.22
N_1999	1 921	4 221	9.88
N_2000	1 727	2 200	5.15
N_2001	1 528	2 908	6.80
N_2002	510	908	2.12
N_2003	2 824	5 674	13.28
N_2004	3 856	6 921	16.20
N_2005	1 448	2 497	5.84
N_2007	829	1 189	2.78
N_2008	1 087	1 587	3.71
N_2010	948	1 632	3.82
N_2011	3 273	6 881	16.10
N_2013	2 613	3 847	9.00
N_2014	403	789	1.85

A4. 12: Numbers of scampi measured, estimated multinomial N sample size, and effective sample size used within the SCI 3 NT_0.25 model for length frequency distributions for observer samples, MN time step 2.

	Measured	Multinomial N	Effective sample size
N_1993	1 639	3 306	11.13
N_1994	2 923	5 285	17.79
N_1995	1 260	1 800	6.06
N_2006	1 086	1 635	5.50
N_2008	535	699	2.35
N_2009	186	245	0.82
N_2011	1 019	1 900	6.40
N_2012	333	588	1.98
N_2013	352	234	0.79
N_2014	1 443	1 378	4.64



A4. 13: Observed (solid line) and fitted (dashed line) length frequency distributions for observer samples, MW time step 1 for SCI 3 NT_0.25.



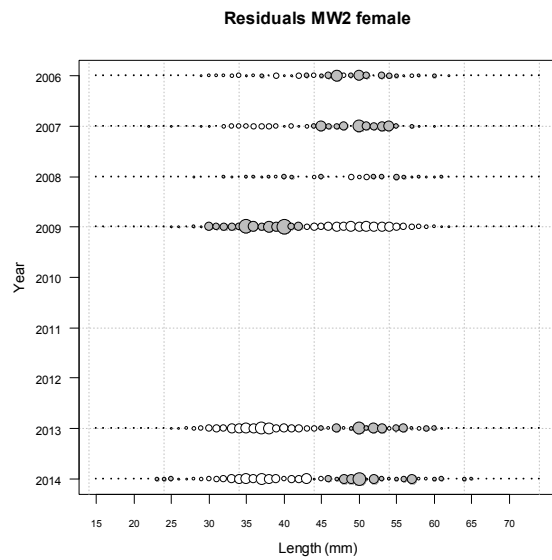
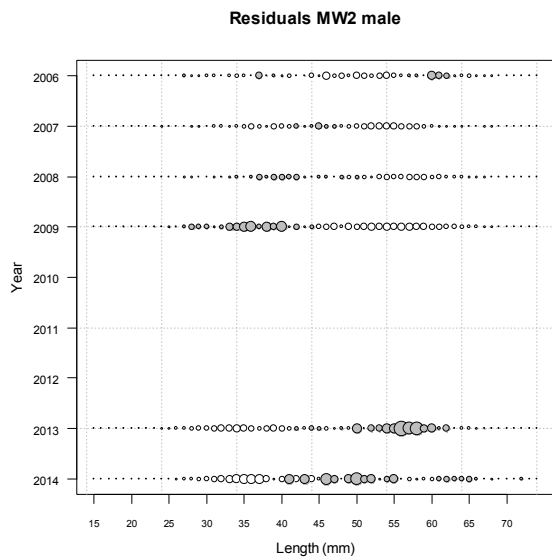
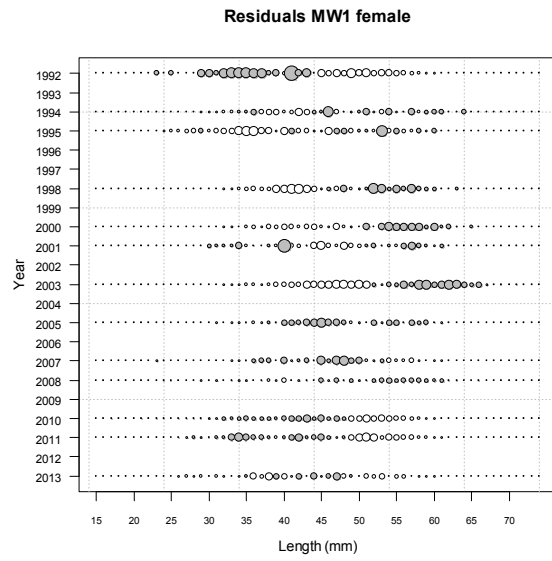
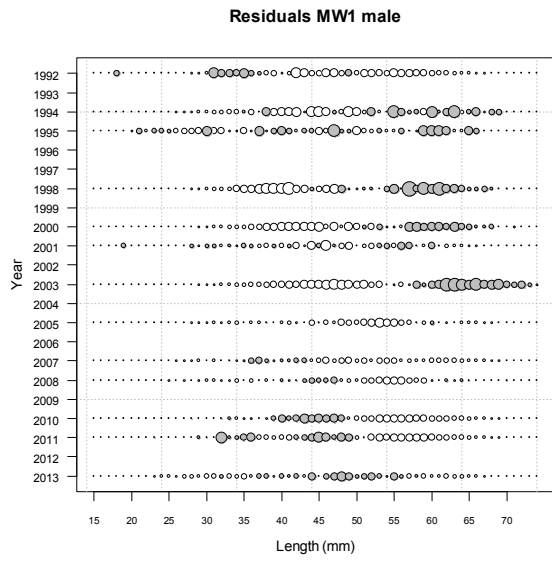
A4. 14: Observed (solid line) and fitted (dashed line) length frequency distributions for observer samples, MW time step 2 for SCI 3 NT_0.25.

A4. 15: Numbers of scampi measured, estimated multinomial N sample size, and effective sample size used within the SCI 3 NT_0.25 model for length frequency distributions for observer samples, MW time step 1.

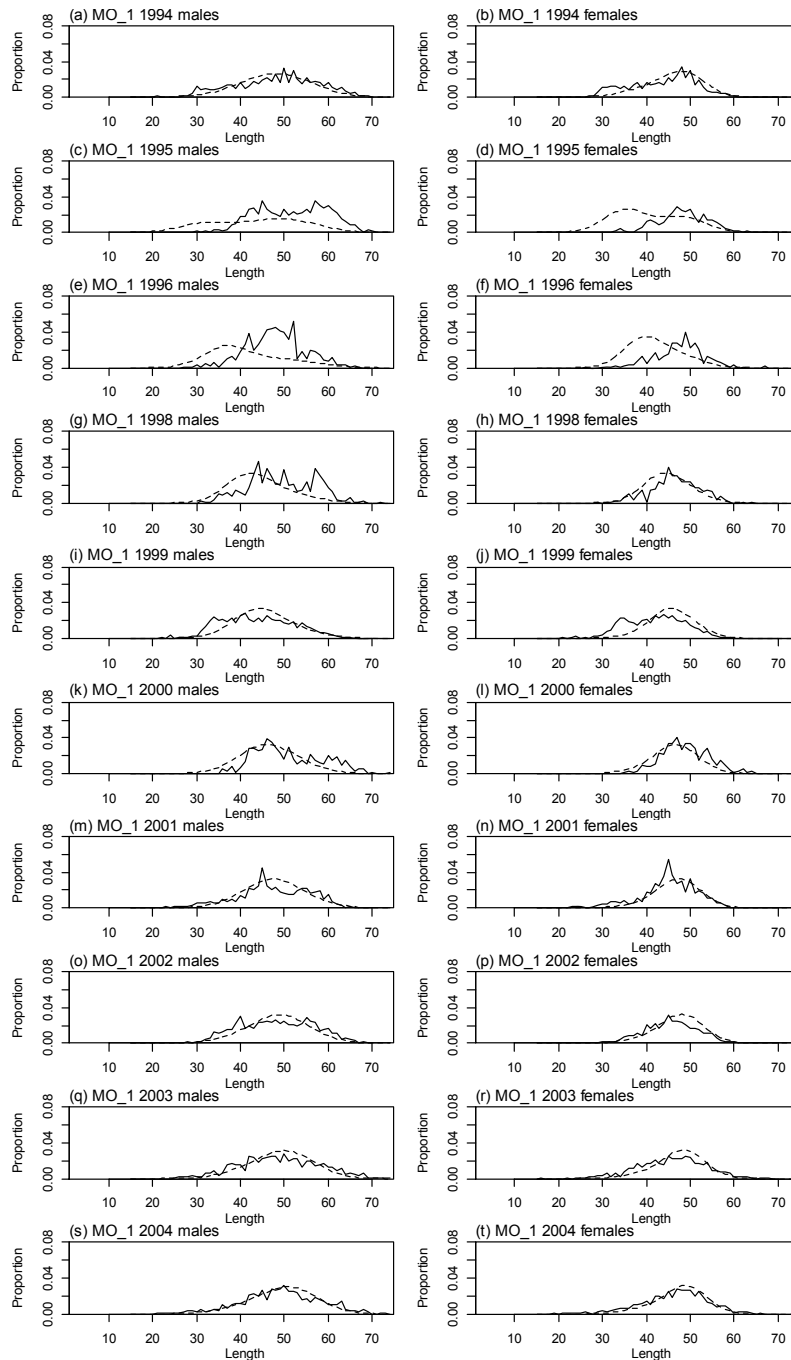
	Measured	Multinomial N	Effective sample size
N_1992	229	107	0.26
N_1994	242	100	0.24
N_1995	241	100	0.24
N_1998	365	365	0.87
N_2000	521	600	1.44
N_2001	251	169	0.40
N_2003	578	799	1.91
N_2005	593	870	2.08
N_2007	1 082	1 669	3.99
N_2008	1 201	1 865	4.46
N_2010	3 163	6 951	16.63
N_2011	712	2 345	5.61
N_2013	495	616	1.47

A4. 16: Numbers of scampi measured, estimated multinomial N sample size, and effective sample size used within the SCI 3 NT_0.25 model for length frequency distributions for observer samples, MW time step 2.

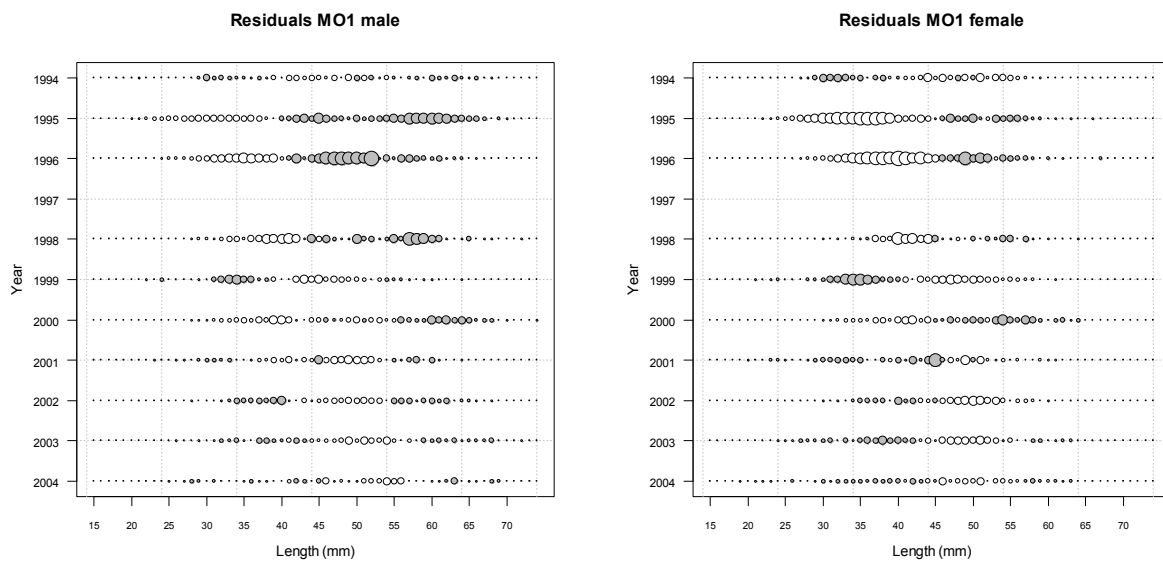
	Measured	Multinomial N	Effective sample size
N_2006	659	699	2.14
N_2007	1 333	2 406	7.35
N_2008	2 278	4 100	12.53
N_2009	693	1 340	4.09
N_2013	550	483	1.48
N_2014	460	317	0.97



A4. 17: Bubble plots of residuals of fits to length frequency distributions for observer sampling from MW, time step 1 and 2, for SCI 3 NT_0.25.



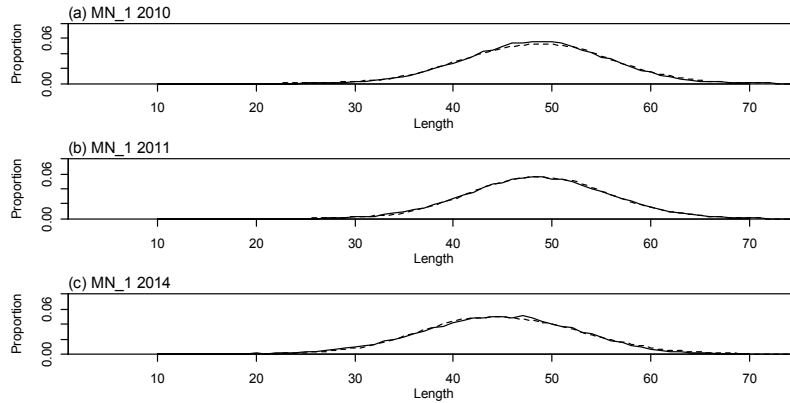
A4. 18: Observed (solid line) and fitted (dashed line) length frequency distributions for observer samples, MO time step 1 for SCI 3 NT_0.25.



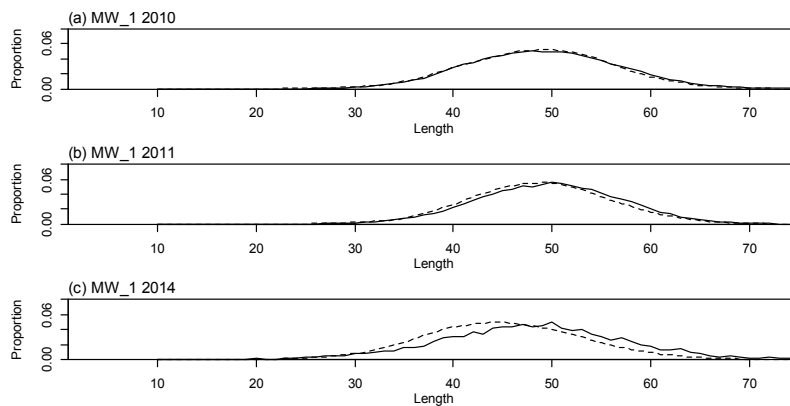
A4. 19: Bubble plots of residuals of fits to length frequency distributions for observer sampling from MO, time step 1, for SCI 3 NT_0.25.

A4. 20: Numbers of scampi measured, estimated multinomial N sample size, and effective sample size used within the SCI 3 NT_0.25 model for length frequency distributions for observer samples, MO time step 1.

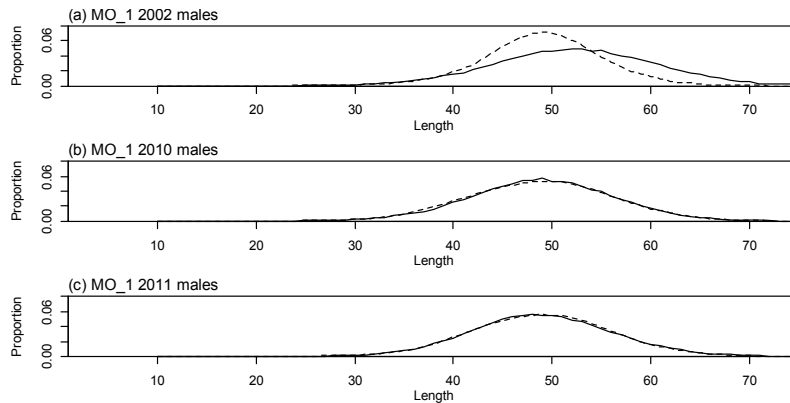
	Measured	Multinomial N	Effective sample size
N_1994	2 665	4 814	11.48
N_1995	2 474	2 500	5.96
N_1996	752	1 200	2.86
N_1998	870	900	2.15
N_1999	1 492	2 996	7.15
N_2000	608	600	1.43
N_2001	1 749	3 118	7.44
N_2002	1 768	3 442	6.29
N_2003	1 367	2 224	5.31
N_2004	1 557	2 881	6.87



A4. 21: Observed (solid line) and fitted (dashed line) length frequency distributions for MN photographic survey scampi size estimation within the SCI 3 NT_0.25 model.



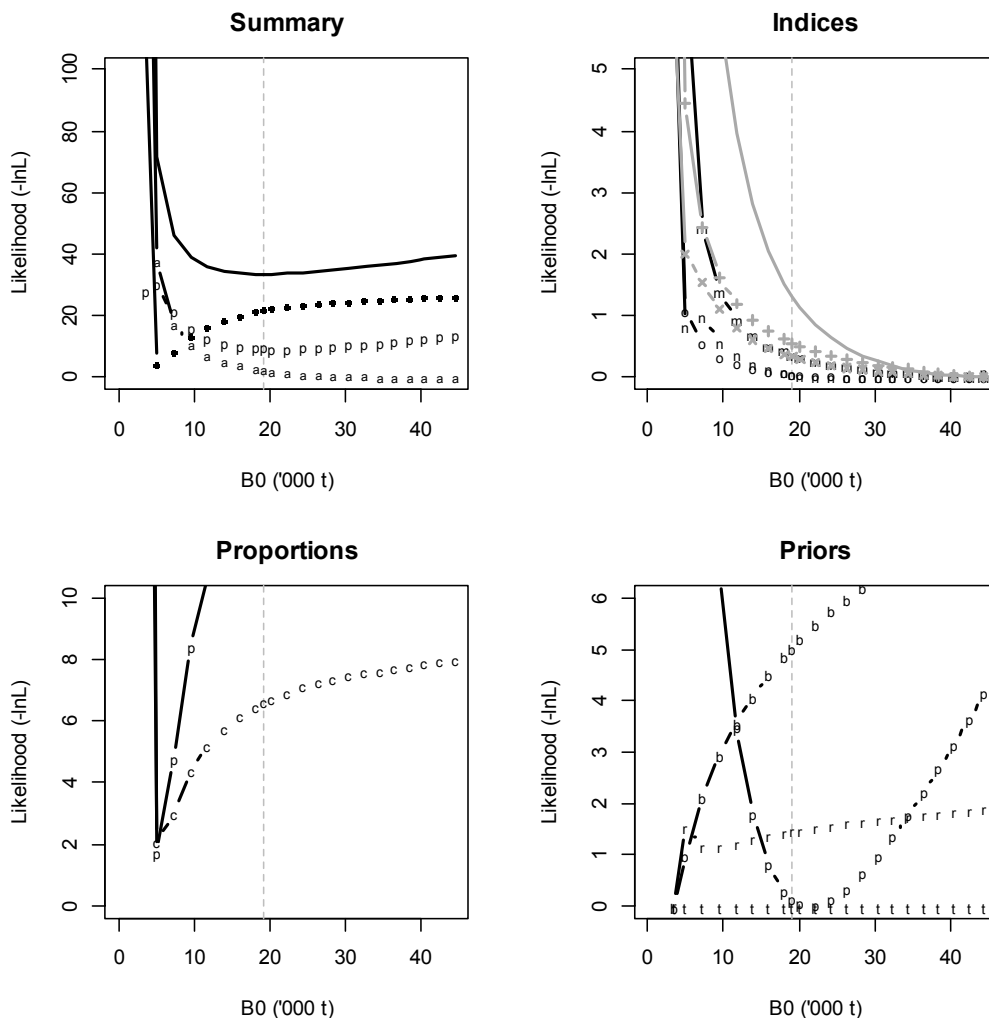
A4. 22: Observed (solid line) and fitted (dashed line) length frequency distributions for MW photographic survey scampi size estimation within the SCI 3 NT_0.25 model.



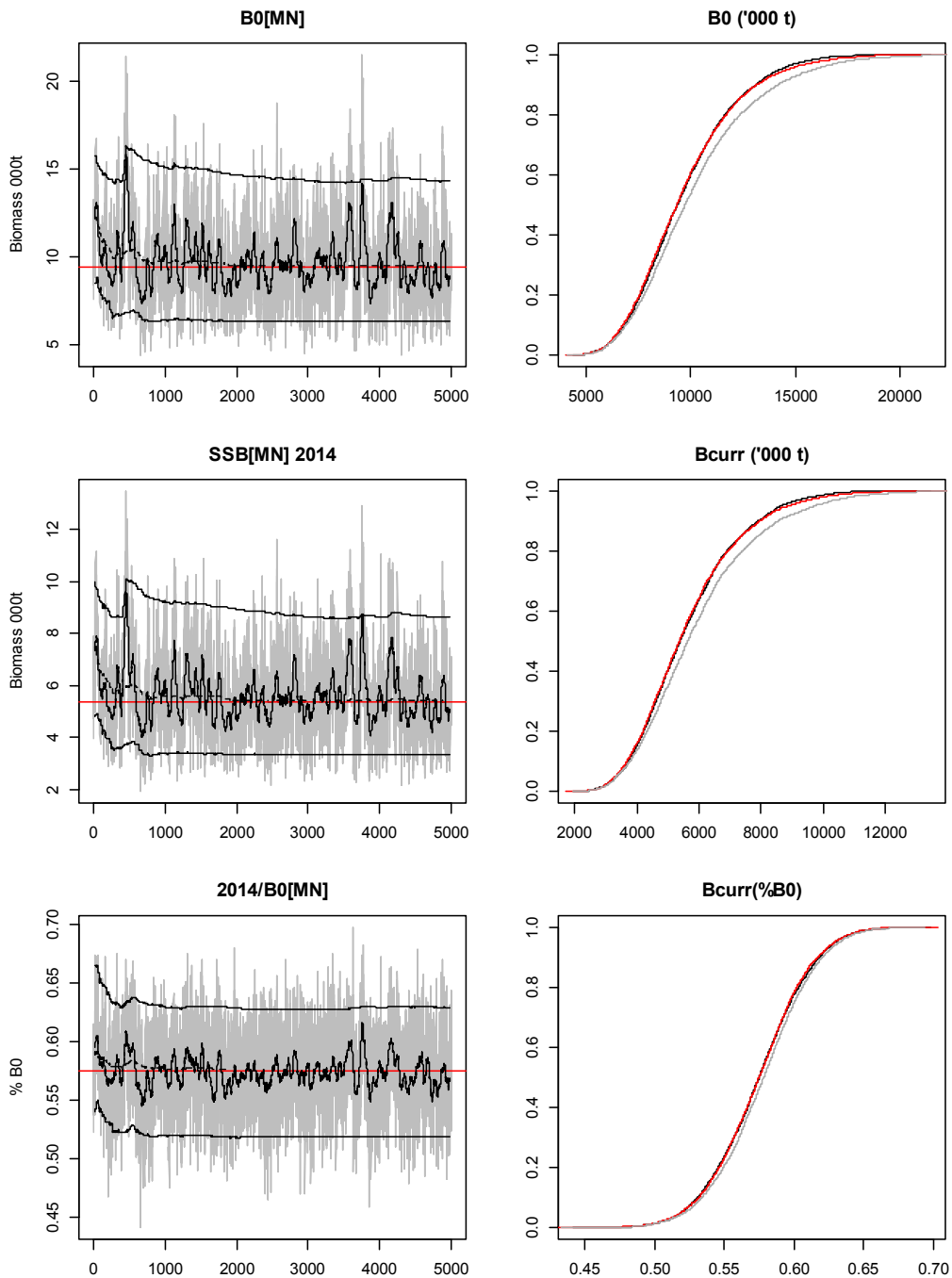
A4. 23: Observed (solid line) and fitted (dashed line) length frequency distributions for MO photographic survey scampi size estimation within the SCI 3 NT_0.25 model.

A4. 24: Numbers of scampi burrows measured, estimated multinomial N sample size, and effective sample size used within the model for length frequency distributions for photographic survey samples within the SCI 3 NT_0.25 model.

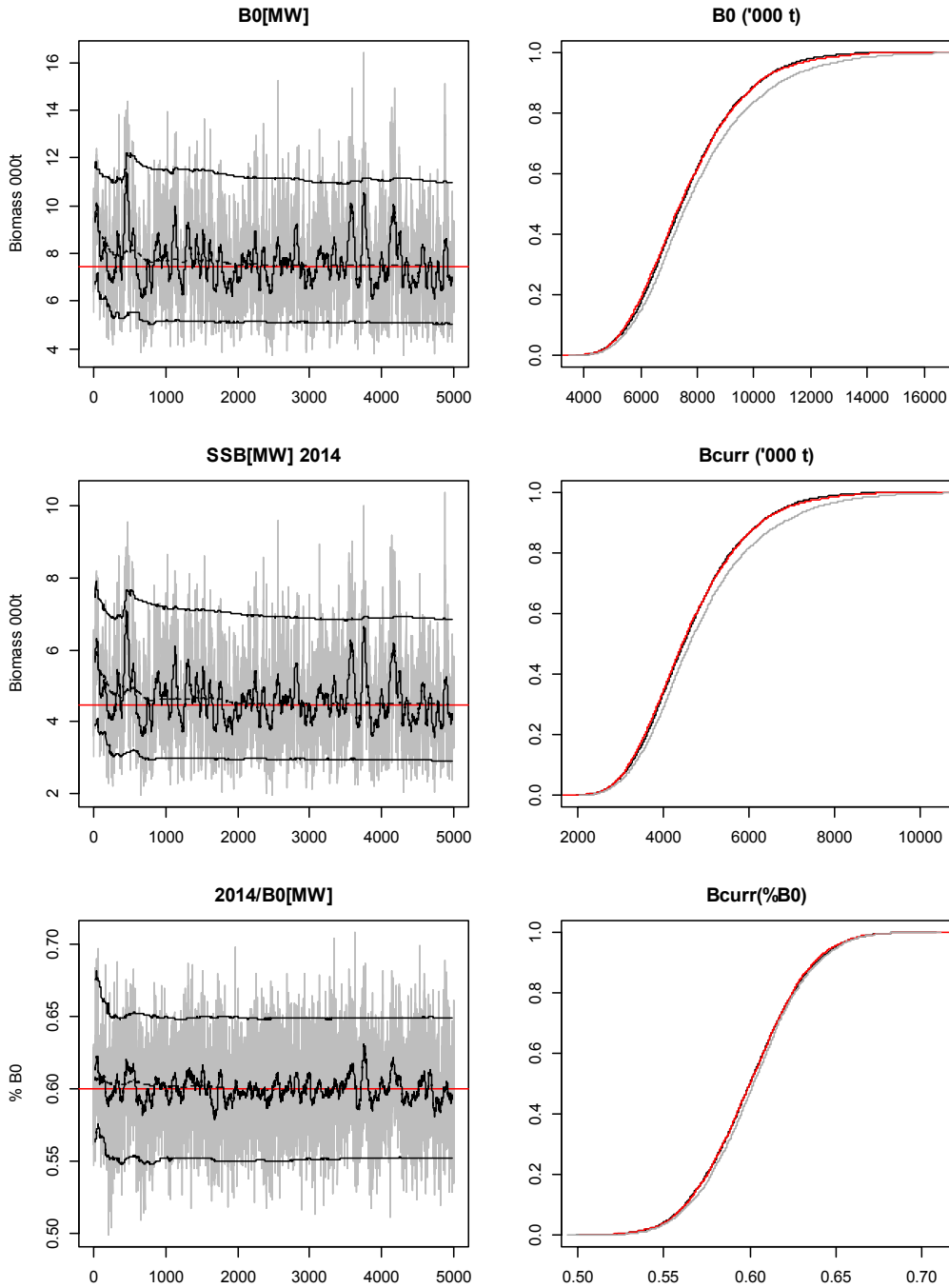
MN	Measured	Multinomial N	Effective sample size
N_2010	360	214	3 069.21
N_2011	536	426	4 569.71
N_2014	227	125	1 935.31
MW	Measured	Multinomial N	Effective sample size
N_2010	303	173	876.84
N_2011	232	128	671.38
N_2014	47	24	136.01
MO	Measured	Multinomial N	Effective sample size
N_2002	397	249	16.36
N_2010	205	113	8.45
N_2011	549	120	22.63
N_2014	117	62	4.82



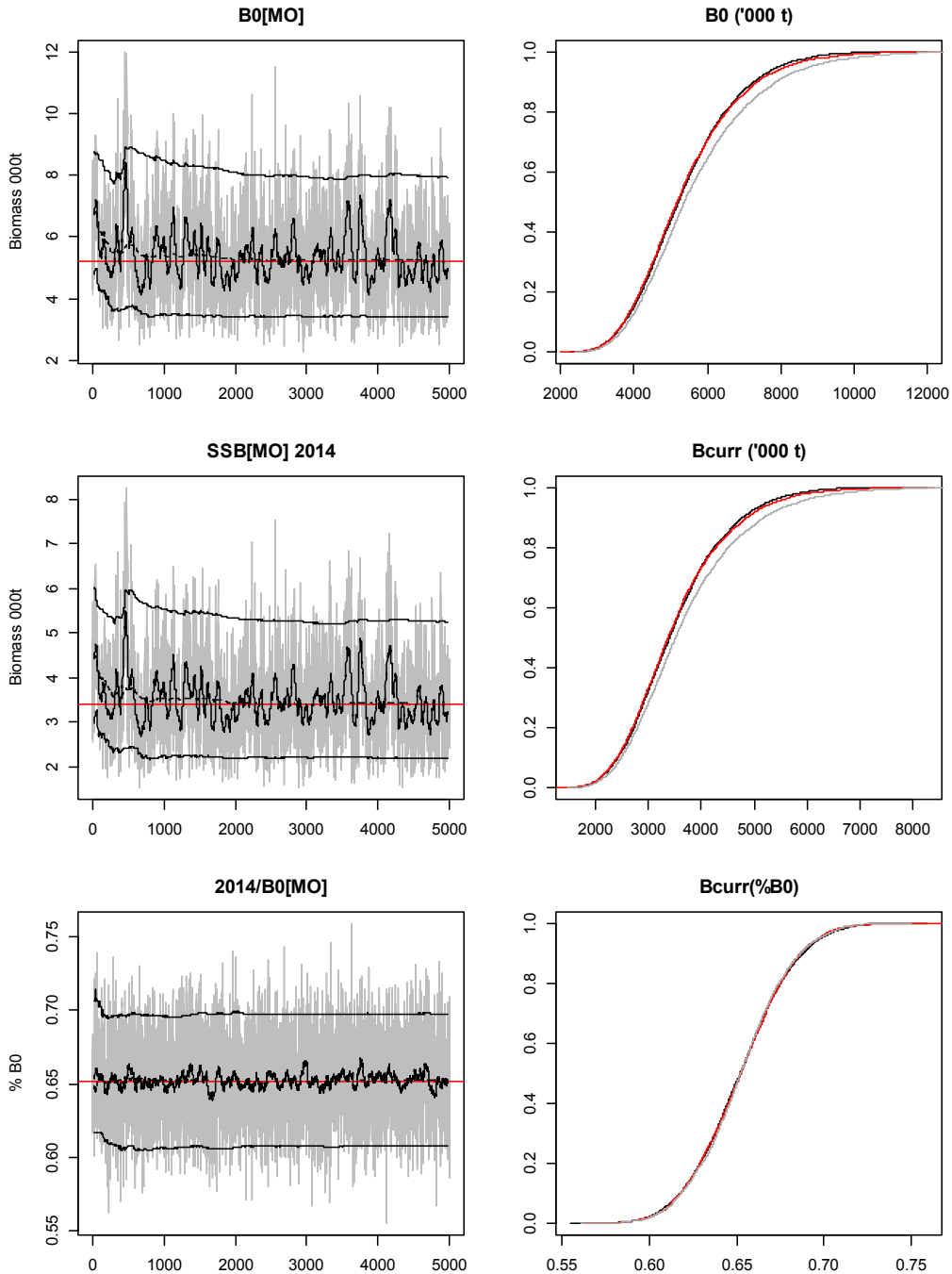
A4. 25: Likelihood profiles for the SCI 3 NT_0.25 model for SCI 3 when B_0 is fixed in the model. Figures show profiles for main priors (top left, p – priors, a – abundance indices, • – proportions at length, r – recapture data), abundance indices (top right, t - trawl survey, c - CPUE, p – photo survey), proportion at length data (bottom left, a-trawl, 1 – observer time step 1, 2 – observer time step 2, 3 – observer time step 3, p - photo) and priors (bottom right, b- B_0 , YCS - r, p- q-Photo). Vertical dashed line represents MPD.



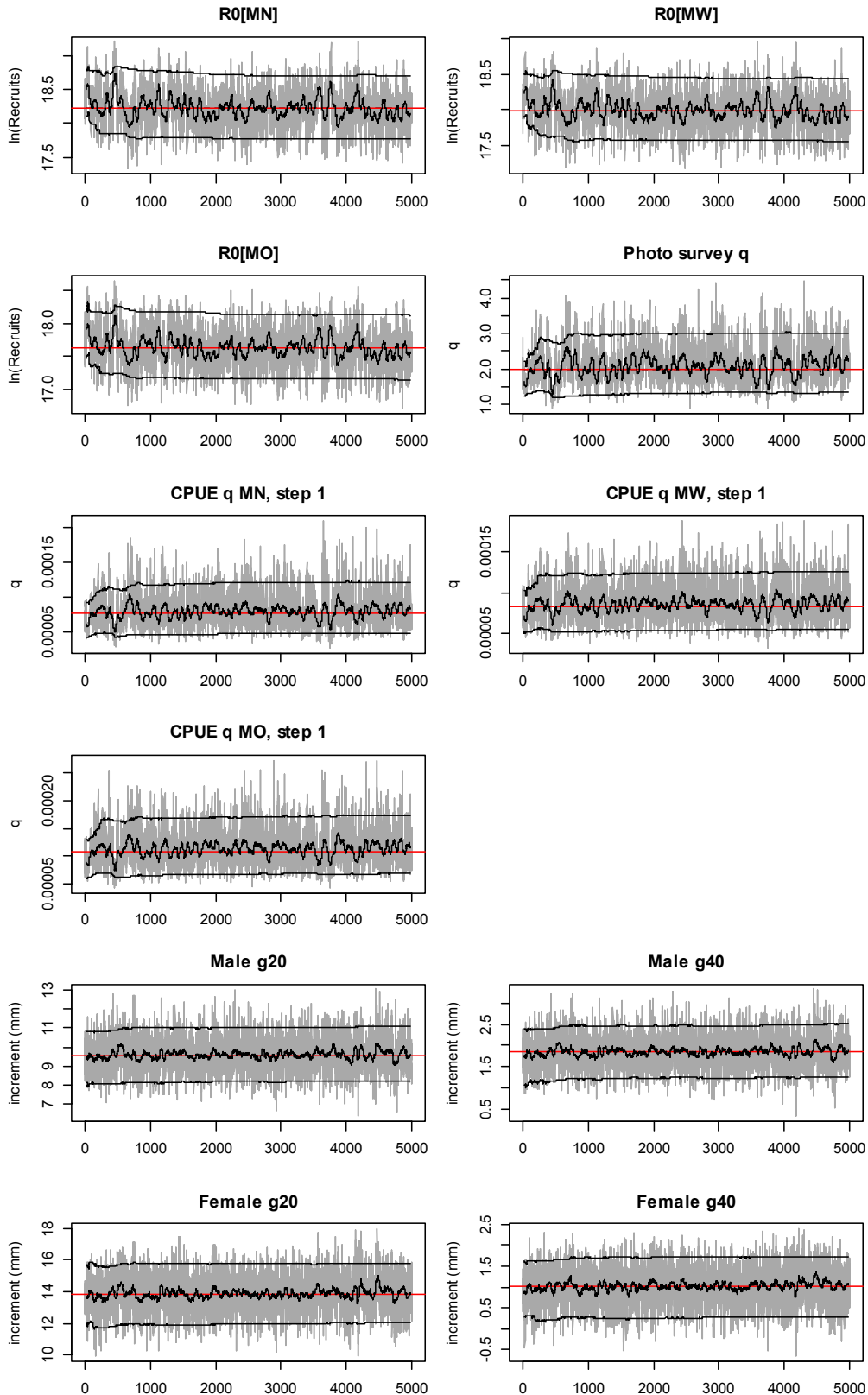
A4. 26: MCMC traces for SSB_0 , SSB_{2014} , and SSB_{2014}/SSB_0 terms for the MN subarea within the SCI 3 NT_0.25 model for SCI 3 (trace – grey line, cumulative moving median – dashed black line, moving average and cumulative moving 2.5%, 97.5% quantiles – solid black lines, overall median – solid red line, left plots), along with cumulative frequency distributions for three independent MCMC chains (shown as red, grey and black lines, right plots).



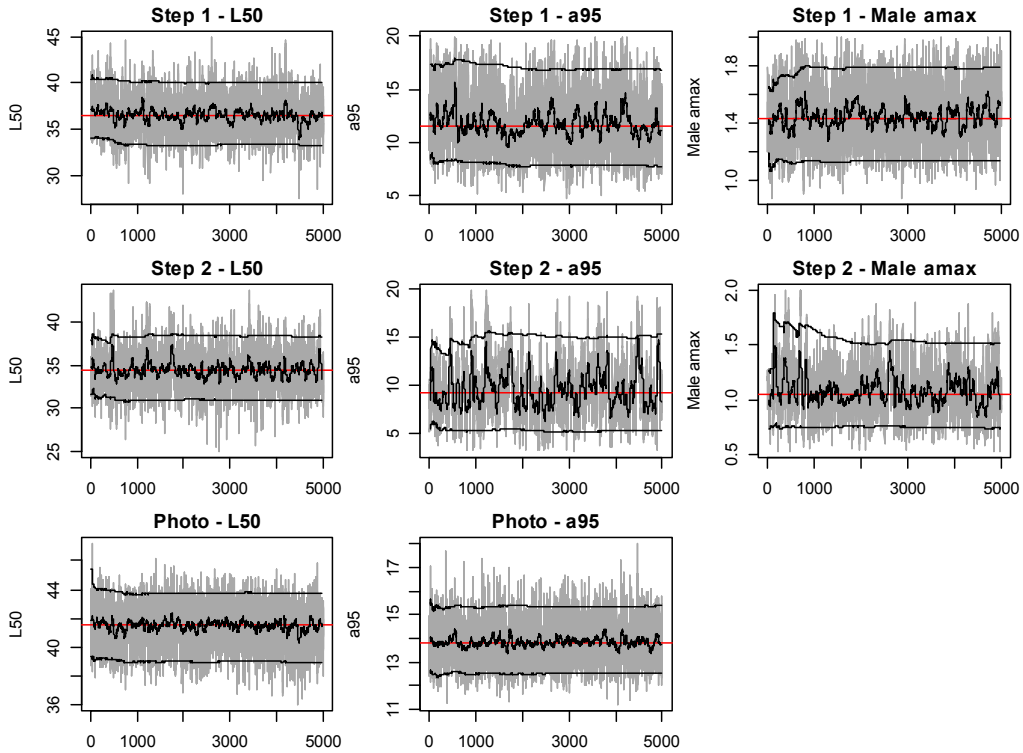
A4. 27: MCMC traces for SSB_0 , SSB_{2014} , and SSB_{2014}/SSB_0 terms for the MW subarea within the SCI 3 NT_0.25 model for SCI 3 (trace – grey line, cumulative moving median – dashed black line, moving average and cumulative moving 2.5%, 97.5% quantiles – solid black lines, overall median – solid red line, left plots), along with cumulative frequency distributions for three independent MCMC chains (shown as red, grey and black lines, right plots).



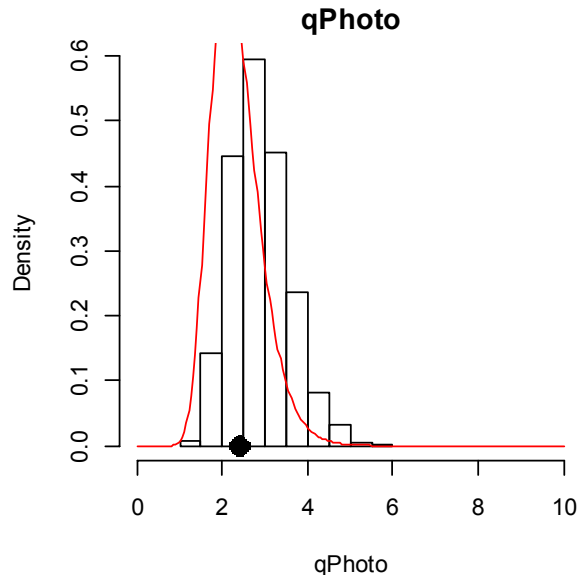
A4. 28: MCMC traces for SSB_0 , SSB_{2014} , and SSB_{2014}/SSB_0 terms for the MO subarea within the SCI 3 NT_0.25 model for SCI 3 (trace – grey line, cumulative moving median – dashed black line, moving average and cumulative moving 2.5%, 97.5% quantiles – solid black lines, overall median – solid red line, left plots), along with cumulative frequency distributions for three independent MCMC chains (shown as red, grey and black lines, right plots).



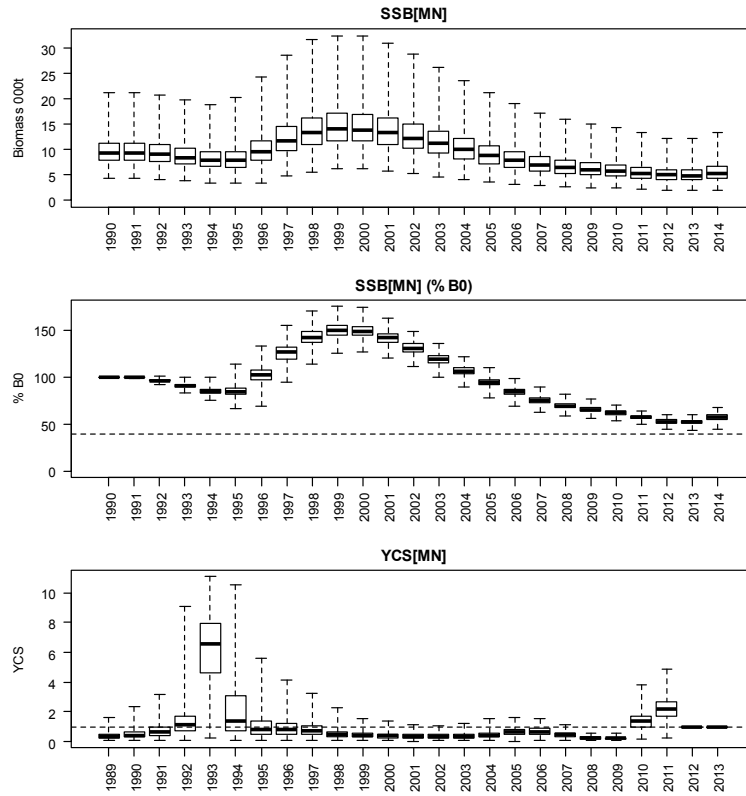
A4. 29: MCMC traces for R_0 , photo survey q , commercial fishery q , and growth increment terms within the SCI 3 NT_0.25 model for SCI 3 (trace – grey line, cumulative moving median – dashed black line, moving average and cumulative moving 2.5%, 97.5% quantiles – solid black lines, overall median – solid red line, left plots), along with cumulative frequency distributions for three independent MCMC chains (shown as red, grey and black lines, right plots).



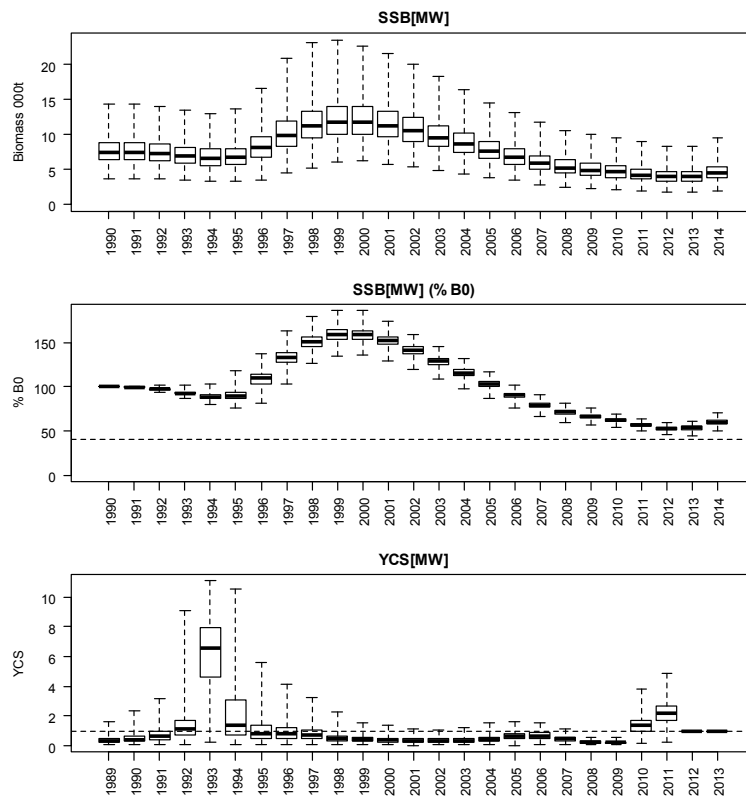
A4. 30: MCMC traces for selectivity parameters within the SCI 3 NT_0.25 model for SCI 3 (trace – grey line, cumulative moving median – dashed black line, moving average and cumulative moving 2.5%, 97.5% quantiles – solid black lines, overall median – solid red line, left plots), along with cumulative frequency distributions for three independent MCMC chains (shown as red, grey and black lines, right plots).



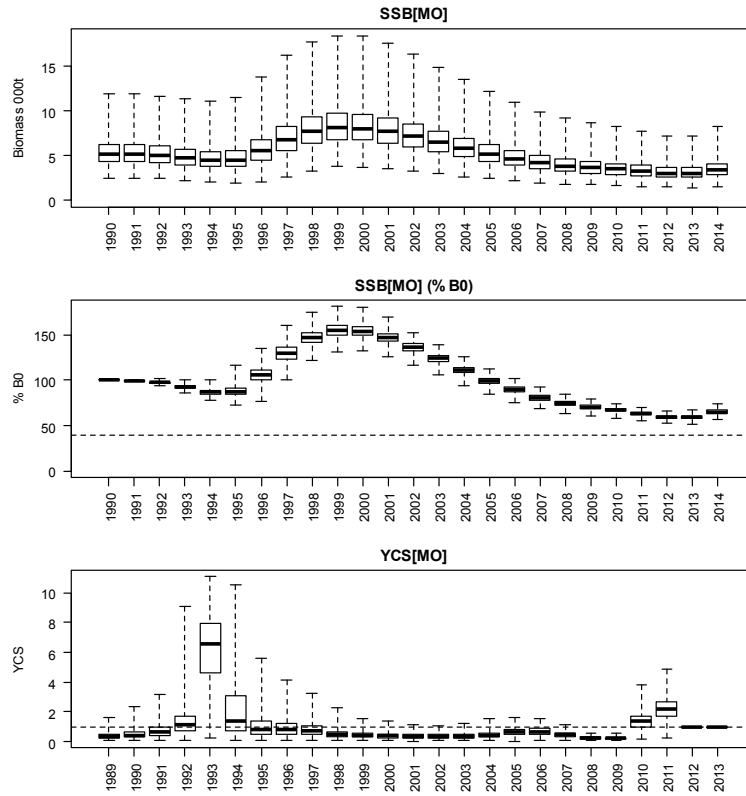
A4. 31: Marginal posterior distribution (histogram), MPD estimate (solid symbol) and distribution of prior (line) for photo survey catchability term within the SCI 3 NT_0.25 model.



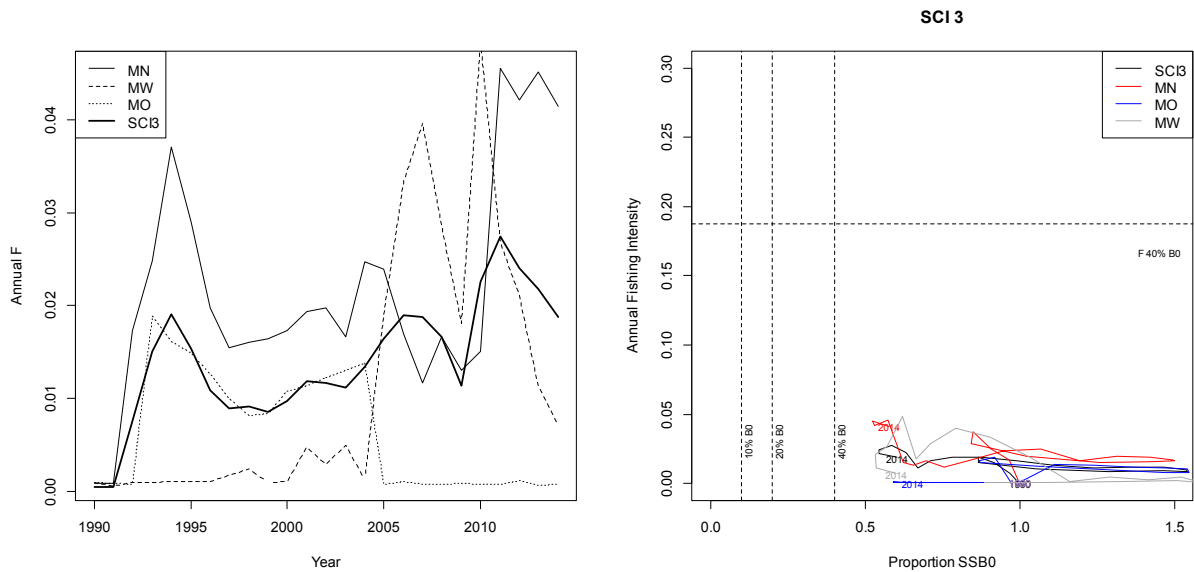
A4. 32: Posterior trajectory of SSB, SSB₂₀₁₄/SSB₀ and YCS for the MN subarea within the SCI 3 NT_0.25 model.



A4. 33: Posterior trajectory of SSB, SSB₂₀₁₄/SSB₀ and YCS for the MW subarea within the SCI 3 NT_0.25 model.

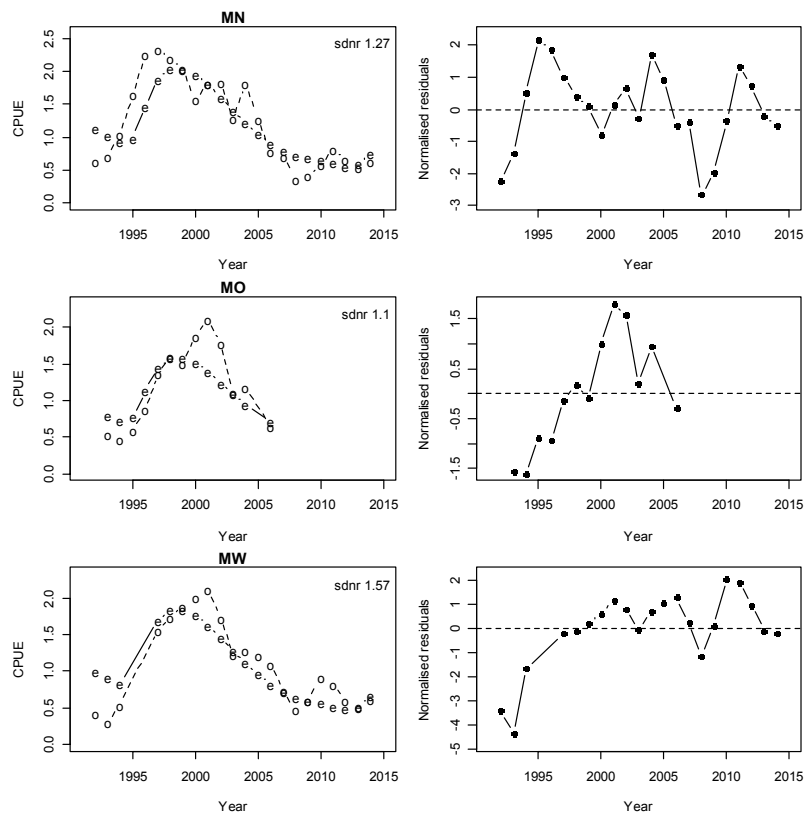


A4. 34: Posterior trajectory of SSB, SSB_{2014}/SSB_0 and YCS for the MO subarea within the SCI 3 NT_0.25 model.

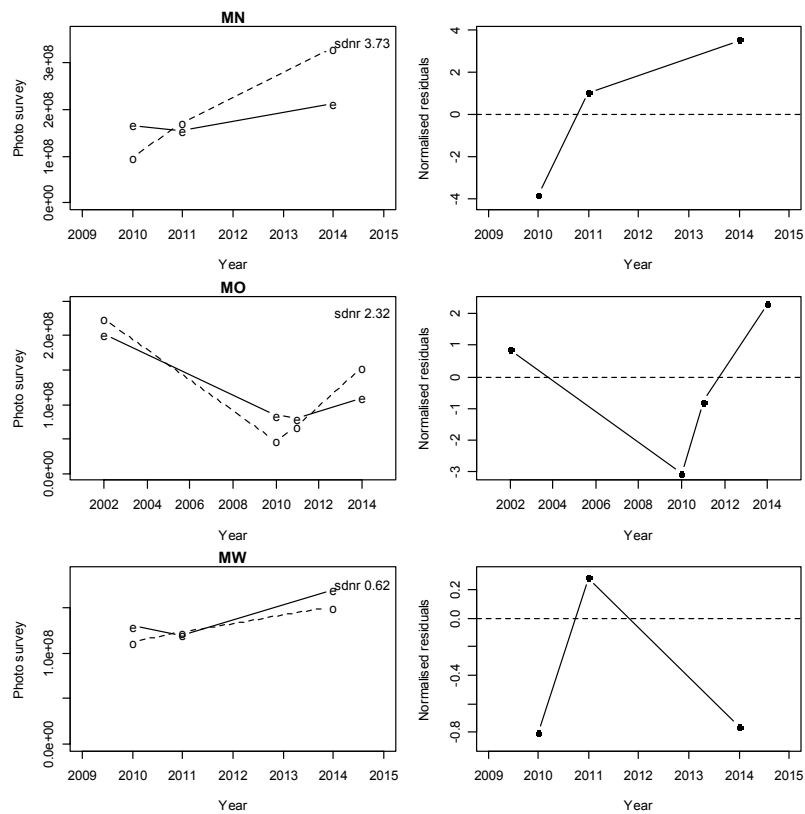


A4. 35: Estimated annual equivalent F (left) and phase plot (right) from the SCI 3 NT_0.25 model.

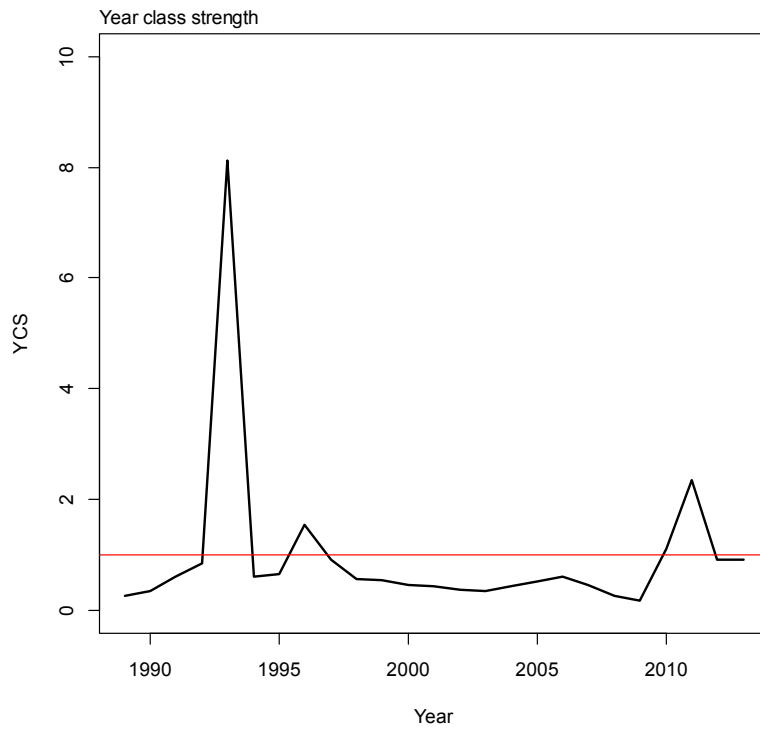
APPENDIX 5. MODEL NT_0.35



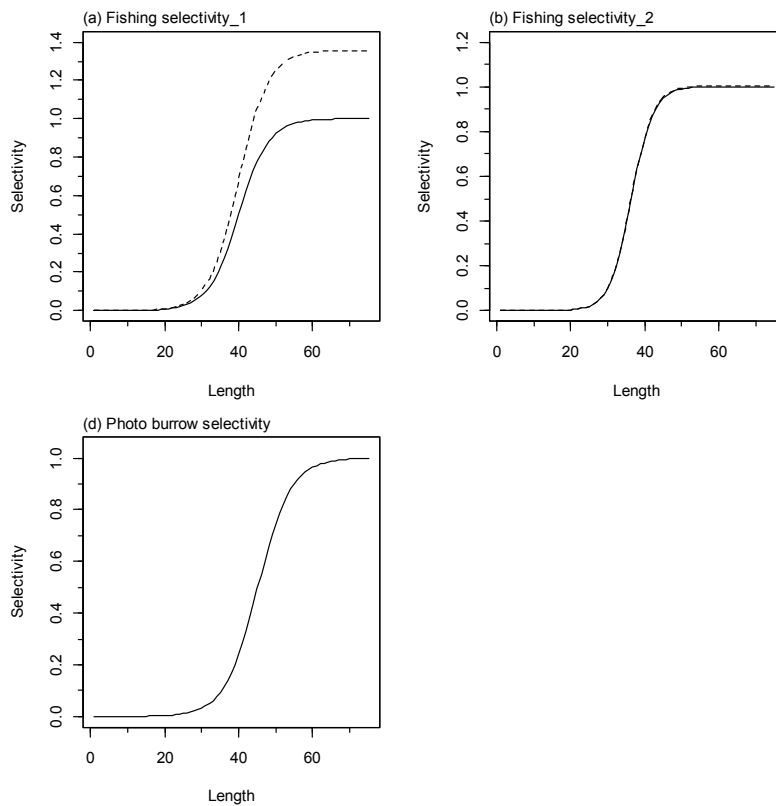
A5. 1: Fits to CPUE indices (left column) and normalised residuals (right column) for each subarea for SCI 3 NT_0.25.



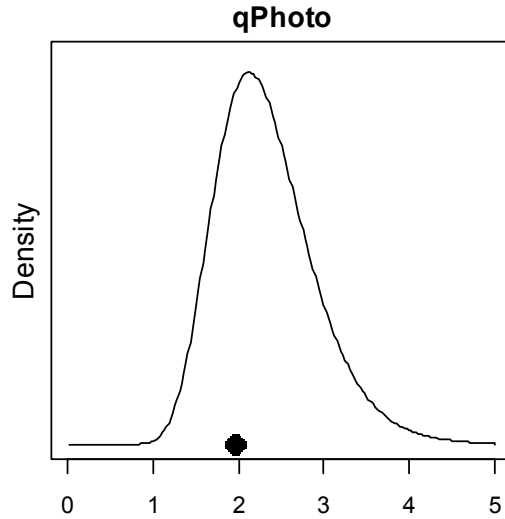
A5. 2: Fits to photographic survey indices (left column) and normalised residuals (right column) for each subarea for SCI 3 NT_0.35.



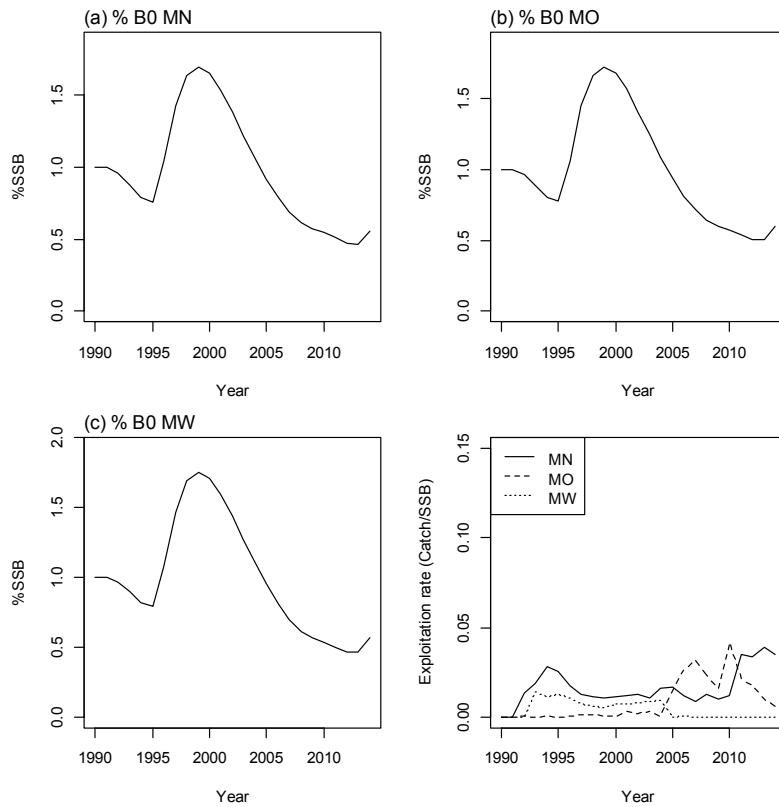
A5. 3: Year class strength for SCI 3 NT_0.35.



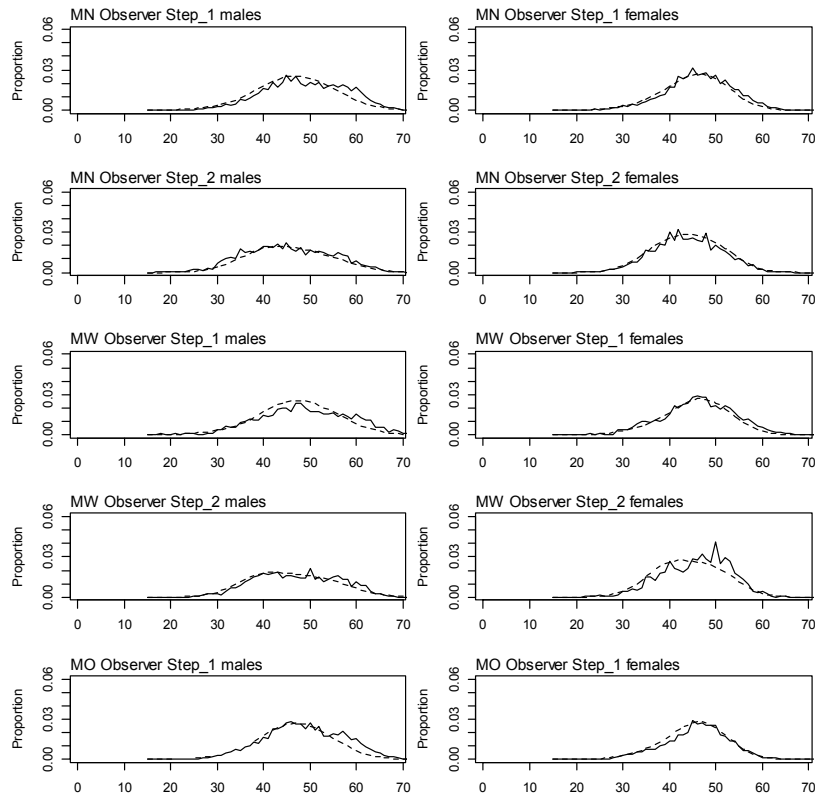
A5. 4: Fishery and survey selectivity curves for SCI 3 NT_0.35. Solid line – females, dotted line – males. The scampi photo index is not sexed, and a single selectivity applies.



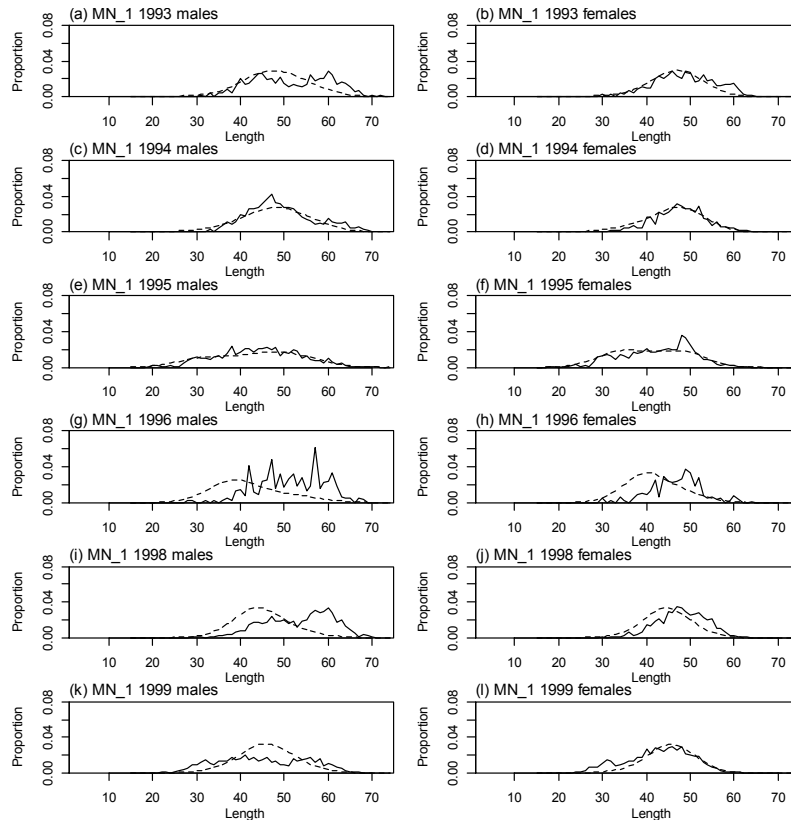
A5. 5: Catchability estimate from MPD model run, plotted in relation to prior distribution for SCI 3 NT_0.35.



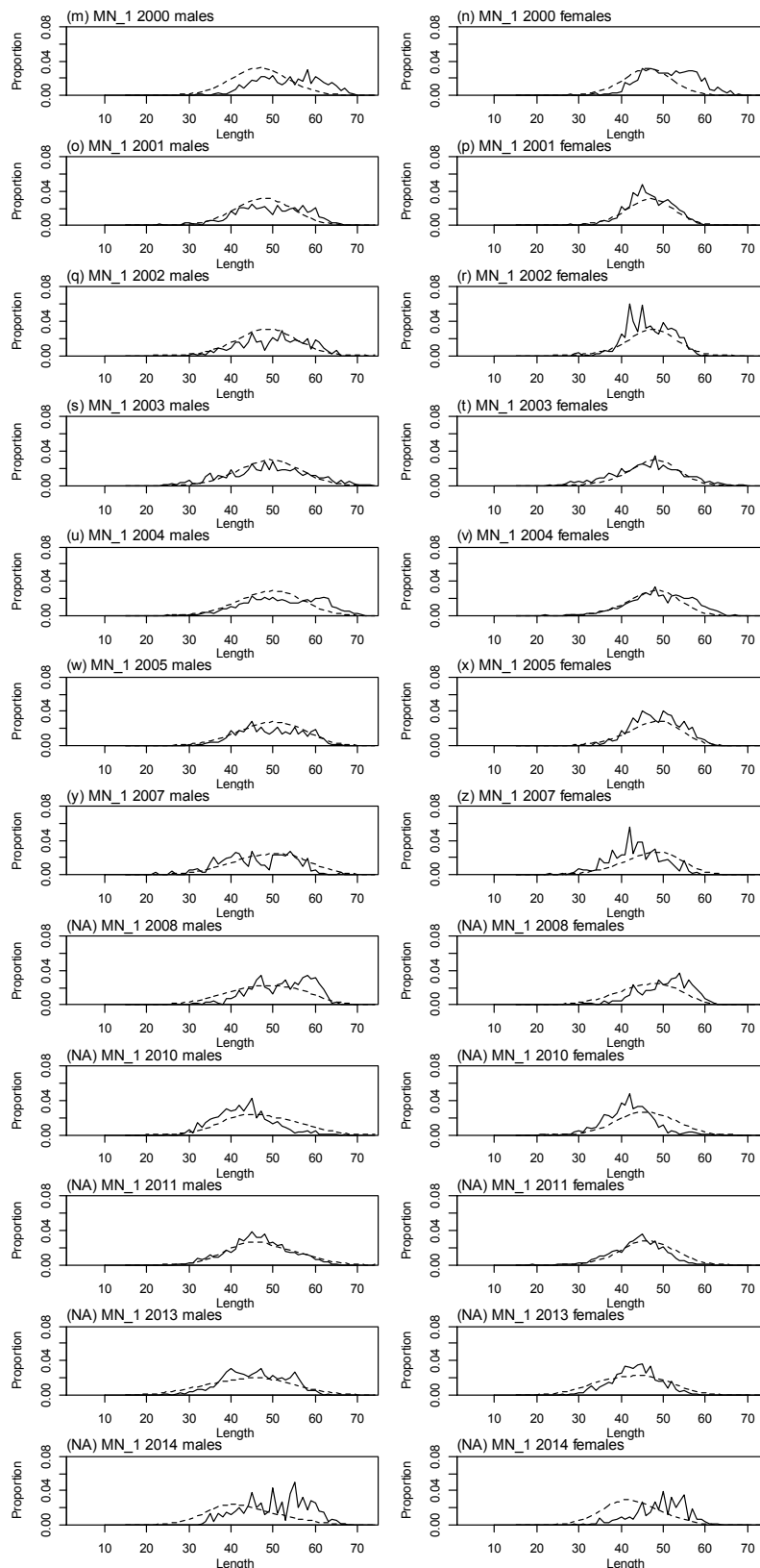
A5. 6: Stock trajectories (% SSB₀) for each subarea estimated from the MPD model run, and estimated exploitation rates for SCI 3 NT_0.35.



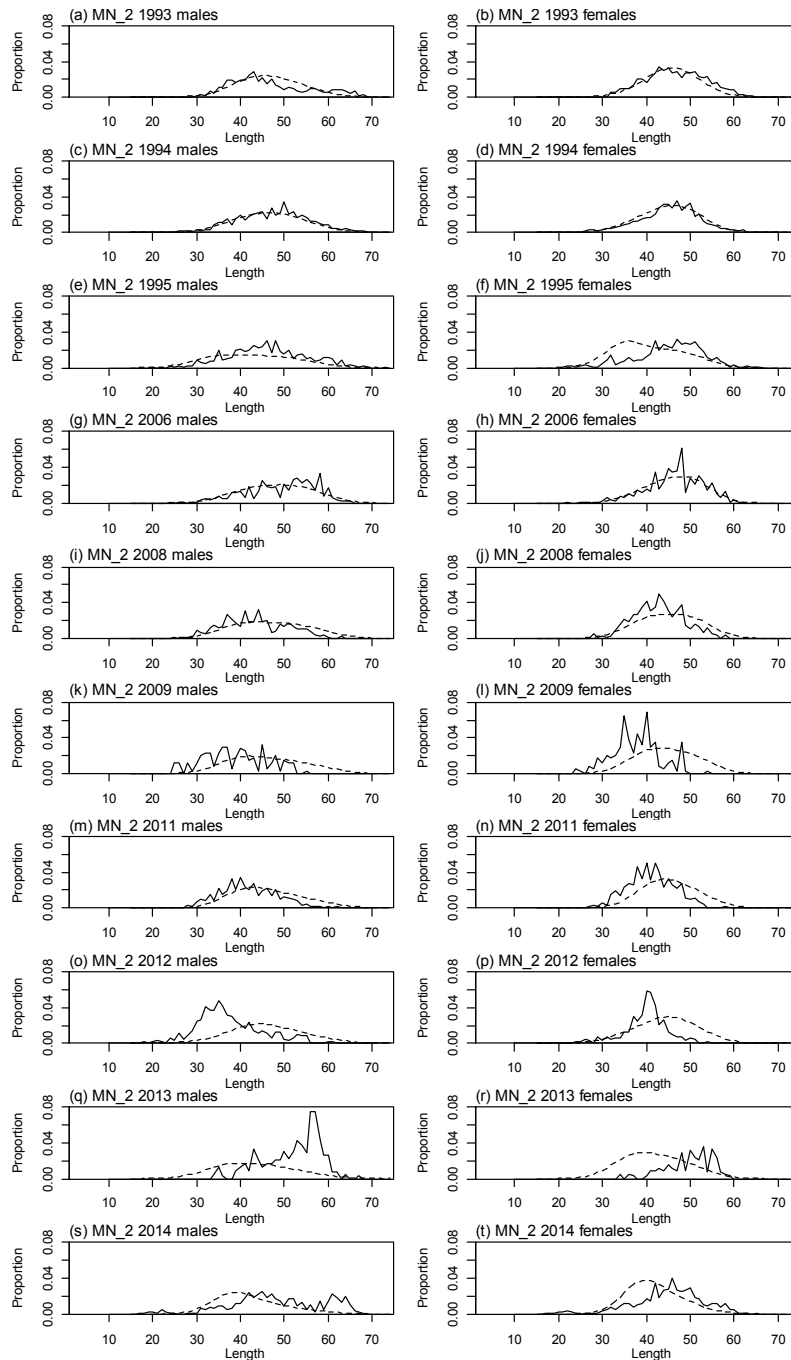
A5. 7: Average observed (solid line) and fitted (dashed line) length frequency distributions for observer samples for SCI 3 NT_0.35.



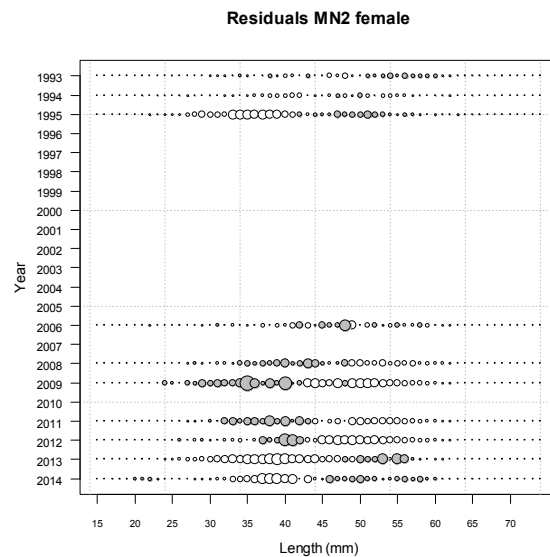
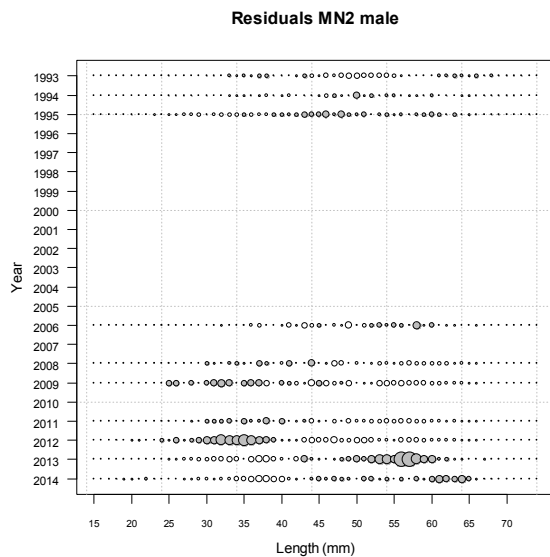
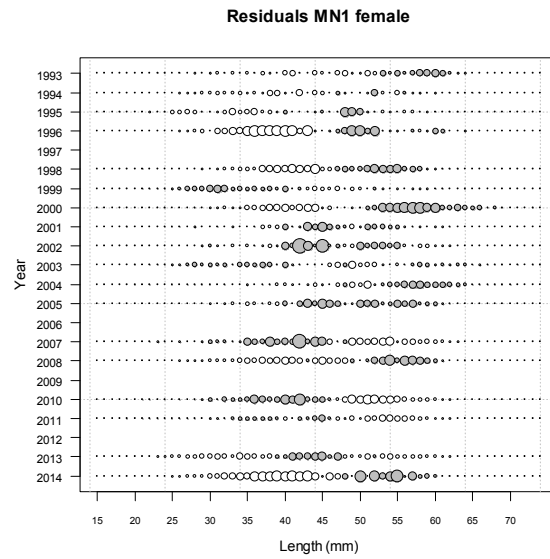
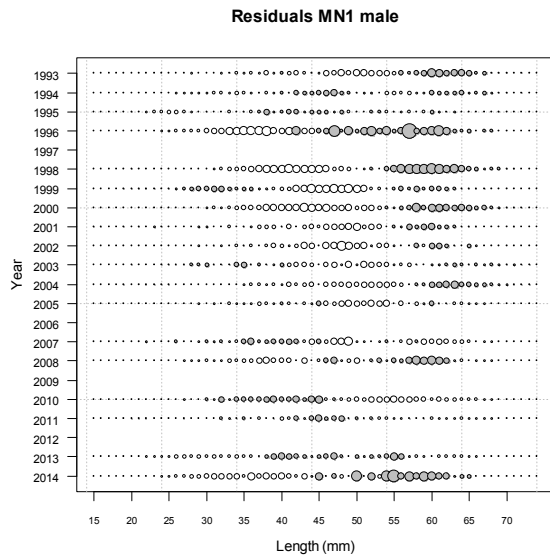
A5. 8: Observed (solid line) and fitted (dashed line) length frequency distributions for observer samples, MN time step 1 for SCI 3 NT_0.35.



A5. 8 ctd: Observed (solid line) and fitted (dashed line) length frequency distributions for observer samples, MN time step 1 for SCI 3 NT_{0.35}.



A5. 9: Observed (solid line) and fitted (dashed line) length frequency distributions for observer samples, MN time step 2 for SCI 3 NT_{0.35}.



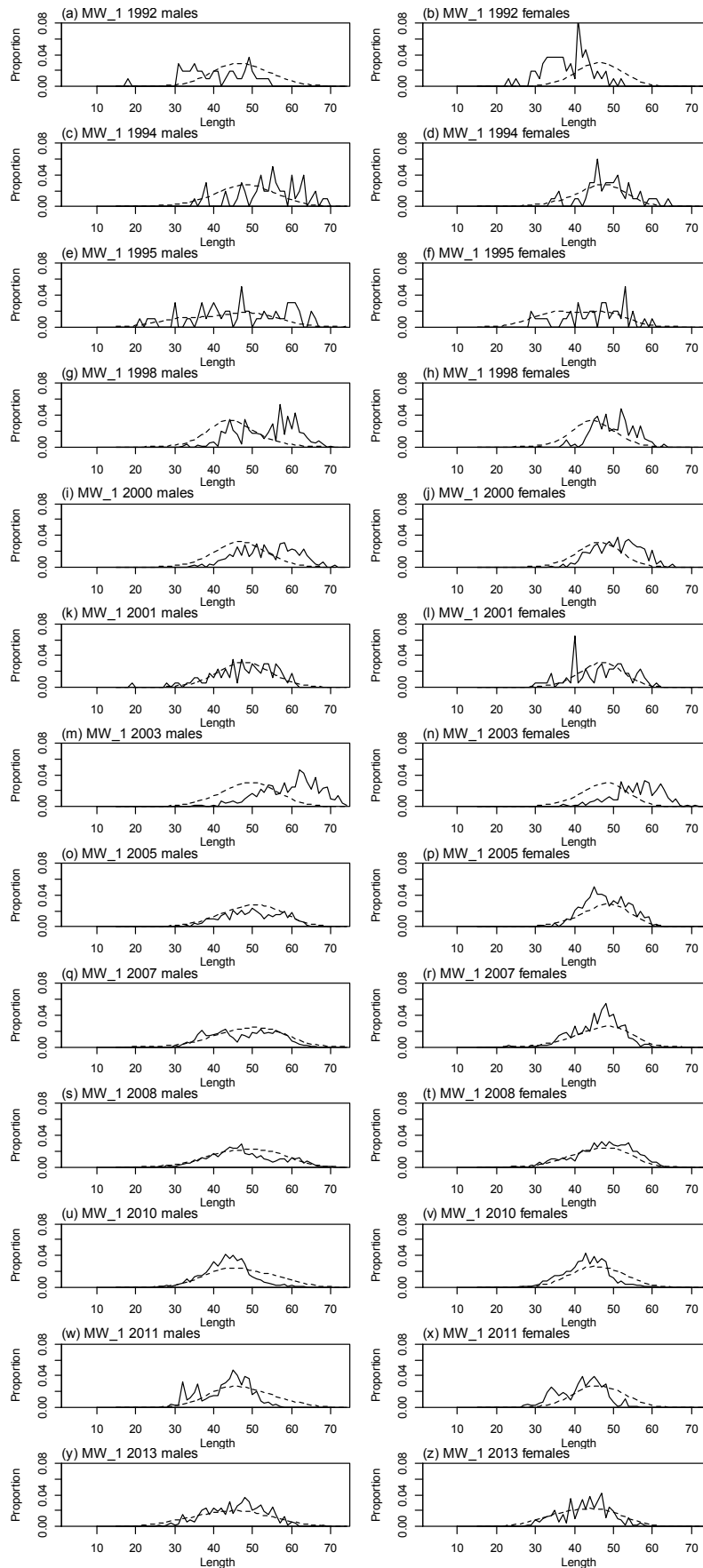
A5. 10: Bubble plots of residuals of fits to length frequency distributions for observer sampling from MN, time step 1 and 2, for SCI 3 NT_0.35.

A5. 11: Numbers of scampi measured, estimated multinomial N sample size, and effective sample size used within the SCI 3 NT_0.35 model for length frequency distributions for observer samples, MN time step 1.

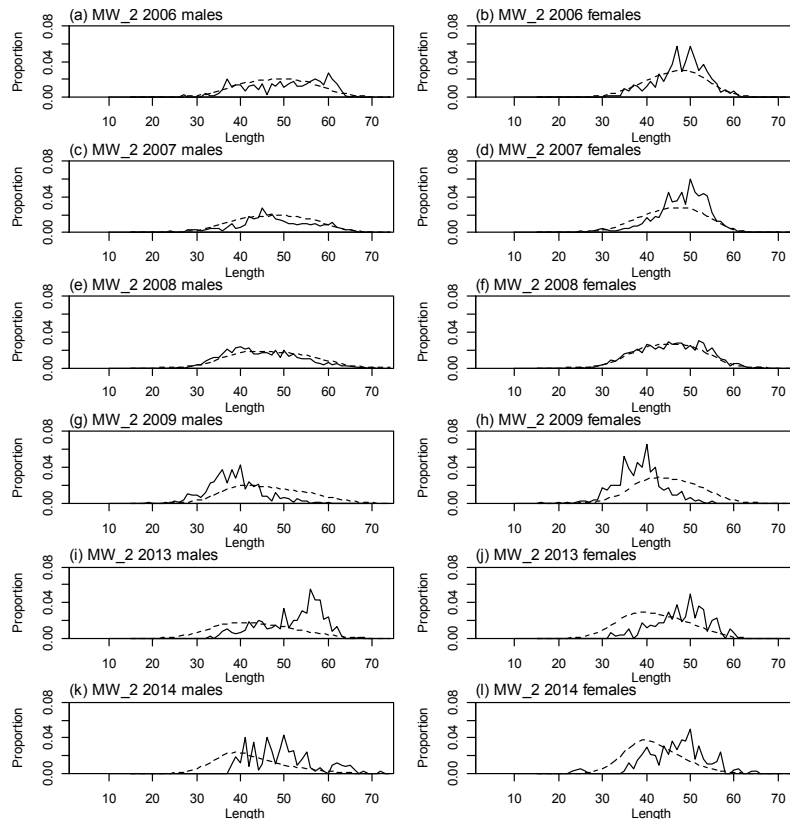
	Measured	Multinomial N	Effective sample size
N_1993	1 089	1 520	3.83
N_1994	2 090	3 036	7.65
N_1995	1 498	2 300	5.79
N_1996	465	500	1.26
N_1998	1 843	3 085	7.77
N_1999	1 921	4 221	10.63
N_2000	1 727	2 200	5.54
N_2001	1 528	2 908	7.33
N_2002	510	908	2.29
N_2003	2 824	5 674	14.29
N_2004	3 856	6 921	17.44
N_2005	1 448	2 497	6.29
N_2007	829	1 189	3.00
N_2008	1 087	1 587	4.00
N_2010	948	1 632	4.11
N_2011	3 273	6 881	17.33
N_2013	2 613	3 847	9.69
N_2014	403	789	1.99

A5. 12: Numbers of scampi measured, estimated multinomial N sample size, and effective sample size used within the SCI 3 NT_0.35 model for length frequency distributions for observer samples, MN time step 2.

	Measured	Multinomial N	Effective sample size
N_1993	1 639	3 306	11.12
N_1994	2 923	5 285	17.78
N_1995	1 260	1 800	6.06
N_2006	1 086	1 635	5.50
N_2008	535	699	2.35
N_2009	186	245	0.82
N_2011	1 019	1 900	6.39
N_2012	333	588	1.98
N_2013	352	234	0.79
N_2014	1 443	1 378	4.64



A5. 13: Observed (solid line) and fitted (dashed line) length frequency distributions for observer samples, MW time step 1 for SCI 3 NT_0.35.



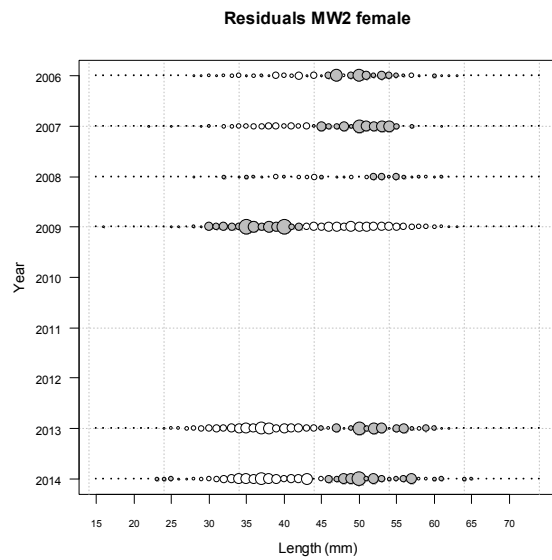
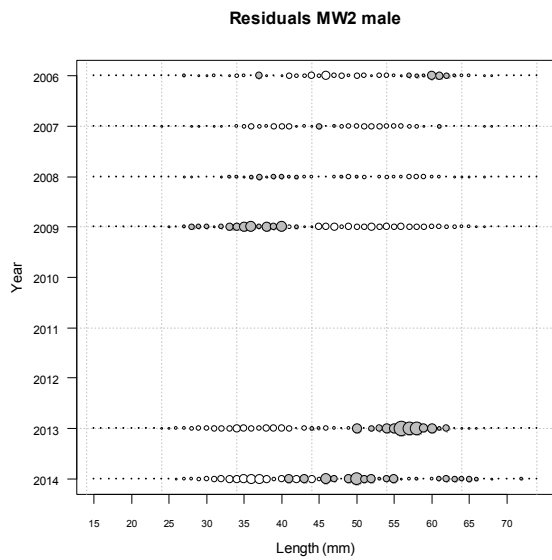
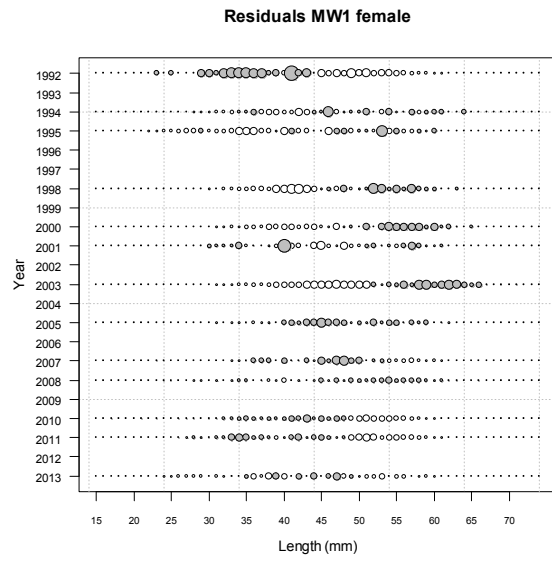
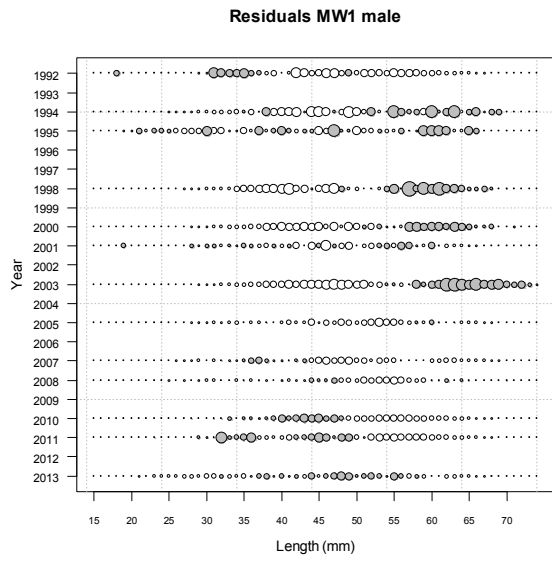
A5. 14: Observed (solid line) and fitted (dashed line) length frequency distributions for observer samples, MW time step 2 for SCI 3 NT_0.35.

A5. 15: Numbers of scampi measured, estimated multinomial N sample size, and effective sample size used within the SCI 3 NT_0.35 model for length frequency distributions for observer samples, MW time step 1.

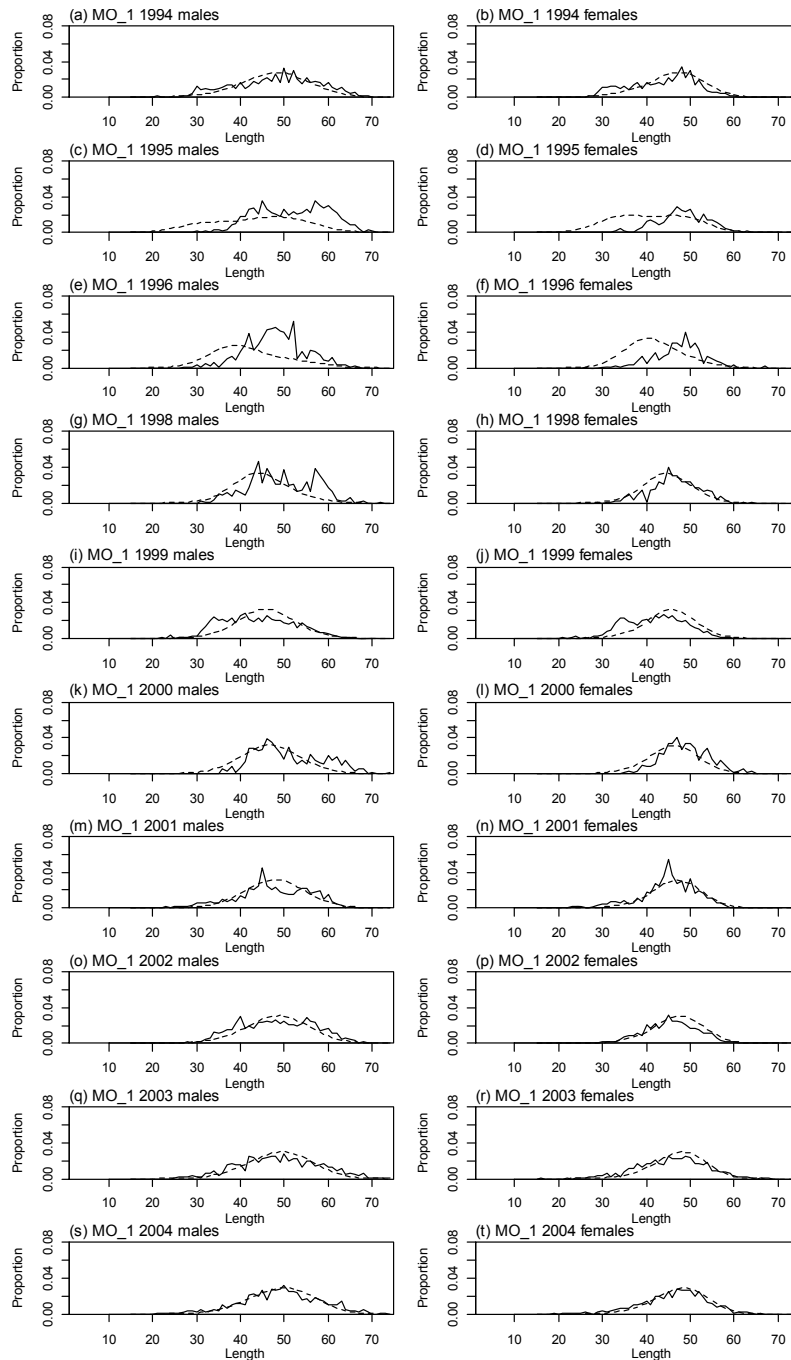
	Measured	Multinomial N	Effective sample size
N_1992	229	107	0.28
N_1994	242	100	0.26
N_1995	241	100	0.26
N_1998	365	365	0.95
N_2000	521	600	1.56
N_2001	251	169	0.44
N_2003	578	799	2.07
N_2005	593	870	2.26
N_2007	1 082	1 669	4.33
N_2008	1 201	1 865	4.84
N_2010	3 163	6 951	18.03
N_2011	712	2 345	6.08
N_2013	495	616	1.60

A5. 16: Numbers of scampi measured, estimated multinomial N sample size, and effective sample size used within the SCI 3 NT_0.35 model for length frequency distributions for observer samples, MW time step 2.

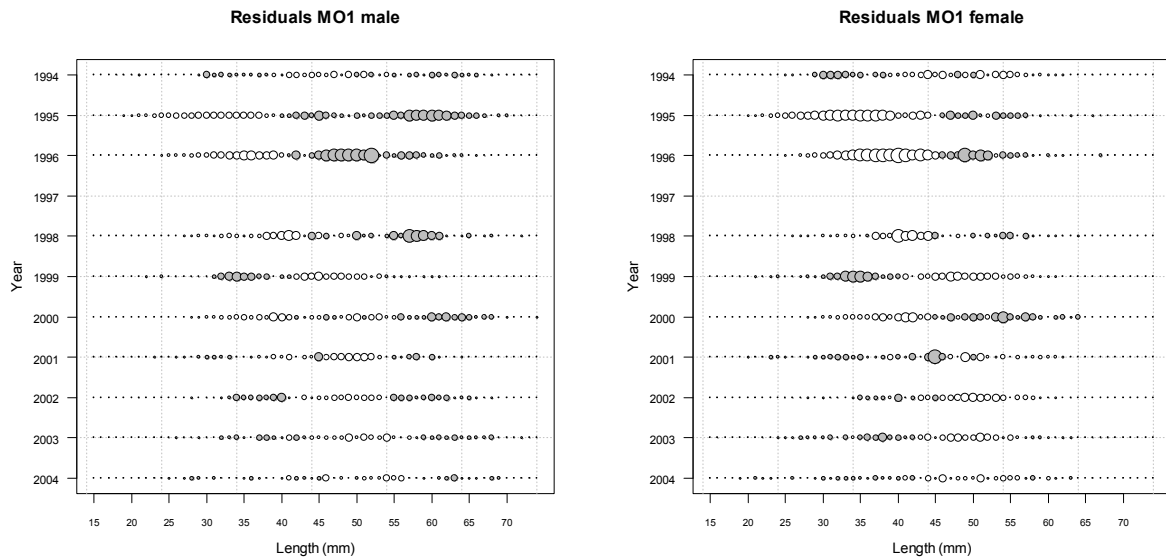
	Measured	Multinomial N	Effective sample size
N_2006	659	699	2.14
N_2007	1 333	2 406	7.38
N_2008	2 278	4 100	12.57
N_2009	693	1 340	4.11
N_2013	550	483	1.48
N_2014	460	317	0.97



A5. 17: Bubble plots of residuals of fits to length frequency distributions for observer sampling from MW, time step 1 and 2, for SCI 3 NT_0.35.



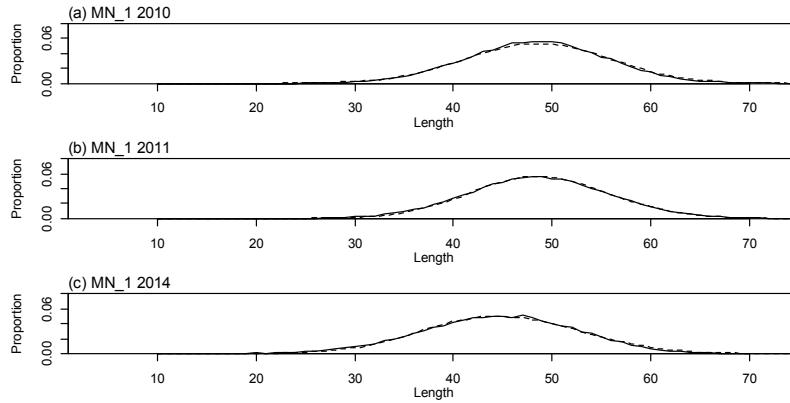
A5. 18: Observed (solid line) and fitted (dashed line) length frequency distributions for observer samples, MO time step 1 for SCI 3 NT_0.35.



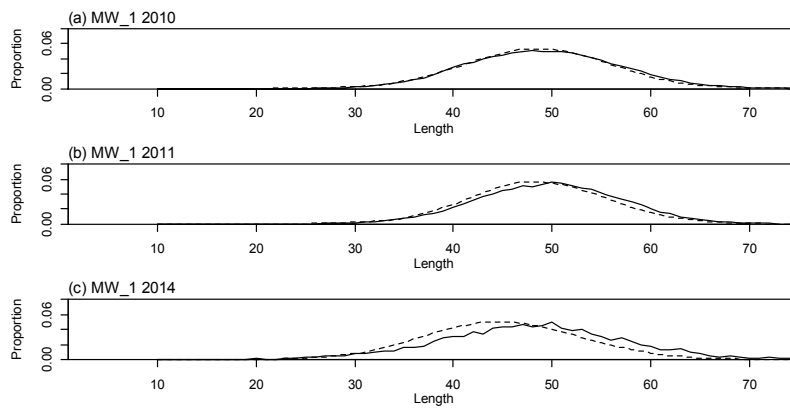
A5. 19: Bubble plots of residuals of fits to length frequency distributions for observer sampling from MO, time step 1, for SCI 3 NT_0.35.

A5. 20: Numbers of scampi measured, estimated multinomial N sample size, and effective sample size used within the SCI 3 NT_0.35 model for length frequency distributions for observer samples, MO time step 1.

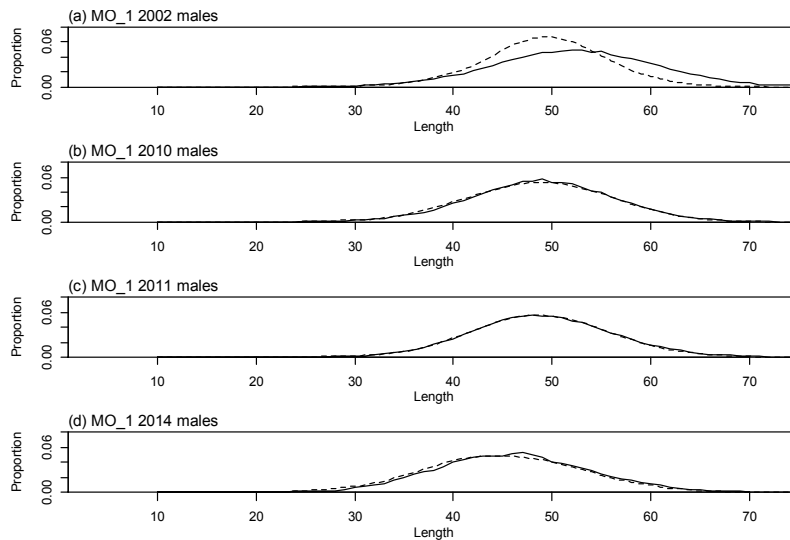
	Measured	Multinomial N	Effective sample size
N_1994	2 665	4 814	13.04
N_1995	2 474	2 500	6.77
N_1996	752	1 200	3.25
N_1998	870	900	2.44
N_1999	1 492	2 996	8.11
N_2000	608	600	1.63
N_2001	1 749	3 118	8.44
N_2002	1 768	3 442	7.14
N_2003	1 367	2 224	6.02
N_2004	1 557	2 881	7.80



A5. 21: Observed (solid line) and fitted (dashed line) length frequency distributions for MN photographic survey scampi size estimation within the SCI 3 NT_0.35 model.



A5. 22: Observed (solid line) and fitted (dashed line) length frequency distributions for MW photographic survey scampi size estimation within the SCI 3 NT_0.35 model.



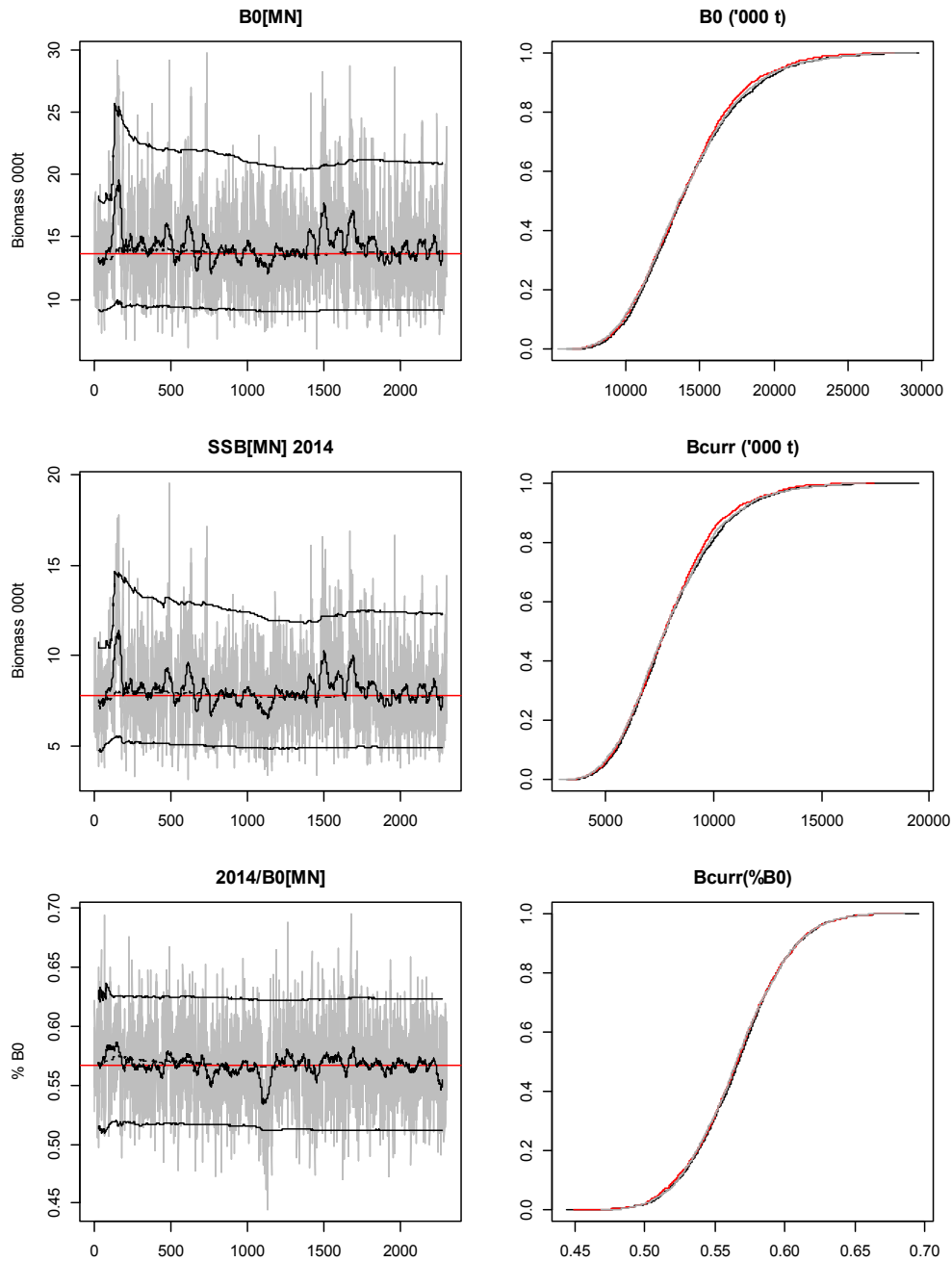
A5. 23: Observed (solid line) and fitted (dashed line) length frequency distributions for MO photographic survey scampi size estimation within the SCI 3 NT_0.35 model.

A5. 24: Numbers of scampi burrows measured, estimated multinomial N sample size, and effective sample size used within the model for length frequency distributions for photographic survey samples within the SCI 3 NT_0.35 model.

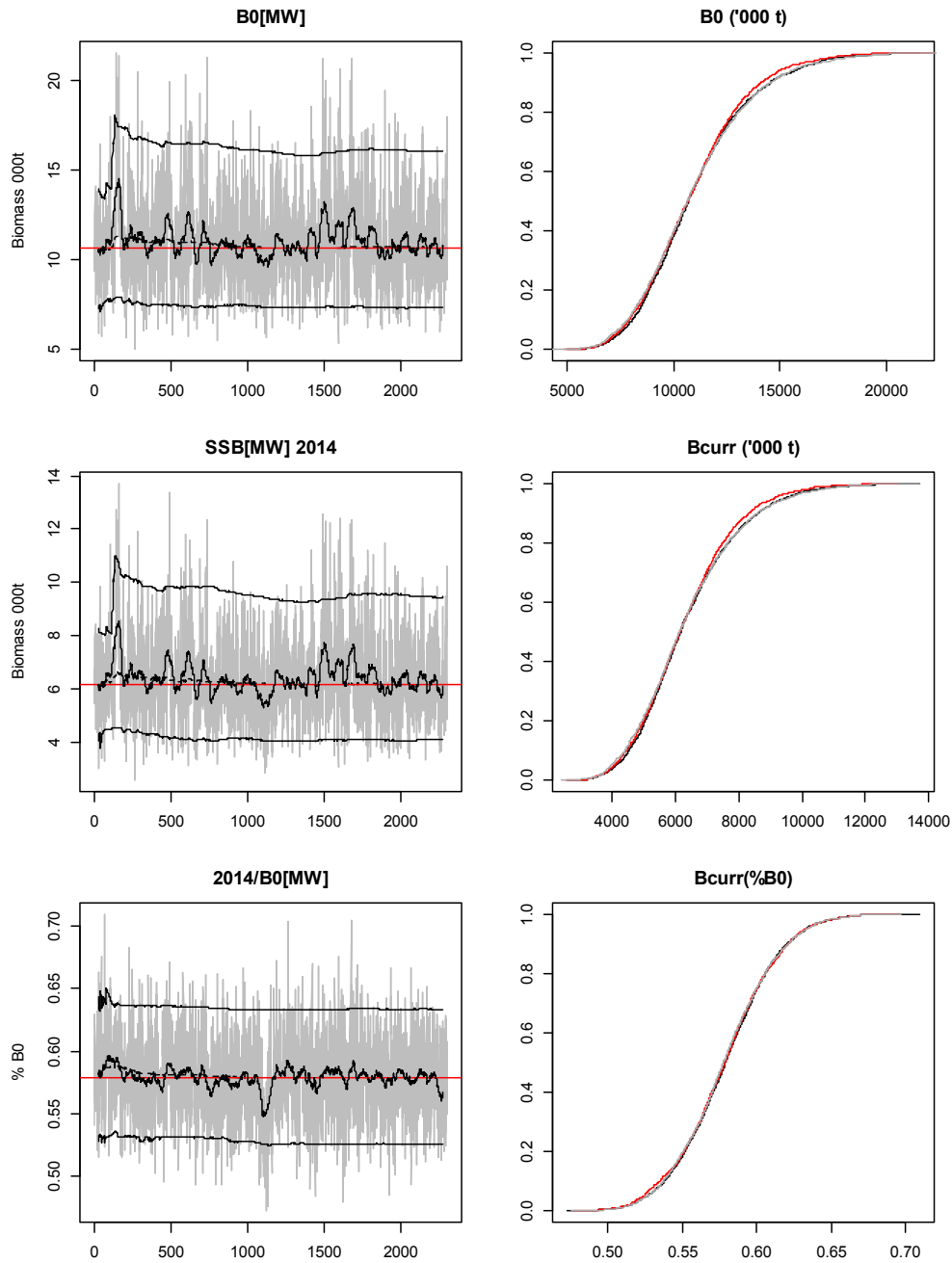
MN	Measured	Multinomial N	Effective sample size
N_2010	360	214	3 908.30
N_2011	536	426	5 819.03
N_2014	227	125	2 464.40

MW	Measured	Multinomial N	Effective sample size
N_2010	303	173	976.18
N_2011	232	128	747.44
N_2014	47	24	151.42

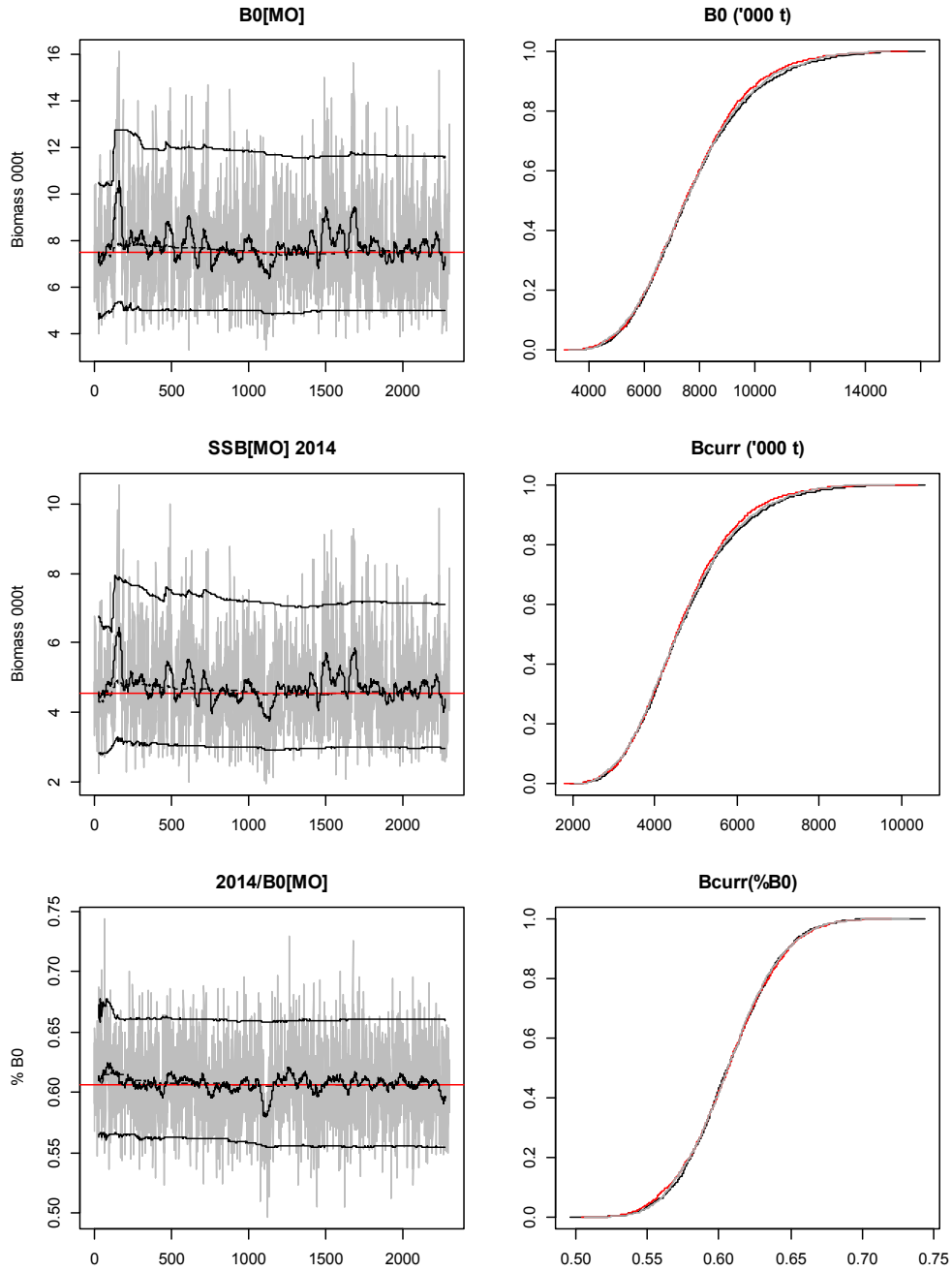
MO	Measured	Multinomial N	Effective sample size
N_2002	397	249	21.30
N_2010	205	113	11.00
N_2011	549	120	29.46
N_2014	117	62	6.28



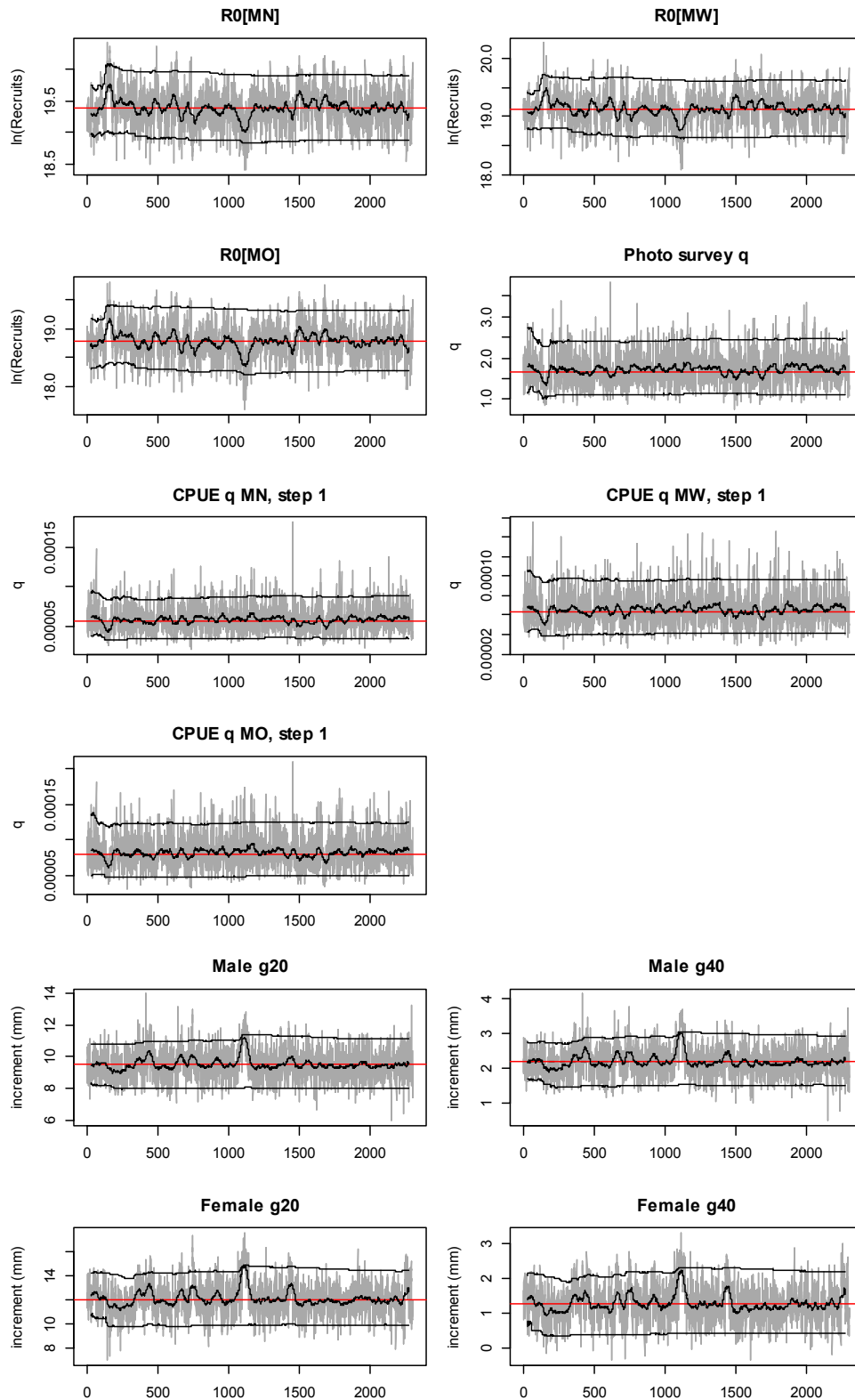
A5. 25: MCMC traces for SSB_0 , SSB_{2014} , and SSB_{2014}/SSB_0 terms for the MN subarea within the SCI 3 NT_0.35 model for SCI 3 (trace – grey line, cumulative moving median – dashed black line, moving average and cumulative moving 2.5%, 97.5% quantiles – solid black lines, overall median – solid red line, left plots), along with cumulative frequency distributions for three independent MCMC chains (shown as red, grey and black lines, right plots).



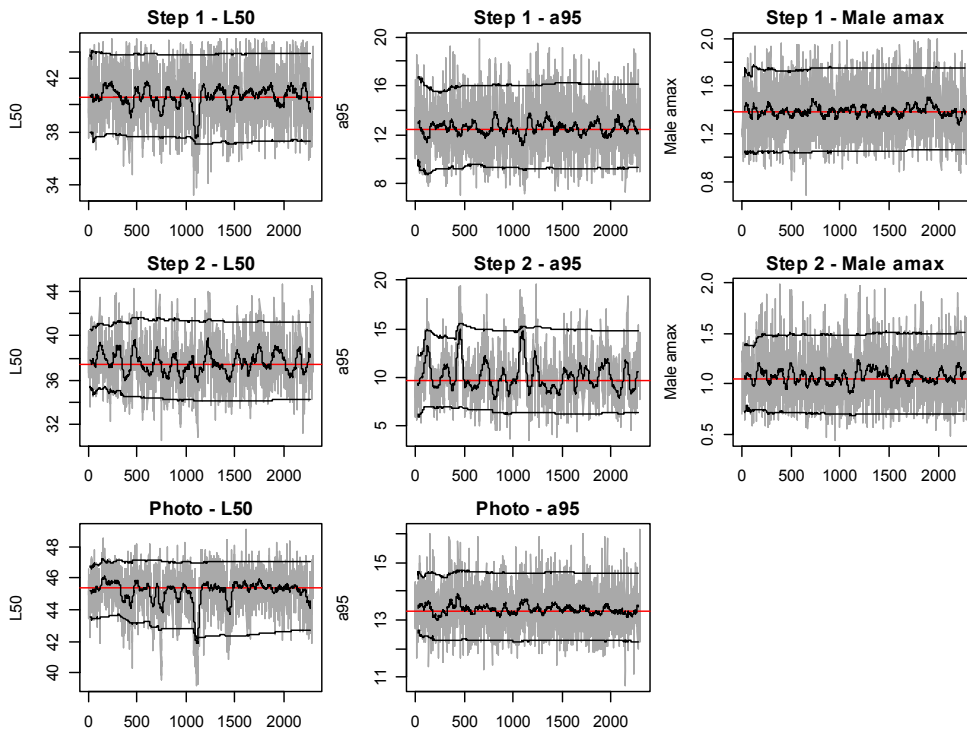
A5. 26: MCMC traces for SSB₀, SSB₂₀₁₄, and SSB₂₀₁₄/SSB₀ terms for the MW subarea within the SCI 3 NT_0.35 model for SCI 3 (trace – grey line, cumulative moving median – dashed black line, moving average and cumulative moving 2.5%, 97.5% quantiles – solid black lines, overall median – solid red line, left plots), along with cumulative frequency distributions for three independent MCMC chains (shown as red, grey and black lines, right plots).



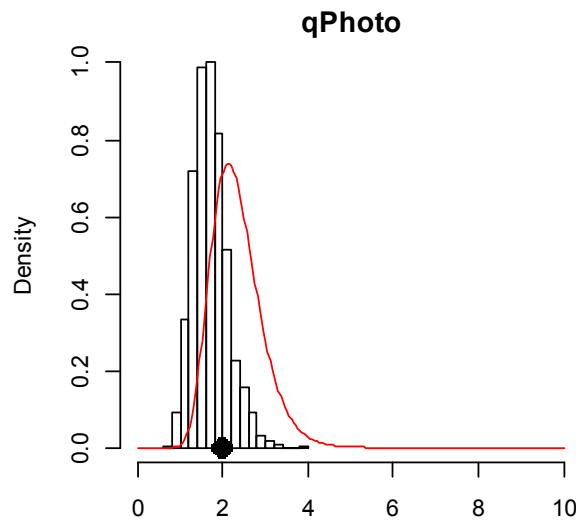
A5. 27: MCMC traces for SSB_0 , SSB_{2014} , and SSB_{2014}/SSB_0 terms for the MO subarea within the SCI 3 NT_0.35 model for SCI 3 (trace – grey line, cumulative moving median – dashed black line, moving average and cumulative moving 2.5%, 97.5% quantiles – solid black lines, overall median – solid red line, left plots), along with cumulative frequency distributions for three independent MCMC chains (shown as red, grey and black lines, right plots).



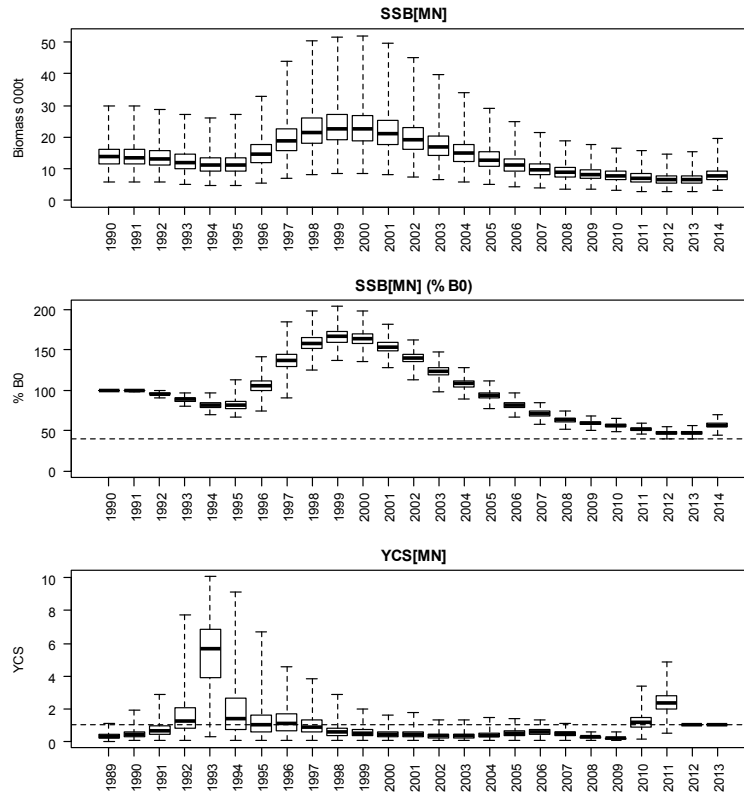
A5. 28: MCMC traces for R_0 , photo survey q , commercial fishery q , and growth increment terms within the SCI 3 NT_0.35 model for SCI 3 (trace – grey line, cumulative moving median – dashed black line, moving average and cumulative moving 2.5%, 97.5% quantiles – solid black lines, overall median – solid red line, left plots), along with cumulative frequency distributions for three independent MCMC chains (shown as red, grey and black lines, right plots).



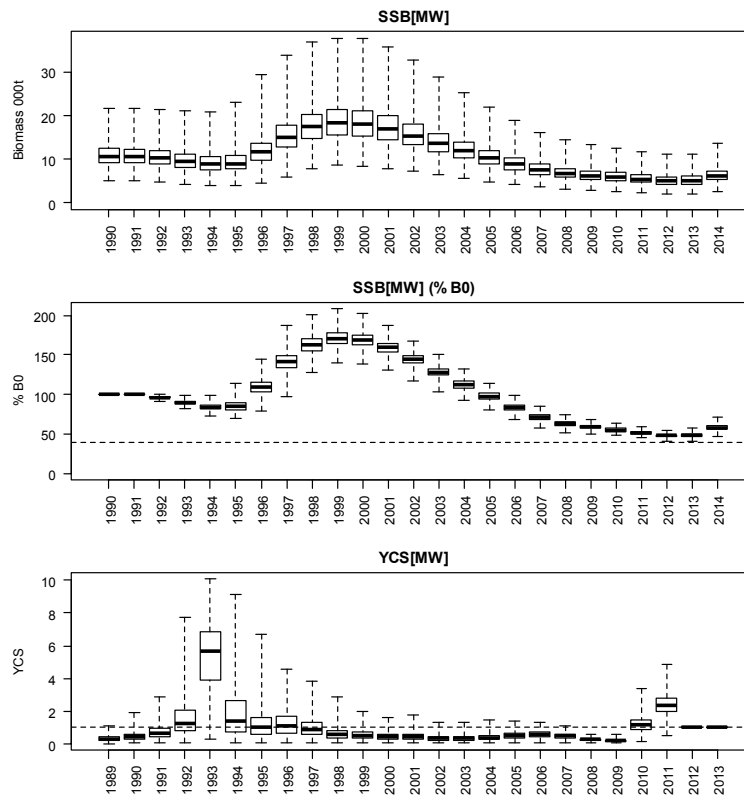
A5. 29: MCMC traces for selectivity parameters within the SCI 3 NT_0.35 model for SCI 3 (trace – grey line, cumulative moving median –dashed black line, moving average and cumulative moving 2.5%, 97.5% quantiles – solid black lines, overall median – solid red line, left plots), along with cumulative frequency distributions for three independent MCMC chains (shown as red, grey and black lines, right plots).



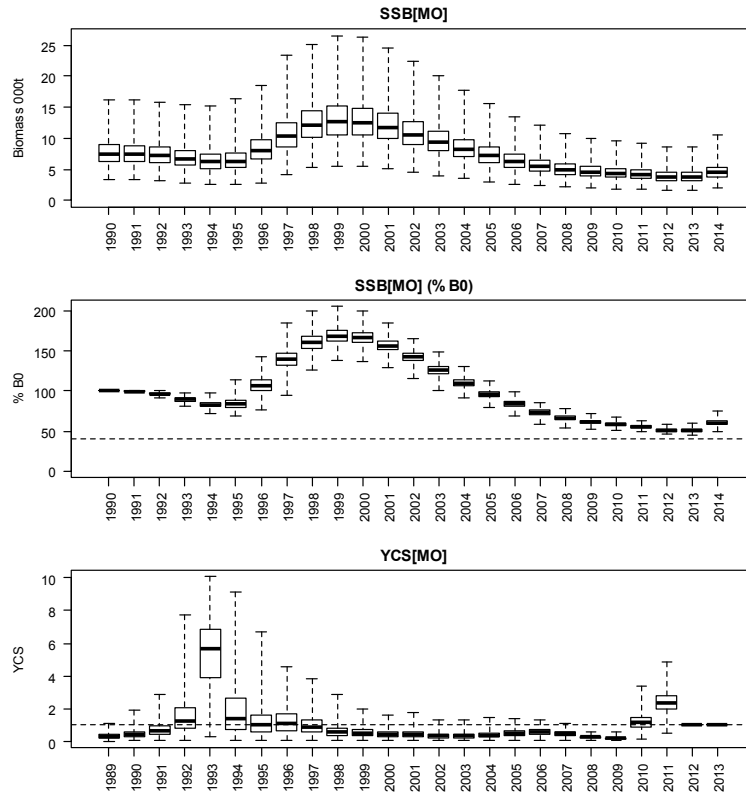
A5. 30: Marginal posterior distribution (histogram), MPD estimate (solid symbol) and distribution of prior (line) for photo survey catchability term within the SCI 3 NT_0.35 model.



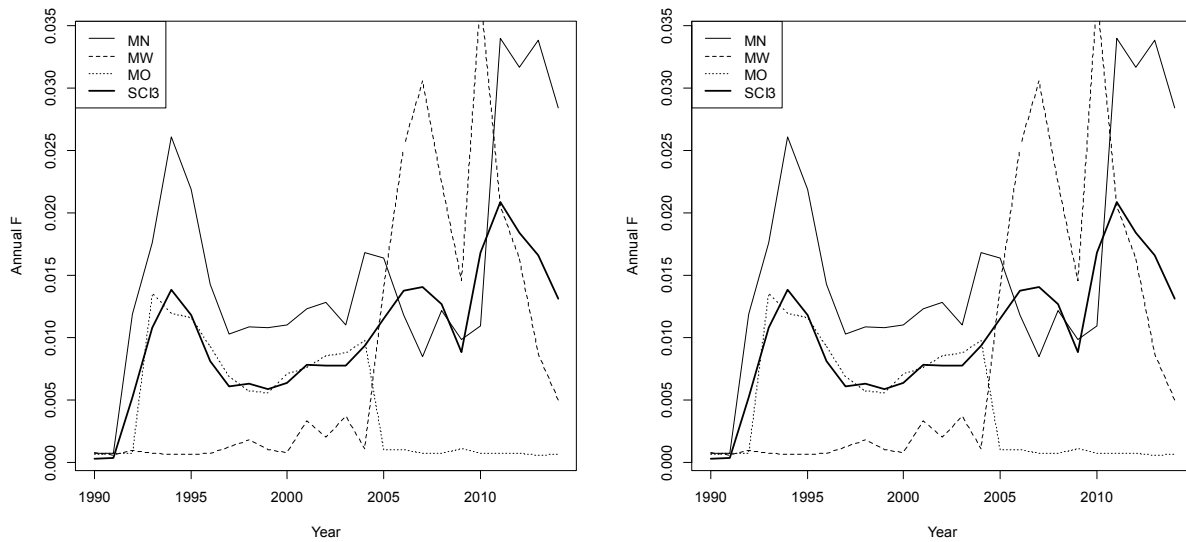
A5. 31: Posterior trajectory of SSB, SSB_{2014}/SSB_0 and YCS for the MN subarea within the SCI 3 NT_0.35 model.



A5. 32: Posterior trajectory of SSB, SSB_{2014}/SSB_0 and YCS for the MW subarea within the SCI 3 NT_0.35 model.

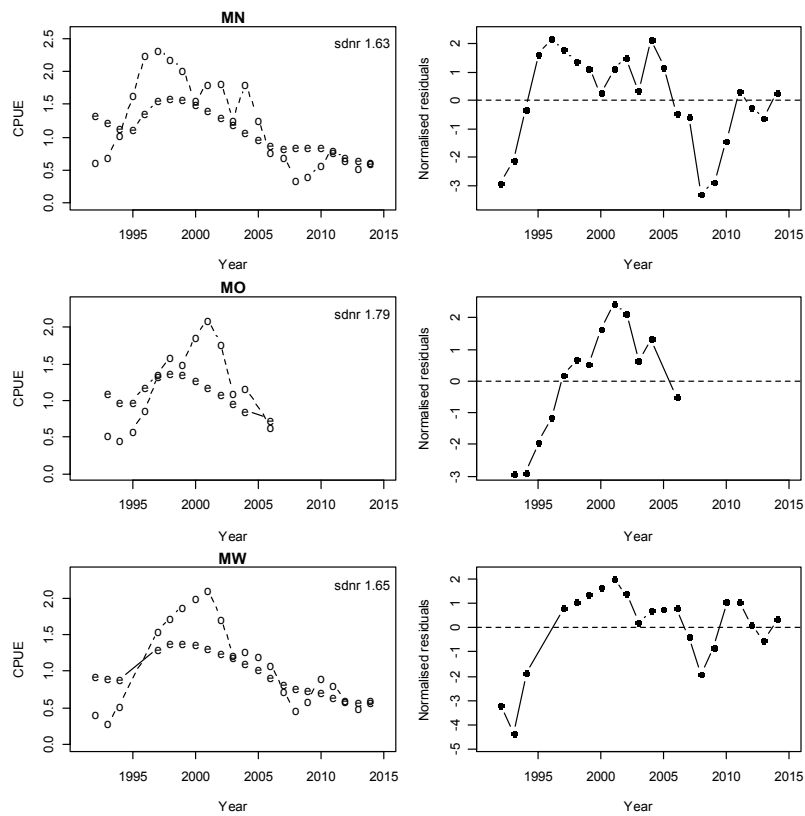


A5. 33: Posterior trajectory of SSB, SSB₂₀₁₄/SSB₀ and YCS for the MO subarea within the SCI 3 NT_0.35 model.

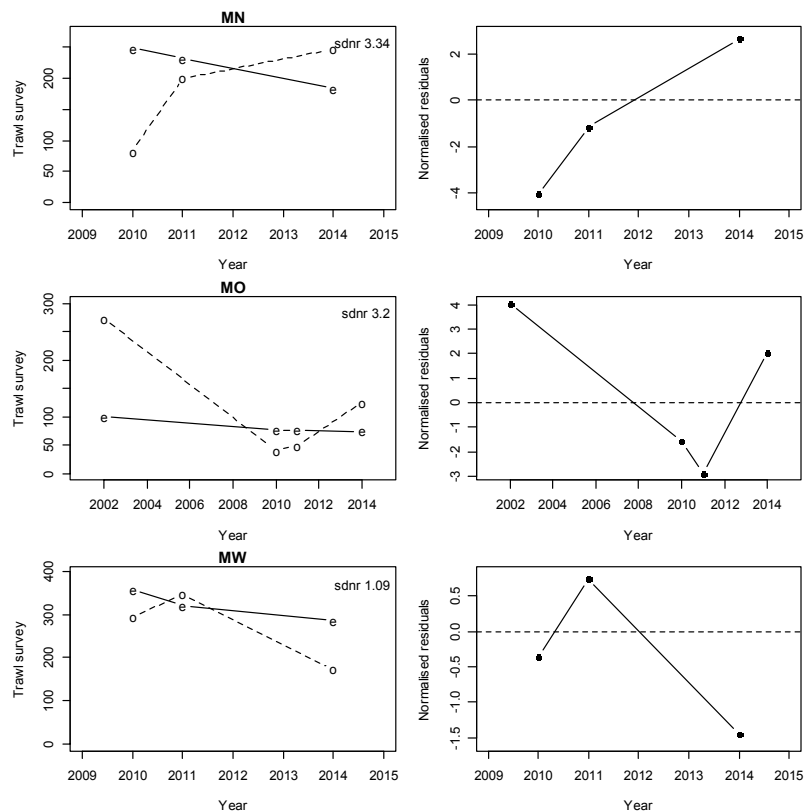


A5. 34: Estimated annual equivalent F (left) and phase plot (right) from the SCI 3 NT_0.35 model.

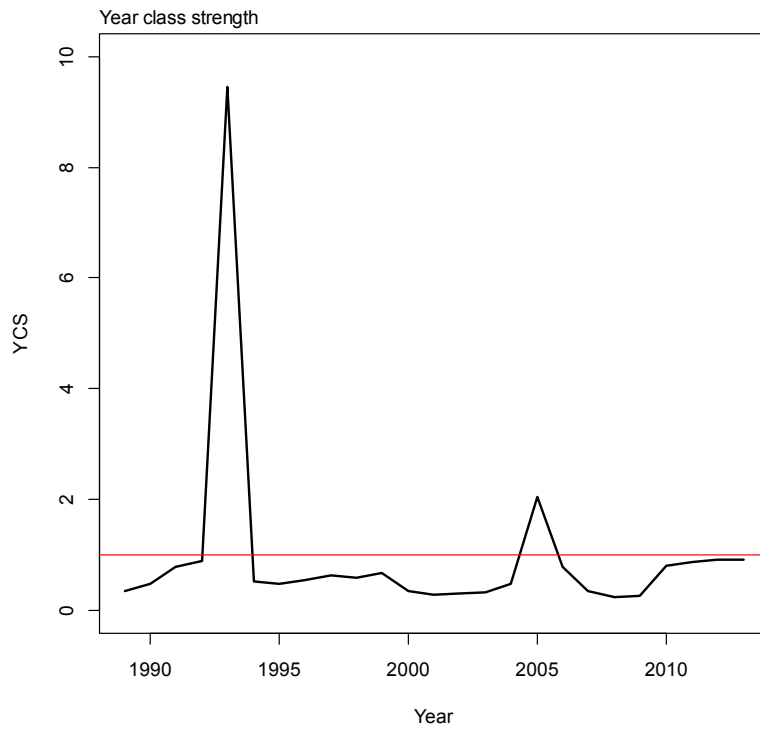
APPENDIX 6. MODEL NP_0.15



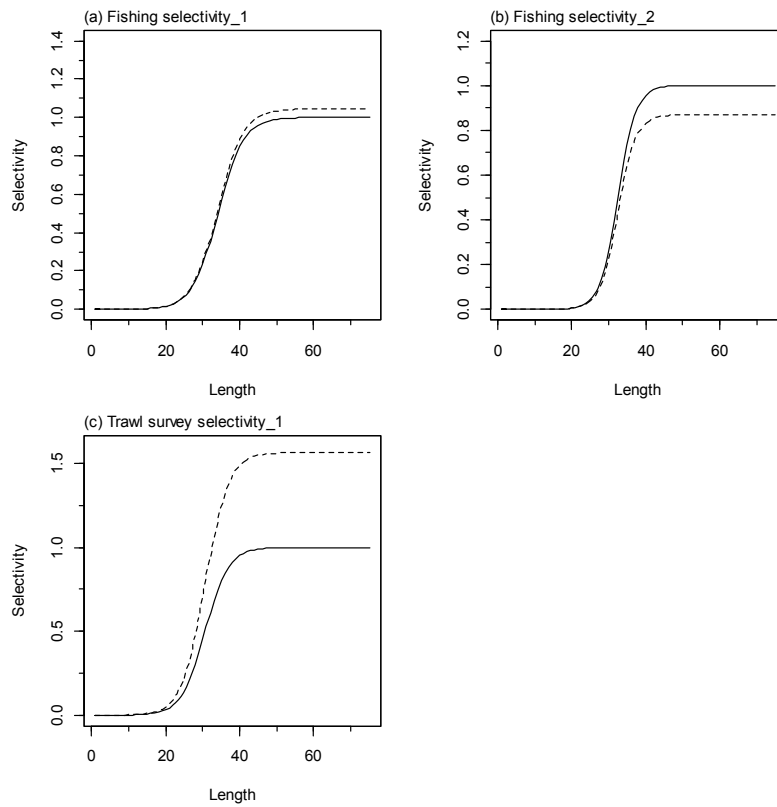
A6. 1: Fits to CPUE indices (left column) and normalised residuals (right column) for each subarea for SCI 3 NP_0.15.



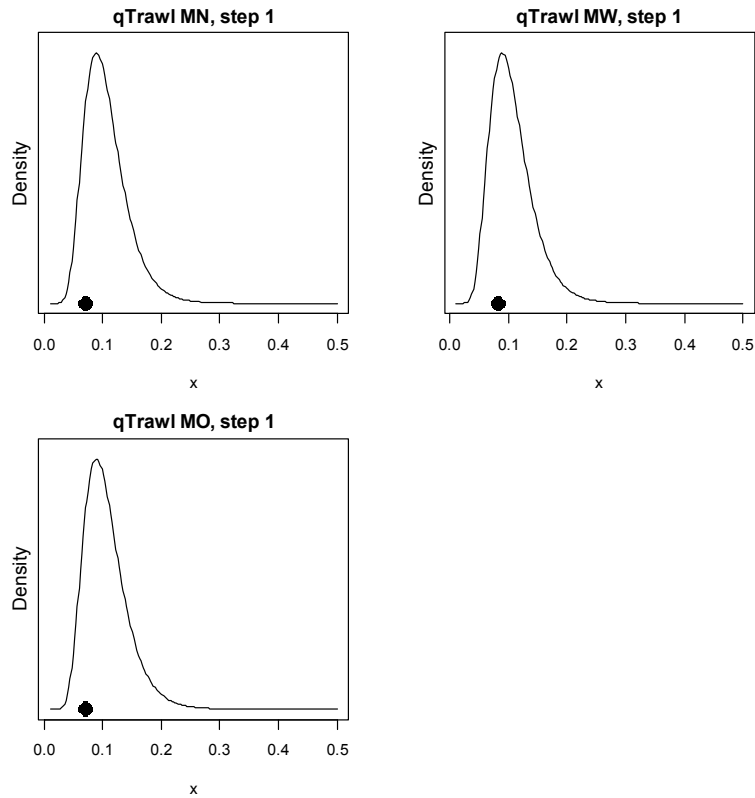
A6. 2: Fits to trawl survey indices (left column) and normalised residuals (right column) for each subarea for SCI 3 NP_0.15.



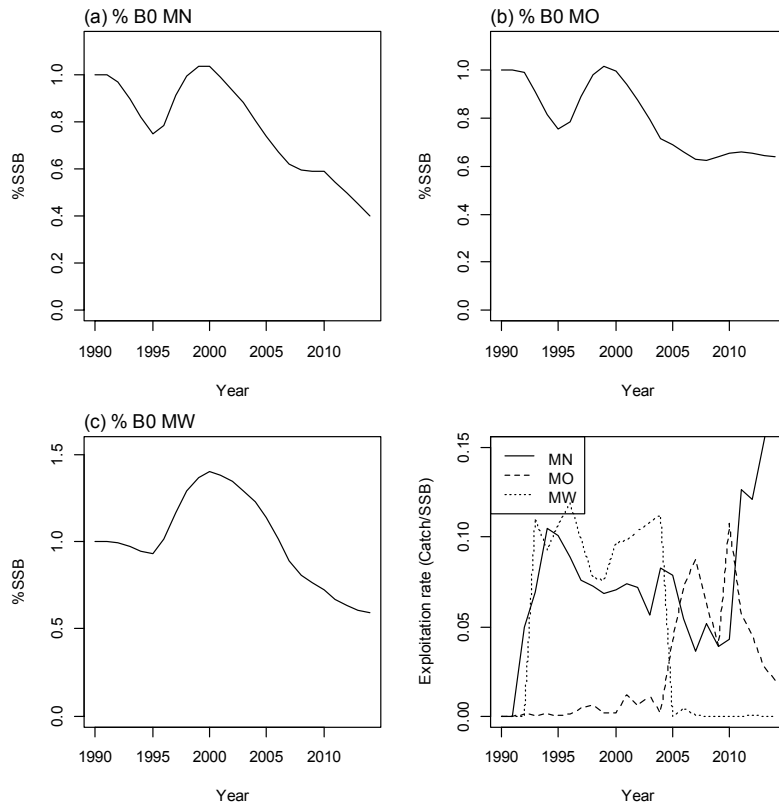
A6. 3: Year class strength for SCI 3 NP_0.15.



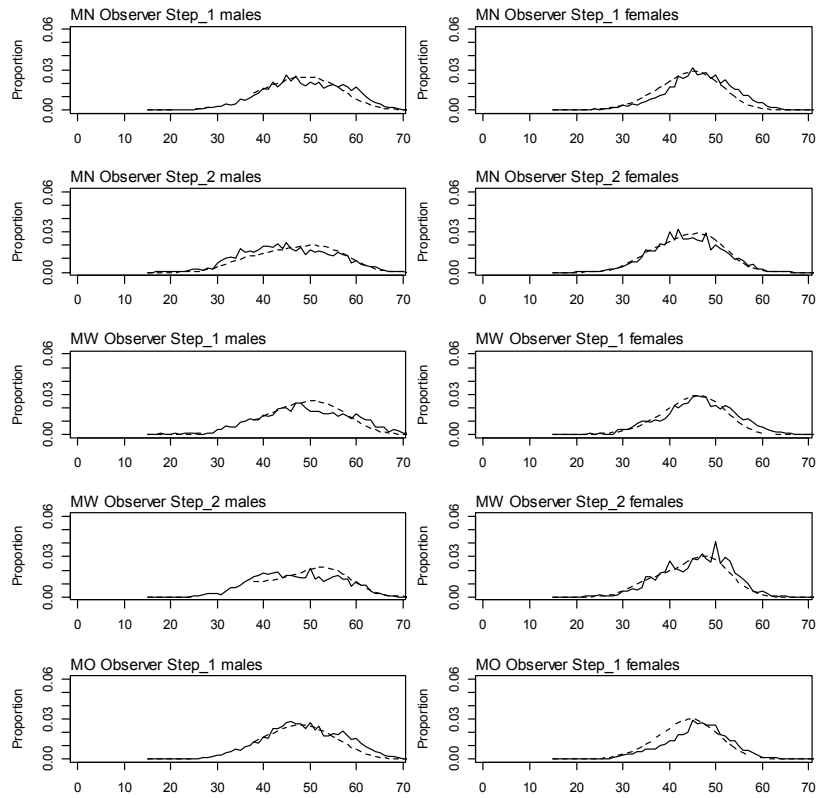
A6. 4: Fishery and survey selectivity curves for SCI 3 NP_0.15. Solid line – females, dotted line – males.



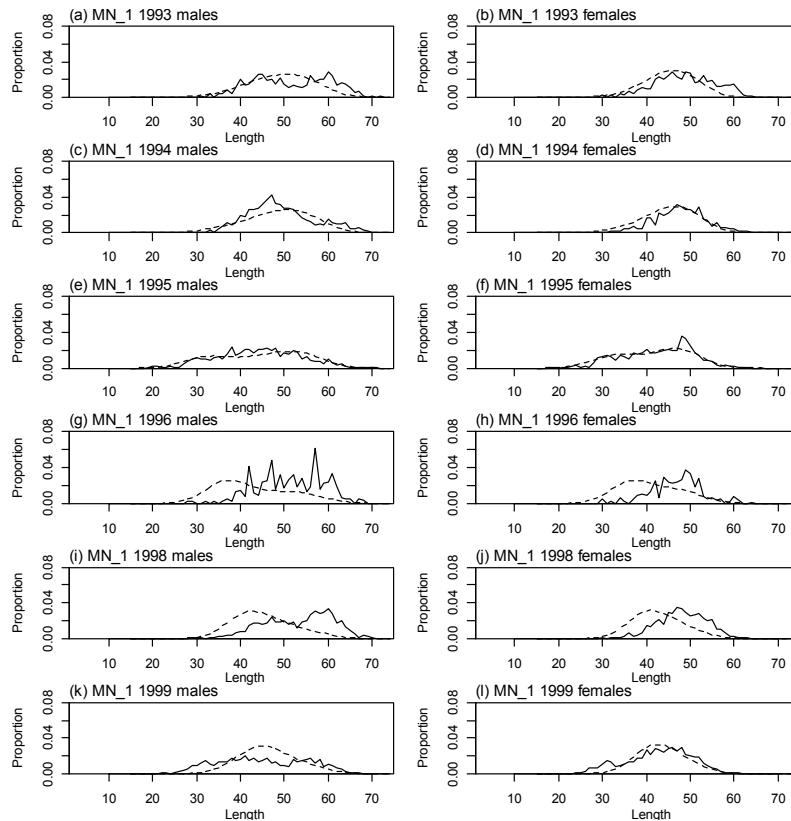
A6. 5: Catchability estimates from MPD model run, plotted in relation to prior distribution for SCI 3 NP_0.15.



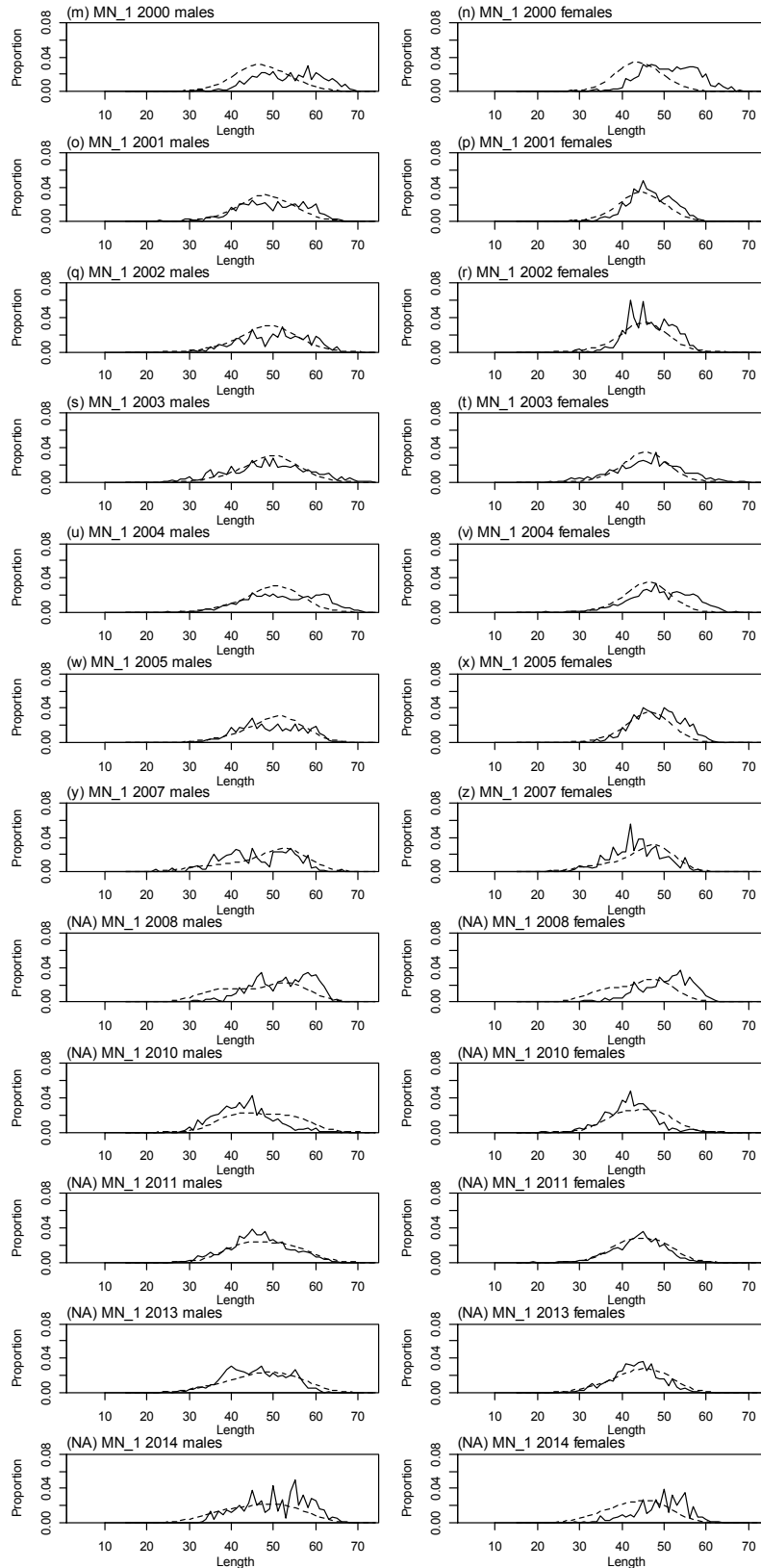
A6. 6: Stock trajectories (% SSB₀) for each subarea estimated from the MPD model run, and estimated exploitation rates for SCI 3 NP_0.15.



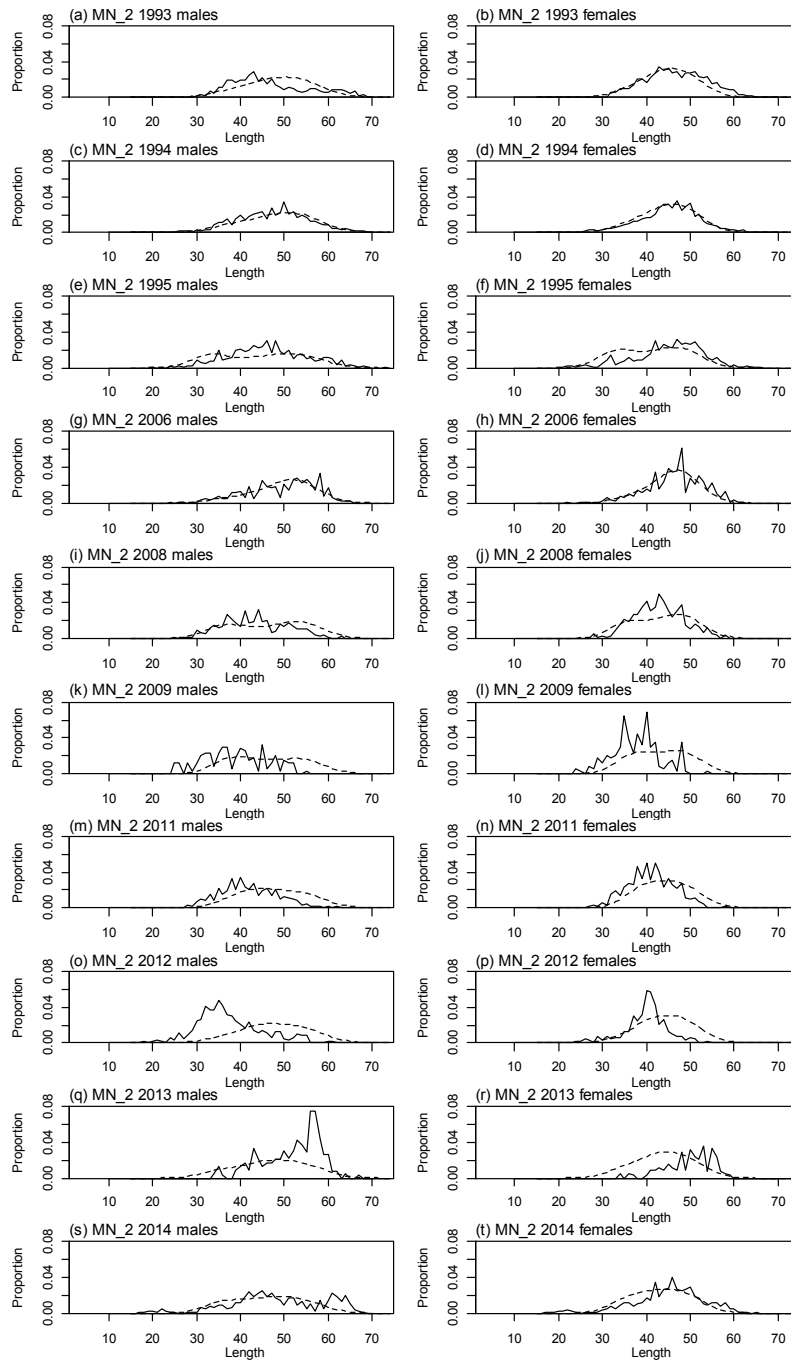
A6. 7: Average observed (solid line) and fitted (dashed line) length frequency distributions for observer samples for SCI 3 NP_0.15.



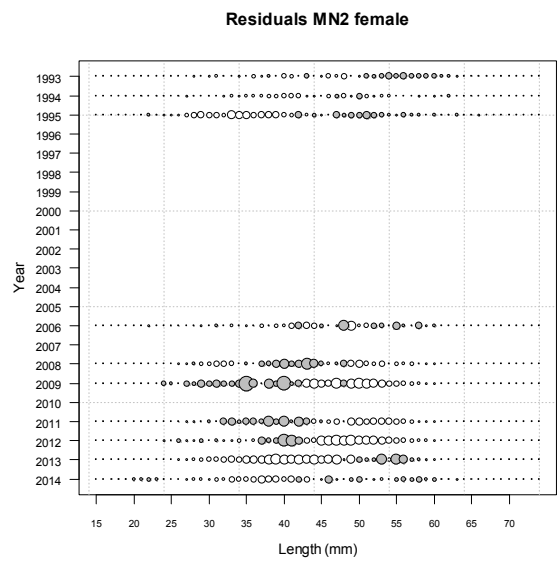
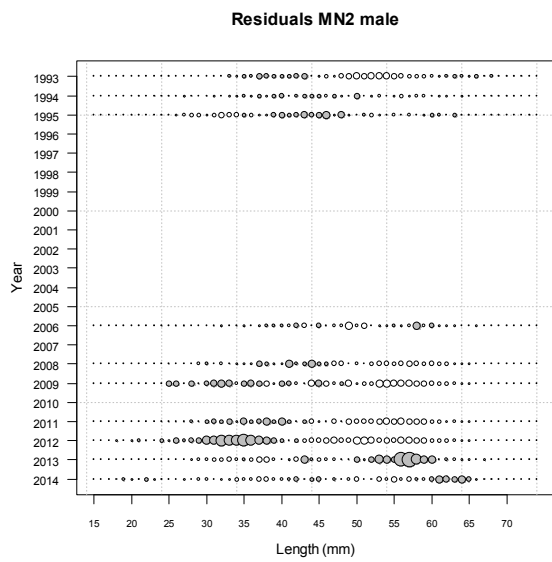
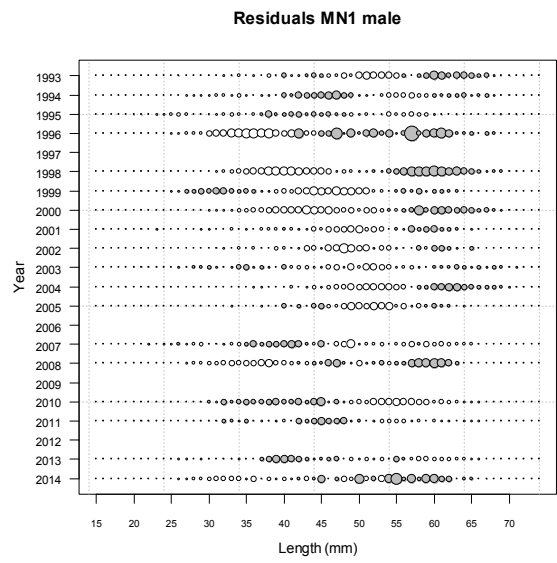
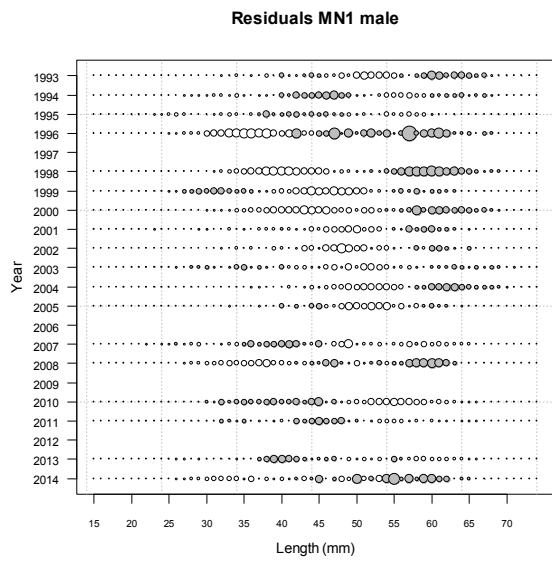
A6. 8: Observed (solid line) and fitted (dashed line) length frequency distributions for observer samples, MN time step 1 for SCI 3 NP_0.15.



A6.8 ctd.: Observed (solid line) and fitted (dashed line) length frequency distributions for observer samples, MN time step 1 for SCI 3 NP_0.15.



A6. 9: Observed (solid line) and fitted (dashed line) length frequency distributions for observer samples, MN time step 2 for SCI 3 NP_0.15.



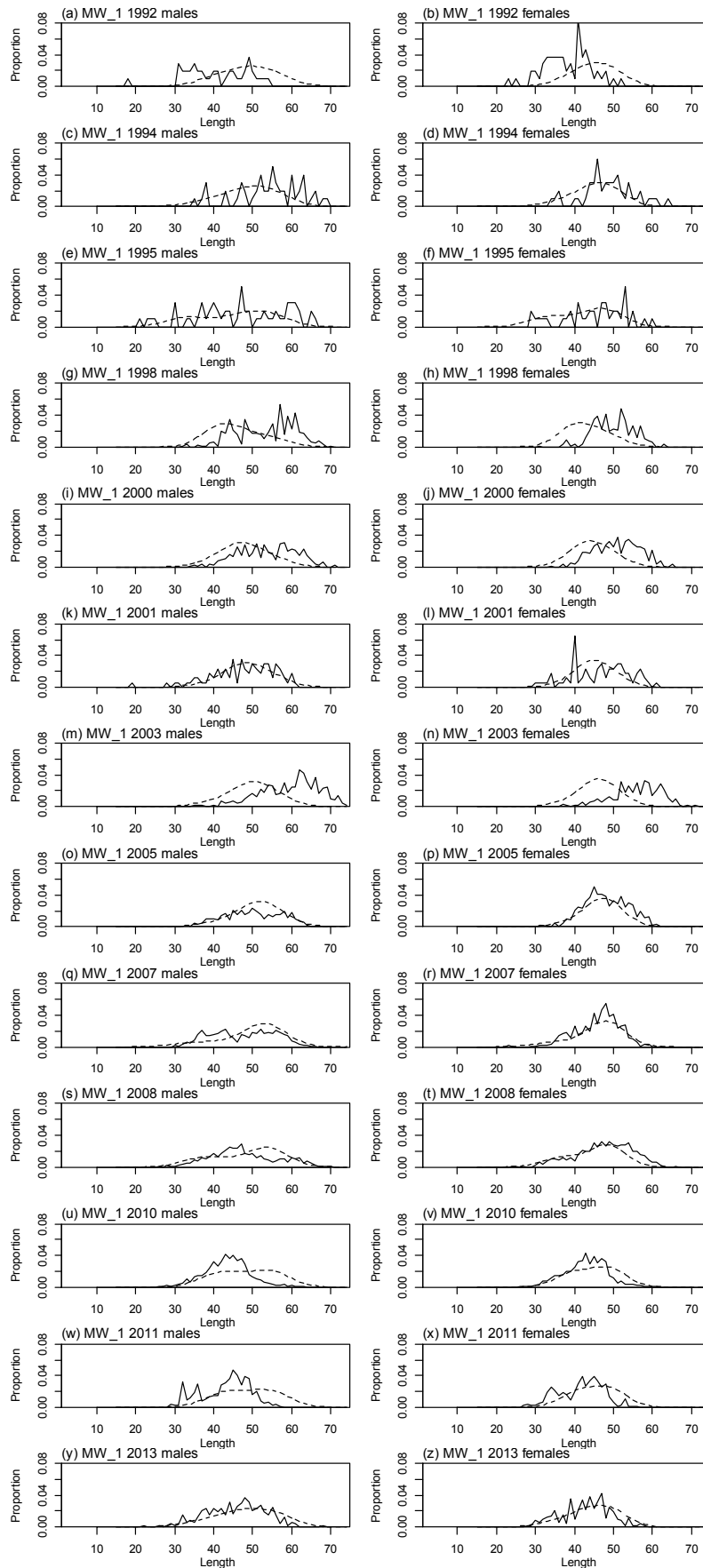
A6. 10: Bubble plots of residuals of fits to length frequency distributions for observer sampling from MN, time step 1 and 2, for SCI 3 NP_0.15.

A6. 11: Numbers of scampi measured, estimated multinomial N sample size, and effective sample size used within the SCI 3 NP_0.15 model for length frequency distributions for observer samples, MN time step 1.

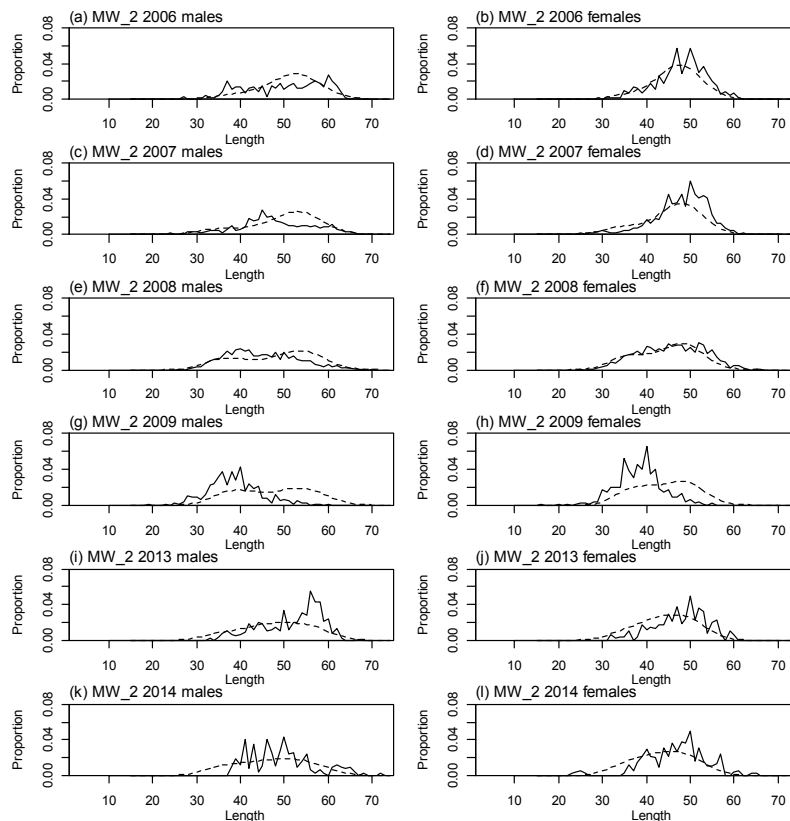
	Measured	Multinomial N	Effective sample size
N_1993	1 089	1 520	3.73
N_1994	2 090	3 036	7.46
N_1995	1 498	2 300	5.65
N_1996	465	500	1.23
N_1998	1 843	3 085	7.58
N_1999	1 921	4 221	10.37
N_2000	1 727	2 200	5.40
N_2001	1 528	2 908	7.14
N_2002	510	908	2.23
N_2003	2 824	5 674	13.94
N_2004	3 856	6 921	17.00
N_2005	1 448	2 497	6.13
N_2007	829	1 189	2.92
N_2008	1 087	1 587	3.90
N_2010	948	1 632	4.01
N_2011	3 273	6 881	16.90
N_2013	2 613	3 847	9.45
N_2014	403	789	1.94

A6. 12: Numbers of scampi measured, estimated multinomial N sample size, and effective sample size used within the SCI 3 NP_0.15 model for length frequency distributions for observer samples, MN time step 2.

	Measured	Multinomial N	Effective sample size
N_1993	1 639	3 306	16.77
N_1994	2 923	5 285	26.80
N_1995	1 260	1 800	9.13
N_2006	1 086	1 635	8.29
N_2008	535	699	3.55
N_2009	186	245	1.24
N_2011	1 019	1 900	9.64
N_2012	333	588	2.98
N_2013	352	234	1.19
N_2014	1 443	1 378	6.99



A6. 13: Observed (solid line) and fitted (dashed line) length frequency distributions for observer samples, MW time step 1 for SCI 3 NP_0.15.



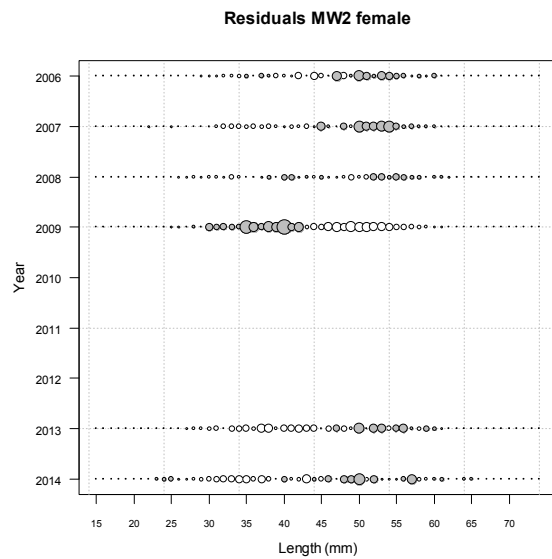
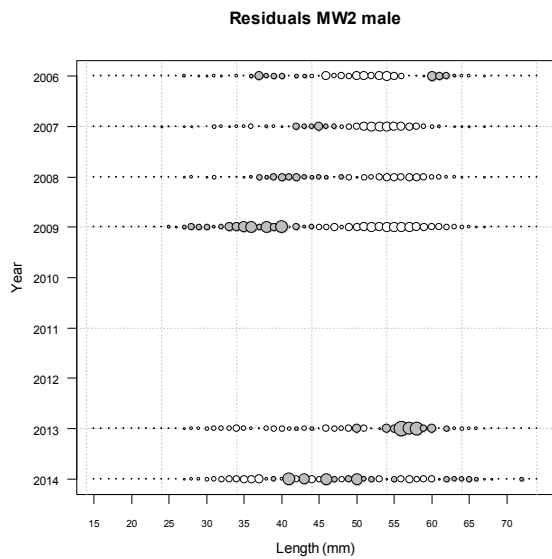
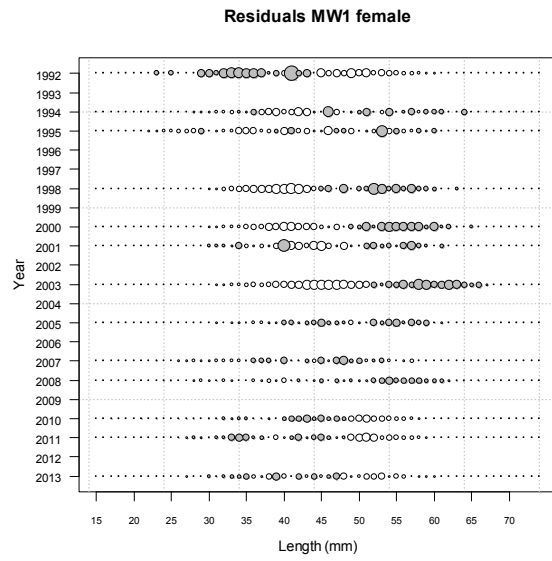
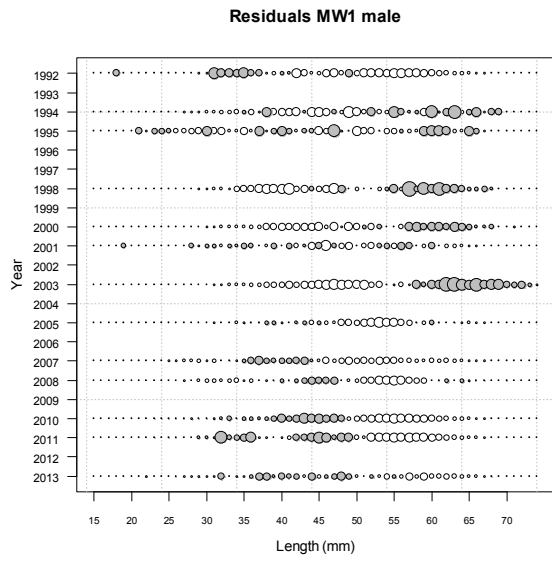
A6. 14: Observed (solid line) and fitted (dashed line) length frequency distributions for observer samples, MW time step 2 for SCI 3 NP_0.15.

A6. 15: Numbers of scampi measured, estimated multinomial N sample size, and effective sample size used within the SCI 3 NP_0.15 model for length frequency distributions for observer samples, MW time step 1.

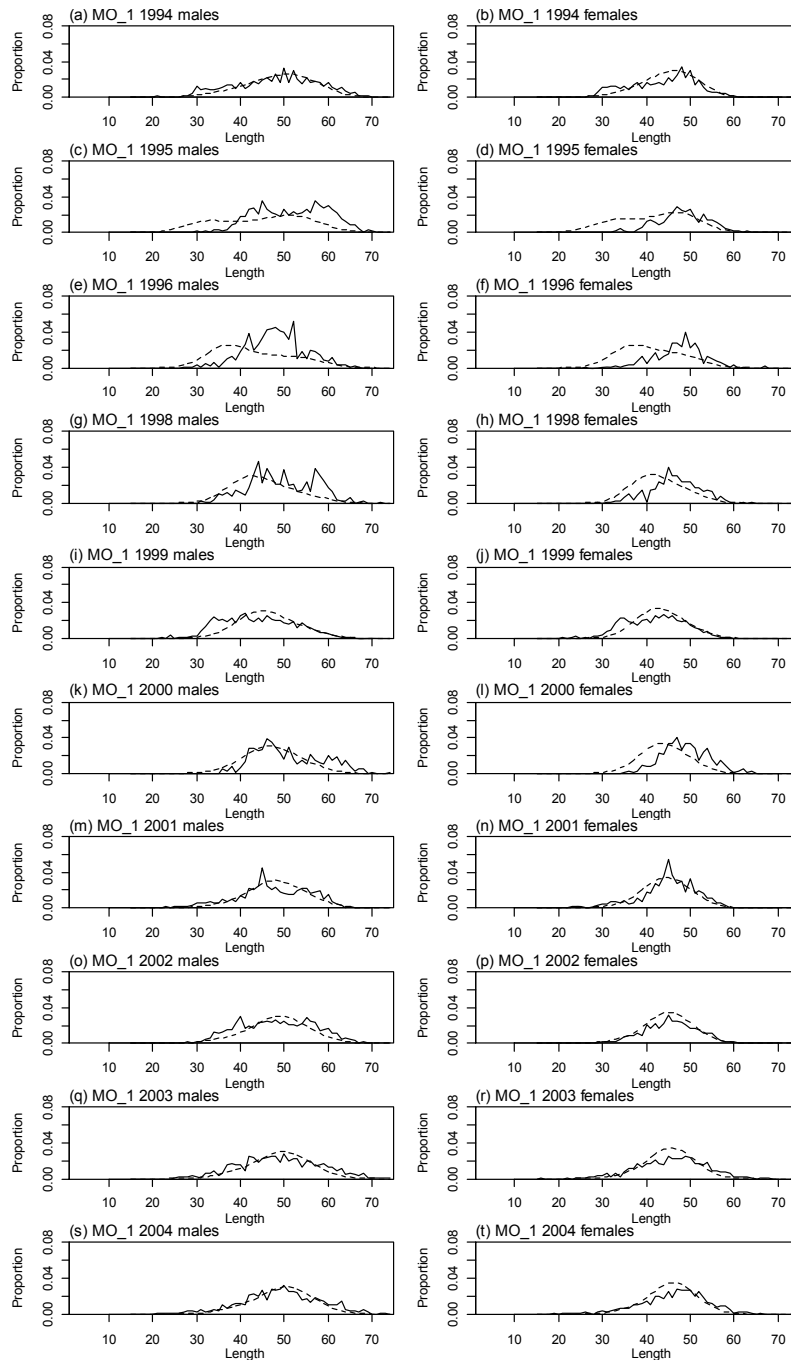
	Measured	Multinomial N	Effective sample size
N_1992	229	107	0.25
N_1994	242	100	0.23
N_1995	241	100	0.23
N_1998	365	365	0.84
N_2000	521	600	1.38
N_2001	251	169	0.39
N_2003	578	799	1.84
N_2005	593	870	2.00
N_2007	1 082	1 669	3.84
N_2008	1 201	1 865	4.29
N_2010	3 163	6 951	15.98
N_2011	712	2 345	5.39
N_2013	495	616	1.42

A6. 16: Numbers of scampi measured, estimated multinomial N sample size, and effective sample size used within the SCI 3 NP_0.15 model for length frequency distributions for observer samples, MW time step 2.

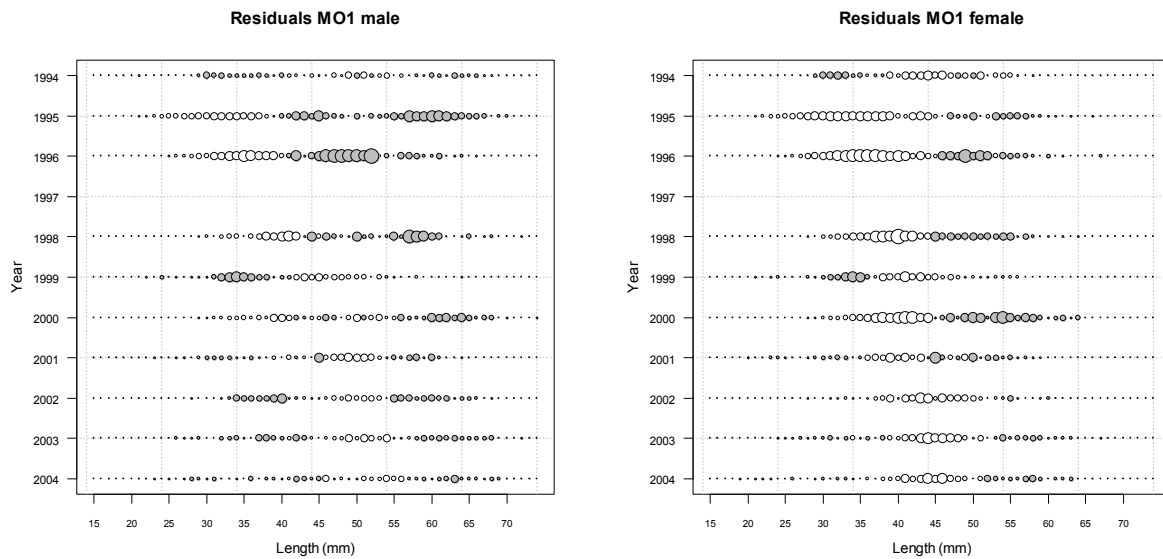
	Measured	Multinomial N	Effective sample size
N_2006	659	699	3.09
N_2007	1 333	2 406	10.64
N_2008	2 278	4 100	18.13
N_2009	693	1 340	5.92
N_2013	550	483	2.14
N_2014	460	317	1.40



A6. 17: Bubble plots of residuals of fits to length frequency distributions for observer sampling from MW, time step 1 and 2, for SCI 3 NP_0.15.



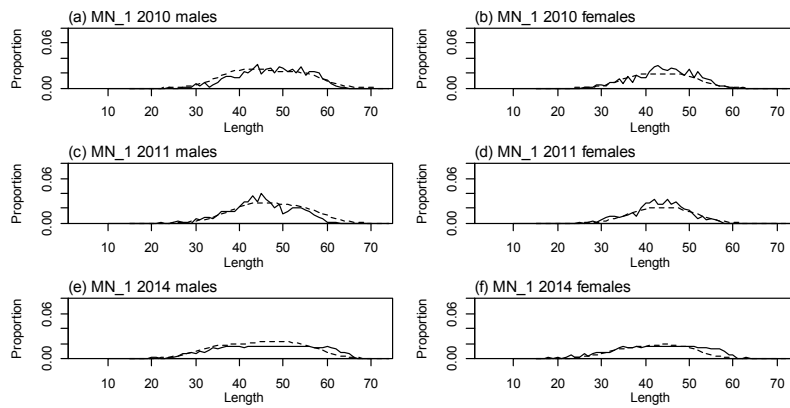
A6. 18: Observed (solid line) and fitted (dashed line) length frequency distributions for observer samples, MO time step 1 for SCI 3 NP_0.15.



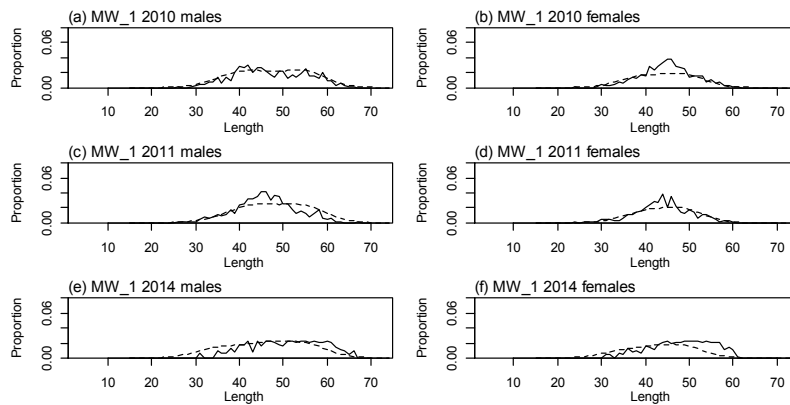
A6. 19: Bubble plots of residuals of fits to length frequency distributions for observer sampling from MO, time step 1, for SCI 3 NP_0.15.

A6. 20: Numbers of scampi measured, estimated multinomial N sample size, and effective sample size used within the SCI 3 NP_0.15 model for length frequency distributions for observer samples, MO time step 1.

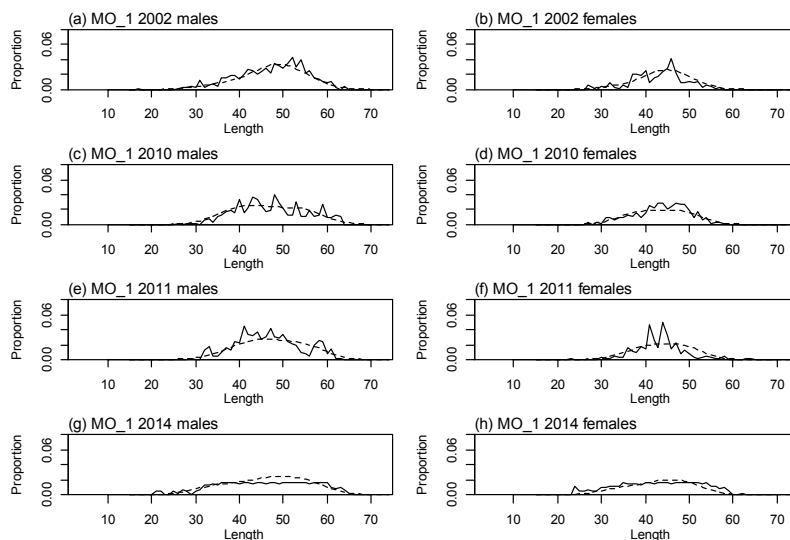
	Measured	Multinomial N	Effective sample size
N_1994	2 665	4 814	18.68
N_1995	2 474	2 500	9.70
N_1996	752	1 200	4.66
N_1998	870	900	3.49
N_1999	1 492	2 996	11.62
N_2000	608	600	2.33
N_2001	1 749	3 118	12.10
N_2002	1 768	3 442	7.71
N_2003	1 367	2 224	6.51
N_2004	1 557	2 881	8.43



A6. 21: Observed (solid line) and fitted (dashed line) length frequency distributions for MN trawl survey samples within the SCI 3 NP_0.15 model.



A6. 22: Observed (solid line) and fitted (dashed line) length frequency distributions for MW trawl survey samples within the SCI 3 NP_0.15 model.



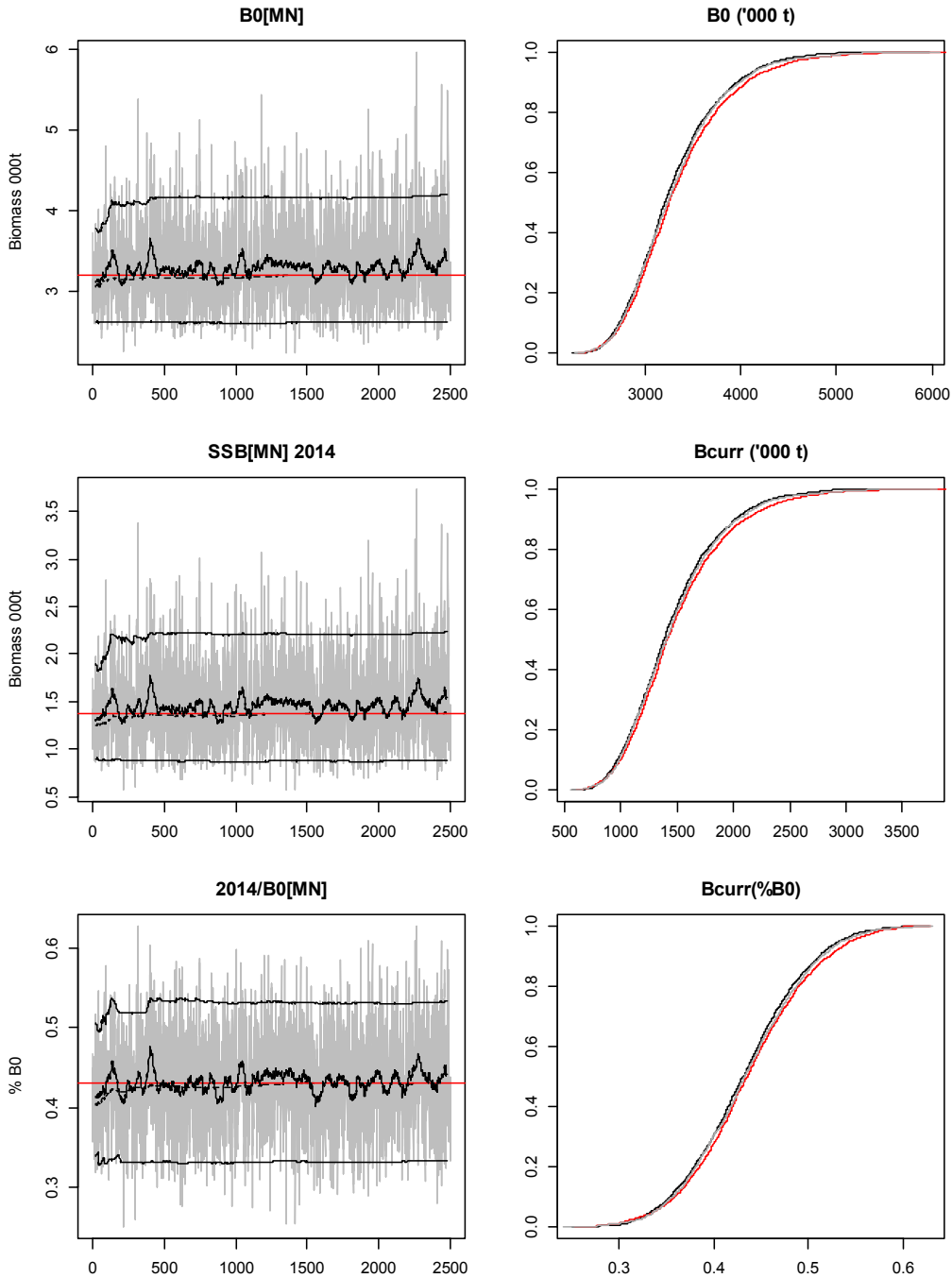
A6. 23: Observed (solid line) and fitted (dashed line) length frequency distributions for MO trawl survey samples within the SCI 3 NP_0.15 model.

A6. 24: Numbers of scampi burrows measured, estimated multinomial N sample size, and effective sample size used within the model for length frequency distributions for photographic survey samples within the SCI 3 NP_0.15 model.

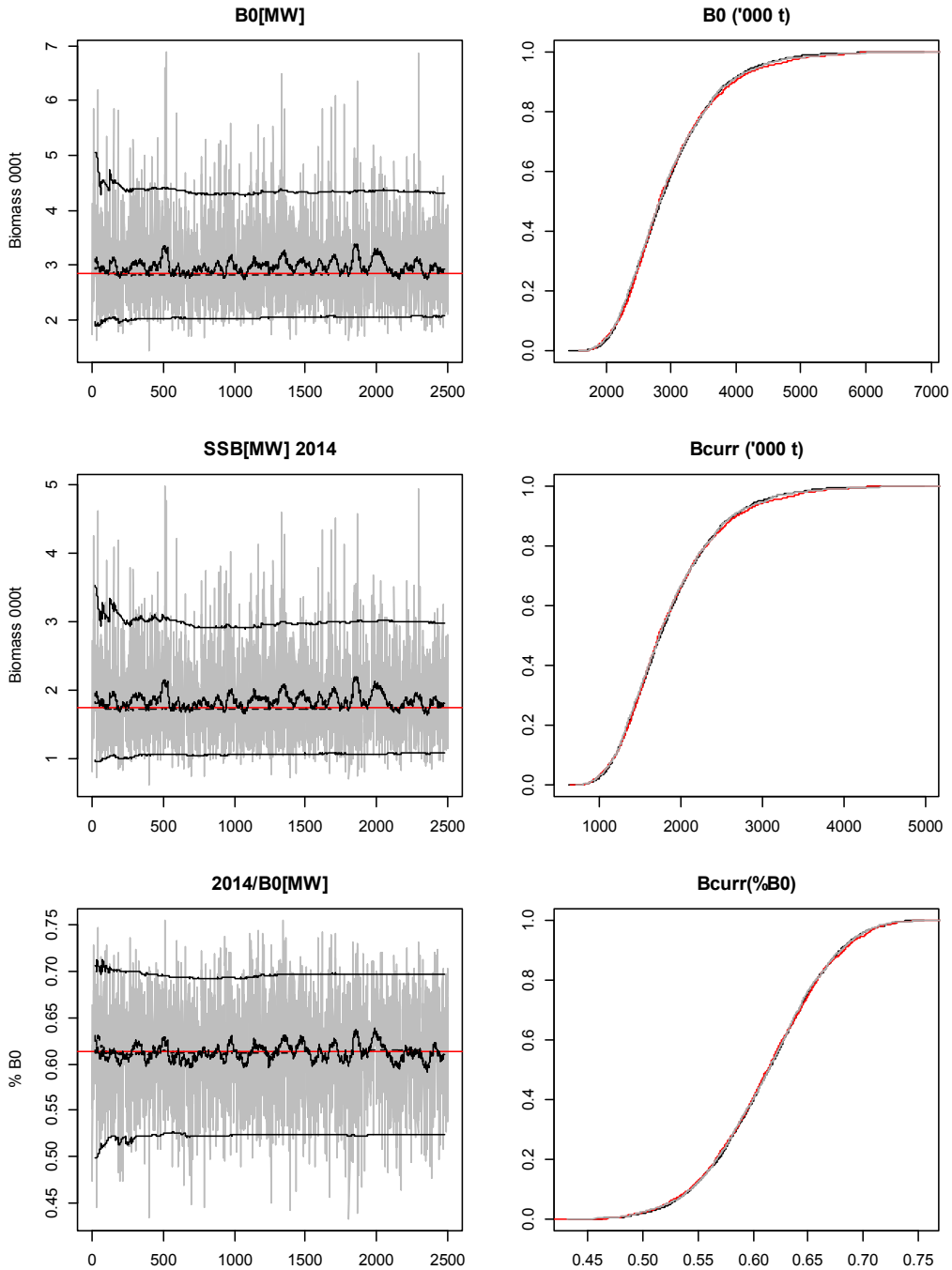
MN	Measured	Multinomial N	Effective sample size
N_2010	2 595	1 276	19.50
N_2011	4 429	2 362	33.27
N_2014	1 077	602	8.09

MW	Measured	Multinomial N	Effective sample size
N_2010	2 254	1 110	25.07
N_2011	2 636	1 295	29.31
N_2014	385	208	4.28

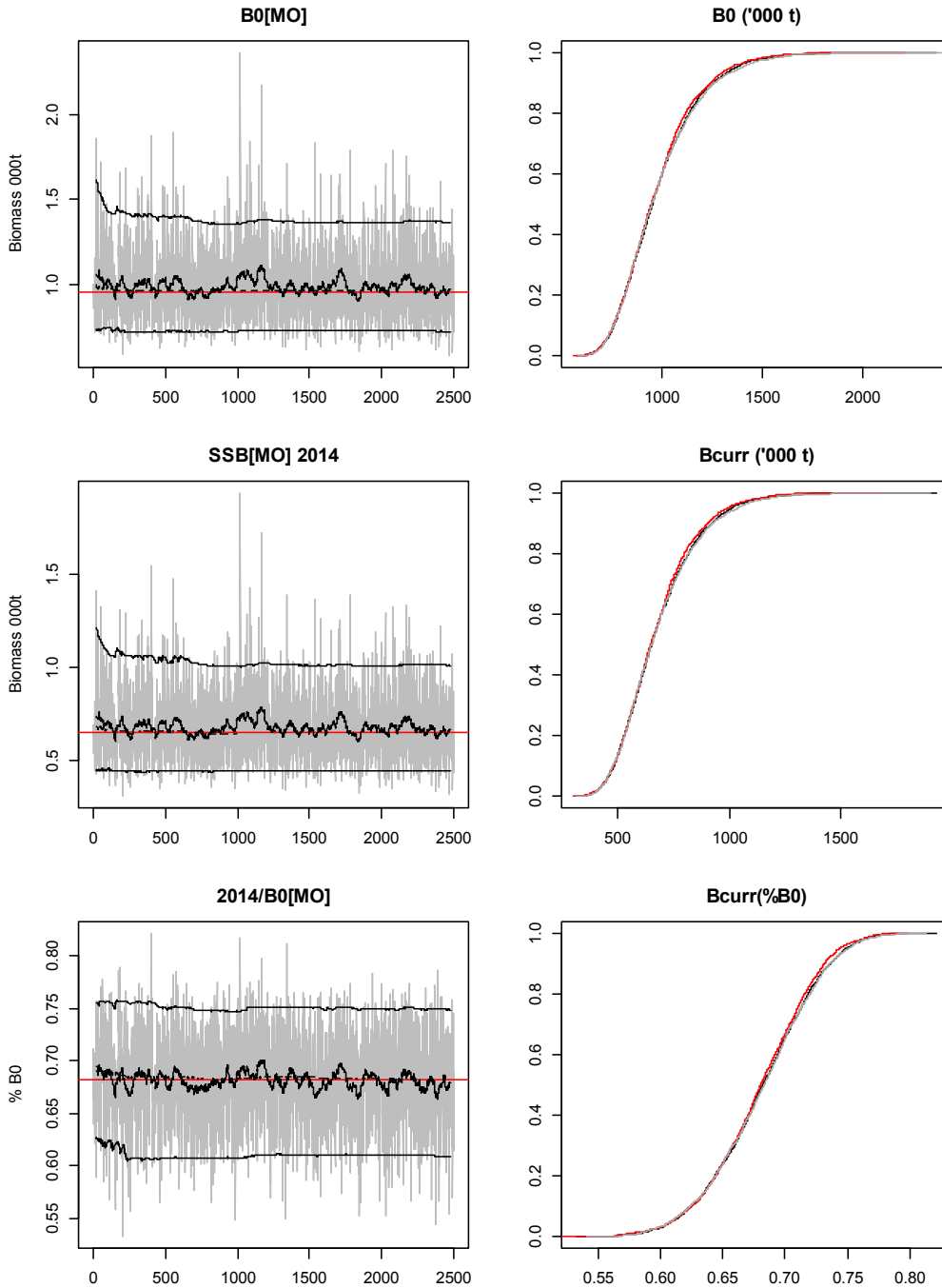
MO	Measured	Multinomial N	Effective sample size
N_2002	1 367	1 418	339.49
N_2010	1 123	551	278.89
N_2011	1 163	611	288.82
N_2014	523	339	129.88



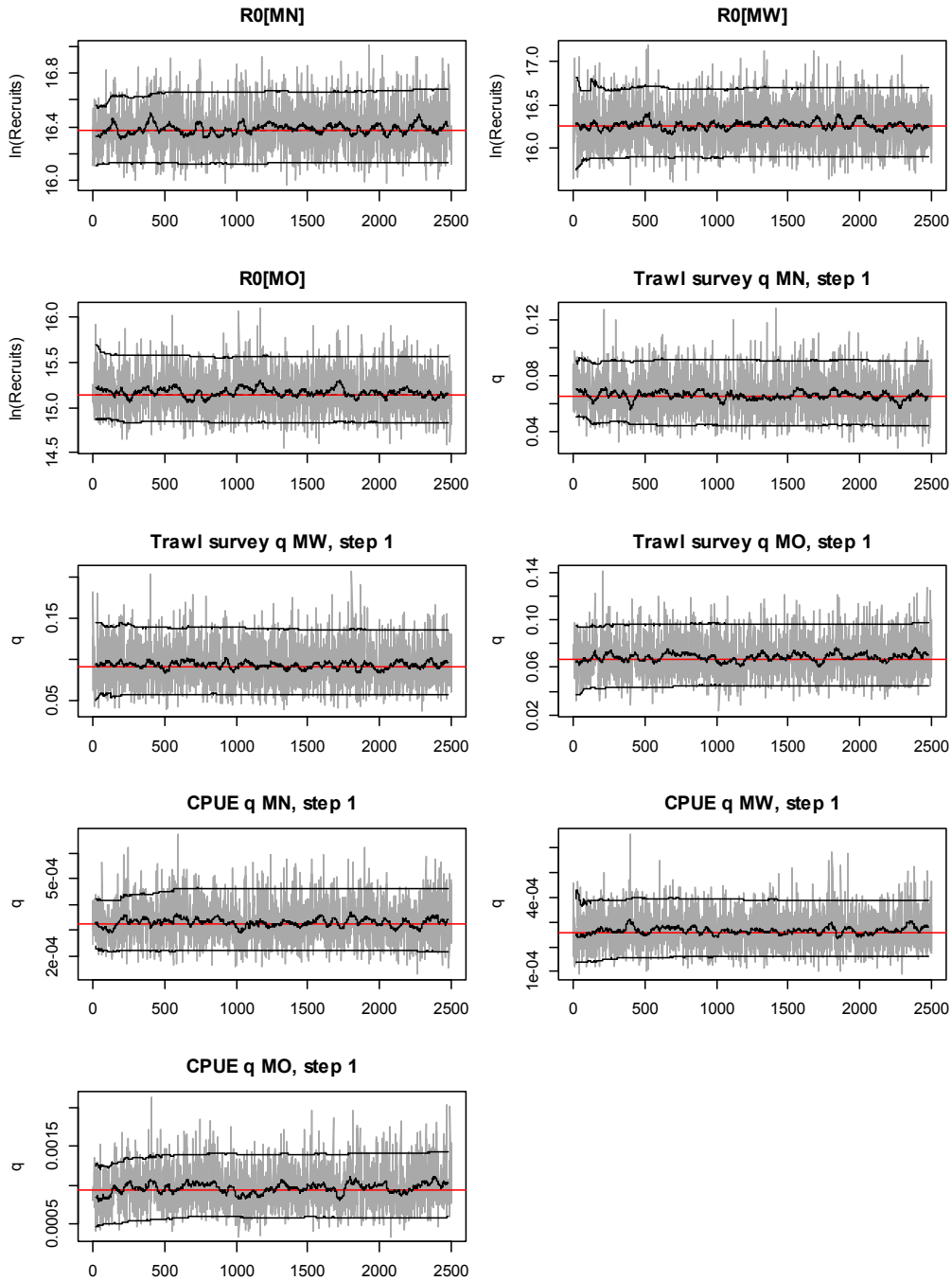
A6. 25: MCMC traces for B_0 , SSB_{2014} , and SSB_{2014}/SSB_0 terms for the MN subarea within the SCI 3 NP_0.15 model for SCI 3 (trace – grey line, cumulative moving median – dashed black line, moving average and cumulative moving 2.5%, 97.5% quantiles – solid black lines, overall median – solid red line, left plots), along with cumulative frequency distributions for three independent MCMC chains (shown as red, grey and black lines, right plots).



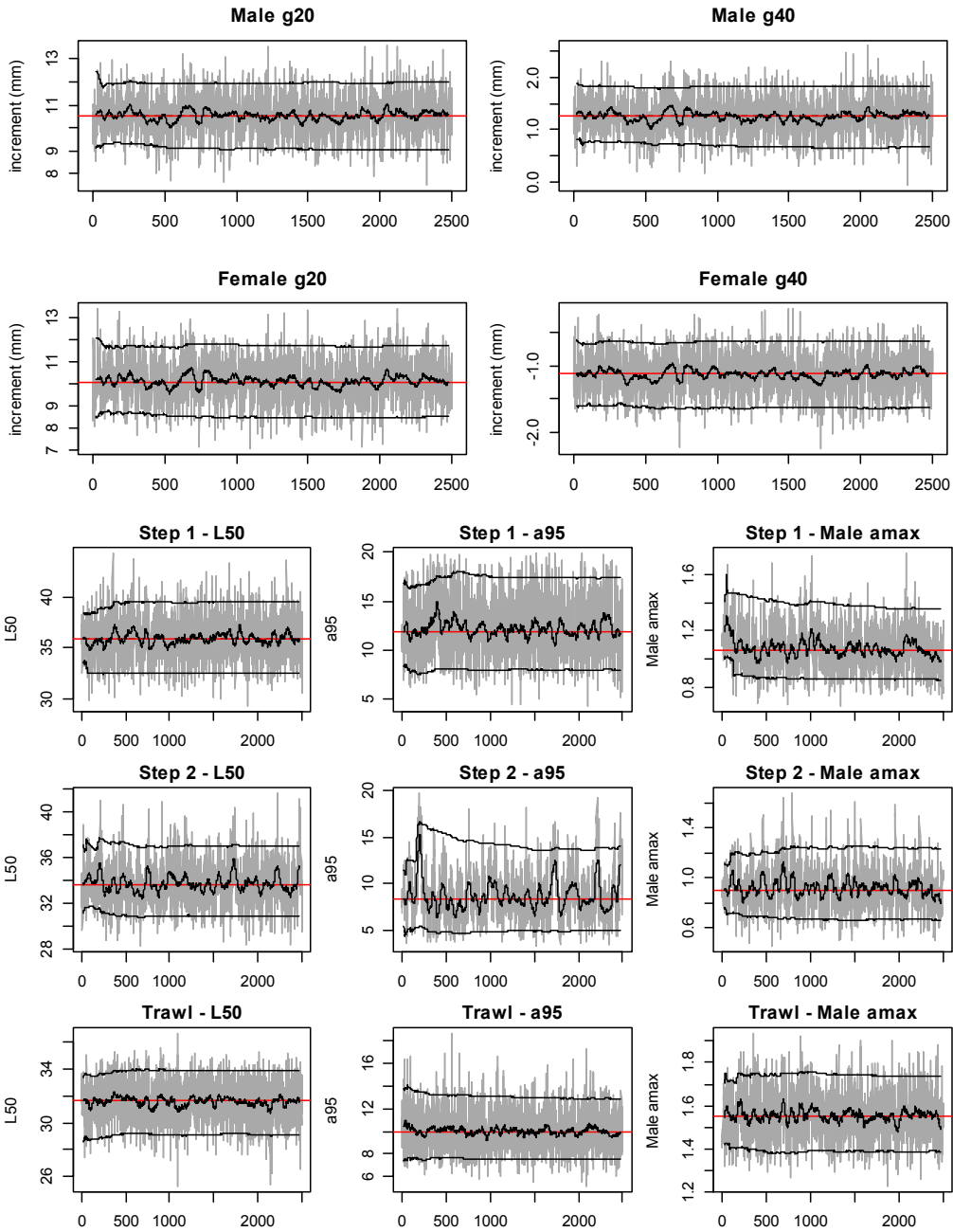
A6. 26: MCMC traces for B_0 , SSB_{2014} , and SSB_{2014}/SSB_0 terms for the MW subarea within the SCI 3 NP_0.15 model for SCI 3 (trace – grey line, cumulative moving median – dashed black line, moving average and cumulative moving 2.5%, 97.5% quantiles – solid black lines, overall median – solid red line, left plots), along with cumulative frequency distributions for three independent MCMC chains (shown as red, grey and black lines, right plots).



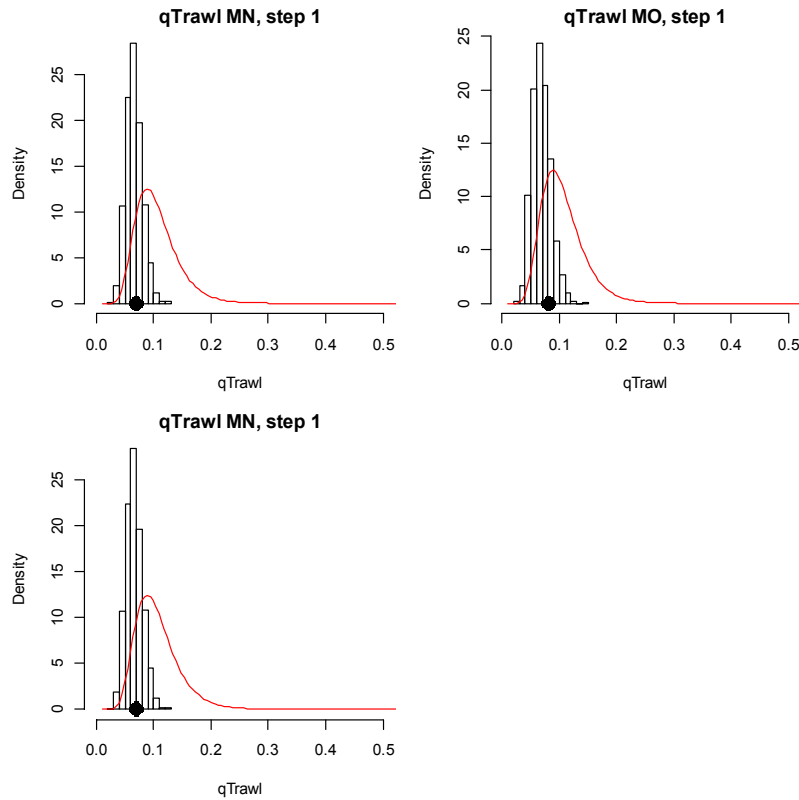
A6. 27: MCMC traces for B_0 , SSB_{2014} , and SSB_{2014}/SSB_0 terms for the MN subarea within the SCI 3 NP_0.15 model for SCI 3 (trace – grey line, cumulative moving median – dashed black line, moving average and cumulative moving 2.5%, 97.5% quantiles – solid black lines, overall median – solid red line, left plots), along with cumulative frequency distributions for three independent MCMC chains (shown as red, grey and black lines, right plots).



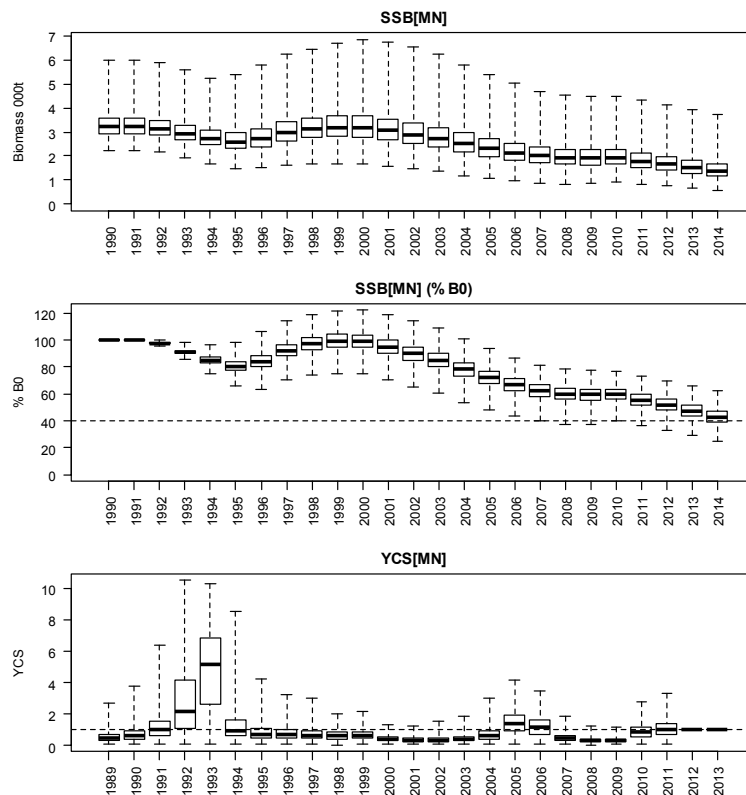
A6. 28: MCMC traces for R_0 , trawl survey q s, and commercial fishery q terms within the SCI 3 NP_0.15 model for SCI 3 (trace – grey line, cumulative moving median – dashed black line, moving average and cumulative moving 2.5%, 97.5% quantiles – solid black lines, overall median – solid red line, left plots), along with cumulative frequency distributions for three independent MCMC chains (shown as red, grey and black lines, right plots).



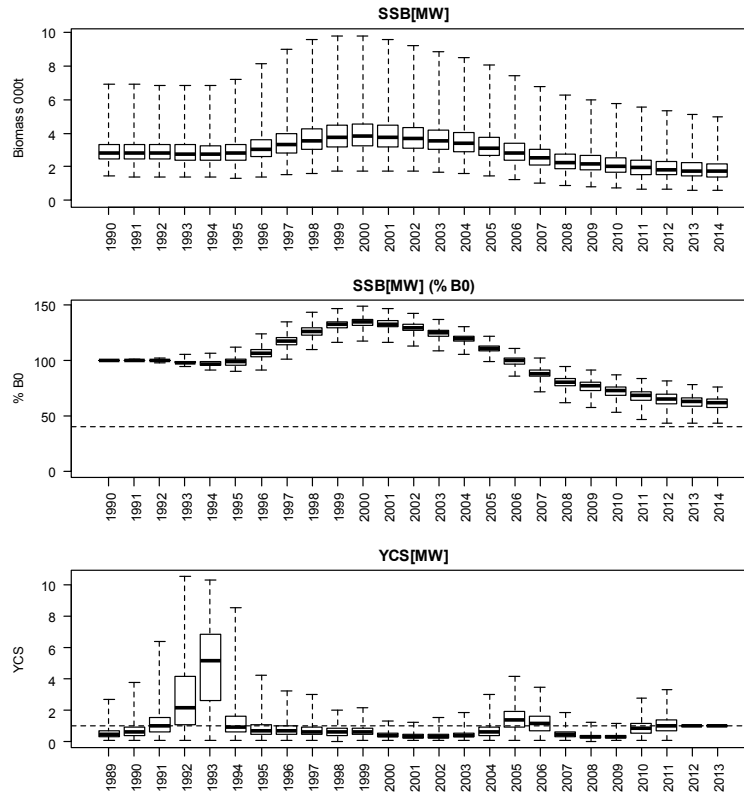
A6. 29: MCMC traces for growth increment and selectivity parameters within the SCI 3 NP_0.15 model for SCI 3 (trace – grey line, cumulative moving median – dashed black line, moving average and cumulative moving 2.5%, 97.5% quantiles – solid black lines, overall median – solid red line, left plots), along with cumulative frequency distributions for three independent MCMC chains (shown as red, grey and black lines, right plots).



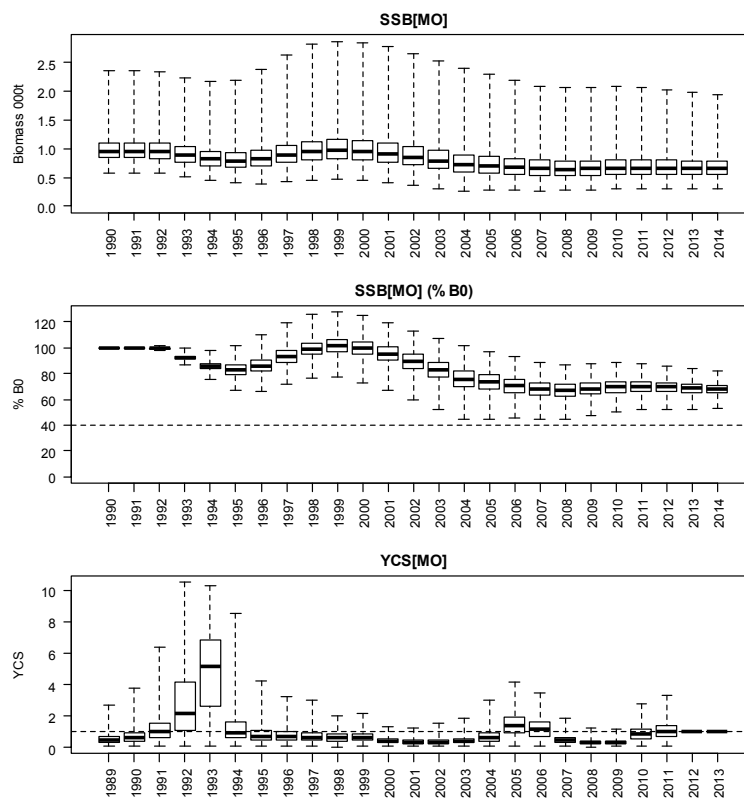
A6. 30: Marginal posterior distribution (histogram), MPD estimate (solid symbols) and distribution of prior (line) for photo survey catchability term within the SCI 3 NP_0.15 model.



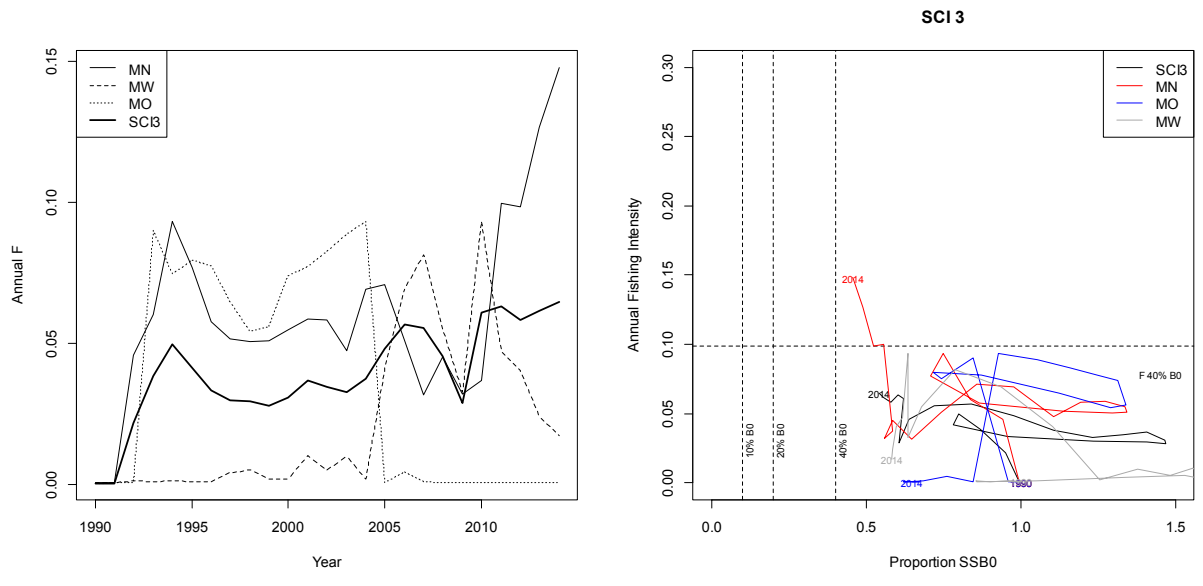
A6. 31: Posterior trajectory of SSB, SSB_{2014}/SSB_0 and YCS for the MN subarea within the SCI 3 NP_0.15 model.



A6. 32: Posterior trajectory of SSB, SSB_{2014}/SSB_0 and YCS for the MW subarea within the SCI 3 NP_0.15 model.

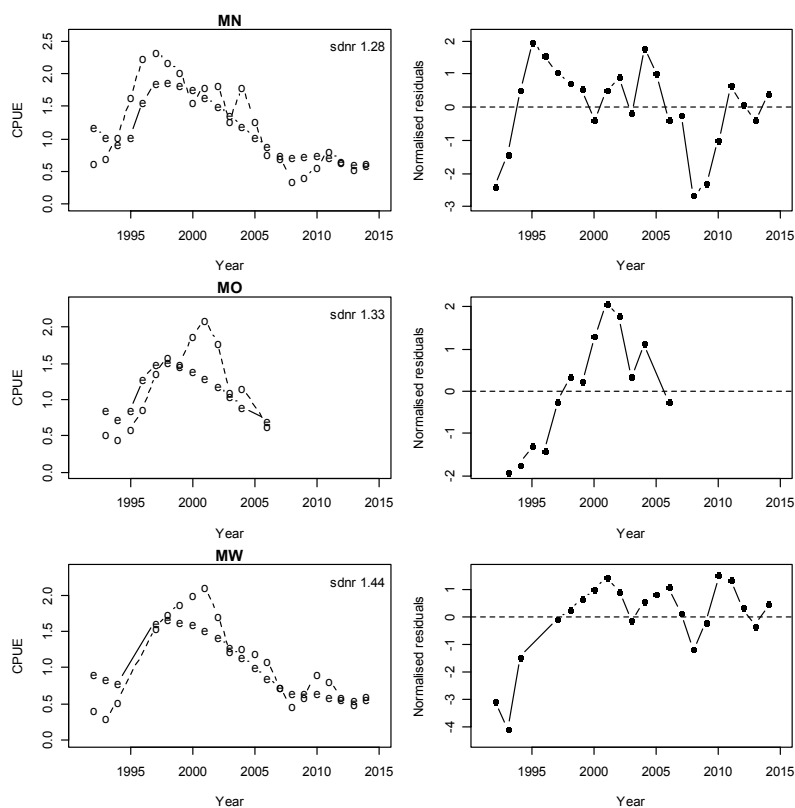


A6. 33: Posterior trajectory of SSB, SSB_{2014}/SSB_0 and YCS for the MO subarea within the SCI 3 NP_0.15 model.

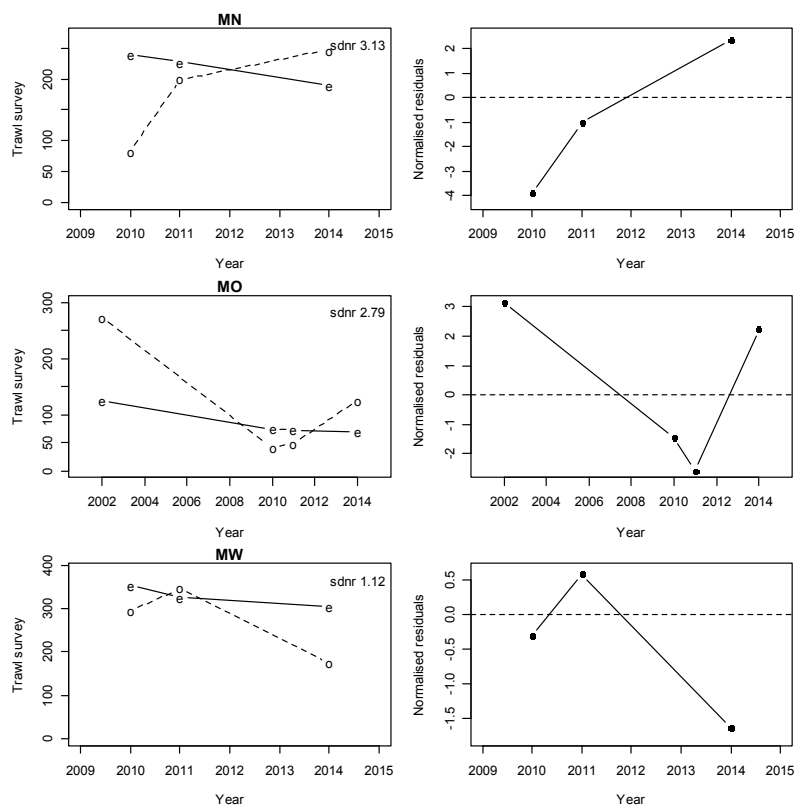


A6. 34: Estimated annual equivalent F (left) and phase plot (right) from the SCI 3 NP_0.15 model.

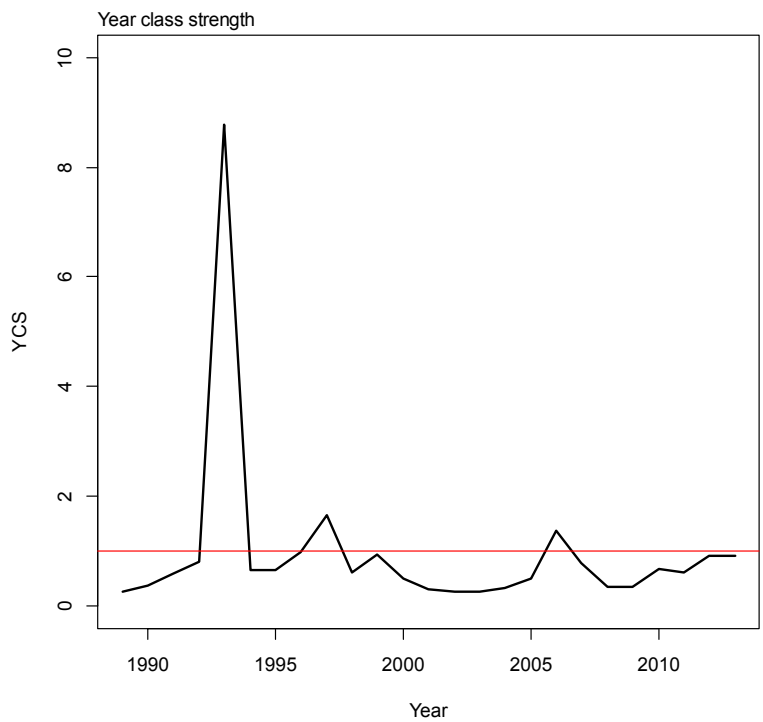
APPENDIX 7. MODEL NP_0.25



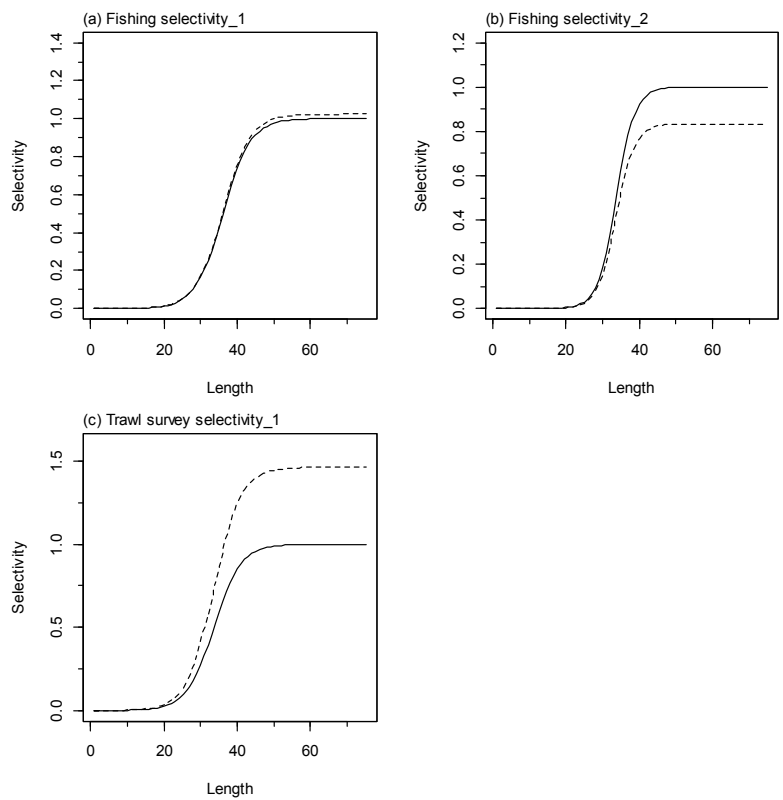
A7.1: Fits to CPUE indices (left column) and normalised residuals (right column) for each subarea for SCI 3 NP_0.25.



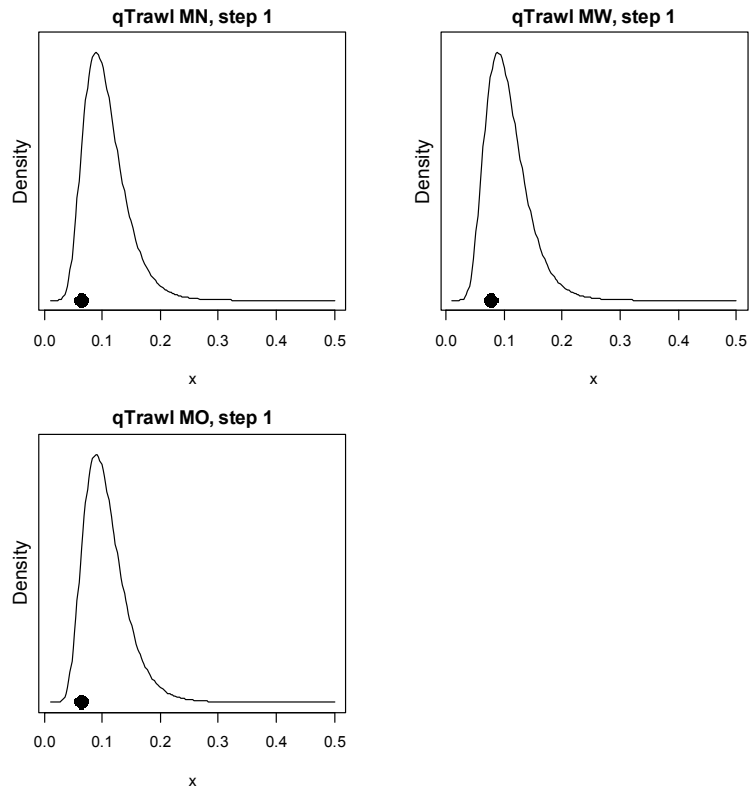
A7.2: Fits to trawl survey indices (left column) and normalised residuals (right column) for each subarea for SCI 3 NP_0.25.



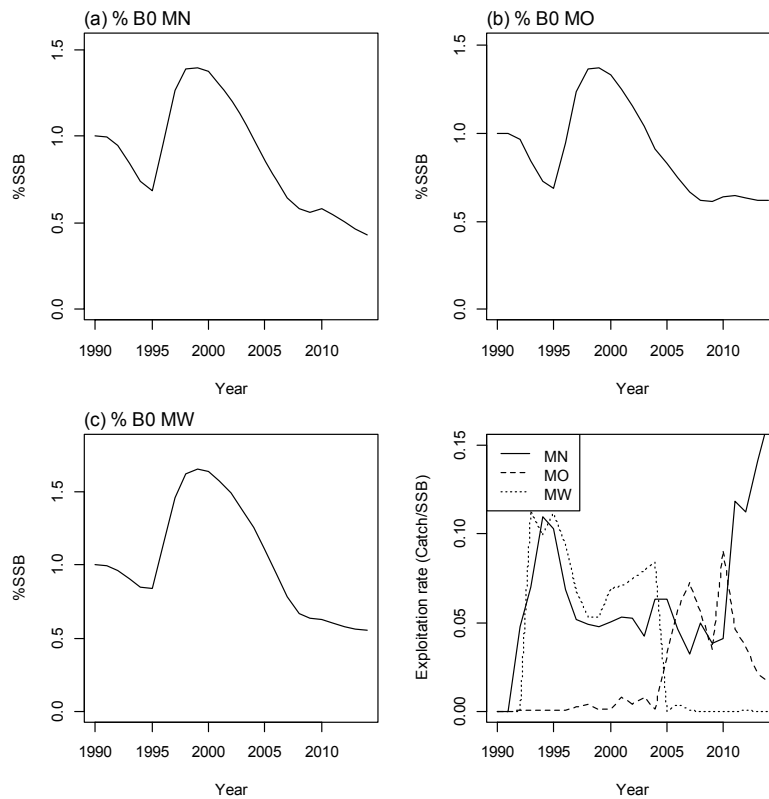
A7. 3: Year class strength for SCI 3 NP_0.25.



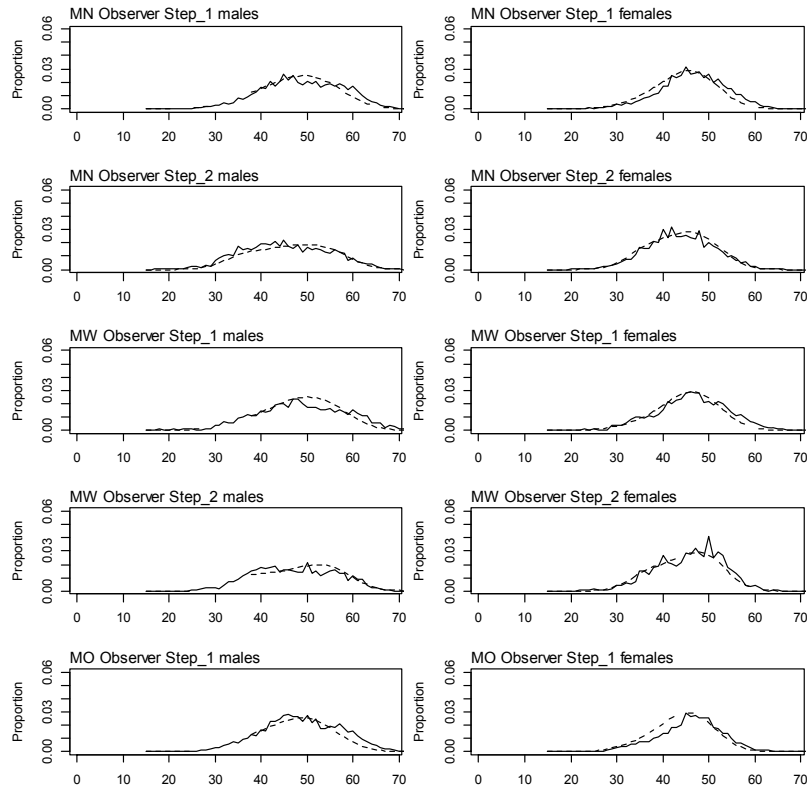
A7. 4: Fishery and survey selectivity curves for SCI 3 NP_0.25. Solid line – females, dotted line – males.



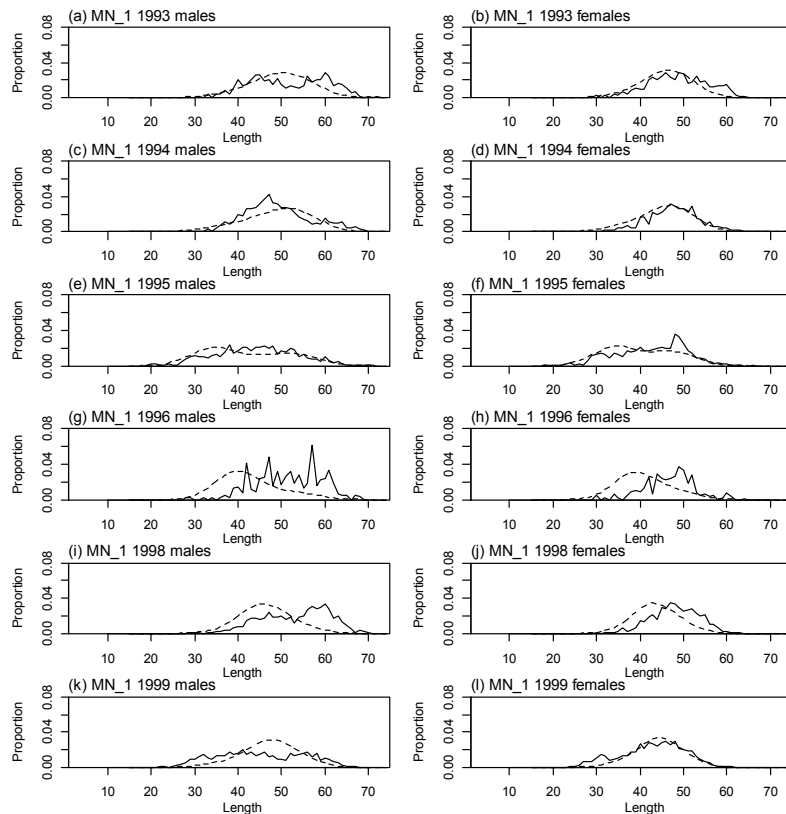
A7. 5: Catchability estimates from MPD model run, plotted in relation to prior distribution for SCI 3 NP_0.25.



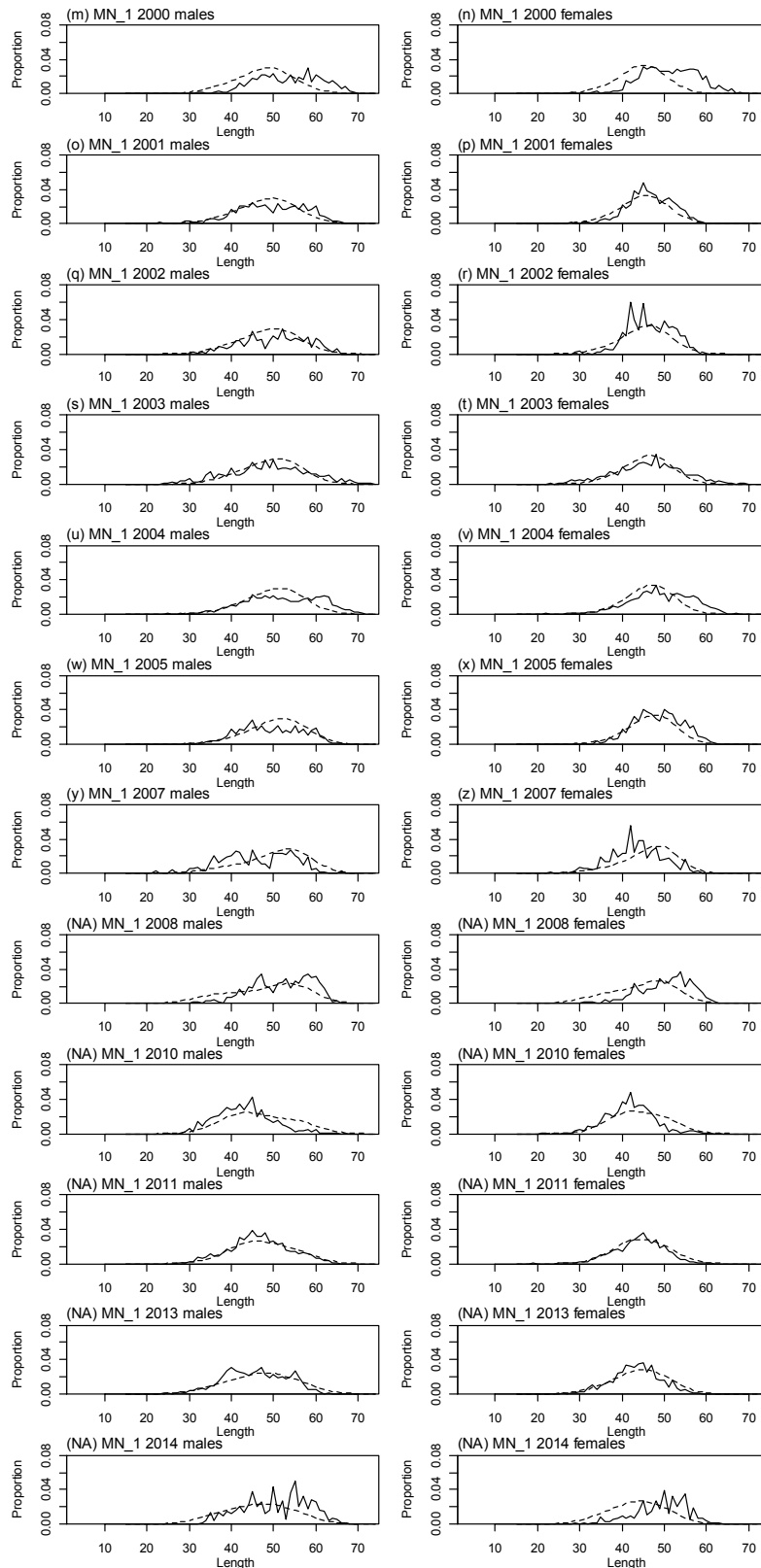
A7. 6: Stock trajectories (%SSB₀) for each subarea estimated from the MPD model run, and estimated exploitation rates for SCI 3 NP_0.25.



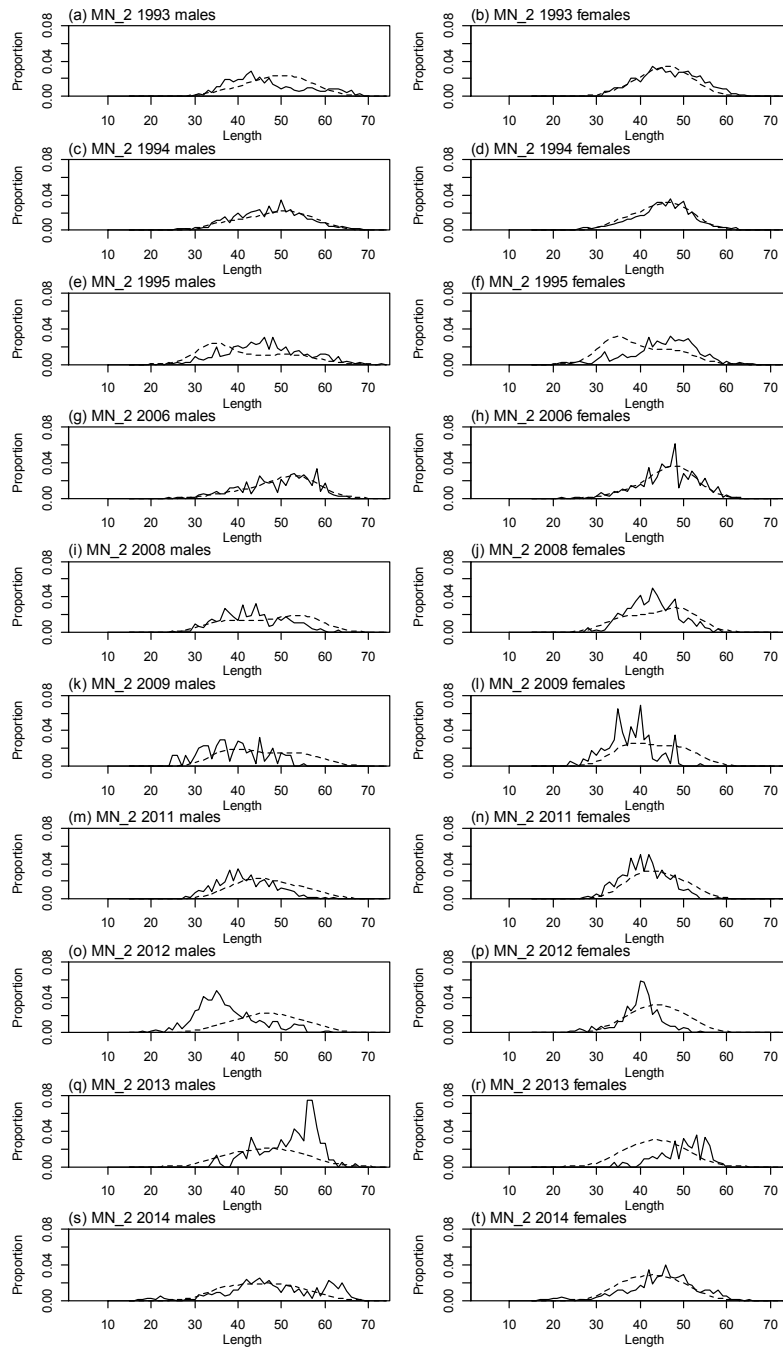
A7. 7: Average observed (solid line) and fitted (dashed line) length frequency distributions for observer samples for SCI 3 NP_0.25.



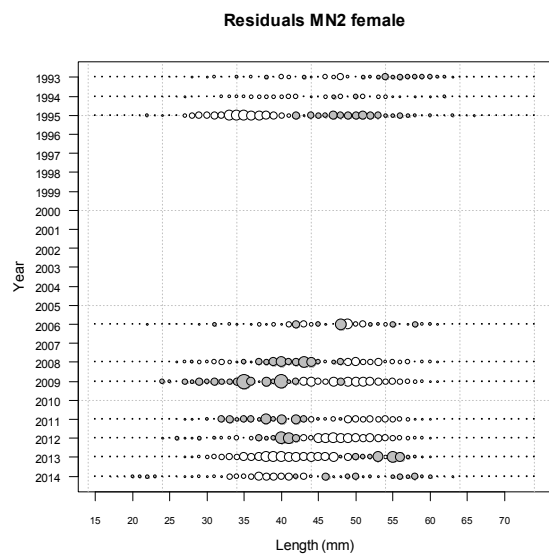
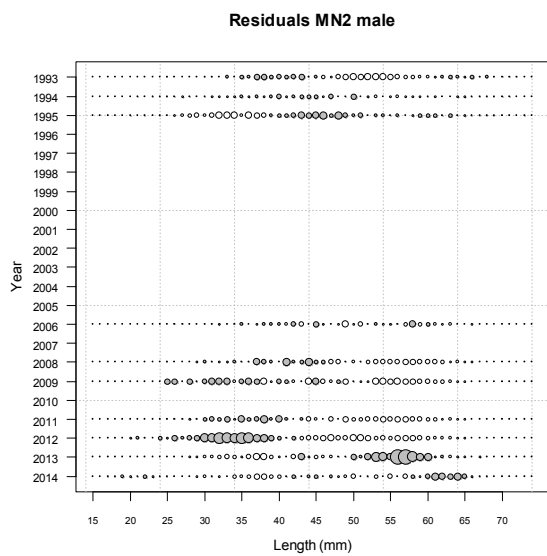
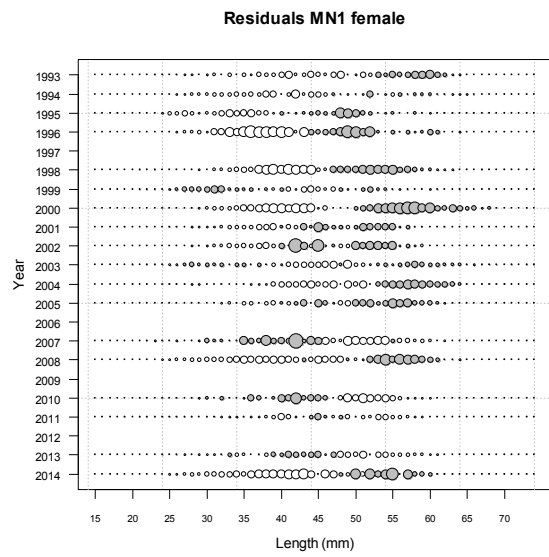
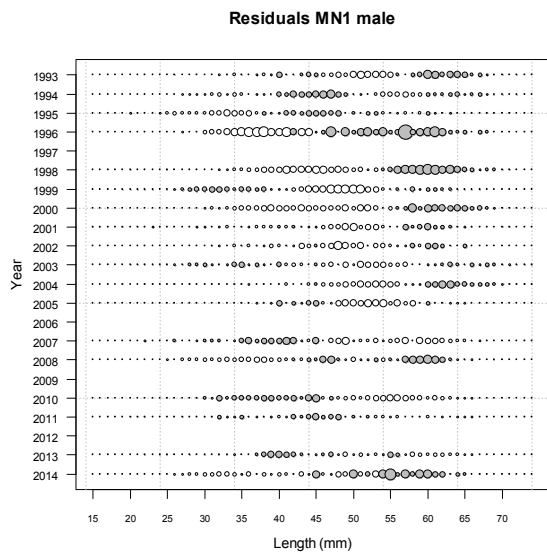
A7. 8: Observed (solid line) and fitted (dashed line) length frequency distributions for observer samples, MN time step 1 for SCI 3 NP_0.25.



A7.8 ctd.: Observed (solid line) and fitted (dashed line) length frequency distributions for observer samples, MN time step 1 for SCI 3 NP_0.25.



A7. 9: Observed (solid line) and fitted (dashed line) length frequency distributions for observer samples, MN time step 2 for SCI 3 NP_0.25.



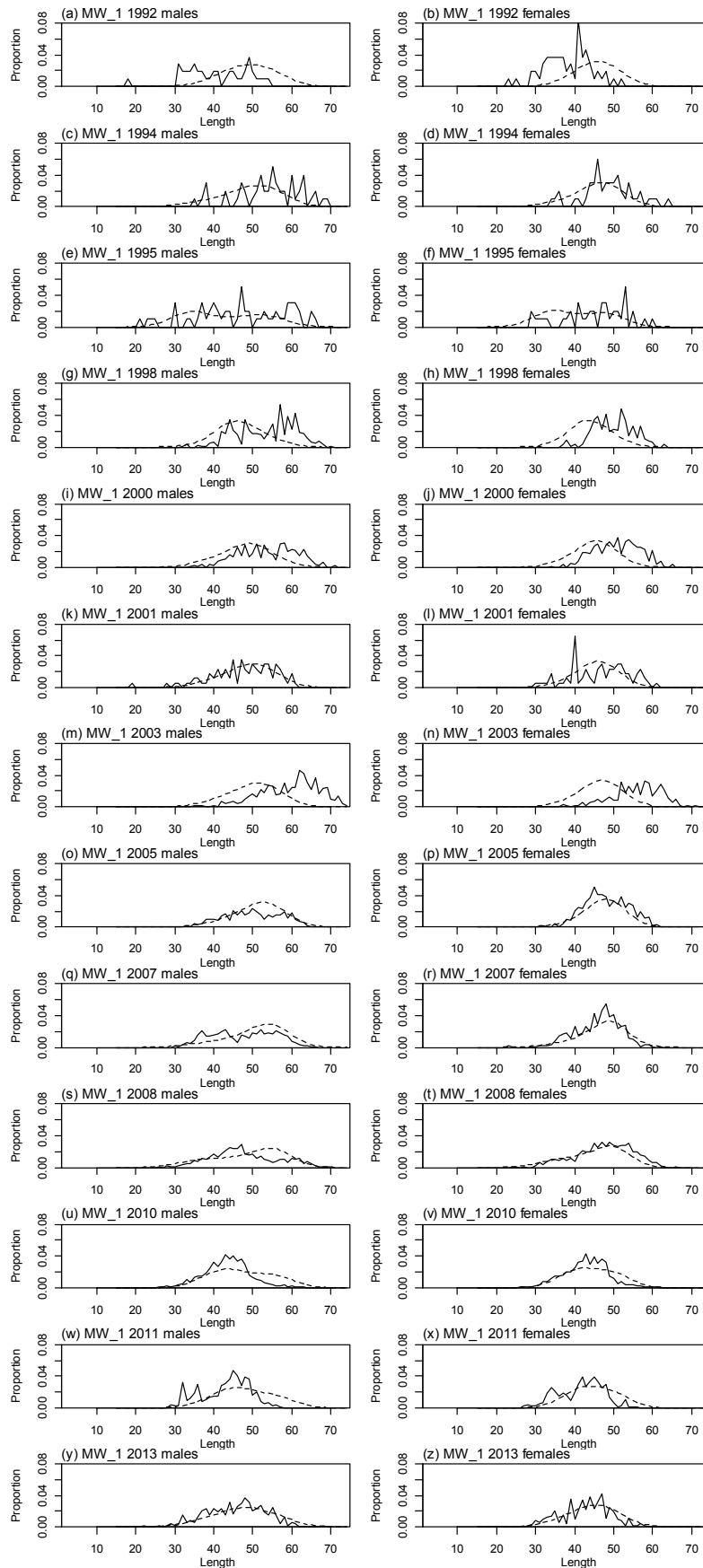
A7. 10: Bubble plots of residuals of fits to length frequency distributions for observer sampling from MN, time step 1 and 2, for SCI 3 NP_0.25.

A7. 11: Numbers of scampi measured, estimated multinomial N sample size, and effective sample size used within the SCI 3 NP_0.25 model for length frequency distributions for observer samples, MN time step 1.

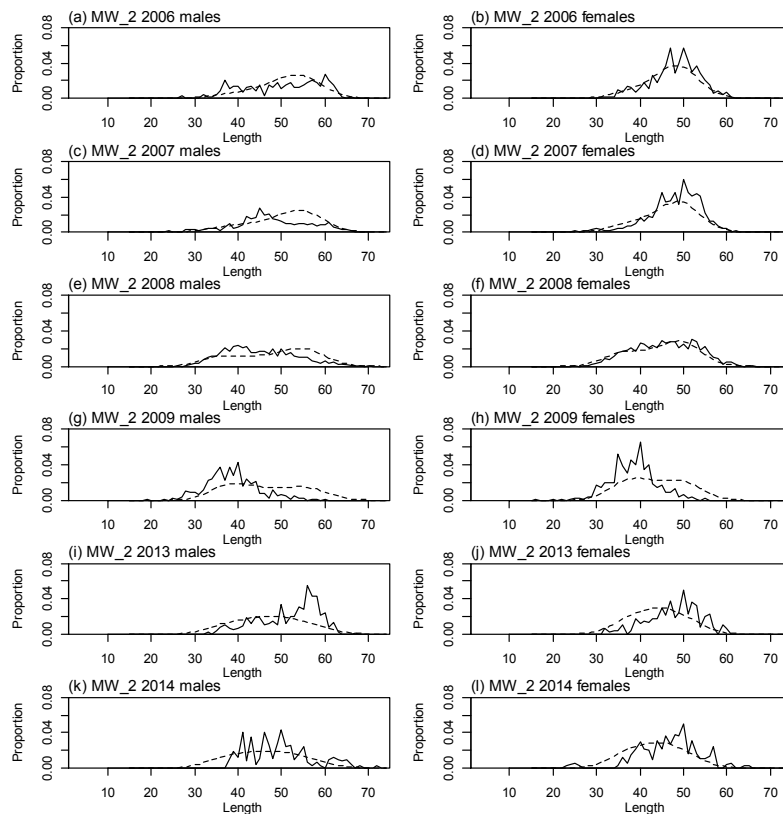
	Measured	Multinomial N	Effective sample size
N_1993	1 089	1 520	4.10
N_1994	2 090	3 036	8.19
N_1995	1 498	2 300	6.21
N_1996	465	500	1.35
N_1998	1 843	3 085	8.32
N_1999	1 921	4 221	11.39
N_2000	1 727	2 200	5.94
N_2001	1 528	2 908	7.85
N_2002	510	908	2.45
N_2003	2 824	5 674	15.31
N_2004	3 856	6 921	18.67
N_2005	1 448	2 497	6.74
N_2007	829	1 189	3.21
N_2008	1 087	1 587	4.28
N_2010	948	1 632	4.40
N_2011	3 273	6 881	18.56
N_2013	2 613	3 847	10.38
N_2014	403	789	2.13

A7. 12: Numbers of scampi measured, estimated multinomial N sample size, and effective sample size used within the SCI 3 NP_0.25 model for length frequency distributions for observer samples, MN time step 2.

	Measured	Multinomial N	Effective sample size
N_1993	1 639	3 306	13.92
N_1994	2 923	5 285	22.24
N_1995	1 260	1 800	7.58
N_2006	1 086	1 635	6.88
N_2008	535	699	2.94
N_2009	186	245	1.03
N_2011	1 019	1 900	8.00
N_2012	333	588	2.47
N_2013	352	234	0.98
N_2014	1 443	1 378	5.80



A7. 13: Observed (solid line) and fitted (dashed line) length frequency distributions for observer samples, MW time step 1 for SCI 3 NP_0.25.



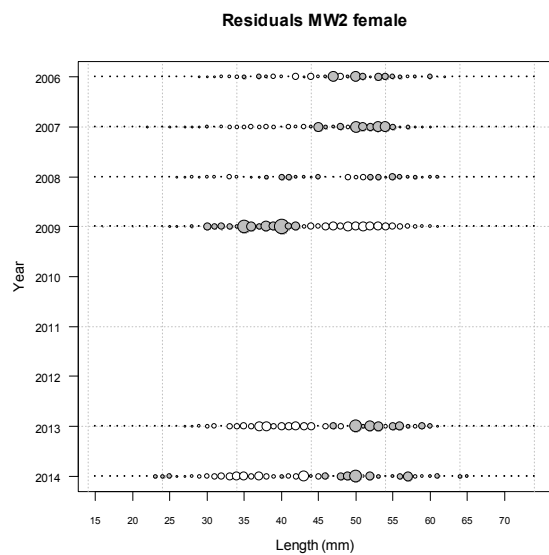
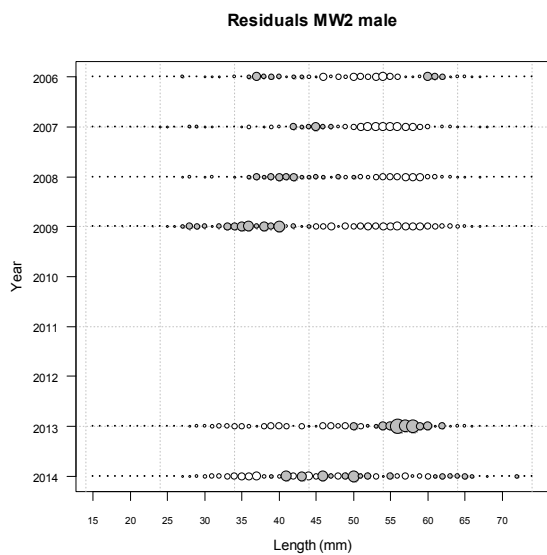
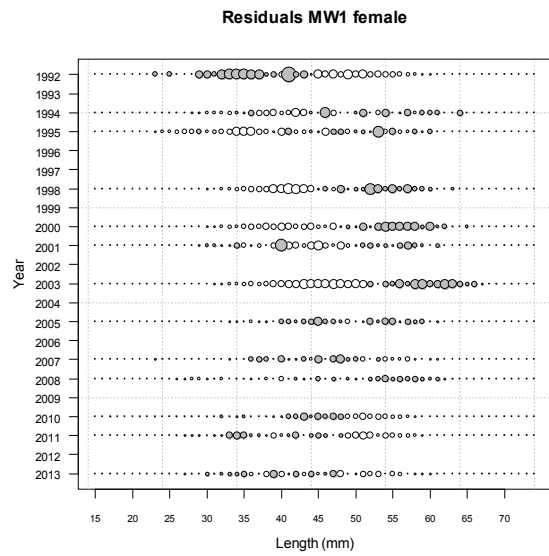
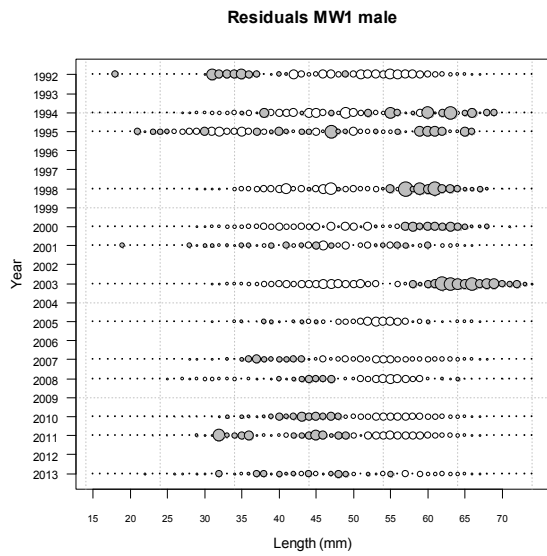
A7.14: Observed (solid line) and fitted (dashed line) length frequency distributions for observer samples, MW time step 2 for SCI 3 NP_0.25.

A7.15: Numbers of scampi measured, estimated multinomial N sample size, and effective sample size used within the SCI 3 NP_0.25 model for length frequency distributions for observer samples, MW time step 1.

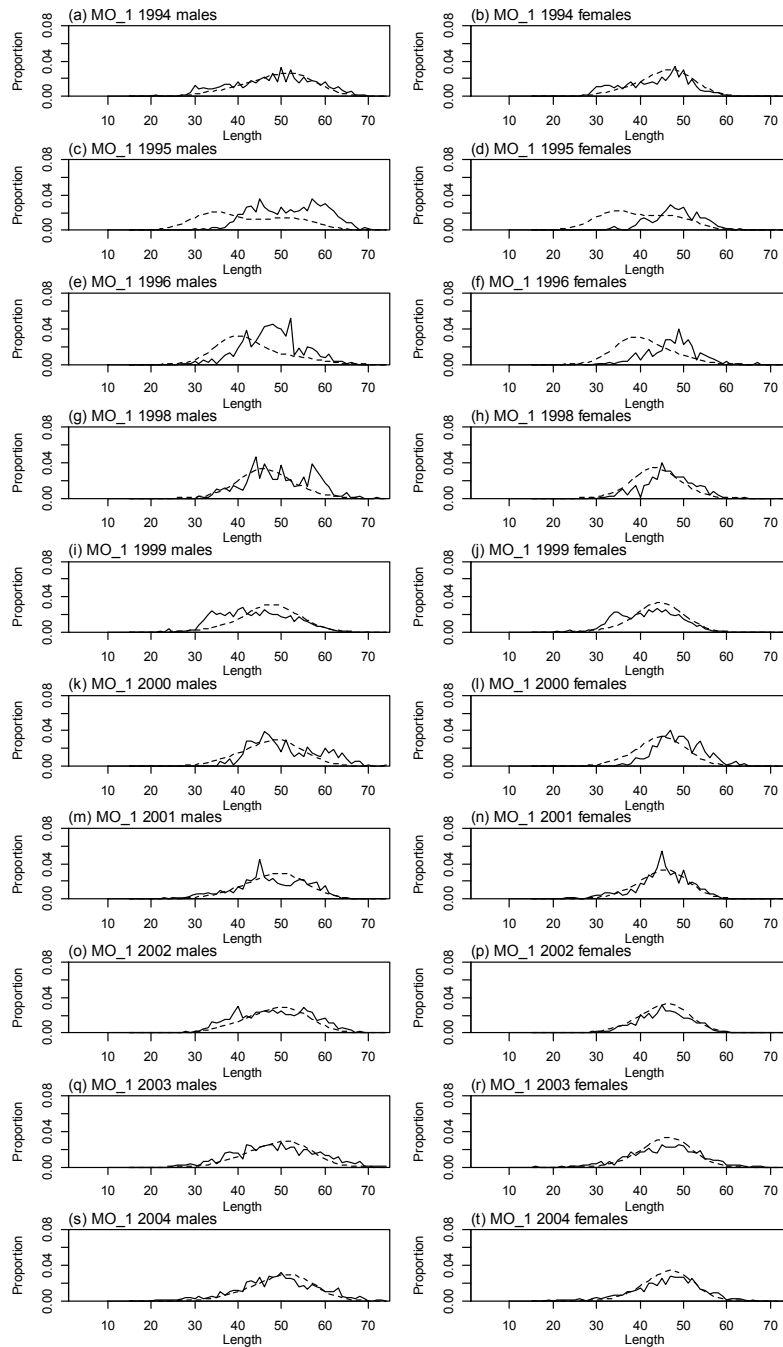
	Measured	Multinomial N	Effective sample size
N_1992	229	107	0.29
N_1994	242	100	0.27
N_1995	241	100	0.27
N_1998	365	365	1.00
N_2000	521	600	1.65
N_2001	251	169	0.46
N_2003	578	799	2.19
N_2005	593	870	2.39
N_2007	1 082	1 669	4.58
N_2008	1 201	1 865	5.12
N_2010	3 163	6 951	19.09
N_2011	712	2 345	6.44
N_2013	495	616	1.69

A7.16: Numbers of scampi measured, estimated multinomial N sample size, and effective sample size used within the SCI 3 NP_0.25 model for length frequency distributions for observer samples, MW time step 2.

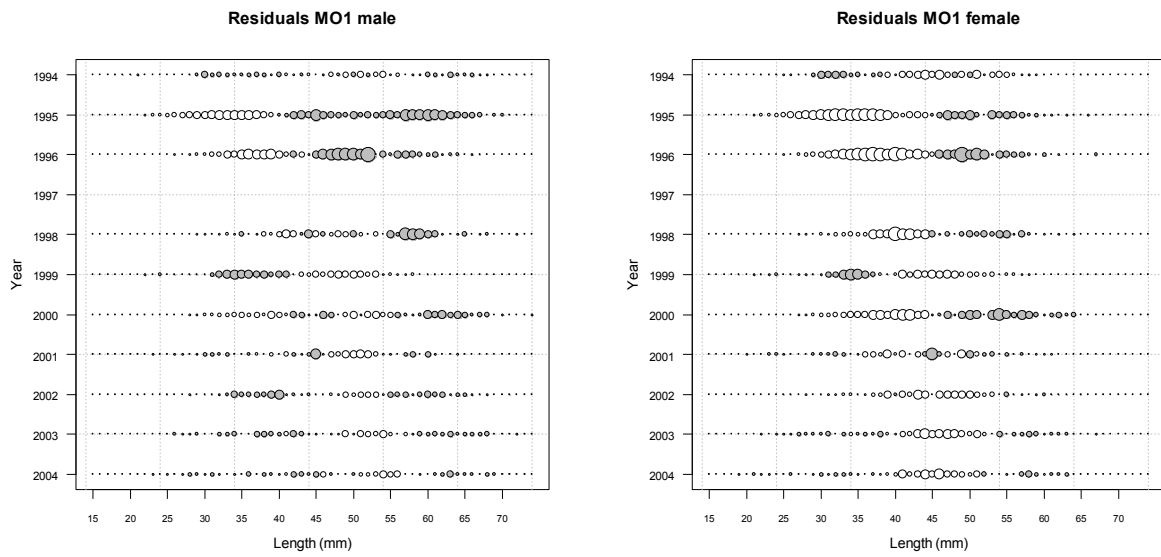
	Measured	Multinomial N	Effective sample size
N_2006	659	699	3.55
N_2007	1 333	2 406	12.21
N_2008	2 278	4 100	20.80
N_2009	693	1 340	6.80
N_2013	550	483	2.45
N_2014	460	317	1.61



A7. 17: Bubble plots of residuals of fits to length frequency distributions for observer sampling from MW, time step 1 and 2, for SCI 3 NP_0.25.



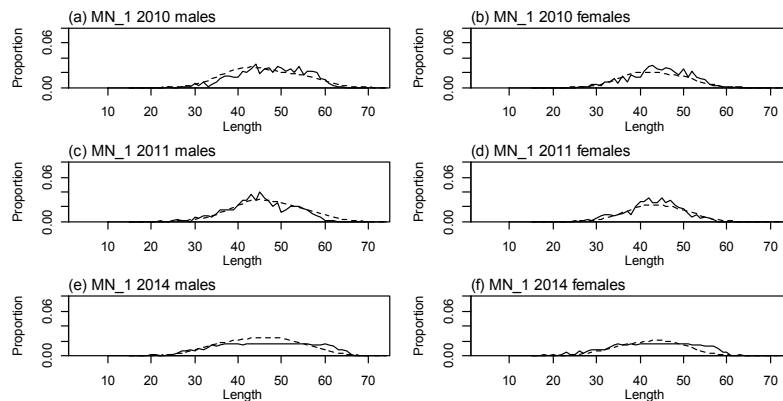
A7. 18: Observed (solid line) and fitted (dashed line) length frequency distributions for observer samples, MO time step 1 for SCI 3 NP_0.25.



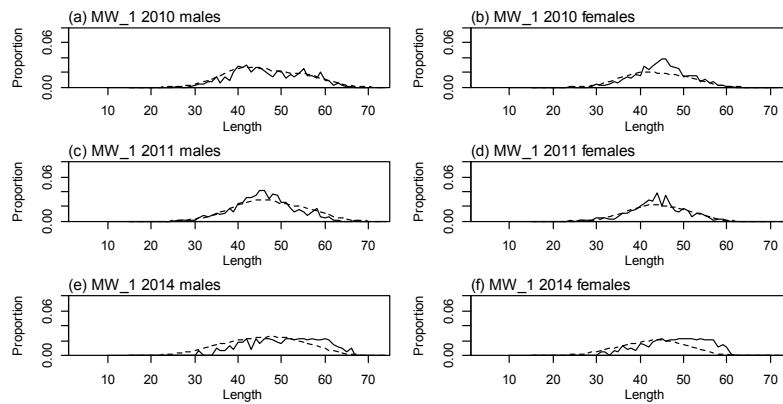
A7. 19: Bubble plots of residuals of fits to length frequency distributions for observer sampling from MO, time step 1, for SCI 3 NP_0.25.

A7. 20: Numbers of scampi measured, estimated multinomial N sample size, and effective sample size used within the SCI 3 NP_0.25 model for length frequency distributions for observer samples, MO time step 1.

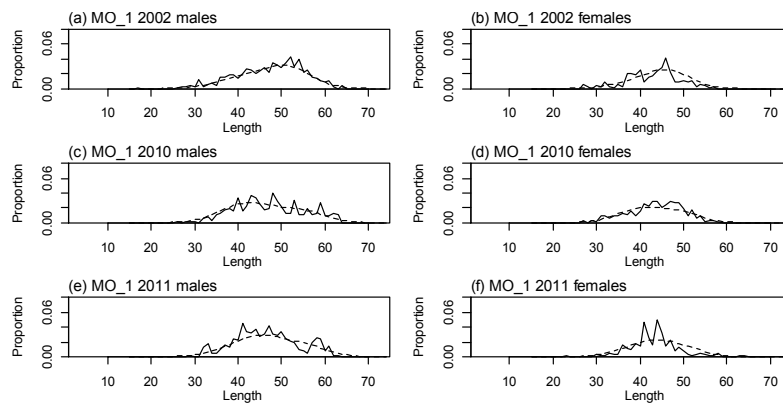
	Measured	Multinomial N	Effective sample size
N_1994	2 665	4 814	11.72
N_1995	2 474	2 500	6.09
N_1996	752	1 200	2.92
N_1998	870	900	2.19
N_1999	1 492	2 996	7.29
N_2000	608	600	1.46
N_2001	1 749	3 118	7.59
N_2002	1 768	3 442	6.42
N_2003	1 367	2 224	5.41
N_2004	1 557	2 881	7.01



A7. 21: Observed (solid line) and fitted (dashed line) length frequency distributions for MN trawl survey samples within the SCI 3 NP_{0.25} model.



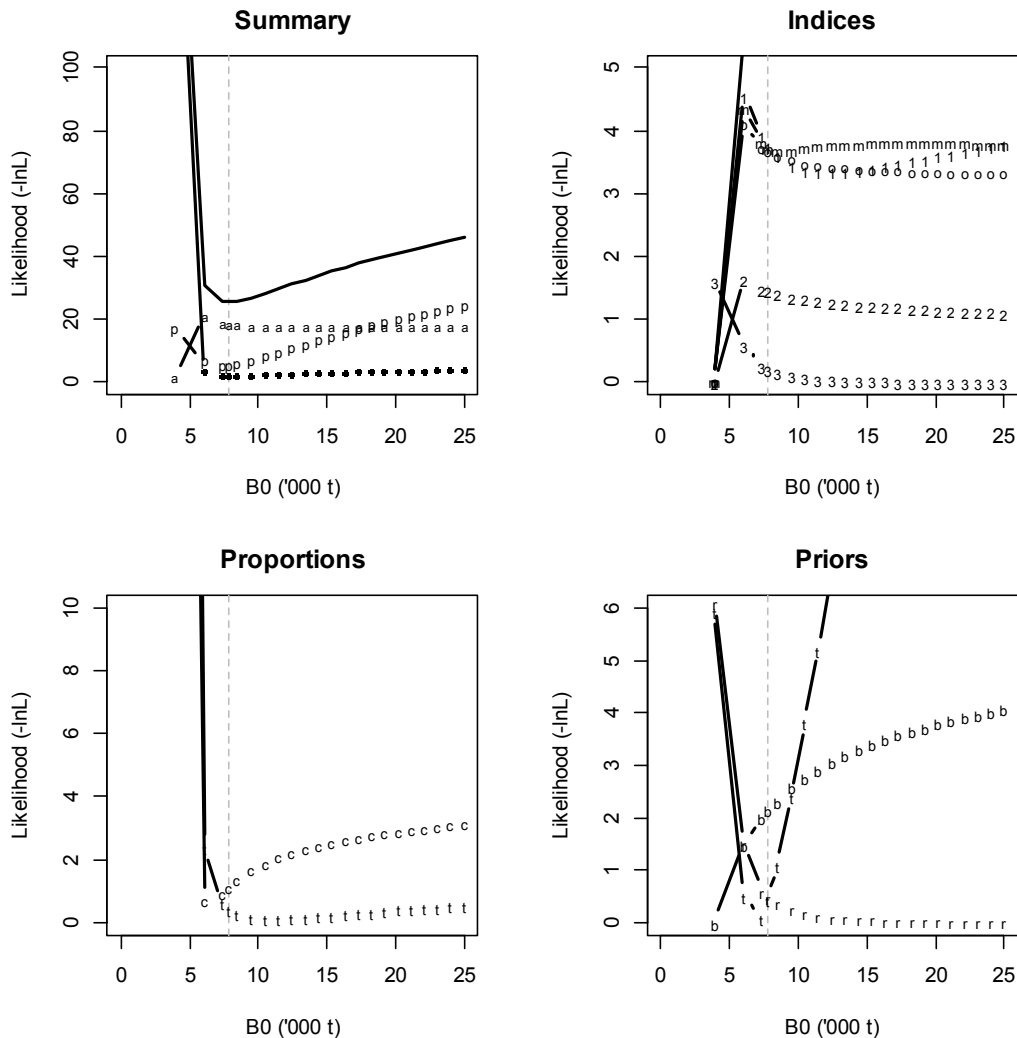
A7. 22: Observed (solid line) and fitted (dashed line) length frequency distributions for MW trawl survey samples within the SCI 3 NP_{0.25} model.



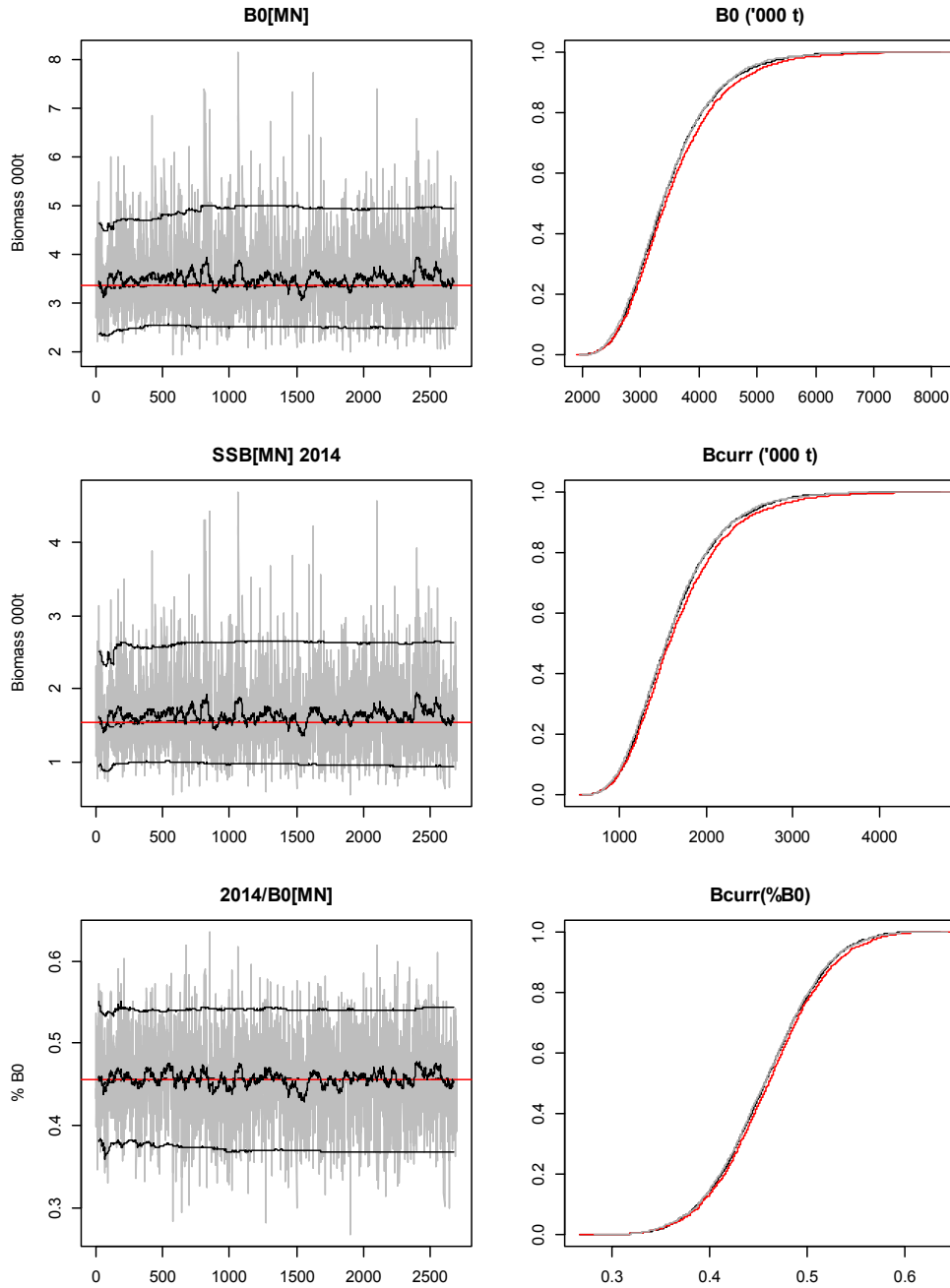
A7. 23: Observed (solid line) and fitted (dashed line) length frequency distributions for MO trawl survey samples within the SCI 3 NP_{0.25} model.

A7. 24: Numbers of scampi burrows measured, estimated multinomial N sample size, and effective sample size used within the model for length frequency distributions for photographic survey samples within the SCI 3 NP_0.25 model.

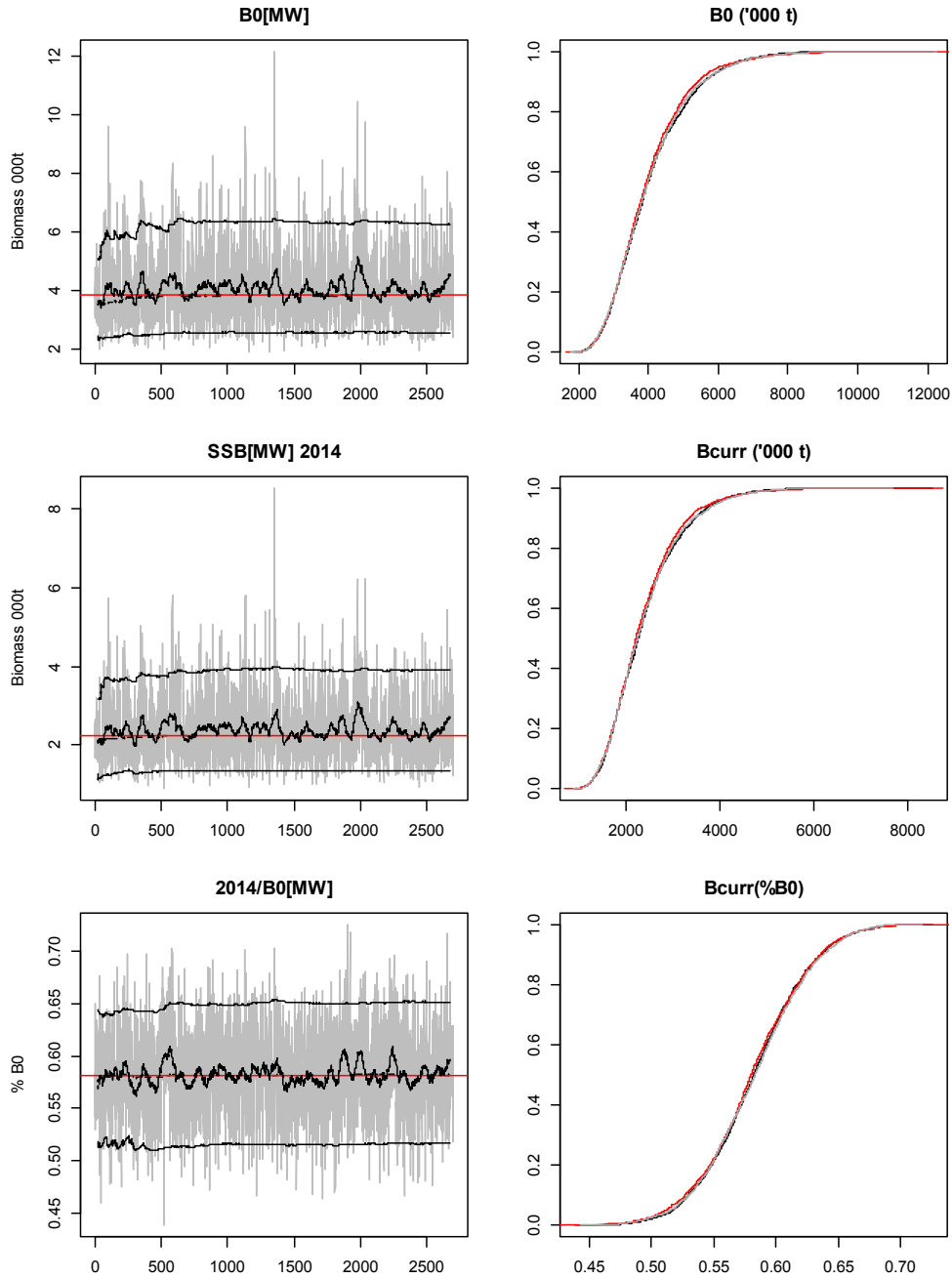
MN	Measured	Multinomial N	Effective sample size
N_2010	2 595	1 276	21.56
N_2011	4 429	2 362	36.79
N_2014	1 077	602	8.95
MW	Measured	Multinomial N	Effective sample size
N_2010	2 254	1 110	35.71
N_2011	2 636	1 295	41.76
N_2014	385	208	6.10
MO	Measured	Multinomial N	Effective sample size
N_2002	1 367	1 418	221.29
N_2010	1 123	551	181.79
N_2011	1 163	611	188.27
N_2014	523	339	84.66



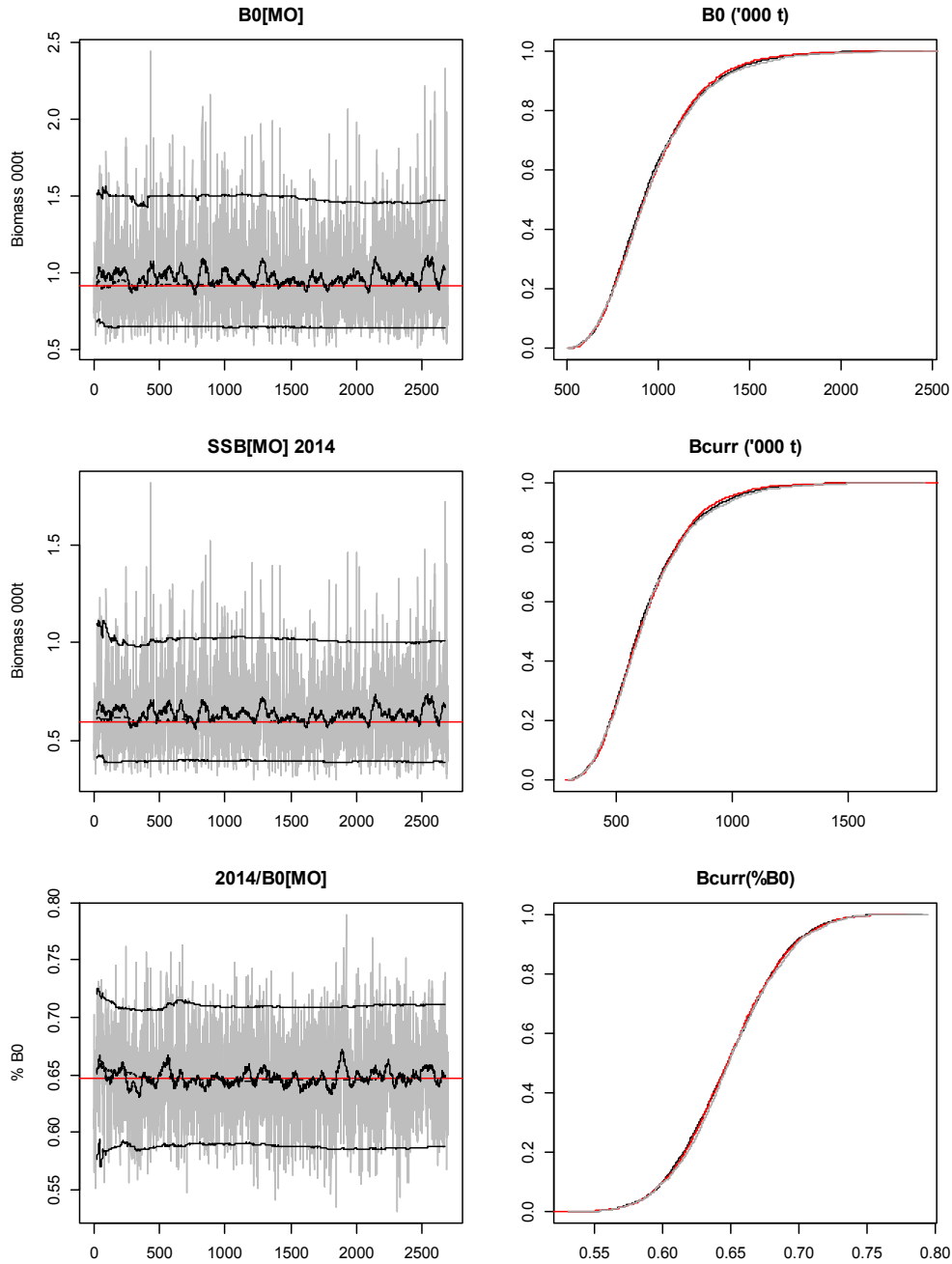
A7. 25: Likelihood profiles for the SCI 3 NP_0.25 model for SCI 3 when B_0 is fixed in the model. Figures show profiles for main priors (top left, p – priors, a – abundance indices, • – proportions at length, r – recapture data), abundance indices (top right, t - trawl survey, c - CPUE, p – photo survey), proportion at length data (bottom left, a-trawl, 1 – observer time step 1, 2 – observer time step 2, 3 – observer time step 3, p - photo) and priors (bottom right, b- B_0 , YCS - r, t – *q-Trawl*). Vertical dashed line represents MPD.



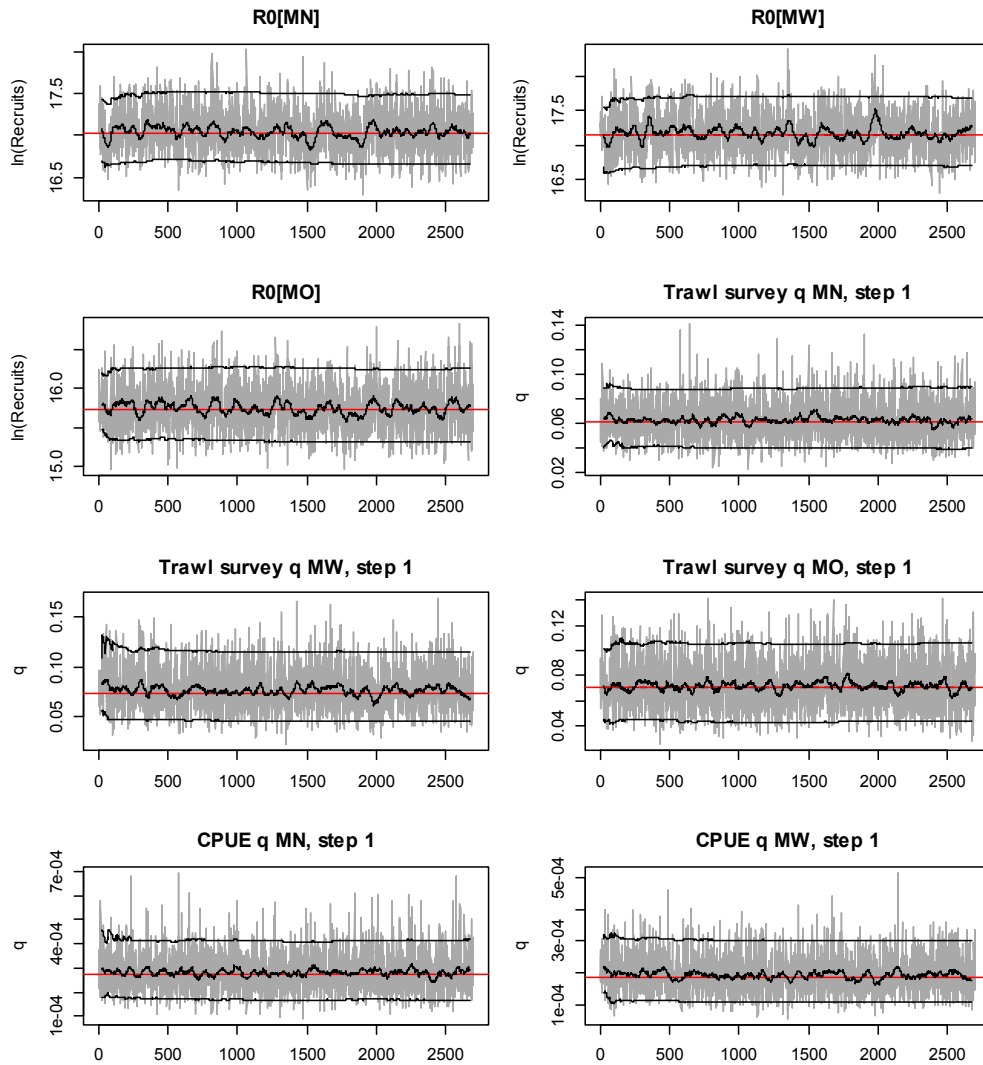
A7. 26: MCMC traces for B_0 , SSB₂₀₁₄, and SSB₂₀₁₄/ B_0 terms for the MN subarea within the SCI 3 NP_0.25 model for SCI 3 (trace – grey line, cumulative moving median – dashed black line, moving average and cumulative moving 2.5%, 97.5% quantiles – solid black lines, overall median – solid red line, left plots), along with cumulative frequency distributions for three independent MCMC chains (shown as red, grey and black lines, right plots).



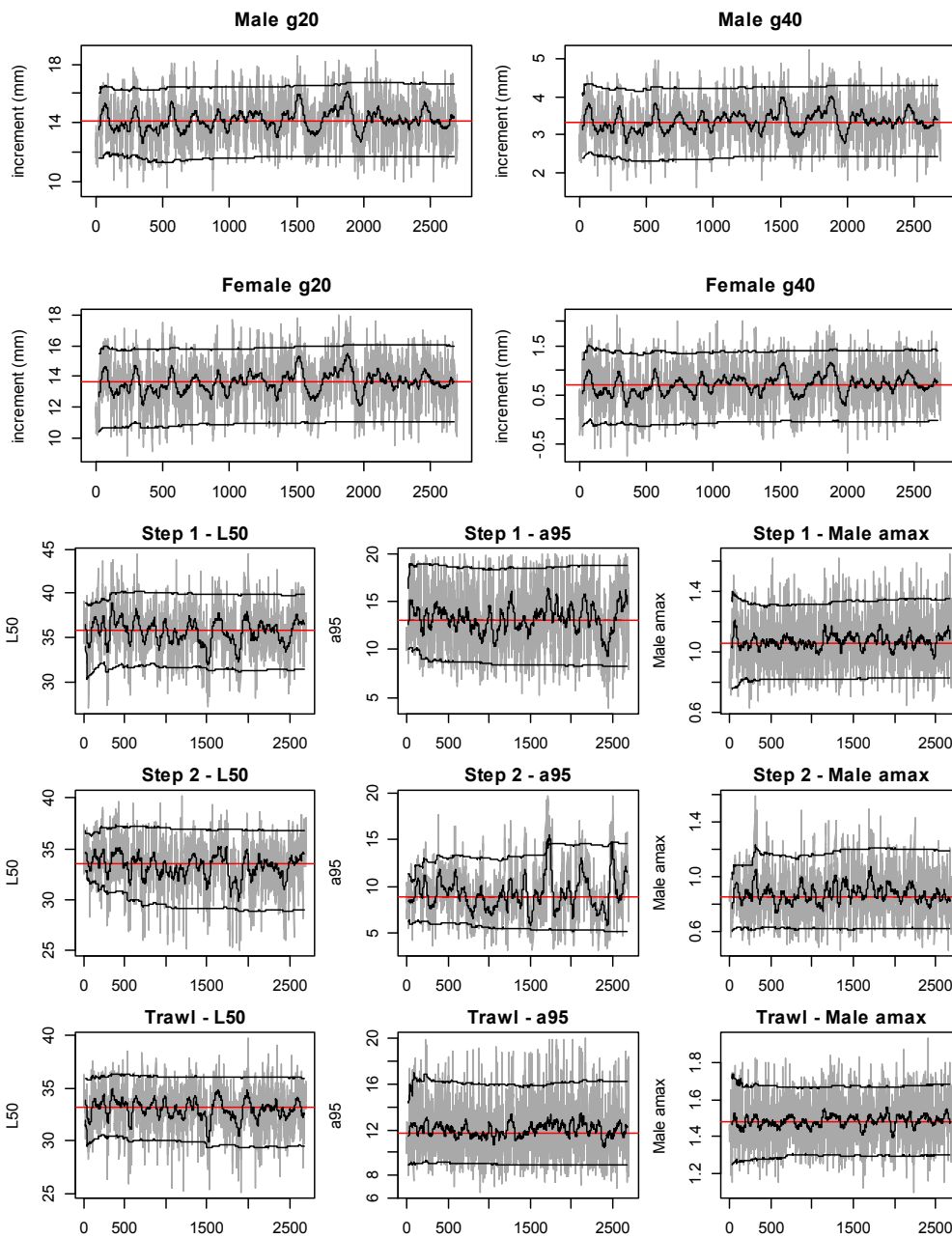
A7. 27: MCMC traces for B_0 , SSB_{2014} , and SSB_{2014}/B_0 terms for the MW subarea within the SCI 3 NP_0.25 model for SCI 3 (trace – grey line, cumulative moving median – dashed black line, moving average and cumulative moving 2.5%, 97.5% quantiles – solid black lines, overall median – solid red line, left plots), along with cumulative frequency distributions for three independent MCMC chains (shown as red, grey and black lines, right plots).



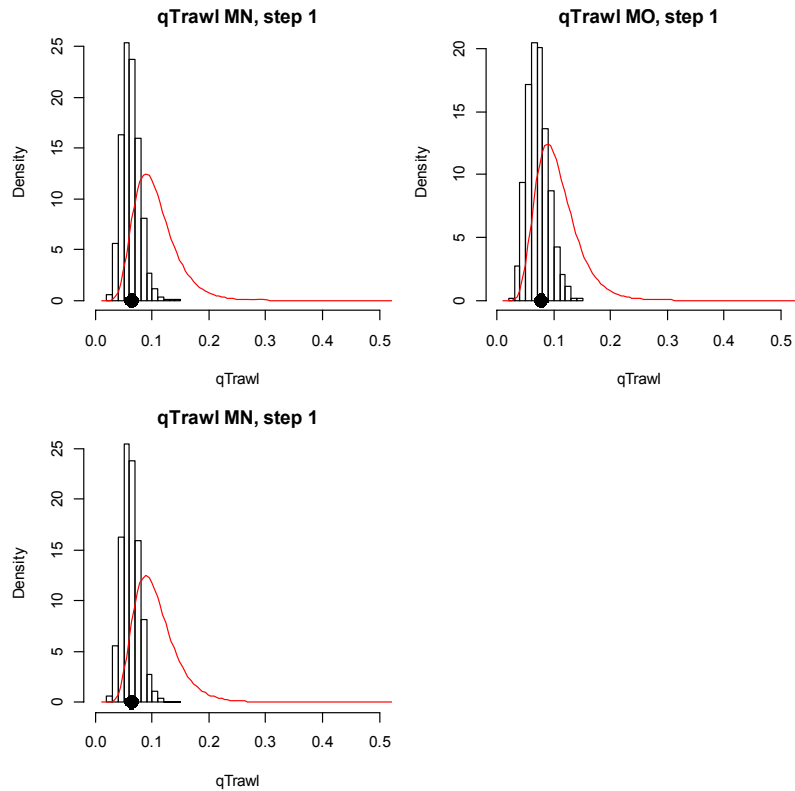
A7. 28: MCMC traces for B_0 , SSB_{2014} , and SSB_{2014}/SSB_0 terms for the MN subarea within the SCI 3 NP_0.25 model for SCI 3 (trace – grey line, cumulative moving median – dashed black line, moving average and cumulative moving 2.5%, 97.5% quantiles – solid black lines, overall median – solid red line, left plots), along with cumulative frequency distributions for three independent MCMC chains (shown as red, grey and black lines, right plots).



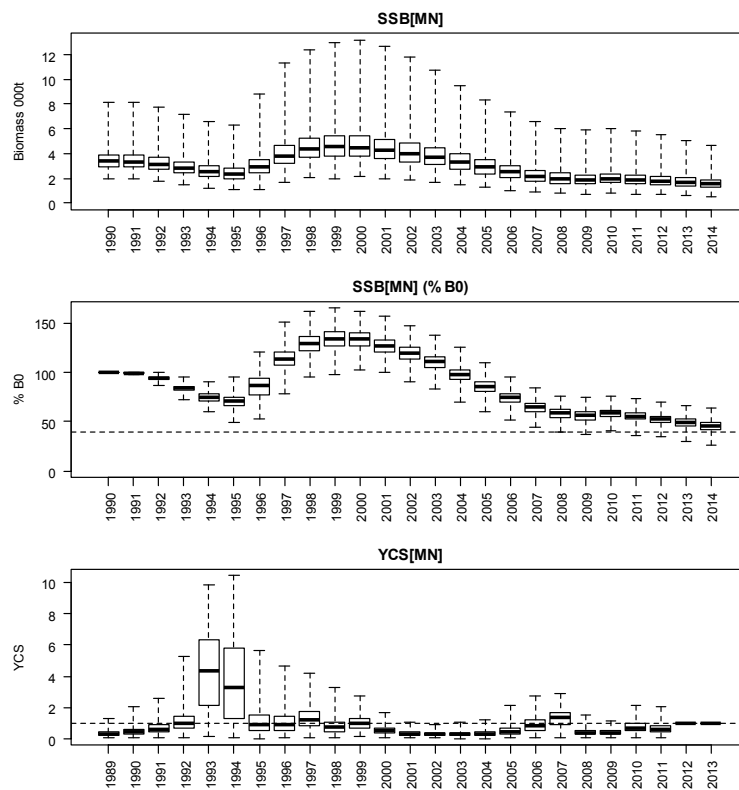
A7. 29: MCMC traces for R_0 , trawl survey q s, and commercial fishery q terms within the SCI 3 NP_0.25 model for SCI 3 (trace – grey line, cumulative moving median – dashed black line, moving average and cumulative moving 2.5%, 97.5% quantiles – solid black lines, overall median – solid red line, left plots), along with cumulative frequency distributions for three independent MCMC chains (shown as red, grey and black lines, right plots).



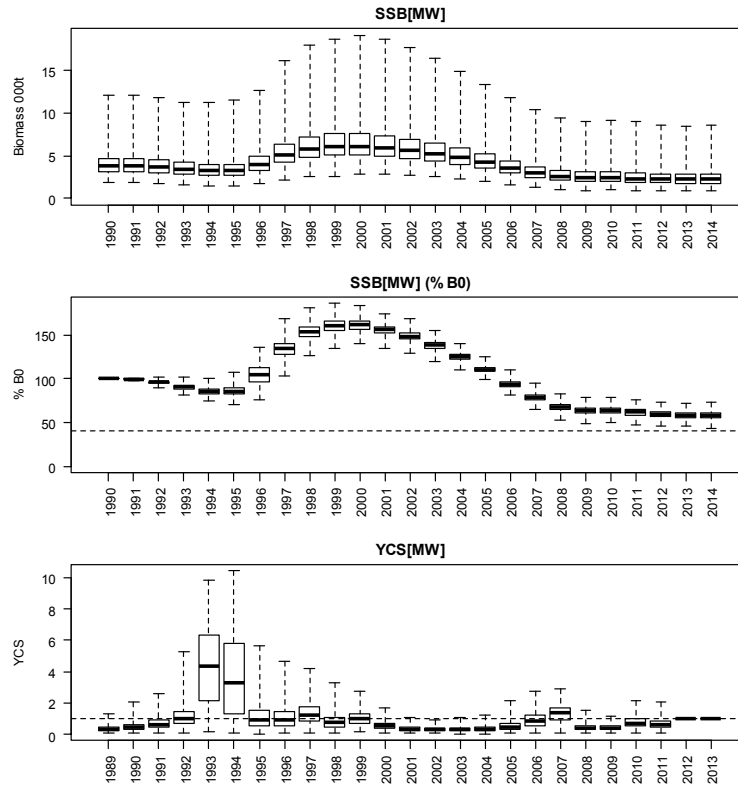
A7. 30: MCMC traces for growth increment and selectivity parameters within the SCI 3 NP_0.25 model for SCI 3 (trace – grey line, cumulative moving median – dashed black line, moving average and cumulative moving 2.5%, 97.5% quantiles – solid black lines, overall median – solid red line, left plots), along with cumulative frequency distributions for three independent MCMC chains (shown as red, grey and black lines, right plots).



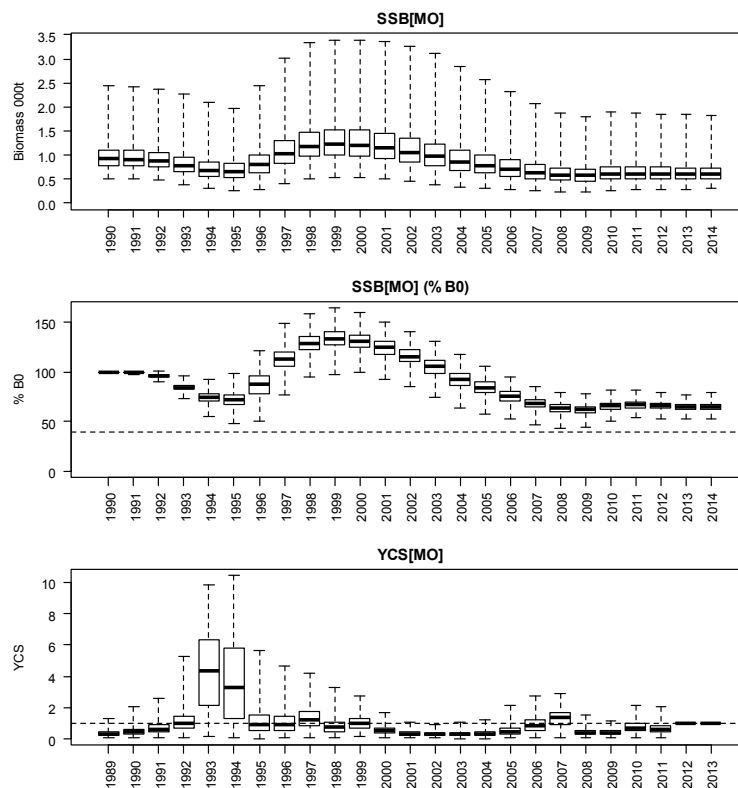
A7. 31: Marginal posterior distribution (histogram), MPD estimate (solid symbols) and distribution of prior (line) for photo survey catchability term within the SCI 3 NP_0.25 model.



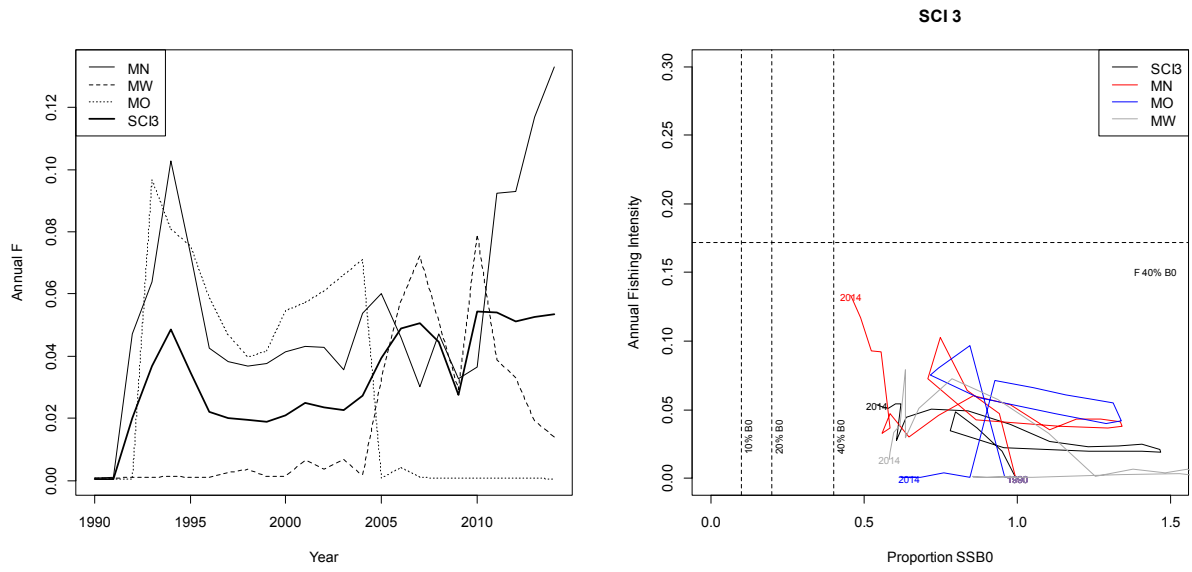
A7. 32: Posterior trajectory of SSB, SSB₂₀₁₄/SSB₀ and YCS for the MN subarea within the SCI 3 NP_0.25 model.



A7. 33: Posterior trajectory of SSB, SSB_{2014}/SSB_0 and YCS for the MW subarea within the SCI 3 NP_0.25 model.

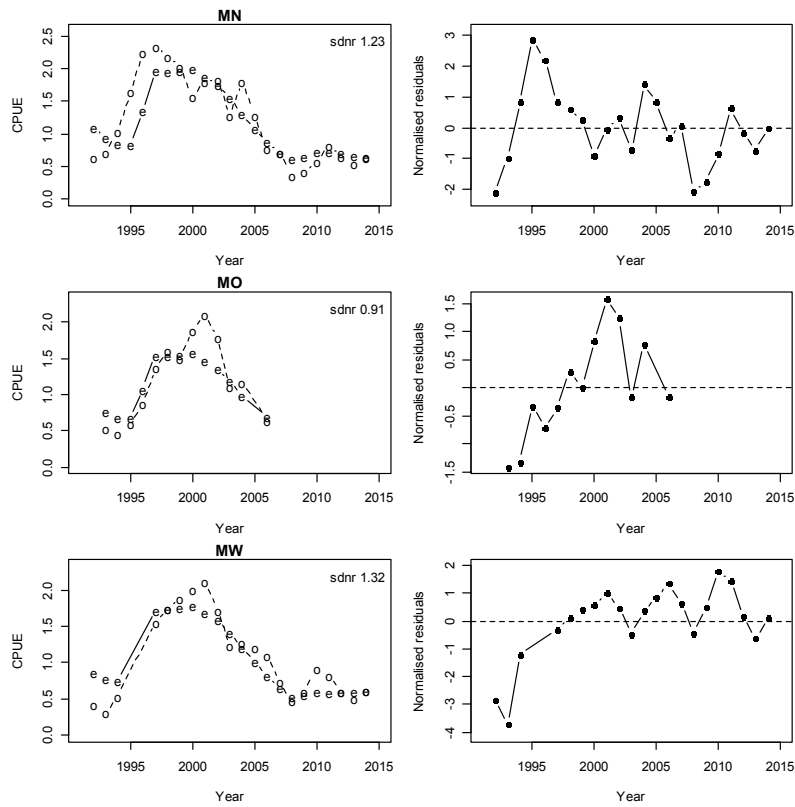


A7. 34: Posterior trajectory of SSB, SSB_{2014}/SSB_0 and YCS for the MO subarea within the SCI 3 NP_0.25 model.

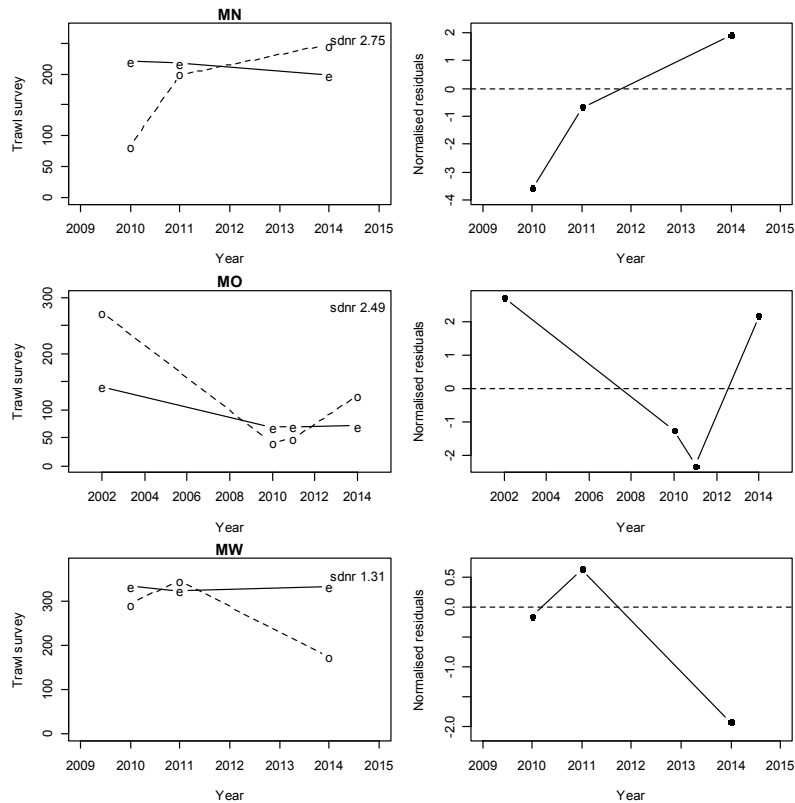


A7. 35: Estimated annual equivalent F (left) and phase plot (right) from the SCI 3 NP_0.25 model.

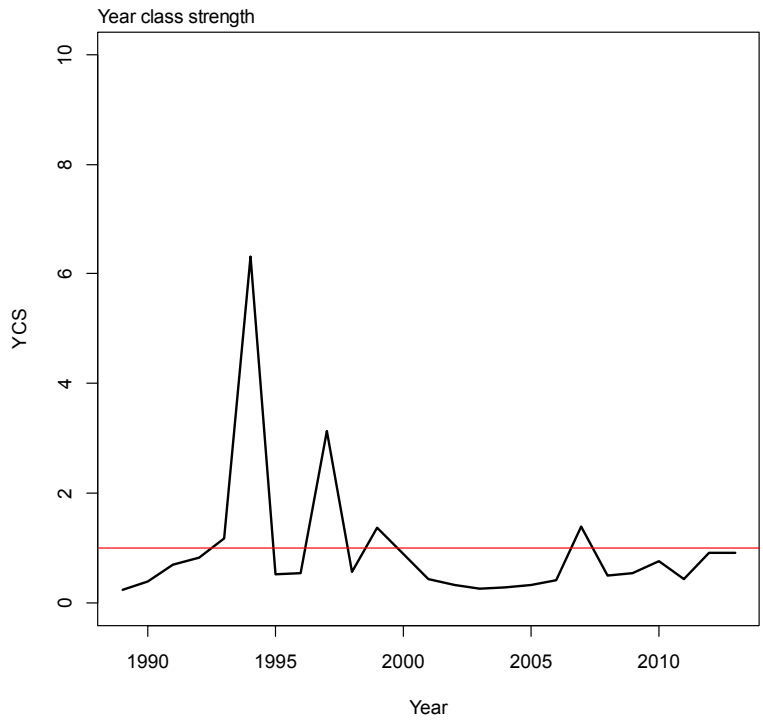
APPENDIX 8. MODEL NP_0.35



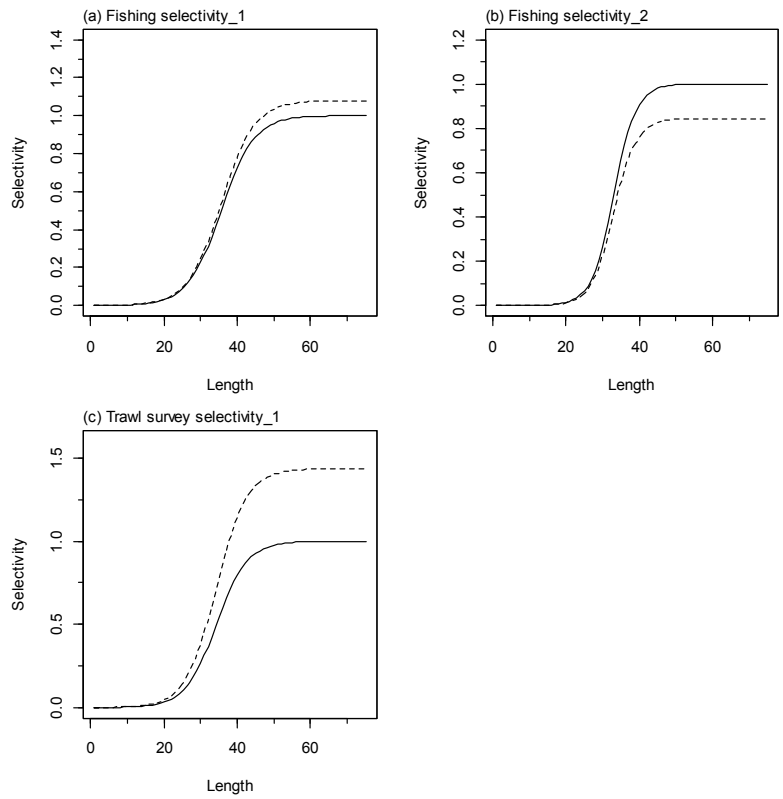
A8. 1: Fits to CPUE indices (left column) and normalised residuals (right column) for each subarea for SCI 3 NP_0.35.



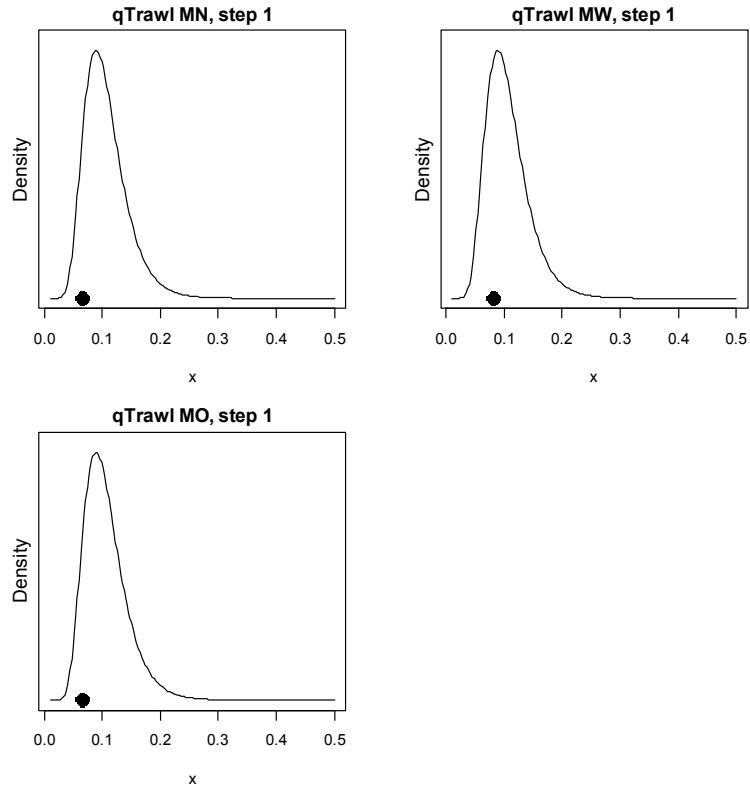
A8. 2: Fits to trawl survey indices (left column) and normalised residuals (right column) for each subarea for SCI 3 NP_0.35.



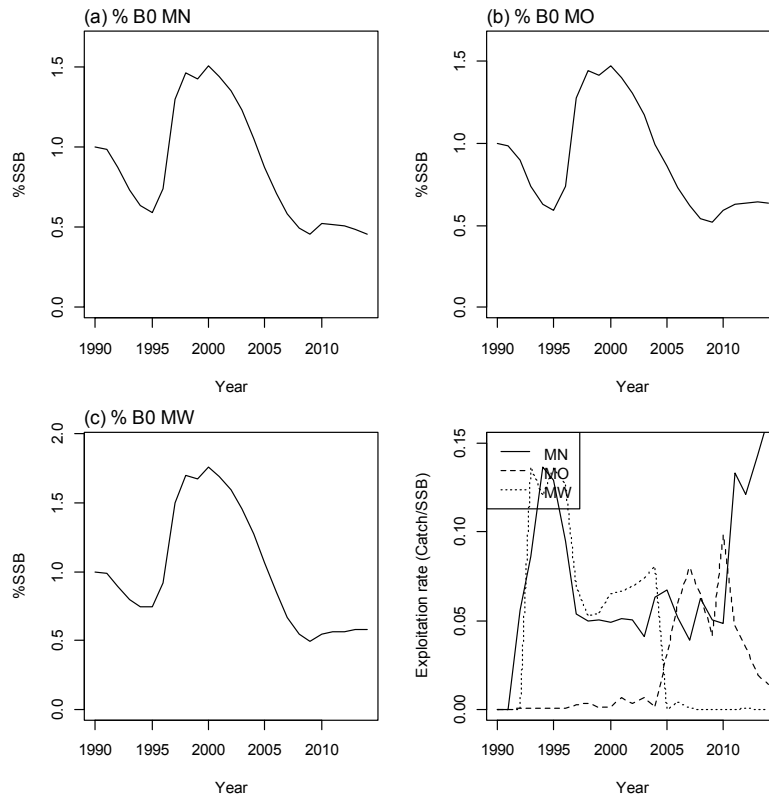
A8. 3: Year class strength for SCI 3 NP_0.35.



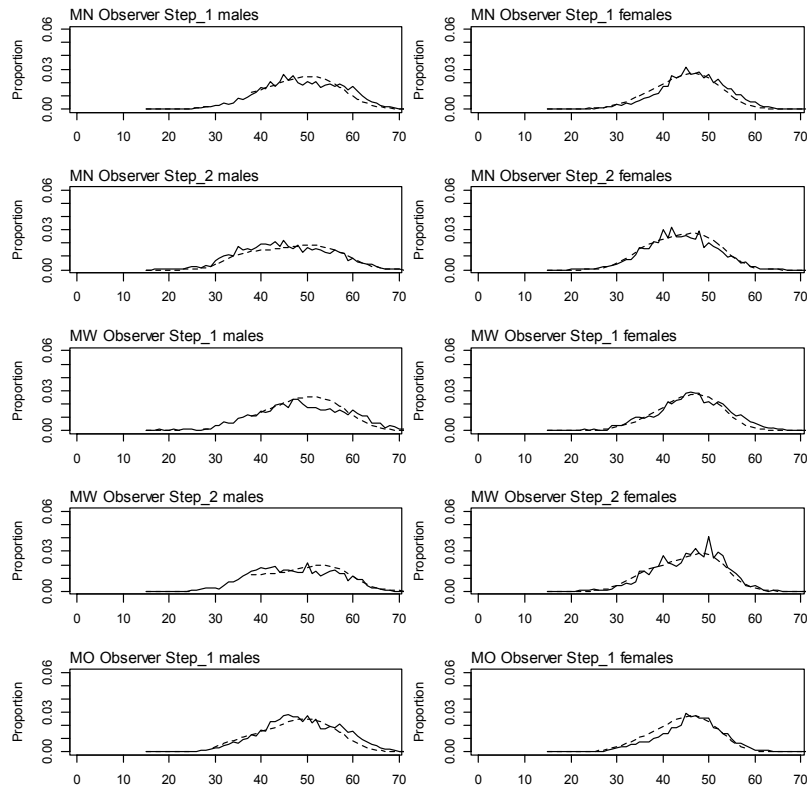
A8. 4: Fishery and survey selectivity curves for SCI 3 NP_0.35. Solid line – females, dotted line – males.



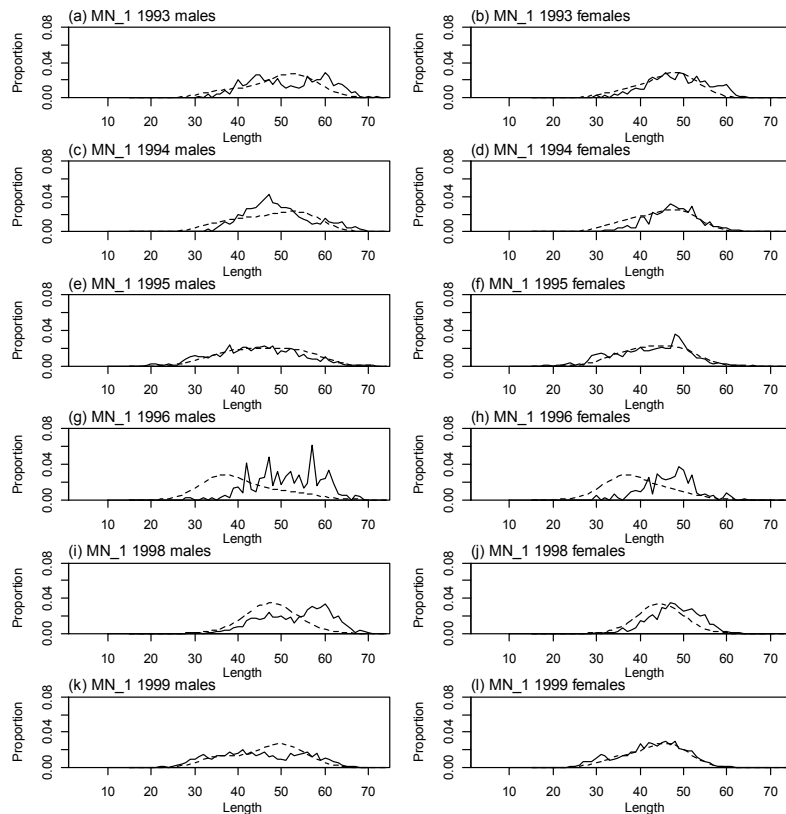
A8. 5: Catchability estimates from MPD model run, plotted in relation to prior distribution for SCI 3 NP_0.35.



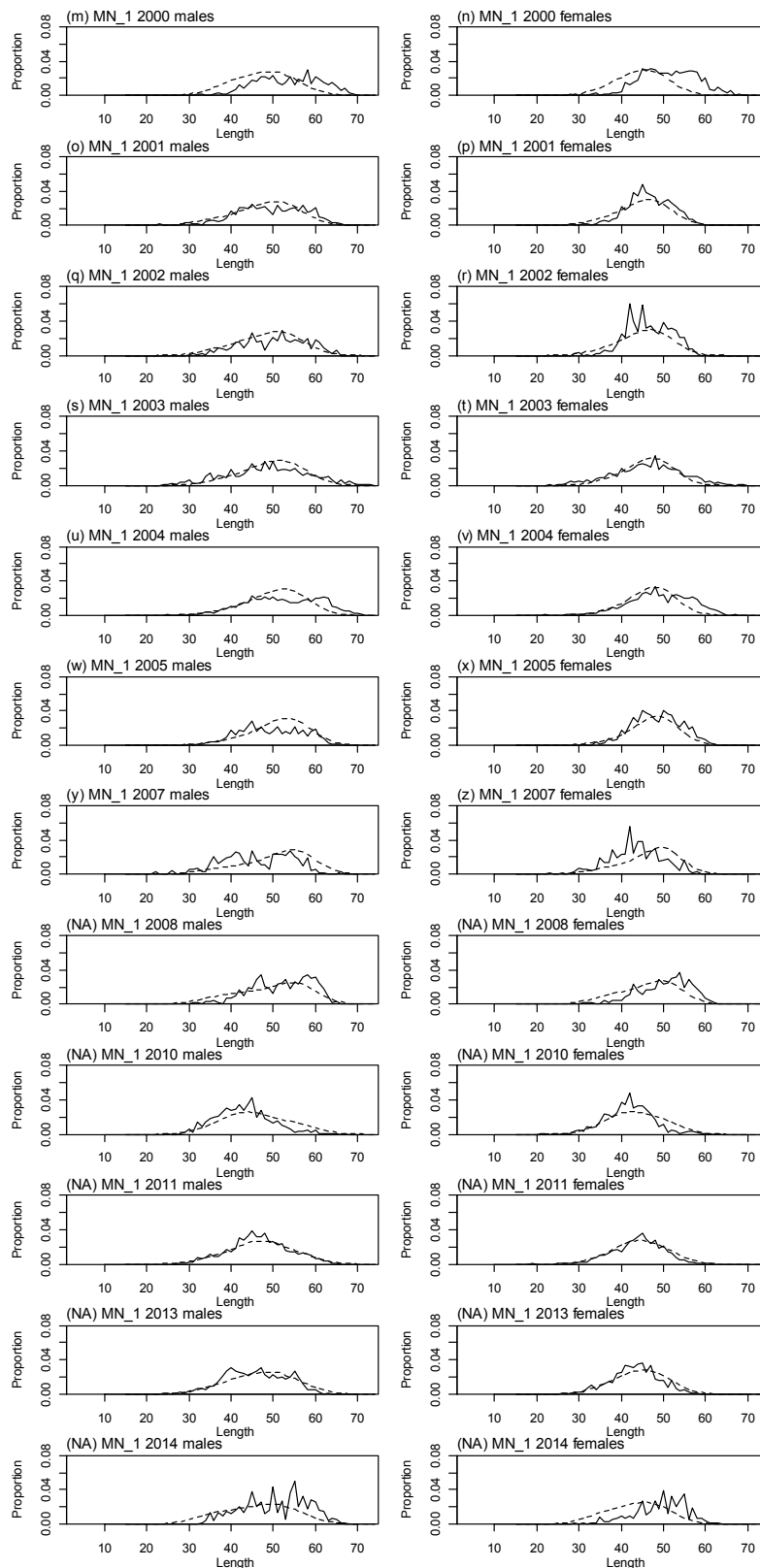
A8. 6: Stock trajectories (% SSB₀) for each subarea estimated from the MPD model run, and estimated exploitation rates for SCI 3 NP_0.35.



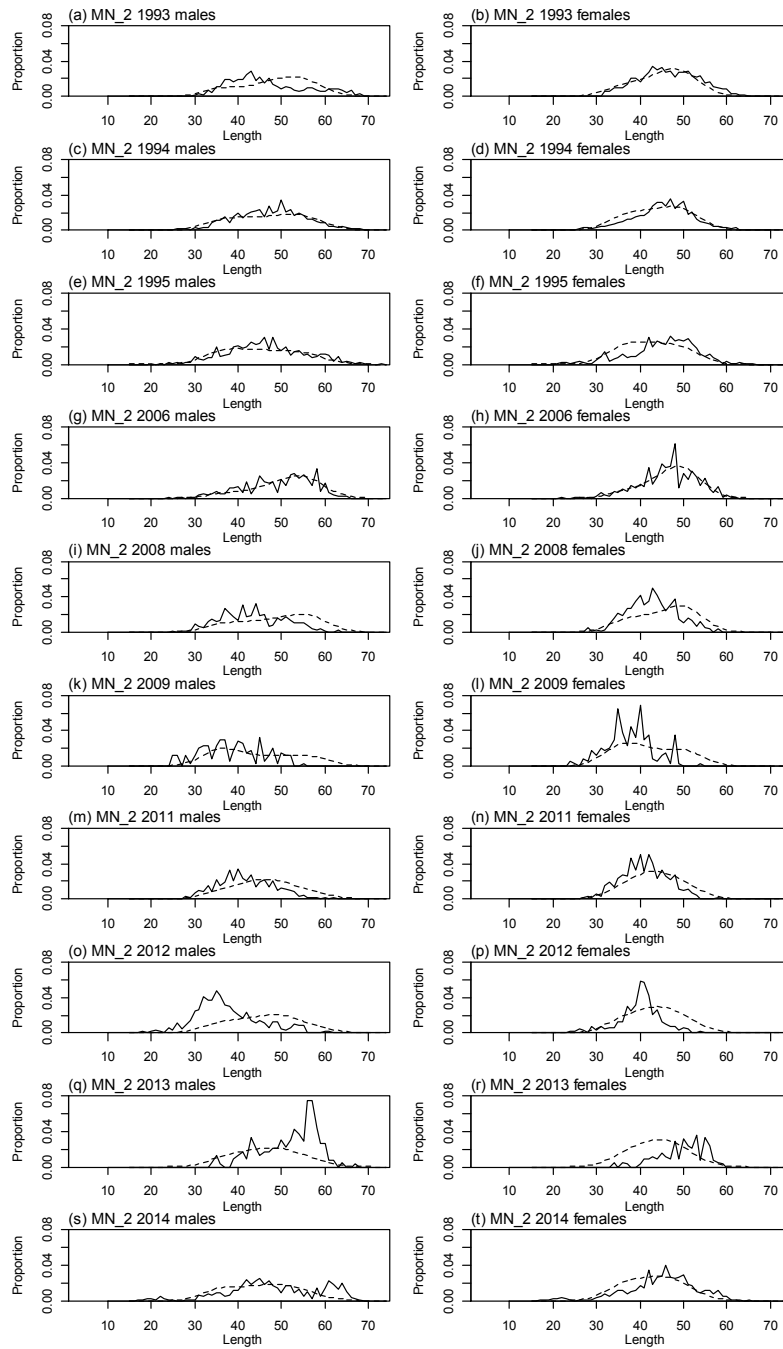
A8. 7: Average observed (solid line) and fitted (dashed line) length frequency distributions for observer samples for SCI 3 NP_0.35.



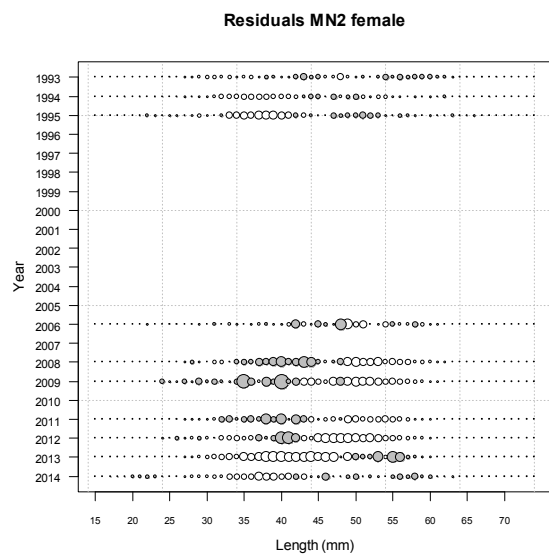
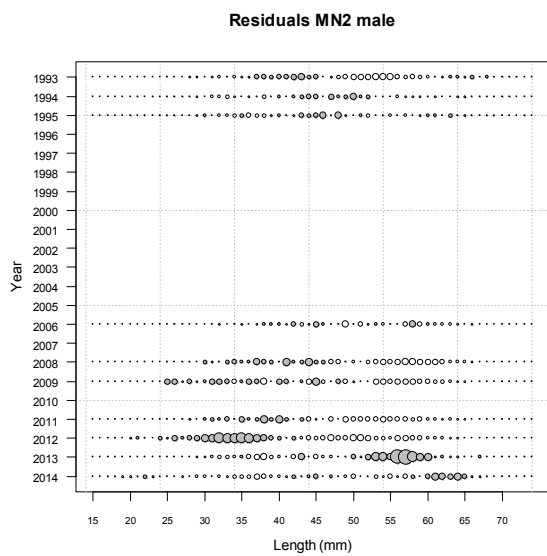
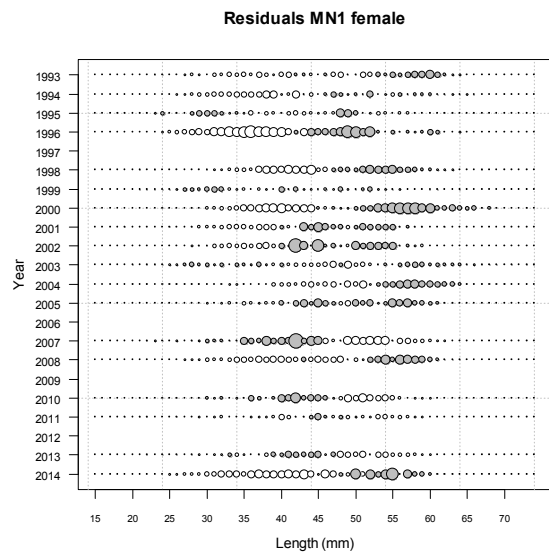
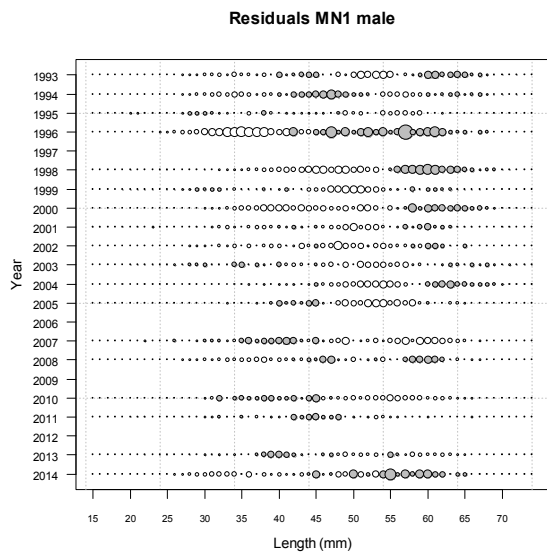
A8. 8: Observed (solid line) and fitted (dashed line) length frequency distributions for observer samples, MN time step 1 for SCI 3 NP_0.35.



A8.8 ctd.: Observed (solid line) and fitted (dashed line) length frequency distributions for observer samples, MN time step 1 for SCI 3 NP_0.35.



A8.9: Observed (solid line) and fitted (dashed line) length frequency distributions for observer samples, MN time step 2 for SCI 3 NP_0.35.



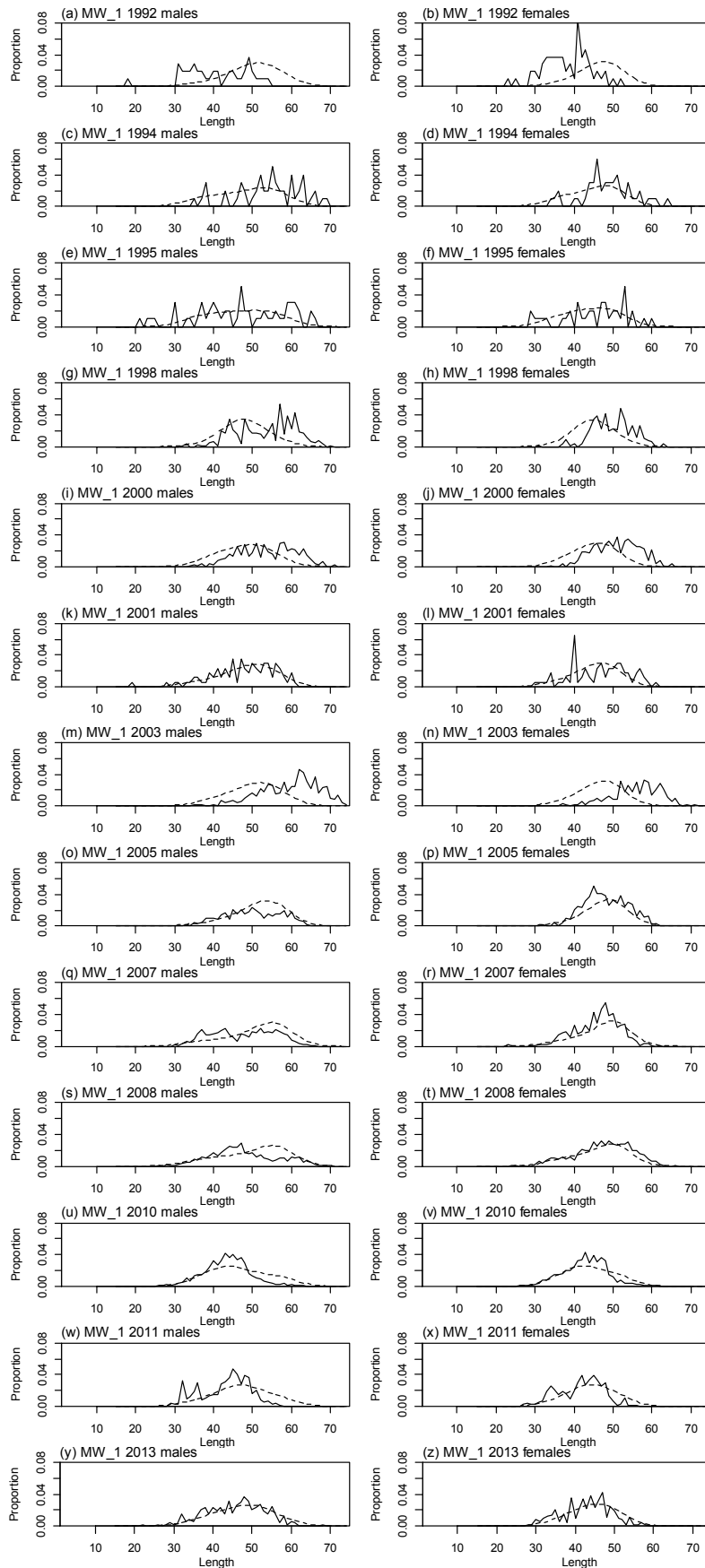
A8. 10: Bubble plots of residuals of fits to length frequency distributions for observer sampling from MN, time step 1 and 2, for SCI 3 NP_0.35.

A8. 11: Numbers of scampi measured, estimated multinomial N sample size, and effective sample size used within the SCI 3 NP_0.35 model for length frequency distributions for observer samples, MN time step 1.

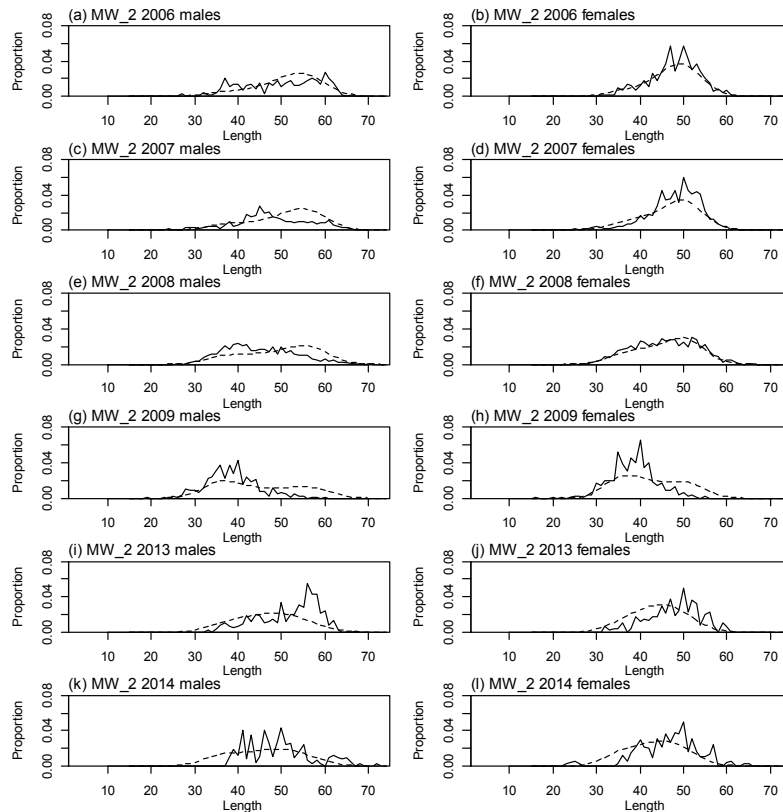
	Measured	Multinomial N	Effective sample size
N_1993	1 089	1 520	4.87
N_1994	2 090	3 036	9.73
N_1995	1 498	2 300	7.37
N_1996	465	500	1.60
N_1998	1 843	3 085	9.88
N_1999	1 921	4 221	13.52
N_2000	1 727	2 200	7.05
N_2001	1 528	2 908	9.32
N_2002	510	908	2.91
N_2003	2 824	5 674	18.18
N_2004	3 856	6 921	22.17
N_2005	1 448	2 497	8.00
N_2007	829	1 189	3.81
N_2008	1 087	1 587	5.08
N_2010	948	1 632	5.23
N_2011	3 273	6 881	22.04
N_2013	2 613	3 847	12.32
N_2014	403	789	2.53

A8. 12: Numbers of scampi measured, estimated multinomial N sample size, and effective sample size used within the SCI 3 NP_0.35 model for length frequency distributions for observer samples, MN time step 2.

	Measured	Multinomial N	Effective sample size
N_1993	1 639	3 306	20.14
N_1994	2 923	5 285	32.19
N_1995	1 260	1 800	10.96
N_2006	1 086	1 635	9.96
N_2008	535	699	4.26
N_2009	186	245	1.49
N_2011	1 019	1 900	11.57
N_2012	333	588	3.58
N_2013	352	234	1.43
N_2014	1 443	1 378	8.39



A8. 13: Observed (solid line) and fitted (dashed line) length frequency distributions for observer samples, MW time step 1 for SCI 3 NP_0.35.



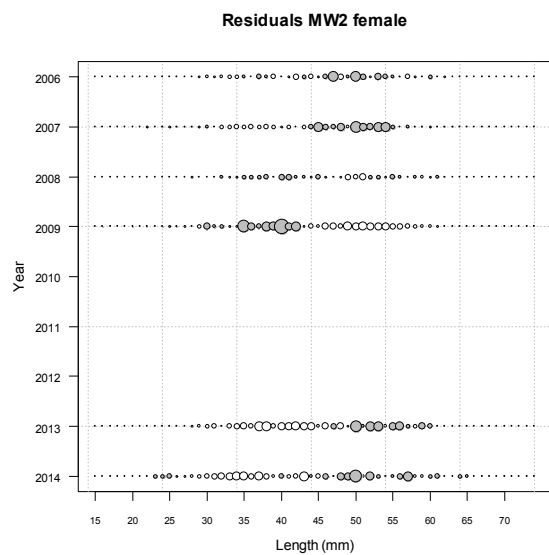
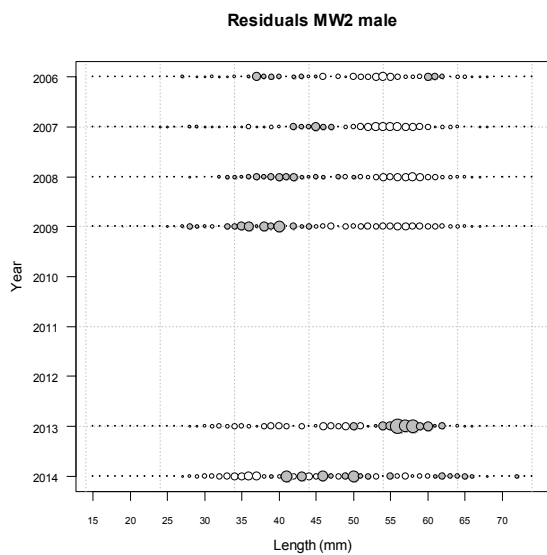
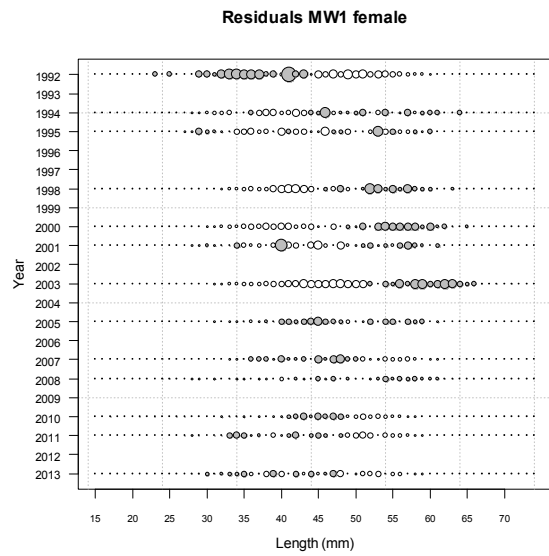
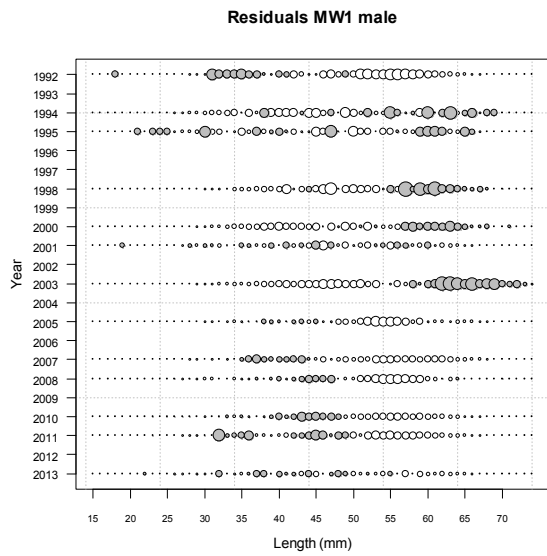
A8. 14: Observed (solid line) and fitted (dashed line) length frequency distributions for observer samples, MW time step 2 for SCI 3 NP_0.35.

A8. 15: Numbers of scampi measured, estimated multinomial N sample size, and effective sample size used within the SCI 3 NP_0.35 model for length frequency distributions for observer samples, MW time step 1.

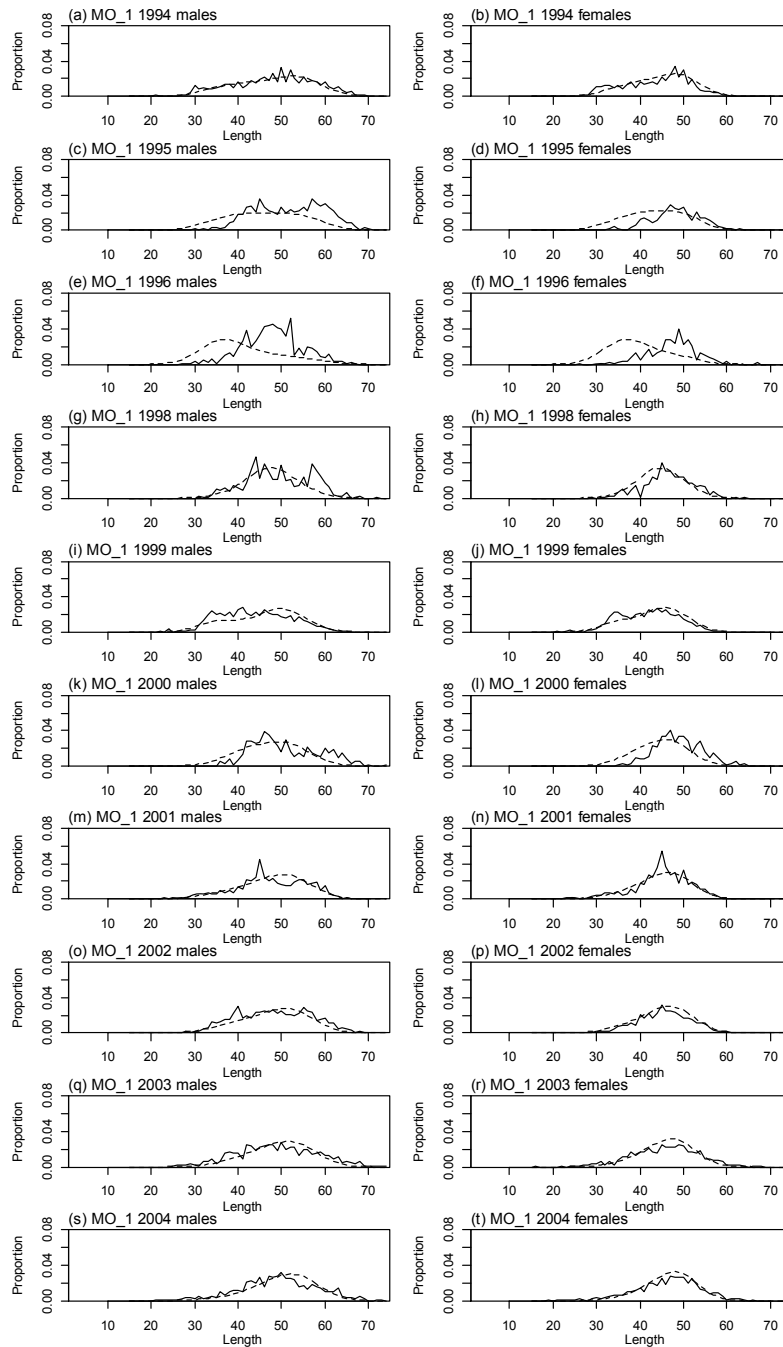
	Measured	Multinomial N	Effective sample size
N_1992	229	107	0.36
N_1994	242	100	0.34
N_1995	241	100	0.34
N_1998	365	365	1.22
N_2000	521	600	2.01
N_2001	251	169	0.57
N_2003	578	799	2.68
N_2005	593	870	2.92
N_2007	1 082	1 669	5.60
N_2008	1 201	1 865	6.25
N_2010	3 163	6 951	23.31
N_2011	712	2 345	7.86
N_2013	495	616	2.07

A8. 16: Numbers of scampi measured, estimated multinomial N sample size, and effective sample size used within the SCI 3 NP_0.35 model for length frequency distributions for observer samples, MW time step 2.

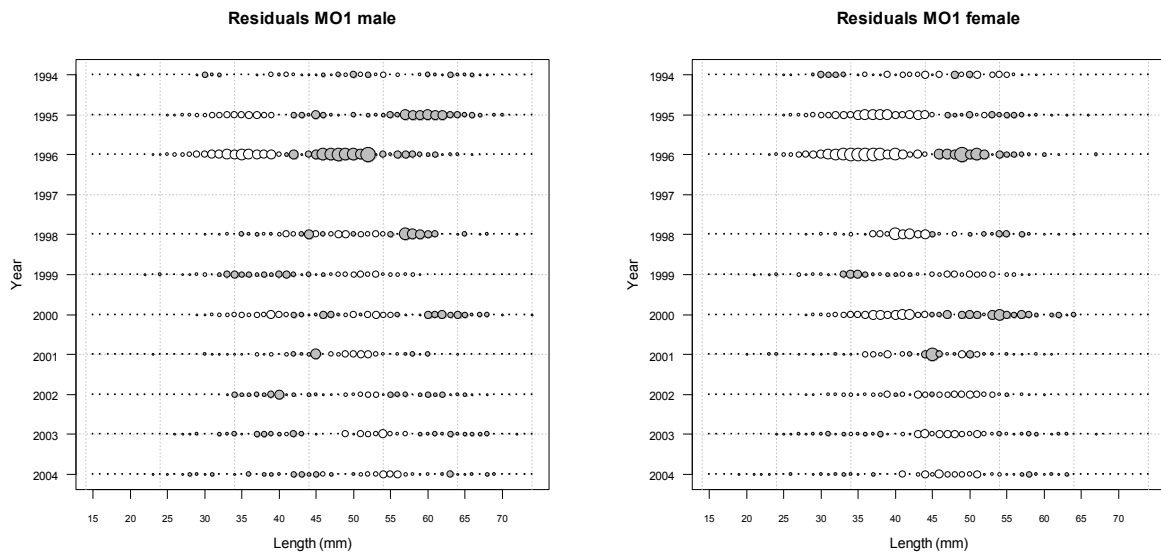
	Measured	Multinomial N	Effective sample size
N_2006	659	699	4.16
N_2007	1 333	2 406	14.30
N_2008	2 278	4 100	24.37
N_2009	693	1 340	7.97
N_2013	550	483	2.87
N_2014	460	317	1.88



A8. 17: Bubble plots of residuals of fits to length frequency distributions for observer sampling from MW, time step 1 and 2, for SCI 3 NP_0.35.



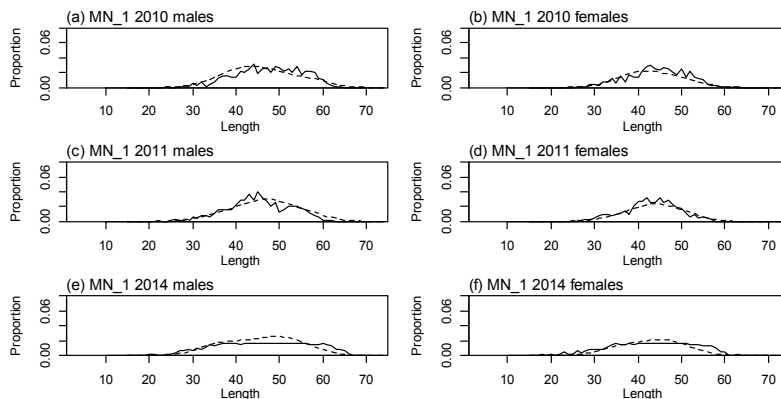
A8. 18: Observed (solid line) and fitted (dashed line) length frequency distributions for observer samples, MO time step 1 for SCI 3 NP_0.35.



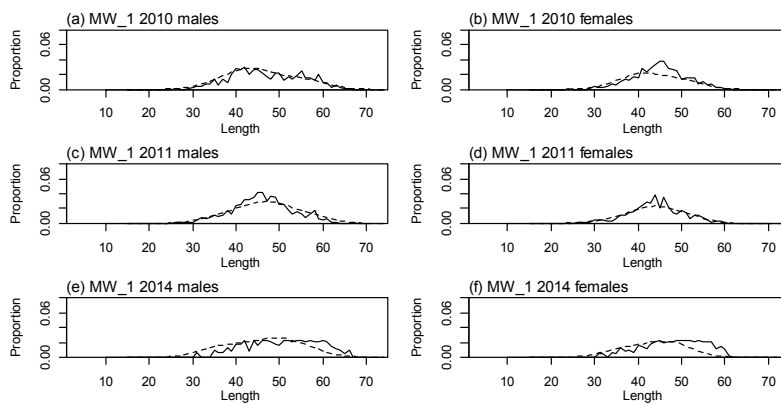
A8. 19: Bubble plots of residuals of fits to length frequency distributions for observer sampling from MO, time step 1, for SCI 3 NP_0.35.

A8. 20: Numbers of scampi measured, estimated multinomial N sample size, and effective sample size used within the SCI 3 NP_0.35 model for length frequency distributions for observer samples, MO time step 1.

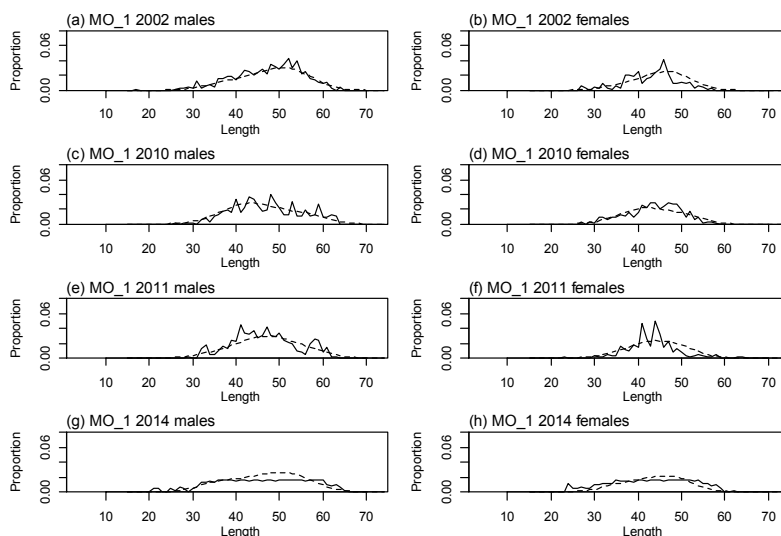
	Measured	Multinomial N	Effective sample size
N_1994	2 665	4 814	19.47
N_1995	2 474	2 500	10.11
N_1996	752	1 200	4.85
N_1998	870	900	3.64
N_1999	1 492	2 996	12.12
N_2000	608	600	2.43
N_2001	1 749	3 118	12.61
N_2002	1 768	3 442	10.66
N_2003	1 367	2 224	9.00
N_2004	1 557	2 881	11.65



A8. 21: Observed (solid line) and fitted (dashed line) length frequency distributions for MN trawl survey samples within the SCI 3 NP_{0.35} model.



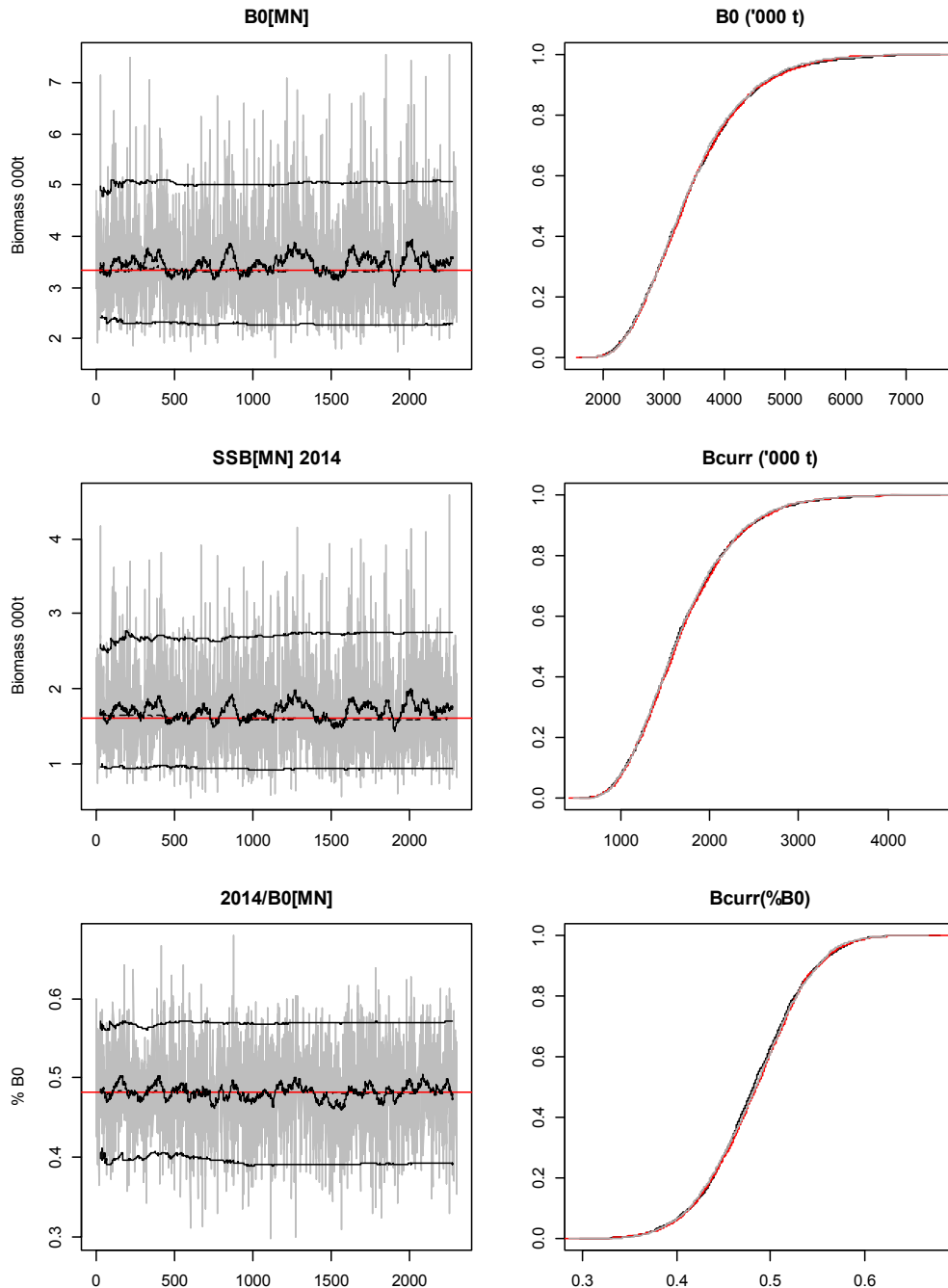
A8. 22: Observed (solid line) and fitted (dashed line) length frequency distributions for MW trawl survey samples within the SCI 3 NP_{0.35} model.



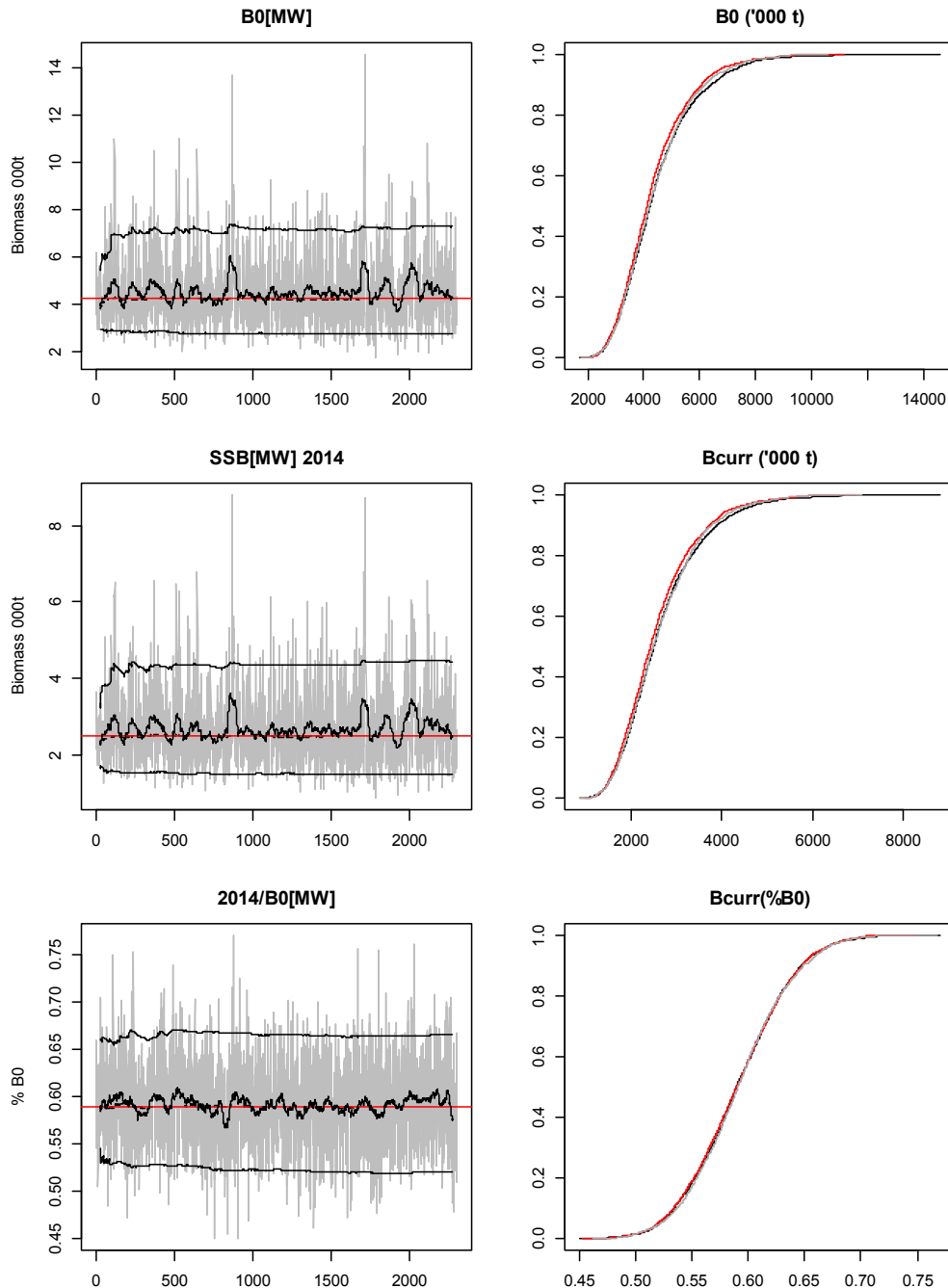
A8. 23: Observed (solid line) and fitted (dashed line) length frequency distributions for MO trawl survey samples within the SCI 3 NP_{0.35} model.

A8. 24: Numbers of scampi burrows measured, estimated multinomial N sample size, and effective sample size used within the model for length frequency distributions for photographic survey samples within the SCI 3 NP_0.35 model.

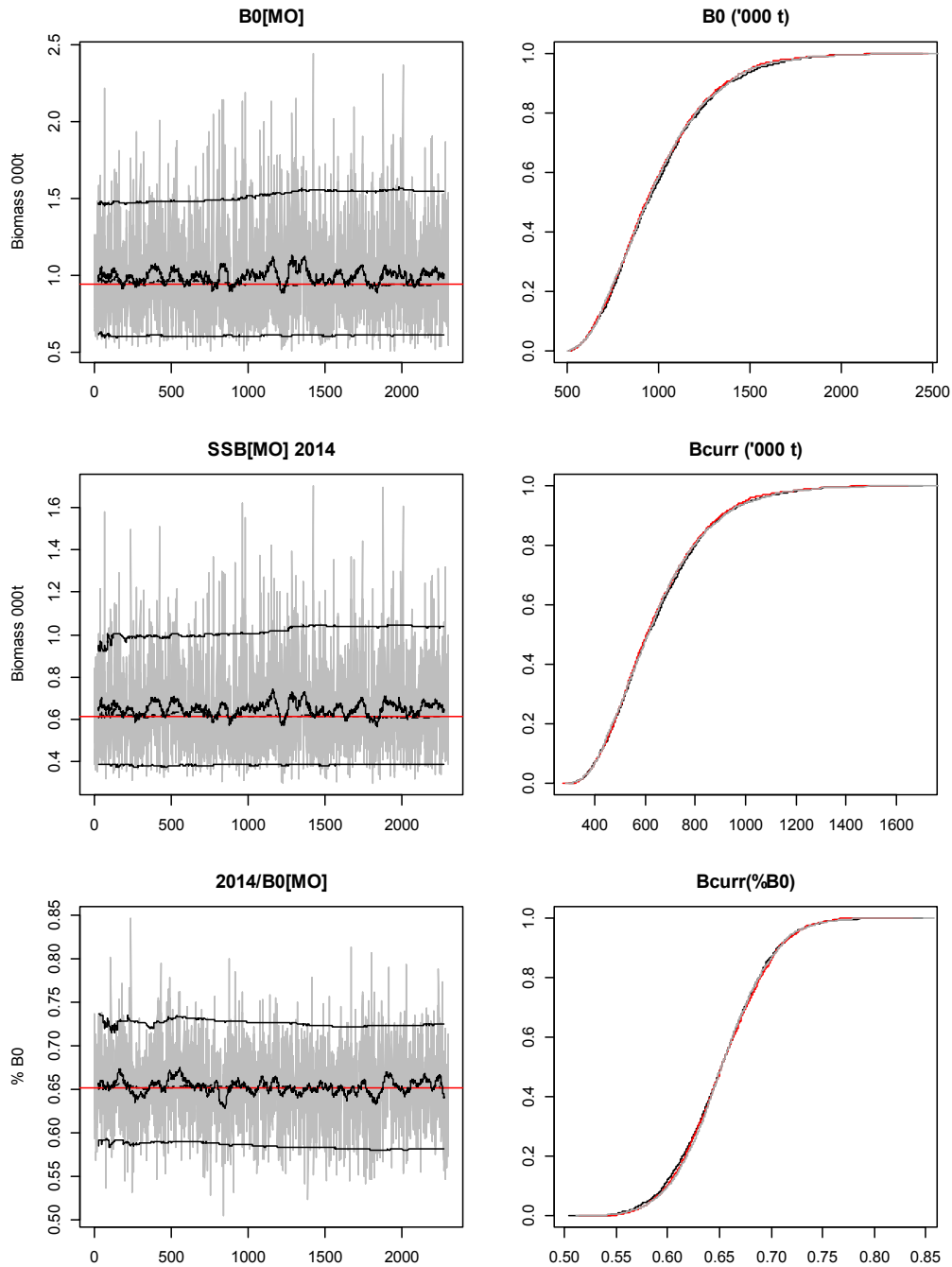
MN	Measured	Multinomial N	Effective sample size
N_2010	2 595	1 276	22.71
N_2011	4 429	2 362	38.76
N_2014	1 077	602	9.42
MW	Measured	Multinomial N	Effective sample size
N_2010	2 254	1 110	45.40
N_2011	2 636	1 295	53.10
N_2014	385	208	7.75
MO	Measured	Multinomial N	Effective sample size
N_2002	1 367	1 418	163.17
N_2010	1 123	551	134.04
N_2011	1 163	611	138.82
N_2014	523	339	62.43



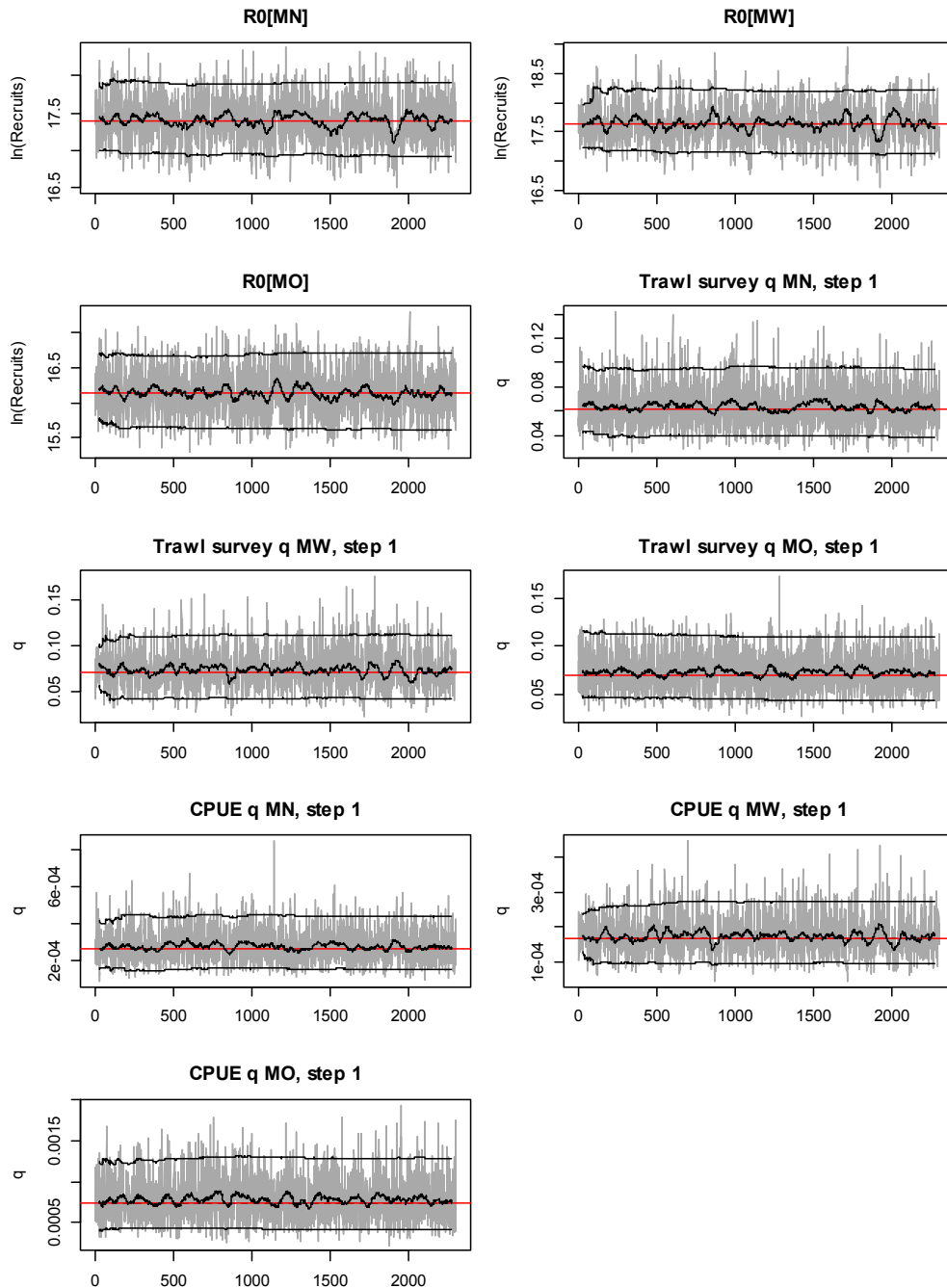
A8. 25: MCMC traces for B_0 , SSB_{2014} , and SSB_{2014}/SSB_0 terms for the MN subarea within the SCI 3 NP_0.35 model for SCI 3 (trace – grey line, cumulative moving median – dashed black line, moving average and cumulative moving 2.5%, 97.5% quantiles – solid black lines, overall median – solid red line, left plots), along with cumulative frequency distributions for three independent MCMC chains (shown as red, grey and black lines, right plots).



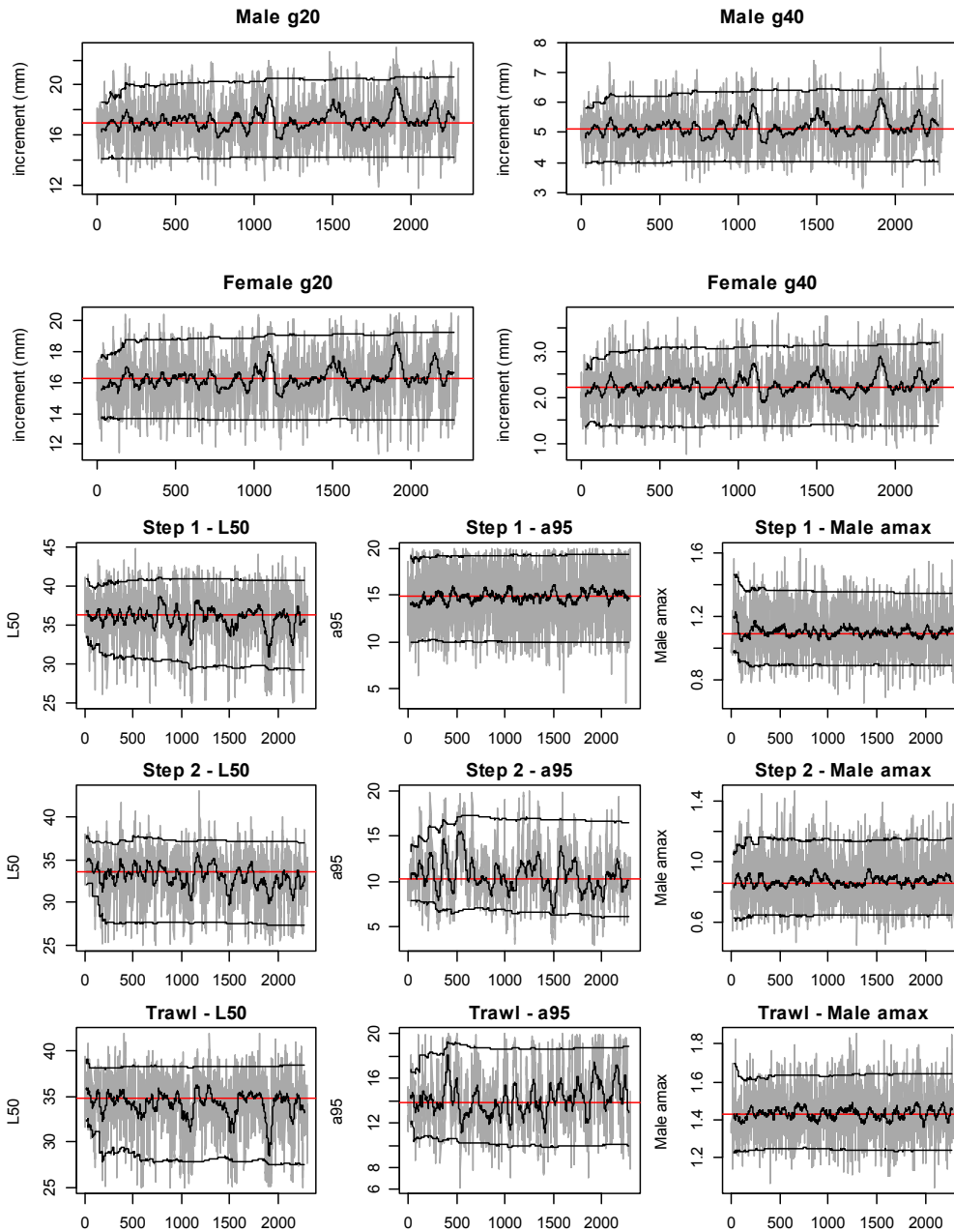
A8. 26: MCMC traces for B_0 , SSB_{2014} , and SSB_{2014}/SSB_0 terms for the MW subarea within the SCI 3 NP_0.35 model for SCI 3 (trace – grey line, cumulative moving median – dashed black line, moving average and cumulative moving 2.5%, 97.5% quantiles – solid black lines, overall median – solid red line, left plots), along with cumulative frequency distributions for three independent MCMC chains (shown as red, grey and black lines, right plots).



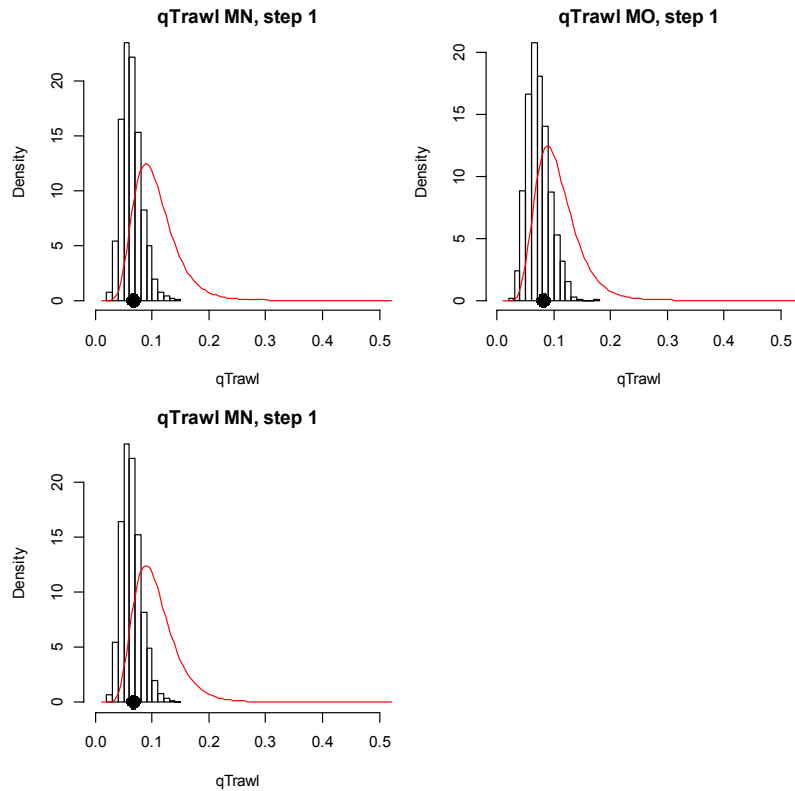
A8. 27: MCMC traces for B_0 , SSB_{2014} , and SSB_{2014}/SSB_0 terms for the MN subarea within the SCI 3 NP_0.35 model for SCI 3 (trace – grey line, cumulative moving median – dashed black line, moving average and cumulative moving 2.5%, 97.5% quantiles – solid black lines, overall median – solid red line, left plots), along with cumulative frequency distributions for three independent MCMC chains (shown as red, grey and black lines, right plots).



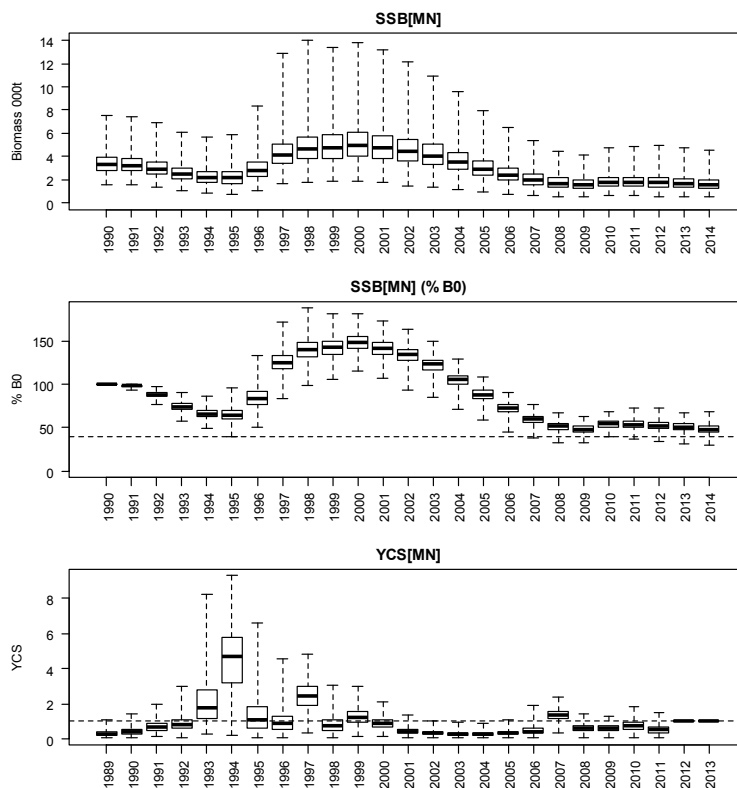
A8. 28: MCMC traces for R_0 , trawl survey q s, and commercial fishery q terms within the SCI 3 NP_0.35 model for SCI 3 (trace – grey line, cumulative moving median – dashed black line, moving average and cumulative moving 2.5%, 97.5% quantiles – solid black lines, overall median – solid red line, left plots), along with cumulative frequency distributions for three independent MCMC chains (shown as red, grey and black lines, right plots).



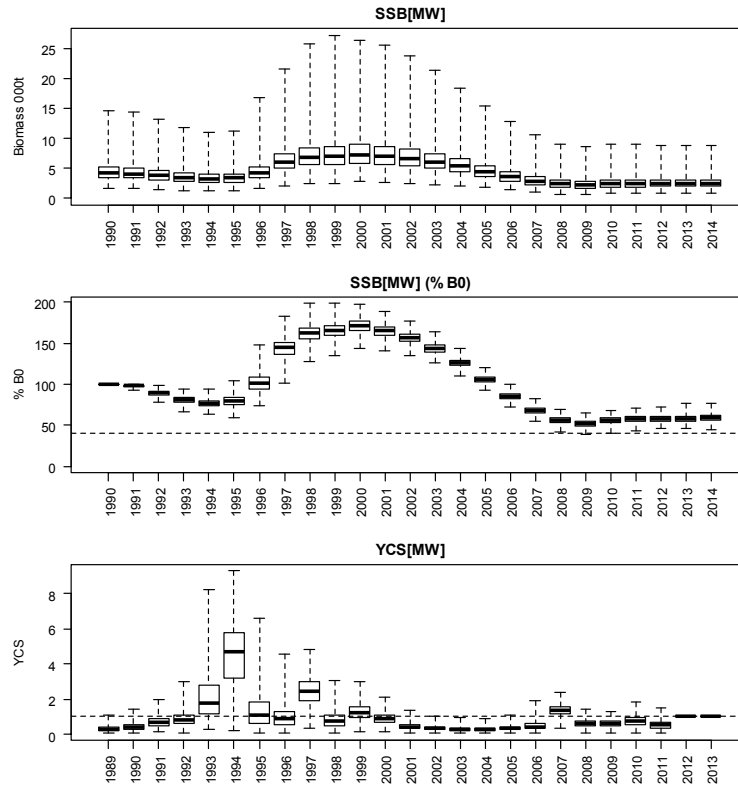
A8. 29: MCMC traces for growth increment and selectivity parameters within the SCI 3 NP_0.35 model for SCI 3 (trace – grey line, cumulative moving median – dashed black line, moving average and cumulative moving 2.5%, 97.5% quantiles – solid black lines, overall median – solid red line, left plots), along with cumulative frequency distributions for three independent MCMC chains (shown as red, grey and black lines, right plots).



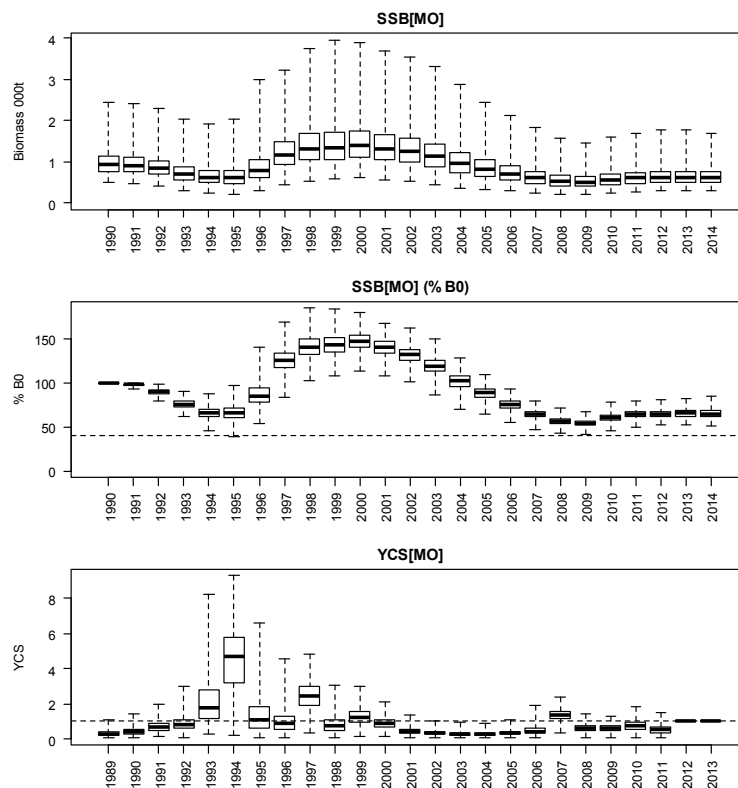
A8. 30: Marginal posterior distribution (histogram), MPD estimate (solid symbols) and distribution of prior (line) for photo survey catchability term within the SCI 3 NP_0.35 model.



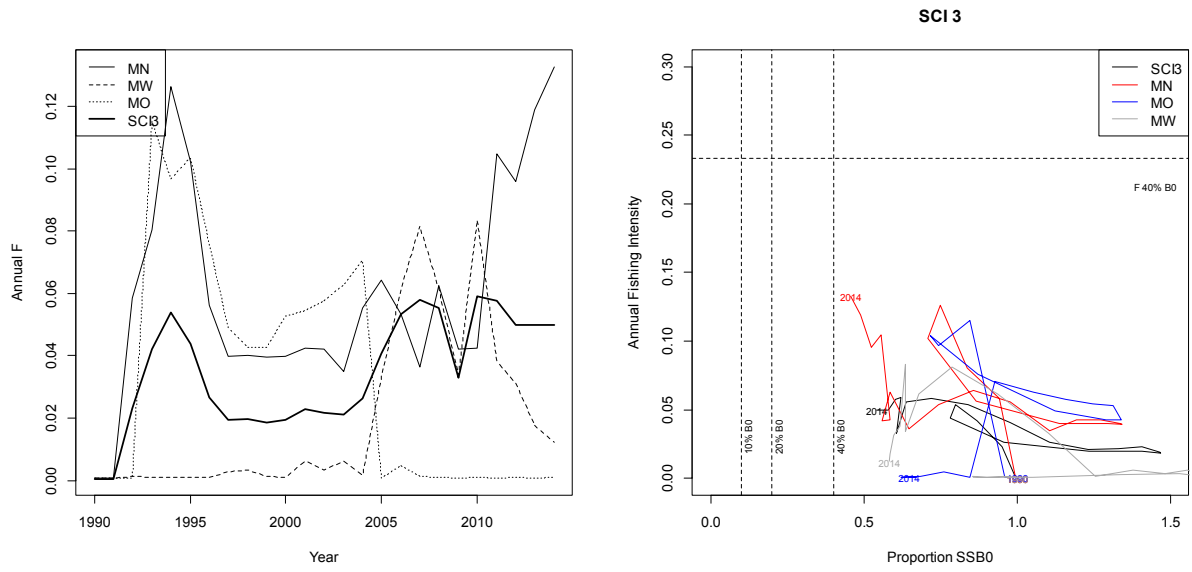
A8. 31: Posterior trajectory of SSB, SSB₂₀₁₄/SSB₀ and YCS for the MN subarea within the SCI 3 NP_0.35 model.



A8. 32: Posterior trajectory of SSB, SSB_{2014}/SSB_0 and YCS for the MW subarea within the SCI 3 NP_0.35 model.



A8. 33: Posterior trajectory of SSB, SSB_{2014}/SSB_0 and YCS for the MO subarea within the SCI 3 NP_0.35 model.



A8. 34: Estimated annual equivalent F (left) and phase plot (right) from the SCI 3 NP_0.35 model.